New Materials for Supramolecular Nanoscale Devices

By

MATTHEW JUROW

A dissertation submitted to the Graduate Faculty in Chemistry in partial fulfillment of the requirements for the degree of Doctor of Philosophy, The City University of New York

2013

This manuscript has been read and accepted for the Graduate Faculty in Chemistry in satisfaction of the dissertation requirement for the degree of Doctor of Philosophy.

_____. _____.

Date Charles M Drain

Chair of Examining Committee

_____. _____.

Date Maria Tamargo

Executive Officer

_____.

Prof. C. Drain

_____.

Prof. H Matsui

_____.

Prof. A Couzis

_____.

Prof. E Galoppini

Supervision Committee

THE CITY UNIVERSITY OF NEW YORK

Abstract

New Materials for Supramolecular Nanoscale Devices

By

Matthew Jurow

Adviser: Professor Charles Michael Drain

Nanotechnology as a scientific discipline embraces the different properties which matter exhibits when confined in physical dimension to particles or more elaborate constructions with relevant features on the order of 10^{-9} meters (1 nanometer). At these length scales materials enter the grey realm of physics governed both by the rules of quantum mechanics and more classical Newtonian or otherwise "normal" physical chemistry. In this blurred area remarkable materials and devices can be produced. Nature has used quantum confinement effects to produce the iridescent color of butterfly wings, the shimmering glow of an opal, the almost impossibly efficient process of turning sunlight into useable energy, and some of the lightest and strongest materials known.

The projects reported here seek to employ the very small – molecules, nanoparticles, films of materials far thinner than a human hair – to create diverse useful systems. We have focused our attention of a class of molecules which strongly absorb light and can be induced to interact with other materials to create devices which can harvest the energy in sunlight, change the way they respond to external stimulus based on the way they are being illuminated, and hopefully in the future make electronic devices more efficient, sustainable, smaller and broadly better.

The majority of our most advanced current technologies are made by "top down" fabrication. Large portions of materials which do not demonstrate any of the strange properties

which emerge when physical dimensions are severely limited, called bulk materials, are whittled down and painstakingly arranged sometimes one molecule at a time to make microchips and the screens in our cell phones. Another driving force of the research described here is to advance the idea of "self assembly" by which molecules can be designed to interact with each other in such a way that they arrange into a precise manner without needing to be moved one at a time.

By advancing our knowledge of self assembled systems, especially those which interact with light, we have strived to make real progress towards new highly applicable functional technologies across many disciplines. Some of our efforts are described in the next chapters.

To my family, friends and teachers

Acknowledgements

I would like to acknowledge everyone who has helped me complete the work detailed in this report. Thank you to my parents for their unwavering support in everything. Thank you Prof. Drain for your guidance and assistance with all of the projects and explorations on which we embarked. Thank you Dr. C Borek for pointing me towards grad school and teaching me the techniques on which I so often relied. Thanks to Dr. Thompson and everyone in his group at USC who helped me at the beginning of my research career. Thank you to all of the lab members who made this work possible; Ivana, Jacopo, Alessandro, Jennifer, Gabby, Dr. Shi, Donna, Ben, Patrick, Chris, Amit, Sunnaina, Ahmed, Stuart, Clayton, Sandeep and especially Brian. Thank you to all of the undergraduates who helped with so much of the work required to finish this book; Waqar, Meroz, Juliya, Danny, Chris and especially Cesar. Thank you David. Thank you to all of the teachers and mentors from Glen Ridge, USC and CUNY who made this all possible through your continued hard work and assistance. Thank you to Dr. Soll and Dr. Devany for helping with endless characterizations and thank you to Dr. Grohmann for his constant help with synthetic design and technique. Thank you to Mirella and everyone in the chemistry office and stock room for helping make all of this possible. Thank you to the staff at the Brookhaven National Labs who assisted with so much of the experimentation required to finish this work; Dr. Nam, Dr. DiMasi, Dr. Black, Dr. Stanic, Dr. Gearba and Dr. Yaeger.

Table of Contents

List of Figures

List of Tables

CHAPTER 1

Introduction and Background

1.1 Introduction

Chemistry continues to play a pivotal role in addressing some of the great challenges in science today and enable new opportunities to make materials to meet societal needs in an environmentally acceptable way.[1,2] These challenges include the development of cost-effective solar energy harvesting systems and devices with lower power consumption in order to meet the ever increasing energy requirements of the US and the world.[3] Similarly, development of low-cost and 'green' catalysts, chemical sensors, and photonic materials will reduce environmental impacts and improve health. The design and synthesis of molecules for directed self-organization and self-assembly into functional materials remains a fundamental scientific issue in the chemical sciences that can also provide practical materials for these and many other applications.[4-6] The overarching theme of this text has been to synthesize molecules designed to continue pushing the limits of self-organization and self-assembly to create functional, photonic materials and prototypical devices containing the various porphyrinoid dyes, graphitic materials, and biopolymers. The majority of the projects described in this thesis deal with the synthesis, characterization, photophysics, surface deposition, and applications of hierarchically organized porphyrinoids (Fig. 1) and other materials.[7-61]

Directed self-organization is the formation of materials by both designed intermolecular interactions and external forces or stimuli such as solvent dynamics,[62,63] surface energetics,[38,55,64] confined spaces,[38,65-67] electromagnetic fields, templates,[68,69] or gravity.[70,71] Self-organized materials may be designed to respond to environmental changes or stimuli.[9,18] Specific intermolecular interactions are directional motifs designed to recognize complementary

components to yield predictable intermolecular interactions and predictable self-assembled, discrete architectures. These motifs include H-bonds and coordination chemistry. Self-assembly allows the predictable formation of nanoarchitectures with predictable photonic properties. Nonspecific intermolecular interactions such as dispersion forces are generally nondirectional and lead to self-organized, open structures that are less ordered and difficult to predict, or that are different depending on the conditions used to make the material. Hierarchical organization defines structures that have different molecular organization at different length scales.[72-75] The number of publications on the supramolecular chemistry of porphyrinoid systems has grown exponentially since the late 1980s[76] because of the potential to make functional materials from components that are significantly easier to synthesize compared to covalently linked arrays, and the large number of potential applications.[77-86] The photophysical, electronic, and catalytic properties of porphyrinoids can be tuned by metal ion coordination, exocyclic motifs, and axial ligands. These properties enable new materials for photonics, sensors, catalysts, electronics, and solar energy harvesting devices.[87-110]

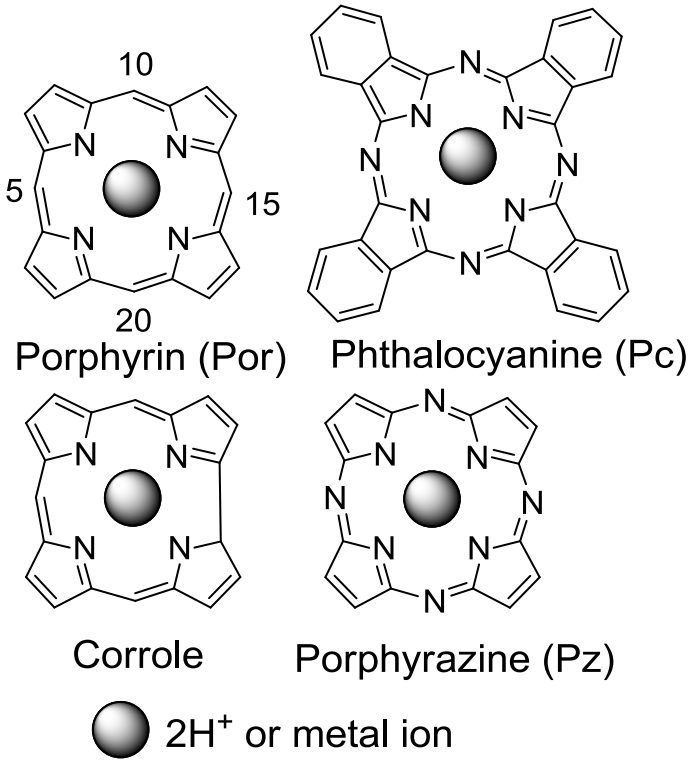

Figure 1.1 Some porphyrinoids.

An important advantage afforded by directed self-organization of materials is the high yield syntheses of molecular components that enable commercially viable technologies.[22,111-113] The disadvantages of self-assembled/organized systems largely stem from the complex equilibriums inherent to supramolecular entities (often thermodynamic products) that make both characterization and material/device stability keystone issues in real-world applications. Conversely, these equilibriums can be exploited to anneal the material, exploit external forces in materials design, and afford a mechanism of self-repair.[114,115] One goal of the work we have done over the last five years has been to further develop the concepts for directed self-organization of porphyrinoids into predictable nanoarchitectures in photonic materials.

1.2 Porphyrinoids

Porphyrinoids (Figure 1-1) are topologically rigid macrocyclic chromophores that display a range of photophysical and chemical properties. The photophysics, redox potentials, catalytic activities, magnetism,[116-123] optical cross sections, and structural dynamics can be controlled by chelation of almost every metal ion in the periodic table, substituents on the macrocycle, and environmental factors such as solvent, matrix, and surface. Importantly, porphyrinoid functionality is profoundly affected by the architectural organization. Porphyrinoid materials can be remarkably stable to real-world conditions, e.g. light, elevated temperatures, O_2, water.[111,124-127] Thus porphyrinoids are versatile tectons that afford a rich diversity in supramolecular nanoarchitecures and are ideal components of hierarchical functional materials.[128-134] The supramolecular chemistry of porphyrins (Por) is well studied.[85,86,113,135-138] The self-assembly and properties of discrete arrays of other porphryinoids such as porphyrazines (Pz)[48,139] and phthalocyanine (Pc) are only beginning to emerge, as are systems containing different chromophores with complementary properties (e.g. photonic, catalytic, and chelation).[79,81,82,140-145]

1.3 Surfaces

The structure of functional supramolecular materials can be directed via interactions with surfaces and patterns on surfaces as part of the design process. While porphyrinoids can be organized on a variety of surfaces as chemically bound self-assembled monolayers (SAMs) or by adsorption, deposition of discrete arrays, such as square tetramers pre-assembled by metal ion coordination or H-bonds, is much more difficult.[11,55,146] Surface interactions play a complex role in hierarchical self-organization and the resulting morphology of porphyrinoid materials because of convoluted factors affecting the equilibriums: e.g. concentration changes during solvent

evaporation, fluid dynamics, and surface energetics.[26,57,58,84,117,147] Accordingly, self-assembled arrays can: (a) disassemble and components separate, (b) aggregate into amorphous or hierarchical structures, (c) reorganize into different structures.[148] The reliable and predictable control of the structure of supramolecular materials at interfaces is a specific goal of the work described herein because this remains a significant challenge and barrier to commercially viable applications.[22,26]

1.4 Fullerenes

Fullerenes and other graphitic materials are active substrates or surfaces for photonics. The materials properties and potential photonics applications of fullerenes, graphene, graphene oxide, and reduced graphene oxide are well established. For many of these applications, the addition of a porphryinoid enhances visible light absorption, creates electron donor-acceptor systems, or modulate the electronic properties of the fullerene or graphitic substrate.[101,102,149-154]

1.5 Summary

"Through controlled self-assembly and directed assembly of nanoconstituents of distinct properties, the next-generation nanocomposite material will have the unique and powerful attribute of independent tunability of previously coupled properties."

Roco, Weiss, and coworkers.[6]

While specialization is still important, interdisciplinary training is needed in fields such as nanoscience, chemical biology, and materials chemistry to make key discoveries and develop emerging technologies.[2] The projects described in the body of this thesis range from synthetic to applied and span all of the classical divisions of chemistry.

1.6 References

(1) Committee on Challenges for the Chemical Sciences in the 21st Century *Beyond the Molecular Frontier: Challenges for Chemistry and Chemical Engineering*; The National Academies Press: Washington, DC, 2003.

(2) Whitesides, G. M.; Deutch, J. *Nature* **2011**, *469*, 21.

(3) Service, R. F. *Science* **2005**, *309*, 548.

(4) Service, R. F. *Science* **2005**, *309*, 95.

(5) Casey, C. P. *Chem. International* **2005**, *27*, 8.

(6) Roco, M. C.; Hersam, M. C.; Mirkin, C. A.; Hersam, M.; Weiss, P. S. **2011**, *1*, 467.

(7) Radivojevic, I.; Bazzan, G.; Burton-Pye, B. P.; Ithisuphalap, K.; Saleh, R.; Durstock, M. F.; Francesconi, L. C.; Drain, C. M. *J. Phy. Chem. C* **2012**, *116*, 15867.

(8) Jurow, M.; Farley, C.; Pabon, C.; Hageman, B.; Dolor, A.; Drain, C. M. *Chem. Comm.* **2012**, *48*, 4731.

(9) Aggarwal, A.; Singh, S.; Samson, J.; Drain, C. M. *Macromol Rapid Comm.* **2012**, *33*, 1220.

(10) Varotto, A.; Smeureanu, G.; Aggarwal, A.; Drain, C. M. In *ACS Symposium Series: Fluorine-related Nanoscience with Energy Applications*; American Chemical Society: Washington, 2011; Vol. 1064, p 55.

(11) Singh, S.; Aggarwal, A.; Farley, C.; Hageman, B. A.; Batteas, J. D.; Drain, C. M. *Chem. Comm.* **2011**, *47*, 7134.

(12) Samson, J.; Piscopo, I.; Yampolski, A.; Nahirney, P.; Parpas, A.; Aggarwal, A.; Saleh, R.; Drain, C. M. *Nanomaterials* **2011**, *1*, 64.

(13) Samson, J.; Nahirney, P. C.; Drain, C. M.; Piscopo, I. *Microscopy Today* **2011**, *19*, 38.

(14) Sahar-Halbany, A.; Vance, J. M.; Drain, C. M. *J. Chem. Ed.* **2011**, *88*, 615.

(15) Bazzan, G.; Aggarwal, A.; Drain, C. M. In *ACS Symposium Series, Interfaces and Interphases in Analytical Chemistry*; Helburn, R., Vitha, M. F., Eds.; American Chemical Society: Washington, 2011, p 167.

(16) Aggarwal, A.; Singh, S.; Zhang, Y.; Anthes, M.; Samaroo, D.; Gao, R.; Drain, C. M. *Tetrahedron Lett.* **2011**, *52*, 5456.

(17) Aggarwal, A.; Singh, S.; Drain, C. M. *J. Porphyrins Phthalocyanines* **2011**, *15*, 1.

(18) Aggarwal, A.; Qureshy, M.; Johnson, J.; Batteas, J. D.; Drain, C. M.; Samaroo, D. *J. Porphyrins Phthalocyanines* **2011**, *15*, 338.

(19) Varotto, A.; Nam, C. Y.; Radivojevic, I.; Tome, J. P. C.; Cavaleiro, J. A. S.; Black, C. T.; Drain, C. M. *J. Am. Chem. Soc.* **2010**, *132*, 2552.

(20) Toschi, A.; Lee, E.; Thompson, S.; Gadir, N.; Yellen, P.; Drain, C. M.; Ohh, M.; Foster, D. A. *Cancer Lett.* **2010**, *299*, 72.

(21) Singh, S.; Aggarwal, A.; Thompson, S.; Tome, J. P. C.; Zhu, X. C.; Samaroo, D.; Vinodu, M.; Gao, R. M.; Drain, C. M. *Bioconjugate Chem.* **2010**, *21*, 2136.

(22) Radivojevic, I.; Varotto, A.; Farley, C.; Drain, C. M. *Energy Environm. Sci.* **2010**, *3*, 1897.

(23) Radivojevic, I.; Sfeir, M.; Nam, C.-Y.; Burton-Pye, B. P.; Falber, A.; Black, C. T.; Drain, C. M. *Proc. IEEE: Solar Energ* **2010**, 003280.

(24) Radivojevic, I.; Likhtina, I.; Shi, X.; Singh, S.; Drain, C. M. *Chem. Comm.* **2010**, *46*, 1643.

(25) Nia, S.; Gong, X. C.; Drain, C. M.; Jurow, M.; Rizvi, W.; Qureshy, M. *J. Porphyrins Phthalocyanines* **2010**, *14*, 621.

(26) Jurow, M.; Schuckman, A. E.; Batteas, J. D.; Drain, C. M. *Coord. Chem. Rev.* **2010**, *254*, 2297.

(27) Drain, C. M.; Singh, S. In *The Handbook of Porphyrin Science with Applications to Chemistry, Physics, Materials Science, Engineering, Biology and Medicine*; Kadish, K. M., Smith, K. M., Guilard, R., Eds.; World Scientific Publishers: Singapore, 2010; Vol. 3, p 485.

(28) Smeureanu, G.; Aggarwal, A.; Soll, C. E.; Arijeloye, J.; Malave, E.; Drain, C. M. *Chem. Eur. J.* **2009**, *15*, 12133.

(29) Samson, J.; Varotto, A.; Nahirney, P. C.; Toschi, A.; Piscopo, I.; Drain, C. M. *Acs Nano* **2009**, *3*, 339.

(30) Falber, A.; Burton-Pye, B. P.; Radivojevic, I.; Todaro, L.; Saleh, R.; Francesconi, L. C.; Drain, C. M. *Eur. J. Inorg. Chem.* **2009**, 2459.

(31) Drain, C. M.; Varotto, A.; Radivojevic, I. *Chem. Rev.* **2009**, *109*, 1630.

(32) de la Rica, R.; Thompson, S.; Baldi, A.; Fernandez-Sanchez, C.; Drain, C. M.; Matsui, H. *Anal. Chem.* **2009**, *81*, 10167.

(33) Varotto, A.; Todaro, L.; Vinodu, M.; Koehne, J.; Liu, G. Y.; Drain, C. M. *Chem. Comm.* **2008**, 4921.

(34) Stevens, N.; O'Connor, N.; Vishwasrao, H.; Samaroo, D.; Kandel, E. R.; Akins, D. L.; Drain, C. M.; Turro, N. J. *J. Am. Chem. Soc.* **2008**, *130*, 7182.

(35) Serem, W. K.; Varotto, A.; Castro, G.; Drain, C. M.; Garno, J. C. *NOBCChE Proceedings* **2008**.

(36) Falber, A.; L.Todaro; Goldberg, I.; Favilla, M. V.; Drain, C. M. *Inorg. Chem.* **2008**, *47*, 454.

(37) Chan, Y.-H.; Schuckman, A. E.; Perez, L. M.; Vinodu, M.; Drain, C. M.; Batteas, J. D. *J. Phys. Chem. C* **2008**, *112*, 6110.

(38) Bazzan, G.; Smith, W.; Francesconi, L. C.; Drain, C. M. *Langmuir* **2008**, *24*, 3244.

(39) Samaroo, D.; Vinodu, M.; Chen, X.; Drain, C. M. *J. Combi. Chem.* **2007**, *9*, 998.

(40) Balaban, T. S.; Berova, N.; Drain, C. M.; Hauschild, R.; Kalt, H.; Lebedkin, S.; Lehn, J.-M.; Huang, X.; Nifaitis, F.; Pescitelli, G.; Prokhorenko, V. I.; Riedel, G.; Smeureanu, G.; Zeller, J. *Chem. Eur. J.* **2007**, *13*, 8411.

(41) Xu, C.; Wu, T.; Drain, C. M.; Batteas, J. D.; Fasolka, M. J.; Beers, K. L. *Macromolecules* **2006**, *39*, 3359.

(42) Xu, C.; Wu, T.; Batteas, J. D.; Drain, C. M.; Beers, K. L.; Fasolka, M. J. *Applied Surface Science* **2006**, *252*, 2529.

(43) Vittadello, M.; Stallworth, P. E.; Alamgir, F. M.; Suarez, S.; Abbrent, S.; Drain, C. M.; Noto, V. D.; Greenbaum, S. G. *Inorg. Chim. Acta* **2006**, *339*, 2513.

(44) Samaroo, D.; Soll, C. E.; Todaro, L. J.; Drain, C. M. *Org. Lett.* **2006**, *8*, 4985

(45) Helt, J. M.; Drain, C. M.; Bazzan, G. *J. Am. Chem. Soc.* **2006**, *128*, 9371.

(46) Garno, J. C.; Xu, C.; Bazzan, G.; Batteas, J. D.; Drain, C. M. In *ACS Symposium series: Metal-Containing and Metallo-Supramolecular Polymers and Materials*; Schubert, U. S.,

Newcome, G. R., Manners, I., Eds.; American Chemical Society: Washington, DC., 2006; Vol. 928, p 168.

(47) Drain, C. M.; Smeureanu, G.; Patel, S.; Gong, X.; Garno, J.; Arijeloye, J. *New J. Chem.* **2006**, *30*, 1834.

(48) Cheng, K. F.; Thai, N. A.; Grohmann, K.; Teague, L. C.; Drain, C. M. *Inorg. Chem.* **2006**, *45*, 6928.

(49) Xu, C.; Wu, T.; Mei, Y.; Drain, C. M.; Batteas, J. D.; Beers, K. L. *Langmuir* **2005**, *21*, 11136.

(50) Xu, C.; Wu, T.; Drain, C. M.; Batteas, J. D.; Beers, K. L. *Macromolecules* **2005**, *38*, 6.

(51) Drain, C. M.; Goldberg, I.; Sylvain, I.; Falber, A. *Topics in Current Chemistry* **2005**, *245*, 55.

(52) Drain, C. M.; Bazzan, G.; Milic, T.; Vinodu, M.; Goeltz, J. C. *Israel J. Chem.* **2005**, *45*, 255.

(53) Cheng, K. F.; Thai, N. A.; Teague, L. C.; Grohmann, K.; Drain, C. M. *Chem. Commun.* **2005**, 4678.

(54) Xu, C.; Wu, T.; Drain, C. M.; Batteas, J. D.; Beers, K. L. *ACS Polymer Reprints* **2004**, *45*, 667.

(55) Milic, T.; Garno, J. C.; Batteas, J. D.; Smeureanu, G.; Drain, C. M. *Langmuir* **2004**, *20*, 3974.

(56) Helt, J. M.; Drain, C. M.; Batteas, J. D. *J. Am. Chem. Soc.* **2004**, *136*, 628.

(57) Drain, C. M.; Smeareanu, G.; Batteas, J.; Patel, S. In *Dekker Encyclopedia of Nanoscience and Nanotechnology*; Schwartz, J. A., Contescu, C. I., Putyera, K., Eds.; Marcel Dekker, Inc.: New York, 2004; Vol. 5, p 3481.

(58) Drain, C. M.; Milic, T.; Garno, J. C.; Smeureanu, G.; Batteas, J. D. *ACS Polymer Reprints* **2004**, *45*, 346.

(59) Drain, C. M.; Chen., X. In *Encyclopedia of Nanoscience & Nanotechnology*; Nalwa, H. S., Ed.; American Scientific Press: New York, 2004; Vol. 9, p 593.

(60) Chen, X.; Hui, L.; Foster, D. A.; Drain, C. M. *Biochem.* **2004**, *43*, 10918.

(61) Chen, X.; Drain, C. M. *Drug Design Review - Online* **2004**, *1*, 215.

(62) Peng, X.; Huang, Y.; Gao, C.; Peng, J.; Komatsu, N.; Osuka, A.; Cao, Y. *J. Phys. Chem. C* **2010**, *114*, 18449.

(63) Tanoue, R.; Higuchi, R.; Enoki, N.; Miyasato, Y.; Uemura, S.; Kimizuka, N.; Stieg, A. Z.; Gimzewski, J. K.; Kunitake, M. *ACS Nano* **2011**, *5*, 3923.

(64) Rojas, G.; Simpson, S.; Chen, X.; Kunkel, D. A.; Nitz, J.; Xiao, J.; Dowben, P. A.; Zurek, E.; Enders, A. *Phys. Chem. Chem. Phys.* **2012**, *14*, 4971.

(65) Bai, F.; Sun, Z.; Wu, H.; Haddad, R. E.; Coker, E. N.; Huang, J. Y.; Rodriguez, M. A.; Fan, H. *Nano Letters* **2011**, *11*, 5196.

(66) Li, L.-L.; Fu, X.-F.; Ren, Z.; Zhao, Y.-G.; Feng, W.; Yan, C.-H. *Langmuir* **2010**, *26*, 15730.

(67) Qiu, Y.; Chen, P.; Liu, M. *J. Am. Chem. Soc.* **2010**, *132*, 9644.

(68) Nam, Y. S.; Shin, T.; Park, H.; Magyar, A. P.; Choi, K.; Fantner, G.; Nelson, K. A.; Belcher, A. M. *J. Am. Chem. Soc.* **2010**, *132*, 1462.

(69) Börjesson, K.; Wiberg, J.; El-Sagheer, A. H.; Ljungdahl, T.; Mårtensson, J.; Brown, T.; Nordén, B.; Albinsson, B. *ACS Nano* **2010**, *4*, 5037.

(70) Ariga, K.; Hill, J. P.; Lee, M. V.; Vinu, A.; Charvet, R.; Acharya, S. *Sci. Tech. Adv. Mat.* **2008**, *9*, 014109.
(71) Li, M.; Ishihara, S.; Ji, Q.; Akada, M.; Hill, J. P.; Ariga, K. *Sci. Tech. Adv. Mat.* **2012**, *13*, 053001.
(72) Drain, C. M. *Proc. Natl. Acad. Sci., USA* **2002**, *99*, 5178.
(73) Whitesides, G. M.; Grzybowski, B. *Science* **2002**, *295*, 2418.
(74) Ruthard, C.; Schmidt, M.; Gröhn, F. *Macromol. Rapid Comm.* **2011**, *32*, 706.
(75) Lehn, J.-M. *Science* **2002**, 2400.
(76) Drain, C. M.; Christensen, B.; Mauzerall, D. C. *Proc. Natl. Acad. Sci. USA* **1989**, *86*, 6959.
(77) Webb, M. J.; Bampos, N. *Chem. Sci.* **2012**, *3*, 2351.
(78) Trapani, M.; Plutino, M. R.; Sabatino, G.; Occhiuto, I.; Borriello, A.; De Luca, G.; Scolaro, L. M. *Chem. Comm.* **2012**, *48*, 5136.
(79) Subbaiyan, N. K.; D'Souza, F. *Chem. Comm.* **2012**, *48*, 3641.
(80) Sakuma, T.; Sakai, H.; Hasobe, T. *Chem. Comm.* **2012**, *48*, 4441.
(81) Menting, R.; Ng, D. K. P.; Roder, B.; Ermilov, E. A. *Phys. Chem. Chem. Phys.* **2012**.
(82) Menting, R.; Lau, J. T. F.; Xu, H.; Ng, D. K. P.; Roder, B.; Ermilov, E. A. *Chem. Comm.* **2012**, *48*, 4597.
(83) Ishizuka, T.; Sankar, M.; Yamada, Y.; Fukuzumi, S.; Kojima, T. *Chem. Comm.* **2012**, *48*, 6481.
(84) Guo, P.; Chen, P.; Ma, W.; Liu, M. *J. Mater. Chem.* **2012**, *22*, 20243.
(85) D'Urso, A.; Fragala, M. E.; Purrello, R. *Chem. Comm.* **2012**, *48*, 8165.
(86) Hill, J. P.; D'Souza, F.; Ariga, K. In *Supramol. Chem.*; John Wiley & Sons, Ltd: 2012.
(87) Kadish, K.; Smith, K.; Guilard, R. *The Porphryin Handbook*; Academic Press: New York, 2003; Vol. 1-20.
(88) Kadish, K. M.; Smith, K. M.; Guilard, R. *The Handbook of Porphyrin Science with Applications to Chemistry, Physics, Materials Science, Engineering, Biology and Medicine*; World Scientific Publishers: Singapore, 2010; Vol. 1-10.
(89) Akhigbe, J.; Zeller, M.; Brückner, C. *Organic Letters* **2011**, *13*, 1322.
(90) Diev, V. V.; Schlenker, C. W.; Hanson, K.; Zhong, Q.; Zimmerman, J. D.; Forrest, S. R.; Thompson, M. E. *J. Org. Chem.* **2011**, *77*, 143.
(91) Lee, C. Y.; Farha, O. K.; Hong, B. J.; Sarjeant, A. A.; Nguyen, S. T.; Hupp, J. T. *J. Am. Chem. Soc.* **2011**, *133*, 15858.
(92) Lindsey, J. S.; Bocian, D. F. *Acc. Chem. Res.* **2011**, *44*, 638.
(93) Seol, M.-L.; Choi, S.-J.; Kim, C.-H.; Moon, D.-I.; Choi, Y.-K. *ACS Nano* **2011**, *6*, 183.
(94) Takagi, S.; Shimada, T.; Masui, D.; Tachibana, H.; Ishida, Y.; Tryk, D. A.; Inoue, H. *Langmuir* **2010**, *26*, 4639.
(95) Feese, E.; Sadeghifar, H.; Gracz, H. S.; Argyropoulos, D. S.; Ghiladi, R. A. *Biomacromol.* **2011**, *12*, 3528.
(96) Larsen, R. W.; Wojtas, L.; Perman, J.; Musselman, R. L.; Zaworotko, M. J.; Vetromile, C. M. *J. Am. Chem. Soc.* **2011**, *133*, 10356.
(97) Megiatto, J. D.; Schuster, D. I. *Org. Lett.* **2011**, *13*, 1808.

(98) Brancatelli, G.; De Zorzi, R.; Hickey, N.; Siega, P.; Zingone, G.; Geremia, S. *Crystal Growth Design* **2012**.

(99) Fry, H. C.; Garcia, J. M.; Medina, M. J.; Ricoy, U. M.; Gosztola, D. J.; Nikiforov, M. P.; Palmer, L. C.; Stupp, S. I. *J. Am. Chem. Soc.* **2012**, *134*, 14646.

(100) Sivalingam, Y.; Martinelli, E.; Catini, A.; Magna, G.; Pomarico, G.; Basoli, F.; Paolesse, R.; Di Natale, C. *J. Phys. Chem. C* **2012**, *116*, 9151.

(101) D'Souza, F.; Sandanayaka, A. S. D.; Ito, O. *J. Phys. Chem. Lett.* **2010**, *1*, 2586.

(102) Maligaspe, E.; Sandanayaka, A. S. D.; Hasobe, T.; Ito, O.; D'Souza, F. *J. Am. Chem. Soc.* **2010**, *132*, 8158.

(103) Cho, W. J.; Cho, Y.; Min, S. K.; Kim, W. Y.; Kim, K. S. *J. Am. Chem. Soc.* **2011**, *133*, 9364.

(104) Farha, O. K.; Shultz, A. M.; Sarjeant, A. A.; Nguyen, S. T.; Hupp, J. T. *J. Am. Chem. Soc.* **2011**, *133*, 5652.

(105) Fateeva, A.; Devautour-Vinot, S.; Heymans, N.; Devic, T.; Grenèche, J.-M.; Wuttke, S.; Miller, S.; Lago, A.; Serre, C.; De Weireld, G.; Maurin, G.; Vimont, A.; Férey, G. *Chem. Mater.* **2011**, *23*, 4641.

(106) Zhan, H.; Lamare, S.; Ng, A.; Kenny, T.; Guernon, H.; Chan, W.-K.; Djurišić, A. B.; Harvey, P. D.; Wong, W.-Y. *Macromol.* **2011**, *44*, 5155.

(107) Tian, Y.; Shumway, B. R.; Meldrum, D. R. *Chem. Mater.* **2010**, *22*, 2069.

(108) Morris, W.; Volosskiy, B.; Demir, S.; Gándara, F.; McGrier, P. L.; Furukawa, H.; Cascio, D.; Stoddart, J. F.; Yaghi, O. M. *Inorg. Chem.* **2012**, *51*, 6443−6445.

(109) Fathalla, M.; Neuberger, A.; Li, S.-C.; Schmehl, R.; Diebold, U.; Jayawickramarajah, J. *J. Am. Chem. Soc.* **2010**, *132*, 9966.

(110) Koepf, M.; Conradt, J.; Szmytkowski, J. d.; Wytko, J. A.; Allouche, L.; Kalt, H.; Balaban, T. S.; Weiss, J. *Inorg. Chem.* **2011**, *50*, 6073.

(111) Liu, Z.; Yasseri, A. A.; Lindsey, J. S.; Bocian, D. F. *Science* **2003**, *302*, 1543.

(112) Peet, J.; Heeger, A. J.; Bazan, G. C. *Acc. Chem. Res.* **2009**, *42*, 1700.

(113) Frischmann, P. D.; Mahata, K.; Wurthner, F. *Chem. Soc. Rev.* **2013**.

(114) Schmittel, M.; Kalsani, V.; Bats, J. W. *Inorg. Chem.* **2005**, *44*, 4115.

(115) Lehn, J.-M. *Supramolecular Chemistry: Concepts and Perspectives*; Wiley VCH: Weinheim, 1995.

(116) Lerouge, F.; Cerveau, G.; Corriu, R. J. P.; C., S.; Guilard, R. *Chem. Comm.* **2007**, *2007*, 1553.

(117) Drain, C. M.; Batteas, J. D.; Flynn, G. W.; Milic, T.; Chi, N.; Yablon, D. G.; Sommers, H. *Proc. Natl. Acad. Sci., USA* **2002**, *99*, 6498.

(118) Laget, V.; Hornick, C.; Rabu, P.; Drillon, M.; Ziessel, R. *Coord. Chem. Rev.* **1998**, *178-180*, 1533.

(119) Ishikawa, N.; Sugita, M.; Ishikawa, T.; Koshihara, S.-y.; Kaizu, Y. *J. Phys. Chem. B* **2004**, *108*, 11265.

(120) Zhao, M.; Zhong, C.; Stern, C.; Barrett, A. G. M.; Hoffman, B. M. *J. Am. Chem. Soc.* **2005**, *127*, 9769.

(121) Zhao, M.; Zhong, C.; Stern, C.; Barrett, A. G. M.; Hoffman, B. M. *Inorg. Chem.* **2004**, *43*, 3377.

(122) Miller, J. S. *Polyhedron* **2001**, *20*, 1723.

(123) Ishikawa, N.; Sugita, M.; Ishikawa, T.; Koshihara, S.-Y.; Kaizu, Y. *J. Am. Chem. Soc.* **2003**, *125*, 8694.

(124) Muthukumaran, K.; Loewe, R. S.; Ambroise, A.; Tamaru, S. i.; Li, Q.; Mathur, G.; Bocian, D. F.; Misra, V.; Lindsey, J. S. *J. Org. Chem.* **2004**, *69*, 1444.

(125) Gong, X.; Milic, T.; Xu, C.; Batteas, J. D.; Drain, C. M. *J. Am. Chem. Soc.* **2002**, *124*, 14290.

(126) Pasetto, P.; Chen, X.; Drain, C. M.; Franck, R. W. *Chem. Commun.* **2001**, 81.

(127) Drain, C. M.; Nifiatis, F.; Vasenko, A.; Batteas, J. D. *Angew. Chem. Int. Ed.* **1998**, *37*, 2344.

(128) Lee, S. J.; Malliakas, C. D.; Kanatzidis, M. G.; Hupp, J. T.; Nguyen, S. T. *Adv. Mater.* **2008**, *20*, 3543.

(129) Shi, N.; Yin, G.; Han, M.; Jiang, L.; Xu, Z. *Chem. Eur. J.* **2008**, *14*, 6255.

(130) Zhang, X.; Takeuchi, M. *Angew. Chem. Inter. Ed.* **2009**, *48*, 9646.

(131) Medforth, C. J.; Wang, Z.; Martin, K. E.; Song, Y.; Jacobsen, J. L.; Shelnutt, J. A. *Chem. Comm.* **2009**, 7261.

(132) Tian, Y.; Martin, K. E.; Shelnutt, J. Y. T.; Evans, L.; Busani, T.; Miller, J. E.; Medforth, C. J.; Shelnutt, J. A. *Chem. Comm.* **2011**, *47*, 6069.

(133) Tian, Y.; Busani, T.; Uyeda, G. H.; Martin, K. E.; van Swol, F.; Medforth, C. J.; Montano, G. A.; Shelnutt, J. A. *Chem. Comm.* **2012**, *48*, 4863.

(134) Zaytsev, D. V.; Xie, F.; Mukherjee, M.; Bludin, A.; Demeler, B.; Breece, R. M.; Tierney, D. L.; Ogawa, M. Y. *Biomacromol.* **2010**, *11*, 2602.

(135) Wang, C.-L.; Lan, C.-M.; Hong, S.-H.; Wang, Y.-F.; Pan, T.-Y.; Chang, C.-W.; Kuo, H.-H.; Kuo, M.-Y.; Diau, E. W.-G.; Lin, C.-Y. *Energy Environ. Sci.* **2012**, *5*, 6933.

(136) Alessio, E.; Casanova, M.; Zangrando, E.; Iengo, E. *Chem. Comm.* **2012**, *48*, 5112.

(137) Martinez-Diaz, M. V.; de la Torre, G.; Torres, T. *Chem. Comm.* **2010**, *46*, 7090.

(138) Beletskaya, I.; Tyurin, V. S.; Tsivadze, A. Y.; Guilard, R.; Stern, C. *Chem. Rev.* **2009**, *109*, 1659.

(139) Pietrangeli, D.; Ricciardi, G. *Tetrahedron Let.* **2011**, *52*, 1105.

(140) Imahori, H.; Umeyama, T.; Kurotobi, K.; Takano, Y. *Chem. Comm.* **2012**, *48*, 4032.

(141) Pereira, A. M. V. M.; Soares, A. R. M.; Hausmann, A.; Neves, M. G. P. M. S.; Tome, A. C.; Silva, A. M. S.; Cavaleiro, J. A. S.; Guldi, D. M.; Torres, T. *Phys. Chem. Chem. Phys.* **2011**, *13*, 11858.

(142) Pereira, A. M. V. M.; Hausmann, A.; Tomé, J. P. C.; Trukhina, O.; Urbani, M.; Neves, M. G. P. M. S.; Cavaleiro, J. A. S.; Guldi, D. M.; Torres, T. *Chem. Eur. J.* **2012**, *18*, 3210.

(143) Ngo, T. H.; Nastasi, F.; Puntoriero, F.; Campagna, S.; Dehaen, W.; Maes, W. *Eur. J. Org. Chem.* **2012**, *2012*, 5605.

(144) Panda, D. K.; Goodson, F. S.; Ray, S.; Lowell, R.; Saha, S. *Chem. Comm.* **2012**, *48*, 8775.

(145) Kan, J.; Chen, Y.; Gao, J.; Wan, L.; Lei, T.; Ma, P.; Jiang, J. *Mater. Chem.* **2012**, *22*, 15695.

(146) Milic, T. N.; Chi, N.; Yablon, D. G.; Flynn, G. W.; Batteas, J. D.; Drain, C. M. *Angew. Chem., Int. Ed.* **2002**, *41*, 2117.

(147) De Luca, G.; Romeo, A.; Villari, V.; Micali, N.; Foltran, I.; Foresti, E.; Lesci, I. G.; Roveri, N.; Zuccheri, T.; Scolaro, L. M. *J. Am. Chem. Soc.* **2009**, *131*, 6920.

(148) Teixeira, R.; Andrade, S. M.; Vaz Serra, V.; Paulo, P. M. R.; Sánchez-Coronilla, A.; Neves, M. G. P. M. S.; Cavaleiro, J. A. S.; Costa, S. M. B. *J. Phys. Chem. B* **2012**, *116*, 2396.

(149) Wakahara, T.; D'Angelo, P.; Miyazawa, K. i.; Nemoto, Y.; Ito, O.; Tanigaki, N.; Bradley, D. D. C.; Anthopoulos, T. D. *J. Am. Chem. Soc.* **2012**, *134*, 7204.

(150) Takai, A.; Chkounda, M.; Eggenspiller, A.; Gros, C. P.; Lachkar, M.; Barbe, J.-M.; Fukuzumi, S. *J. Am. Chem. Soc.* **2010**, *132*, 4477.

(151) Yang, Y.; Zhang, Y.-M.; Chen, Y.; Zhao, D.; Chen, J.-T.; Liu, Y. *Chem. Eur. J.* **2012**, *18*, 4208.

(152) Pagona, G.; Zervaki, G. E.; Sandanayaka, A. S. D.; Ito, O.; Charalambidis, G.; Hasobe, T.; Coutsolelos, A. G.; Tagmatarchis, N. *J. Phys. Chem. C* **2012**, *116*, 9439.

(153) Kim, D. *Multiporphyrin Arrays: Fundamentals and Applications*; Pan Stanford Publishing: Singapore, 2012.

(154) Sessler, J. L.; Karnas, E.; Sedenberg, E. In *Supramolecular Chemistry: From Molecules to Nanomaterials.*; Gale, P. A., Steed, J. W., Eds.; John Wiley & Sons: Hoboken, 2012.

CHAPTER 2

Asymmetric Porphyrins as Molecular Electronic Device Components

2.1 Introduction

The proposal that molecules can perform electronic functions in devices such as diodes, rectifiers, wires, capacitors, or serve as functional materials for electronic or magnetic memory, has stimulated intense research across physics, chemistry, and engineering for over 35 years. Because biology uses porphyrins and metalloporphyrins as catalysts, small molecule transporters, electrical conduits, and energy transducers in photosynthesis, porphyrins are an obvious class of molecules to investigate for molecular electronic functions. Of the numerous kinds of molecules under investigation for molecular electronics applications, porphyrins and their related macrocycles are also of particular interest because they are robust and their electronic properties can be tuned by the chelated metal ion and substituents on the macrocycle. The other porphyrinoids have equally variable and adjustable photophysical properties, thus photonic applications are potentiated as well. At least in the near term, realistic architectures for molecular electronics will require self-organization or nanoprinting on surfaces. This review concentrates on self-organized porphyrinoids as components of working electronic devices on electronically active substrates with particular emphasis on how the detailed electronic properties of single molecules are affected by surface, molecular design, orientation, and matrix.

Many current electronic technologies are rapidly approaching the limit of performance and miniaturization in a growing number of applications across science and technology because traditional inorganic materials and component architectures are optimized to the edges of the theoretical limits of performance. The majority of currently employed techniques for mass production of electronic devices involves amazingly expensive facilities with highly specialized

pieces of equipment, extreme conditions, expensive and often toxic materials, and is chemically and energetically wasteful at almost every production step. Additionally, most of the energy used to power these devices is lost as heat rather than used to perform intended functions, so there are additional production and energy costs needed to dissipate heat. A great motivation towards the development of molecular electronics is to increase performance while at the same time diminishing component size, reduce production costs, and minimize the environmental impacts of production and operation.[1] Flexible display and electronics technologies, and ink-jet printing of circuitry will also benefit from molecule based electronics.

Molecules, or collections of molecules, functioning as electronic components have ample precedent in nature. Voltage, ligand, antibiotic, and other ion conducting channels are digital electronics self-assembled into biological membranes in that they have only 'on' or 'off' positions with unit conductance that are unique to a given channel.[2] Photosynthetic reaction centers transport electrons over about eight nm with remarkable efficiency. Ion pumps can also be gated. The photo-driven purple membrane pumps containing bacteriorhodopsin have been studied for many decades in terms of their potential as molecular electronic and photonic materials because they are very robust, can cycle many thousands of times, and the distinctive color changes impart a second functionality to these materials.[3,4] However, the rate of conducting ions in channels and bacteriorhodopsin proteins, and the stability of the former, limit the usefulness of these constructs as components of complex electronic devices. The various photosynthetic systems can provide much inspiration, but are too fragile for real-world applications.

The field of molecular electronics focuses on the molecule, but melds concepts from diverse fields such as: physics, chemistry, biophysics, and electrical engineering. See several

recent reviews that focus on different aspects of molecular electronics ranging from surface chemistry to molecular design, to theory, including a beautiful discussion of mechanical bonds with molecular electronics applications by Stoddart.[5-9] Electronics fabricated from organic materials are potentially much less toxic, easier to recycle, and scalable. In addition, molecular electronics have the potential to contribute to the continuation of Moore's law in the miniaturization of electronic components; pending the further development of bottom up nanofabrication techniques suitable for mass production. In general, classic Coulombic charging, the relative spacing of the highest occupied molecular orbital (HOMO) and lowest unoccupied molecular orbital (LUMO), the spin, and the vibrational modes will determine single electron currents through molecules connected to electrodes with tunneling barriers.[10] Thus, the reversibility of accessible redox states of a molecules are important, e.g. in single molecule transistors.[10] In the case of conducting polymers, the conductance is dependent on the structure and conjugation of the molecular system and the length, but a recent study shows that the mechanical characteristics and topology of a polyfluorene are also important. Pulling the polymer from a gold surface with an STM tip allows about a 20 nm change in length whereupon the conductance curves show a exponential decay with increasing length and oscillations that correspond to a each monomer unit detaching from the surface.[11] The molecular electronic properties are also dependent on the matrix surrounding the molecule and the domain size (number of copies of a molecule in a discrete domain). Image charges generated in the source and the drain can result in the localization of charges in molecules such as conjugated phenyls,[10] or in ensembled domains, until a critical charge density is reached whereupon the transistor switches.

The use of porphyrins in molecular electronics largely came about from the formation of liquid crystalline films and attachment of the molecules to surfaces in the form of the now ubiquitous self-assembled monolayer (SAM).[12-14] It was noted early on that thiols create well ordered structures on gold substrates, and similarly a variety of porphyrins have been bound to gold as SAMs.[15-21] Numerous patterns and arrangements of single molecules and supramolecular assemblies have been reported.[22] Many of the early SAMs were created as Langmuir Blodgett films, and later were fabricated by dipping the substrate into a solution containing the thiol for extended periods of time. Extensive techniques have been developed to fabricate and characterize these assemblies, especially ultrahigh vacuum techniques that allows layers to be patterned with nanoscale precision.[23] Assembly approaches can be further extended by the use of nanopatterning, via techniques such as scanning probe lithography.[13,24,25] In our own work, we have recently shown that porphyrin assemblies may be patterned on Au surfaces using nanografting. In nanografting, an AFM tip is used to displace surface bound matrix molecules (typically an alkanethiol) in a background solution of the molecule of interest. During this process, the molecule of interest, a porphyrin appended with a thiol, then bonds within the open surface region created by the removal of the matrix molecules.[26] Using scanning probe lithography, thiol tethered porphyrin assemblies with features down to *ca.* 10 nm in dimension (Figure 2-1) can be fabricated to create well defined nanostructures on surfaces.

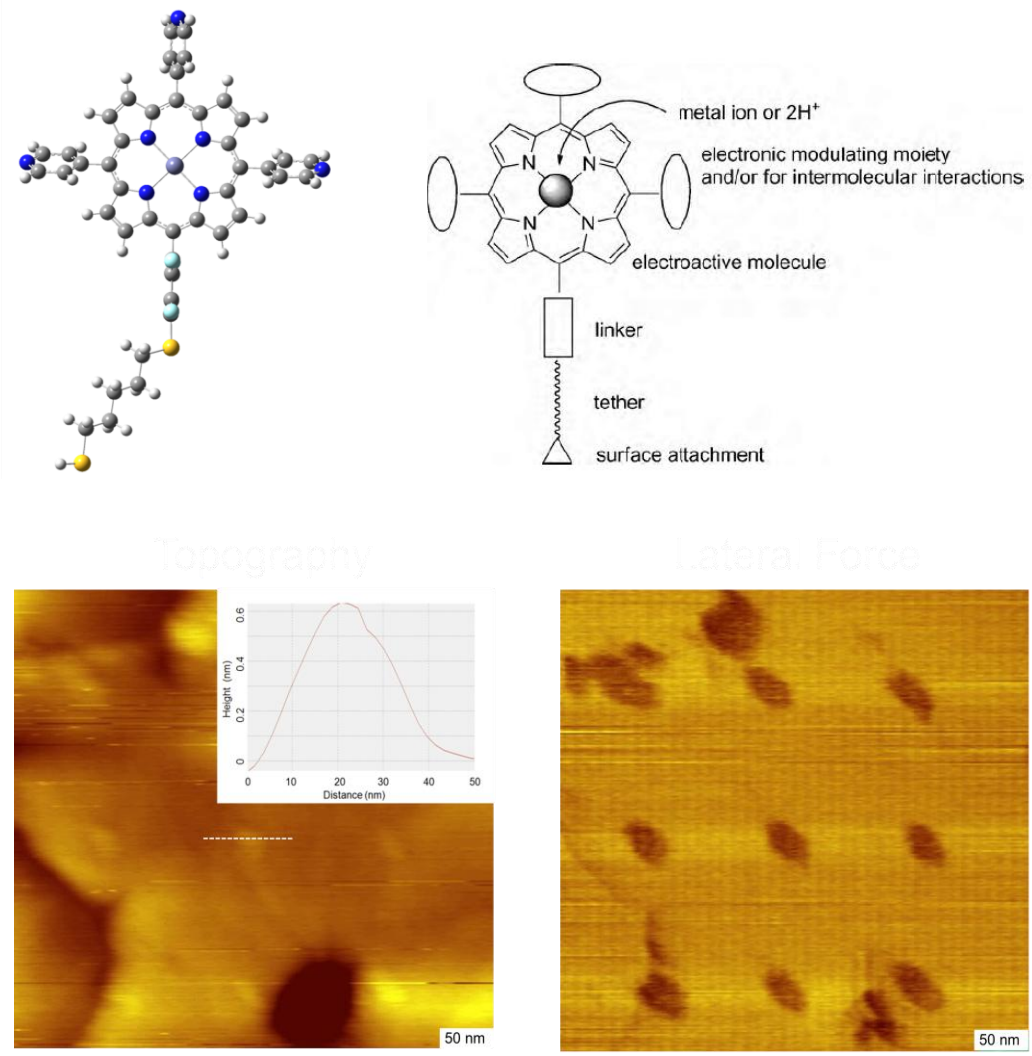

Figure 2-1. Top: calculated structure of a tripyridylporphyrin with an alkanethiol tether. The fluorous phenyl group allows rapid addition of the α-Ω thiols. The chromophore, linker, tether, and exocyclic motifs modulate self-assembly and self-organization. Bottom: A 3x3 array of nanografted islands of a zinc porphyrinthiol (top) patterned in a background matrix of dodecanethiol. The feature size illustrated here is *ca.* 20 nm (FWHM) as determined from the topographic image (left). The porphyrins are found to be protruding above the dodecanethiol matrix by *ca.* 0.6 nm. The friction image (right) more clearly shows the patterned array. (Batteas and coworkers, unpublished results).

There are several modes of porphyrin attachments to gold surfaces depending on the location and size of the linker moieties and attachment groups. For example, Perrine et al, attached thiols directly to the porphyin macrocycle on either opposing pyrrole β positions or on opposing meso positions, therefore coupled to different macrocycle molecular orbitals.[27]

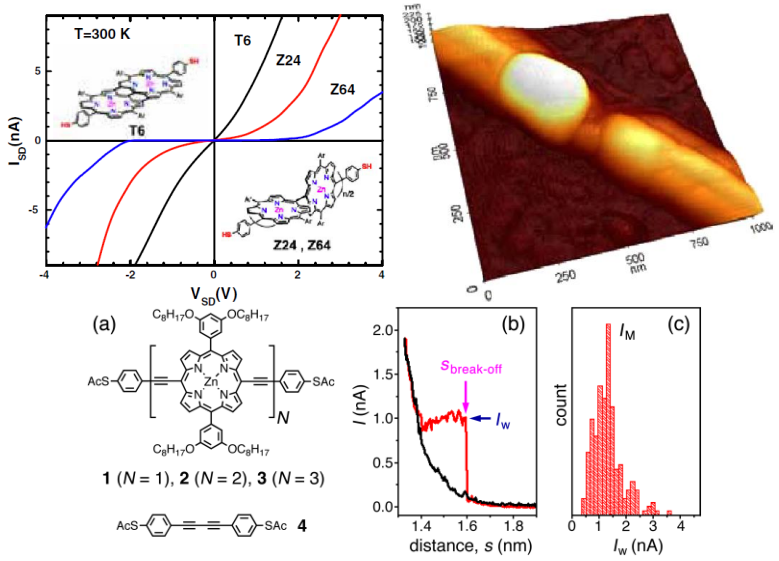

Figure 2-2. Top: Electrical properties of directly linked porphyrin wires across Au nanoelectrodes with spacing of less than 5 nm were prepared using an electromigration-induced break-junction technique (Kang, Materials Science and Engineering C 26 (2006) 1023 – 1027). Bottom: an acetylene-linked porphyrin construct has been studied to look at distance dependence on the conductivity.

This geometry allows the cofacial deposition of the porphyrin with the π-system remarkably close to the Au surface with reasonable reliability (Figure 2-3). Porphyrin oligomers terminated on either end with thiols allow them to bridge, between gold electrodes, and I-V plots show that the fused systems show markedly different electric properties than similar oligomers

directly connected via meso positions (Figure 2-2).[28] Cycling of these electrodes however, indicated that the porprhyrins may be aggregating due to mobility or lability of the Au-S bonds. Similar constructs with multimers of acetylene-bridged zinc porphyrins using phenylacetylene tethers on each end bridged between gold electrodes showed that the conductance is not linearly dependent on the distance (Figure 2-2).[29] A theoretical approach indicated that a porphyrin bearing eight thiols, two on each pyrrole, may bridge between four gold electrodes to serve as a photo gated current router, but construction of this type of device will be problematic.[30]

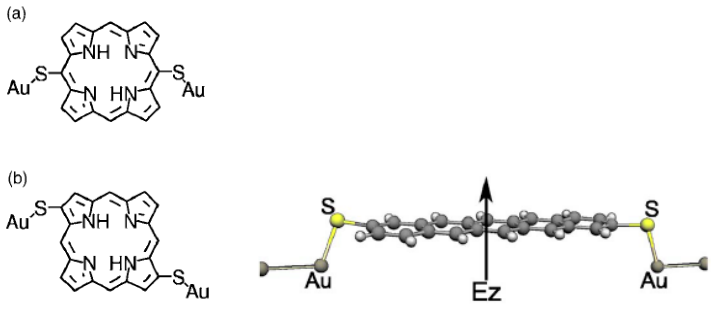

Figure 2-3. Perrine et al. demonstrated cofacial deposition of porphyrins on Au surfaces with thiols directly attached to the porphyrin.

The free base and the Co(II) tetra phenylporphyrins with thiols on the 4-positions on opposing meso positions (5,15 in Figure 1) can be attached to gold nanowires. In this case the metalloporphyrin served as a memory bit wherein the charge was located as the Co(II/III) couple, which then alters the conductance of the nanowire. The free base exhibited no memory effects.[31] In all of the constructs with thiols the facile formation of the disulfides, in the presence of oxygen or from electrode generated redox processes, can complicate the formation of the

material and interpretation of the data. Also, the mobility and lability of the S-Au bond must be considered.

Table 2-1.	**Surface Attachment Chemistry**	
Structure/surface	Comments, and surface bond energies[6]	Recent examples
Por-tether-S-/gold	Migration and lability of S-Au bond can be used to form islands of electroactive molecules and can present issues for preparing useful devices. Surface bond energy ~1.9eV	[15-21]
Por-tether-CH=CH-/Si(100) Por-tether-CH_2-/Si(100)	This bond is less labile, surface bond energy ~3.7 eV.	[32]
Por-tether-O-/Si(100)	Surface bond energy ~3.7 eV	[33]
Adsorption	Surface bond energy <0.5 eV	[24,34-38]

2.2 Attachment Chemistry

The use of a single alkylthiol tether can also be used to implant these molecules into a background matrix, allowing for the investigation of single molecules as well as assemblies of these molecules to be investigated by techniques such as scanning tunneling microscopy (Figure 2-1). Beyond metal surfaces, attachment to semi-conducting and oxide surface can be accomplished via a range of addition reactions. These have different surface bond energies (Table 1). In each of these cases the first key issue surrounding this approach to device fabrication includes understanding the attachment chemistry required to organize the molecular components on surfaces and the role of these bonds in electronic coupling. The implementation

of strategies which link molecular components directly to semiconductors such as Si have a significant advantage in light of the extensive technologies and fabrication methods already developed for Si in the existing semiconductor industry. To this end, several groups are investigating the interactions of small organics with Si surfaces, and are remolding our views of traditional organic chemistry by establishing reaction mechanisms of small organics on semiconductor surfaces.[39-41] Recent work has also shown that porphyrin films can be attached to Si surfaces via Si-O linkages,[33] and that these molecular monolayers are very robust under elevated temperatures, maintaining their electroactivity, thus making them reasonable candidates for device fabrication.[42] Other linking chemistries, including use of chlorosilanes[43] and phosphates[44] can be used for the formation of self-assembled monolayers (SAMs) on oxide surfaces. Additionally, direct attachment to H-terminated Si can be accomplished through the use of alkyne and hydroxyl groups to form Si-C and Si-O bonds.[45,46] Absent from this body of work however are the details of how the film quality (i.e. defect density and local aggregate dimension) impact performance, as well as how the specifics of the electronic structure, packing geometry and coupling group exert influences on the charge transport behavior of the system.

Our groups are interested in designing components for electronics using a porphyrin core system as shown in Figure 2-1. Specifically, we have designed a free-base porphyrin macrocycle bearing three 4-pyridyl moieties and one pentafluorophenyl substituent in the meso positions as a core platform for the rapid, high yield attachment of tethers that can be tailored to both the surface chemistry and other design criteria. In this case the pentafluorophenyl moiety serves as a "universal" linker to which a variety of nucleophiles can be appended via replacement of the 4-fluoro group. The pyridyl motifs allow design of intermolecular interactions to yield hierarchically organized monolayers or can provide a convenient attachment point for additional

molecules via metal-ligand coordination chemistry. Initial studies used a terminal dithioalkane to yield a derivative for immobilization onto a gold surface via strong sulfur-gold chemisorption. Moreover, by controlling the extent of fluorination of linker group, the phenyl moiety can be used as an internal barrier to control the tunneling between the macrocycle and the thiol tether. This barrier can be modulated by systematic variation of the number and position of the fluoro groups on the ring, thus affording some control of the relative orbital energies of this phenyl group and the degree of steric interactions between the 2,6-positions on this phenyl group with the pyrrole β-hydrogens. Thus, control of these interactions provides a means to dictate the electronic coupling between the macrocycle and the tether.

To optimize our ability to investigate these molecules either individually or as small monolayer aggregates (about 6 nm in dimension), we have characterized SAMs of these porphyrin based molecules with thiol linkers mixed into a pre-assembled dodecanethiol matrix.[21] These insertion based experiments afford the means of orienting molecules at the surface by covering the surface with a protective capping group first (in this case a simple alkanethiol). Assemblies of such molecules on clean open metal surfaces show that they will frequently lay down on the surface as described above, driven by the strong interaction between the π system and the metal Au terraces. In characterizing the free-base and zinc porphyrin derivatives, it was found that the molecule inserts on edges of the substrate and into defects in the pre-assembled dodecanethiol SAM. The free base analogue tends to insert as single molecules and small monolayer domains dispersed within the background SAM, whereas the zinc metalated derivative has a much higher proclivity for aggregation thereby creating larger domains that are approximately 10 nm in width on average. These large domains of the metalloporphyrin afford interesting electronic properties that are not seen in the small clusters or free base analogue.

2.3 Devices

In many molecular electronic devices, efficient charge separation and charge stability is essential. Photo initiated charge transfer reactions of porphyrins have been extensively studied and many form long lived charge separate states; when combined with excellent charge carrier mobilities these systems are prime candidates for molecular electronic applications.[47-49] Photo initiated charge injection from porphyrins into semiconducting surfaces has been studied in the context of solar energy devices and the interfacial electron transfer rates of charge injection are generally less than a ps.[50,51] Much work is being done in the design of new molecules capable of forming long lived charge separated states based on the distinct electronic states of porphyrinoids that enable functions such as current routers, gates and field effect transistors.[19,30,52-57] Linear gates and T gates have been fabricated and can be controlled by porphyrin redox chemistry as well as photochemistry.[58,59] Recent studies have also demonstrated that porphyrins on surfaces display stochastic switching.[21] Recently we have found that by forming nanoscale assemblies of porphyrins similar to those in Figure 2-1, stable Coulomb islands can be formed as evidenced by the appearance of a Coulomb staircase in the I-V measurements (unpublished results).

Derivatives of the generic molecule shown in Figure 2-1 have shown promise to serve as molecular capacitors and single electron tunneling devices in which small islands are assembled within electrode gaps and their charge state tuned using a gate voltage. In one example, we investigated the transport properties of zinc metalloporphyrin islands inserted into a dodecanethiol matrix on Au(111). Using scanning tunneling microscopy (STM), it was shown that the zinc porphyrin islands exhibited bias dependent switching at high surface coverage, where the conductance of the molecules increased when sweeping above the threshold voltage and the islands returned to a lower conductance state when the tip was swept to the negative bias.

This switching behavior at high coverage was found to result from the formation of Coulomb islands driven by enhanced aggregation of the macrocycles and zinc metal centers. Low temperature measurements (~4 K) from crossed-wire junctions verified the appearance of a

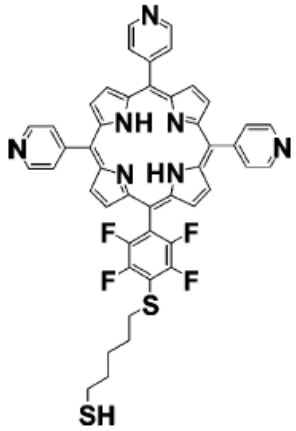

Figure 2-4. Tethered porphyrin

Coulomb staircase and blockade for only aggregates of the zinc porphyrins. In other examples, free base porphyrins in nanogap electrodes (formed as break junctions) have been reported to act as Coulomb islands.[60-62] Wakayama *et al.* observed Coulomb blockade staircases in the I-V measurements of these systems and also showed that the threshold voltages were sensitive to changes in the intermolecular interactions.[63-65] Overall, it has been shown that intermolecular interactions such as aggregation play a significant role in the electronic properties of porphyrin molecules. These aggregates readily show the ability to stabilize charge and this affords a means of creating bias switchable devices.

2.4 Next Generation Molecules

In previous work, the design principle exploited the substitution chemistry of perfluorophenyl groups to rapidly append the tether and the attachment groups in one step using α-Ω thiols (Figure 2-4). In order to probe the mechanism of molecular conductance and the role of self-organized domains in switching for the tethered porphyrin in Figure 2-1, we synthesized a series of molecules to assess the contributions of the different parts of the molecule, specifically the linker on conductance and the roles of the pyridyl groups in self-assembly. These molecules have been sent to the Batteas group at Texas A&M University where they are still under.

Synthetic methodologies for the production of various tethered porphyins are reported below. The tri-pyridyl derivative with a fluorous phenyl linker demonstrated interesting properties when bound to a gold monolayer as discussed above. To investigate the effect of the fluorous phenyl linker we synthesized a tri-pyridyl derivative with a phenyl linker (Figure 2-5, free base **7** and zinc **7**). Similarly, to investigate the contribution of the pyridyl groups, we synthesized tri-phenyl analogues with a fluorous linker (free base **10** and zinc 10). ^{1}H and ^{13}C NMR spectra were recorded in a Bruker 500MHz spectrometer. Electrospray ionization mass spectrometric analyses were performed at the CUNY Mass Spectrometry Facility at Hunter College using an Agilent Technologies HP-1100 LCMSD instrument. The electrospray ionization was run in methanol or dichloromethane with 0.1% formic acid. Uv-Visible spectra were recorded on a Varian Bio3 spectrophotometer. All reagents were obtained form commercial sources and used without further purification. Flash column chromatography was performed using silica gel-60 and the analytical TLC was carried out on precoated sheets with silica gel (0.2mm thick), both from Sorbent Technologies.

The synthesis of **7** and the zinc metalo derivative turned out to be more complex than we anticipated. Therefore, we used the Pummerer rearrangement to deprotect a thiomethyl group on the porphyrin. Other synthetic strategies included treatment with acid and/or base to remove terminal methyl, separate synthesis of a 1-bromo, 5-thiopentane tether, and numerous treatments to break up dithiols. None of these techniques were successful. For the pyridyl derivatives, solubility of the metallocomplexes is less than the free bases because of intermolecular

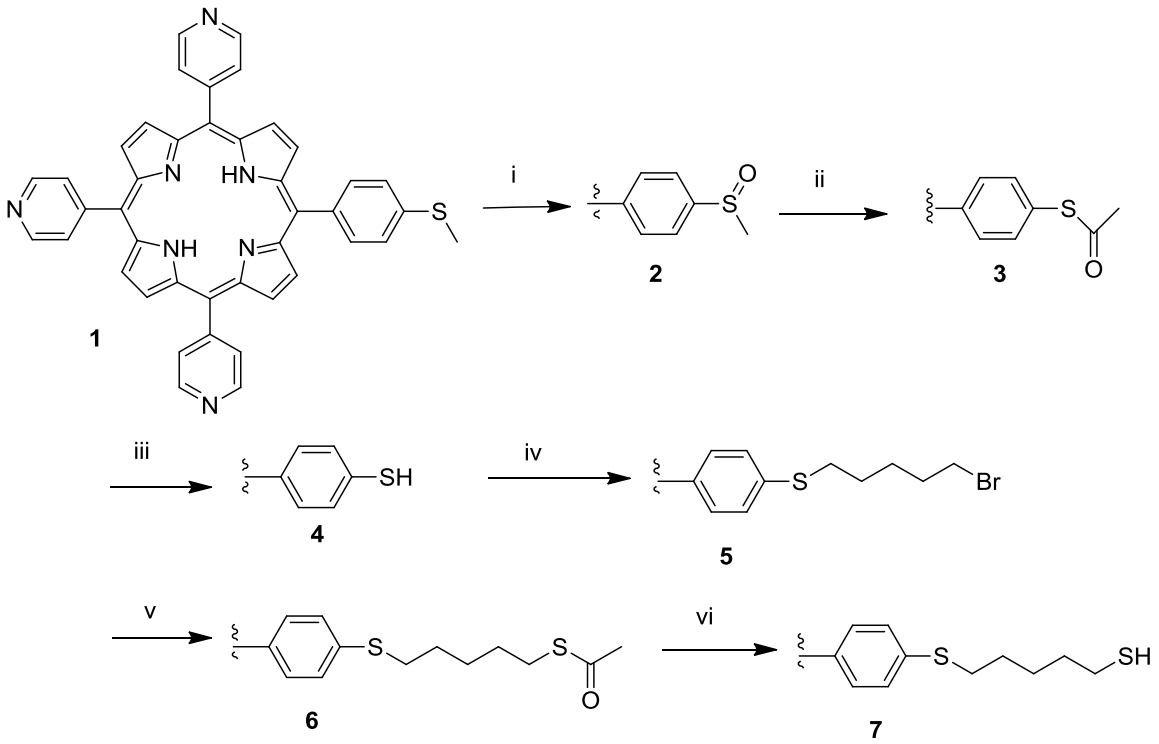

Figure 2-5. Synthetic scheme for alkyl tethered tripyridyl porphyrin with phenyl linker. (i) MCPBA, (ii) acetic anhydride reflux, (iii) ammonium hydroxide, (iv) 1,5 dibromopentane, (v) potassium thioacetate, (vi) sodium methoxide.

coordination of the pyridyl groups to the axial positions of the Zn(II) center. Small amounts of a solvent that competes for the axial sites (THF, pyridine) mitigate this problem.

2.5 Synthetic Details

*5,10,15-tris(4-pyridyl)-20-(4-methylthiophenyl)porphyrin (TPy3PSMe; **1**)*

To a mixture of propionic acid (0.8 L) and nitrobenzene (4 mL) was added 4-methylthiobenzaldehyde (15.38 mmol, 2 mL) and 4-pyridine carboxaldehyde (46.15 mmol, 4.32 mL) with stirring. The mixture was heated to ~ 100 C and pyrrole (61.52 mmol, 4.26 mL) was added slowly. The reaction was refluxed for 3 hours and allowed to cool. 300 mL silica gel was added to the reaction flask and the propionic acid was evaporated. The silica gel was washed with dichloromethane and acetone until no more color eluted. The solution was evaporated to 100 mL and washed with sodium bicarbonate and water, dried over anhydrous sodium sulfate and evaporated to dryness. The organic layer was then recrystallized from hexanes to yield a purple powder. The porphyrin mixture was filtered, dissolved in dichloromethane, loaded onto a 600 mL silica gel column and separated with an eluent of 4:3 toluene : ethyl acetate. The fifth of the six bands was collected and evaporated to yield 2.32 mmol (13% yield) of product **1**. This yields a statistical mixture of six compounds weighted by the reactivity of the aldehydes and the stoichiometry.

*5,10,15-tris(4-pyridyl)-20-(4-methylsulfinylphenyl)porphyrin (Tpy3PSOMe;**2**)*

To a stirring solution of dichloromethane 0°C (500 mL) was added **1** (2.32 mmol, 1.54g). To this stirring mixture MCPBA solution in dichloromethane (2.21 mmol, 0.5091 g) was added drop-wise. The reaction was stirred for 2 hours and allowed to warm to room temperature. The

reaction mixture was reduced to 50 mL, washed with sodium bicarbonate and water, dried over sodium sulfate, and evaporated to dryness.

*5,10,15-tris(4-pyridyl)-20-(4-thioacetylphenyl)porphyrin (TPy3PSAc;**3**)*

To acetic anhydride (100 mL) was added **2** (2.2 mmol, 1.5 g) and refluxed for 3 hours. The mixture was cooled with ice and washed with water, dilute sodium bicarbonate solution, extracted with dichloromethane, and then washed with water again, and dried over sodium sulfate and evaporated to dryness.

*5,10,15-tris(4-pyridyl)-20-(4-thiophenyl)porphyrin (TPy3PSH;**4**)*

To a mixture of dichloromethane:THF:methanol:water:ammonium hydroxide (20:100:65:100:5) was added **3** (2.0 mmol, 1.5 g) dissolved in a minimum volume of dichloromethane. The reaction was stirred for four days at room temperature. The mixture was extracted into chloroform with pH adjusted to less than 7 by addition of acetic acid, washed with water, dried over sodium sulfate, and evaporated to dryness. The product was dissolved in chloroform and loaded onto a 500 mL silica column. The starting material was eluted and recovered first with a 6:1:2 mixture of ethyl acetate: methanol: toluene. Product **4** and its disulfide analogue were then eluted with 93:2:5 chloroform:acetic acid:methanol. Both bands were collected and solvents evaporated.

*5,10,15-tris(4-pyridyl)-20-(4-(1'-thio 5'-bromopentyl)-phenyl)porphyrin (TPy3PSBr;**5**)*

To stirring dry THF (30 mL) was added **4** (0.02 mmol, 31mg). To the stirring solution fresh dithiothreotol (3.686 mg, 1.1 eq.) was added to assure that the free thiol is presents rather

than the disulfide. The mixture was refluxed for 4 hours. The reaction mixture was then cooled to room temperature and 20 mg of potassium carbonate was added. Immediately 1,5 dibromopentane (0.60 mol, 0.1 mL) was added drop wise with stirring and the reaction was stirred at room temperature for 5 days. The solution was washed with water, extracted into dichloromethane, which was dried over sodium sulfate and evaporated to dryness. The crude product was purified by column chromatography to remove starting materials to yield 22 mg of the product (57%).

*5,10,15-tris(4-pyridyl)-20-(4-(5'-thioacetylpentylmercaptyl)-phenyl)porphyrin (Tpy3PSSAc;**6**)*

To freshly distilled DMF (12 mL) was added **5** (0.125 mmol, 100 mg) and solution was degassed for 10 minutes. To the solution was added potassium thioacetate (0.1877 mmol, 21.4 mg). The reaction was refluxed 5 minutes to dissolve all materials and stirred for 3 days at room temperature. The reaction was washed 3 times with ice water, dried over sodium sulfate, the solvent was evaporated. The crude product was re-crystallized from hexanes to yield 68 mg **6** (69% yield).

*5,10,15-tris(4-pyridyl)-20-(4-(1',5'-dithiopentyl)-phenyl)porphyrin (TPy3PSS;**7**)*

To a solution of dichloromethane:methanol (1:1, 5 mL) was added 6 (0.08572 mmol, 68 mg). Sodium methoxide in methanol solution (0.5 M, 0.1714 mmol, 0.342 mL) was added dropwise and the mixture was stirred for 48 hours. The mixture was washed with water, extracted into chloroform, dried over sodium sulfate and evaporated to dryness. The crude product was re-crystallized from hexanes to yield 55 mg pure 9 (85% yield).

UV-vis (CH_2Cl_2): 428.67, 522.81, 562.57, 594.32, 652.88 ^{1}H NMR ($CDCl_3$): δ 9.00 (d 3.8 hz, 9H, 2,6 pyridyl), 8.92 (d 4.1 hz, 2H, β pyrrole), 8.31 (s, 4H, β pyrrole), 8.80 (d 4.1 hz, 2H, β pyrrole), 8.11 (d 7.7 hz, 6H, 3,5 pyridyl), 8.07 (d 7.7 hz, 2H, 3,5 phenyl), 7.66 (d 7.7 hz, 2H, 2,6 phenyl), 7.25 ($CDCl_3$), 5.29 (CH_2Cl_2), 3.204 (t 7.1 hz, 2H, CH_2), 2.815 (t 7.2 hz, 2H, CH_2), 1.87-1.93 (m, 5H, CH_2), 1.73 (m, 3H, CH_2), 0.00 (TMS) ^{13} C NMR ($CDCl_3$): 149.97, 149.92, 148.42, 148.38, 138.64, 137.58, 134.96, 129.36, 126.4, 121.05, 117.49, 117.13, 38.87, 33.13, 28.87, 27.83 ESI MS: found 752.2621 (1.2 ppm)

5,10,15-tris(4-pyridyl)-20-(4-(1',5'-dithiopentyl)-phenyl)porphyrinato zinc (II) (Zn TPy3PSS; ***8****)*

The Zn derivative starts from compound **7**. To stirring distilled stabilized chloroform (5 mL) was added **7** (0.0363 mmol, 27.5 mg). To stirring methanol (5mL) was added zinc acetate dihydrate (0.290 mmol, 63.7 mg). The methanol solution was added to the **7** in chloroform and the mixture was refluxed for 2 hours. The mixture was washed with water, extracted into dichloromethane and 1% pyridine, dried over sodium sulfate, and evaporated to dry to yield mg 17 product and its corresponding disulfide (57% yield). UV-vis (CH_2Cl_2): 426.38, 561.3, 602.3 ^{1}H NMR ($CDCl_3$:Pyridine-d (1:1)): δ 8.98 (d), 8.91 (d), 8.87 (m), 8.58 (s), 8.09 (m), 7.65 (d), 7.60 (s), 7.50 (s), 7.21 ($CDCl_3$), 3.96 (bs), 3.17 (t, 2H, CH_2), 2.80 (t, 2H, CH_2), 1.83 (m, 4H, CH_2), 1.26 (bs, 2H, CH_2) 0.00 (TMS) ^{13} C NMR ($CDCl_3$:Pyridine-d (1:1)): 149.96, 149.93, 149.14, 148.49, 148.42, 148.29, 148.07, 147.92, 147.86, 147.71, 146.69, 146.59, 138.83, 135.43, 134.54, 134.34, 134.25, 134.05, 133.85, 133.7, 131.34, 130.49, 130.38, 130.11, 128.28, 128.25, 124.98, 122.37, 122.12, 122.03, 121.83, 121.63, 120.08, 116.63, 116.33, 116.29, 37.48, 31.88, 27.54, 27.49, 26.42, 121.6(pyr), 121.8(pyr), 122.0(pyr), 133.8(pyr), 134.0(pyr), 134.2(pyr), 147.8(pyr), 148.0(pyr), 148.2(pyr) ESI MS: found 813.1699 (1.5 ppm)

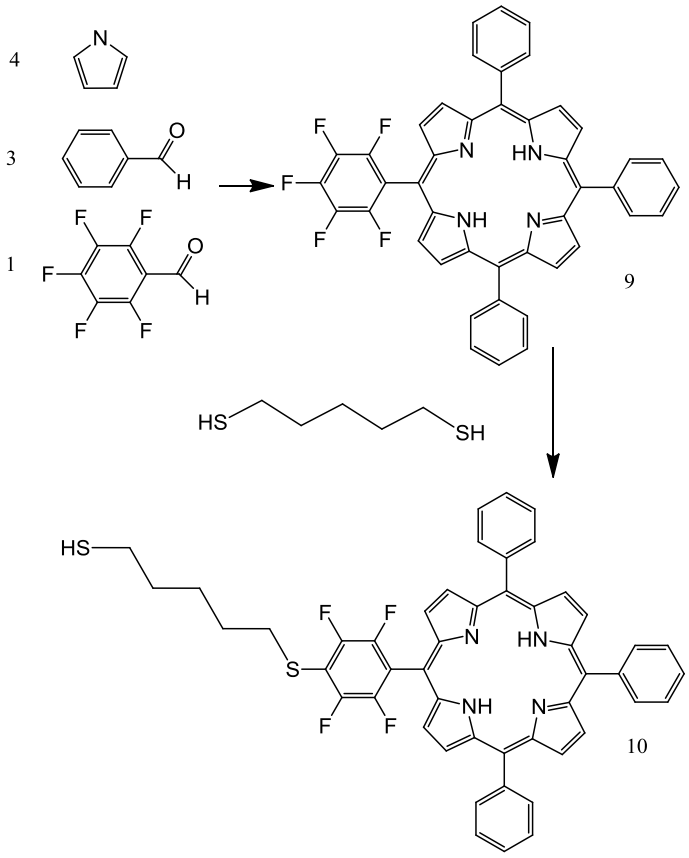

Figure 2-6. Synthesis of the phenylporphyrin starts from the statistical synthesis of six compounds weighted by the thermodynamics of the reaction and the stoichiometry. Substitution of the para fluoro group often proceeds at very high yields.

*5,10,15-tripheynl-20-(2,3,4,5,6-pentafluorophenyl)porphyrin (TPh3Pf;**9**)*

To a mixture of propionic acid (0.6 L) and nitrobenzene (6 mL) was added benzaldehyde (21.34 mmol, 2.17 mL) and pentafluorobenzaldehyde (7.0 mmol, 0.875 mL) with stirring. Mixture was heated to ~ 100 ºC and pyrrole (28.3 mmol, 1.94 mL) was added slowly. The reaction was refluxed for 3 hours, in the dark, and allowed to cool. 300 mL silica was added to the reaction flask and the propionic acid was evaporated. The silica gel was washed with dichloromethane and acetone until no more color eluted. The solution was evaporated to 100 mL

and washed with sodium bicarbonate and water, dried over anhydrous sodium sulfate and evaporated to dryness. The organic layer was then recrystallized from hexanes to yield a purple powder. The porphyrin mixture was filtered, dissolved in dichloromethane, loaded onto a 600 mL silica gel column and separated with an eluent of 30:70 toluene:petroleum ether (v/v). The fifth of the six bands was collected, evaporated and recrystallized from hexanes to yield 228 mg (0.323 mmol, 4.57% yield) of product **9**.

*5,10,15-triphenyl-20-(4-(1',5'-dithio)-2,3,5,6-tetrafluorophenyl)porphyrin (TPh3PfSS;**10**)*

To stirring dry DMF (25 mL) was added **9** (228 mg, 0.323 mmol) under nitrogen atmosphere. To the stirring solution 1,5-pentane-dithiol (0.3472 mL, 2.59 mmol using 8 equivalents) was added followed by diisopropylethylamine (1 mL, 5.18 mmol). The mixture was stirred at room temperature for 24 hours. The reaction mixture was then cooled to room temperature, washed with water, extracted into dichloromethane, dried over sodium sulfate and evaporated to dry under reduced pressure. The crude product was purified by column chromatography to remove starting materials and recrystallized from hexanes to yield 204mg of product **2** (yield 90.79%)

*5,10,15-triphenyl-20-(4-(1',5'-dithio)-2,3,5,6-tetrafluorophenyl)porphyrinato zinc (II) (ZnTPh3PfSS;Zn**10**);*

To stirring chloroform (3.33 mL) was added **2** (0.037 mmol, 0.030 g). To stirring methanol (0.55 mL) was added zinc acetate dihydrate (292 mmol, 0.064 g, 8 eq). The methanol solution was added to the **2** in chloroform and the mixture was refluxed for 3 hours. The mixture

was washed with water, extracted into dichloromethane, dried over sodium sulfate, and evaporated to dry to yield 22 mg product and its corresponding disulfide (73.33% yield).

NMR (500 MHz, $CDCl_3$)) 8.964 (t, *J*), 8H, exterior pyrrole; 8.212 (s *J*), 6H, ortho phenyl; 7.771 (m, *J*), 9H, meta and para phenyl; 3.276 (t, *J*), 2H, thiol (closest to phenyl); 1.779 (m, *J*), 8H, last H's of thiol

2.6 Characterization

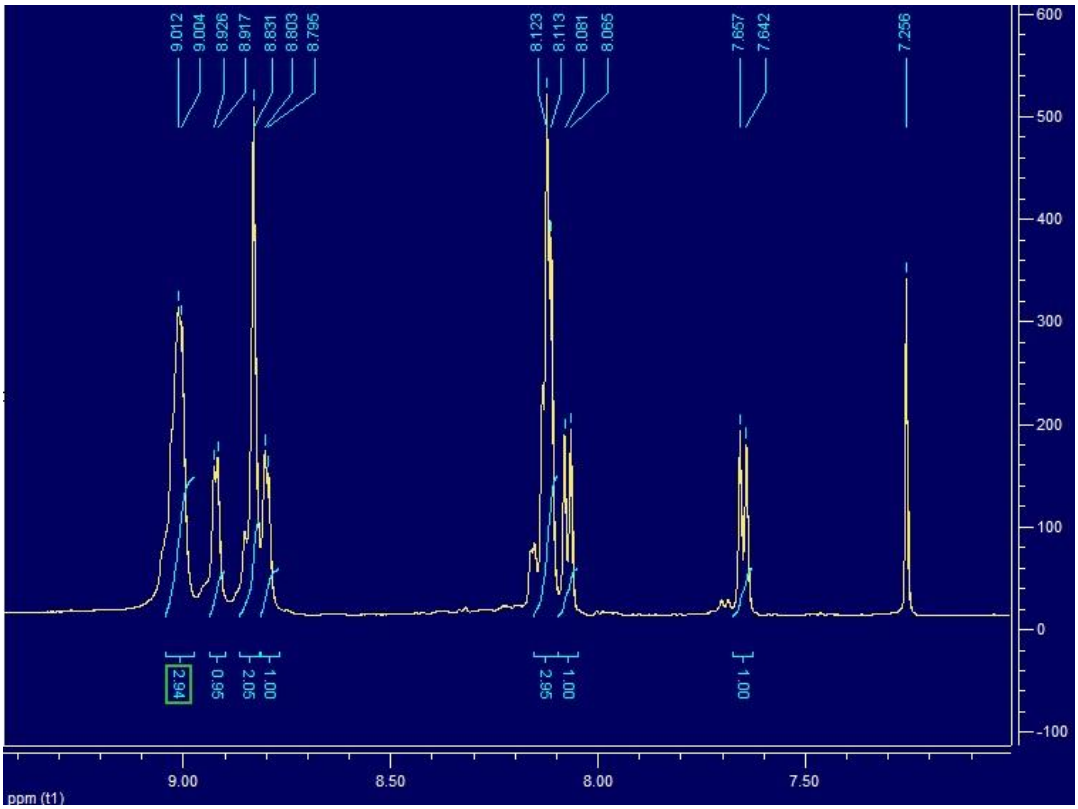

Figure 2-7. Aromatic NMR region of **7.**

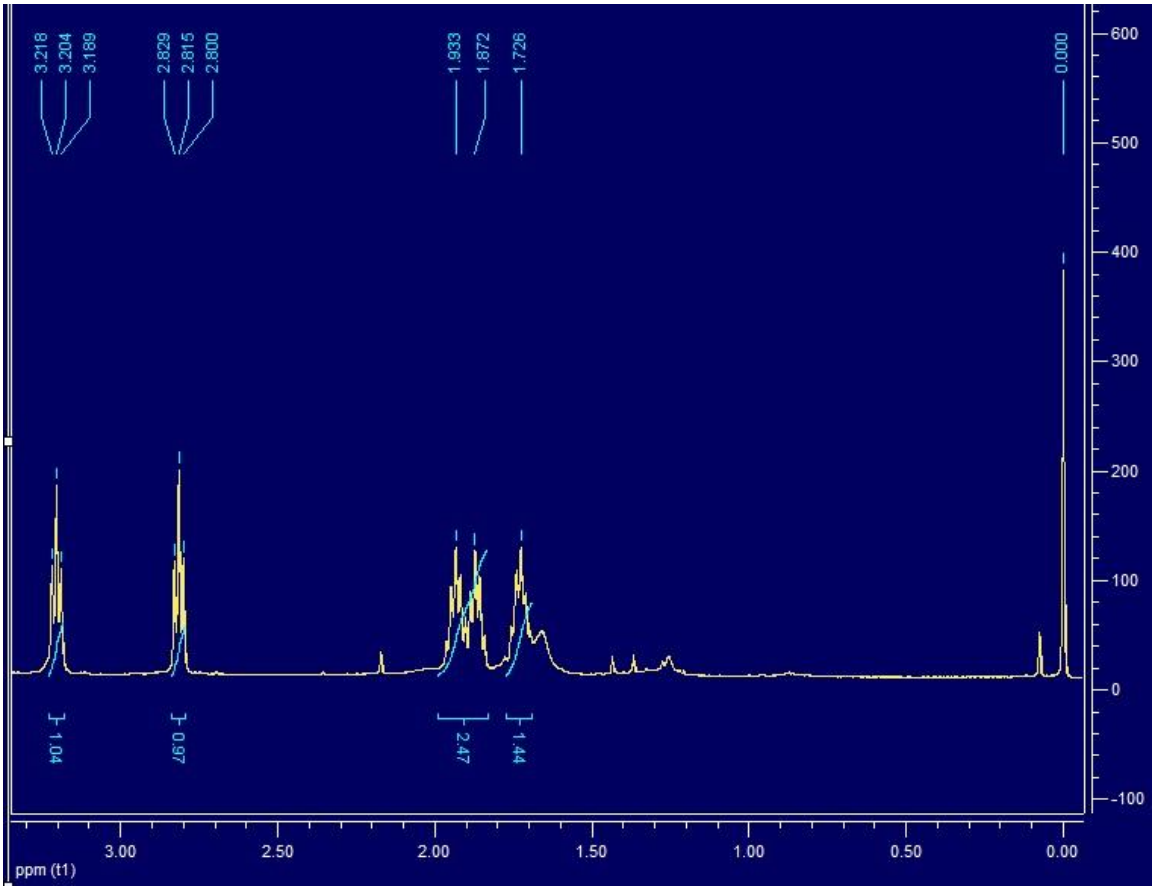

Figure 2-8. Aliphatic NMR region of **7.**

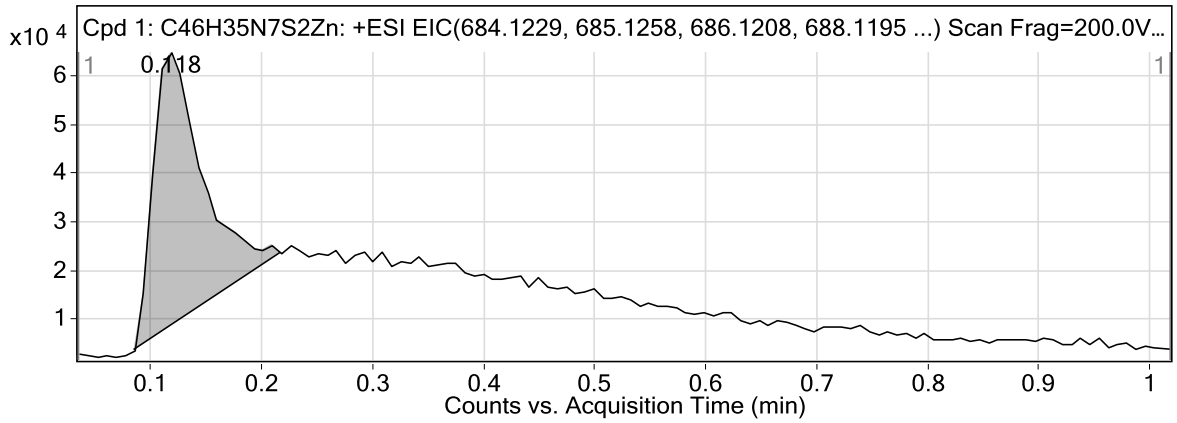

Figure 2-9. ESI/MS of **8.** Calculated M/Z 813.1687, found M/Z 813.1699

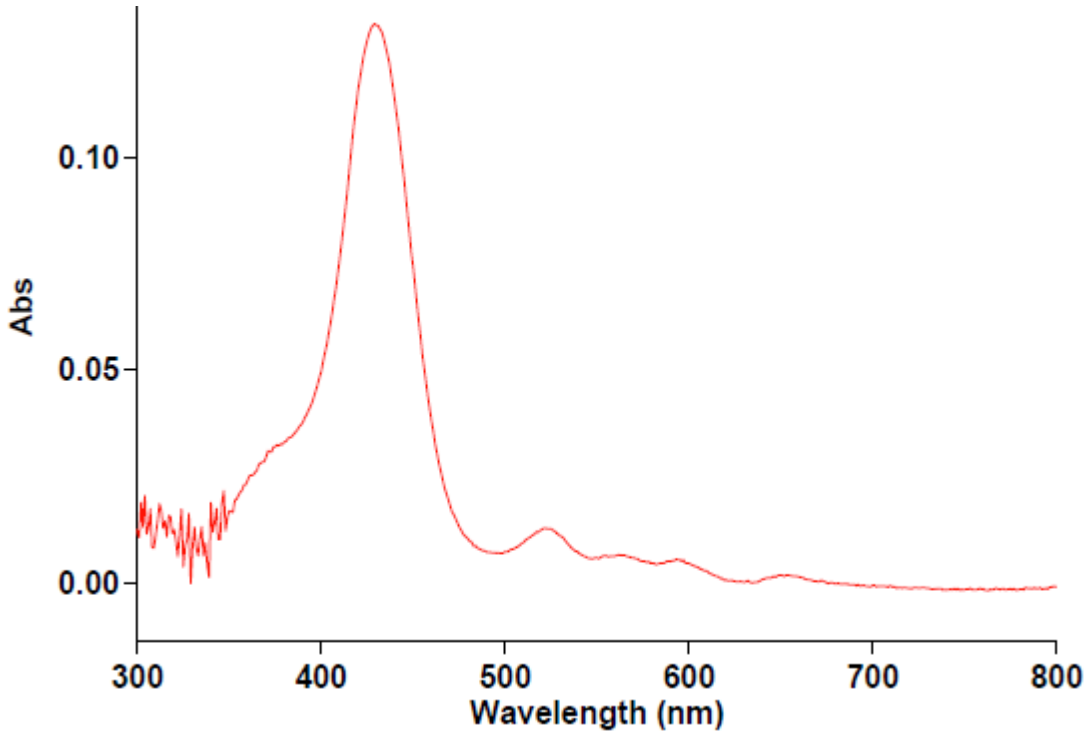

Figure 2-10. UV-Visible absorption spectrum of **7.**

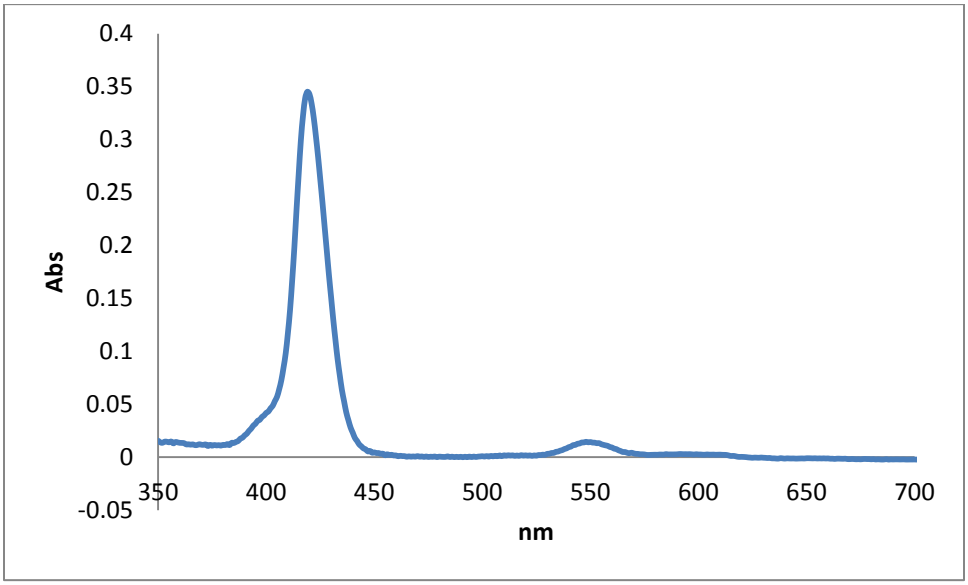

Figure 2-11. UV-Visible absorption of **Zn10** in DCM.

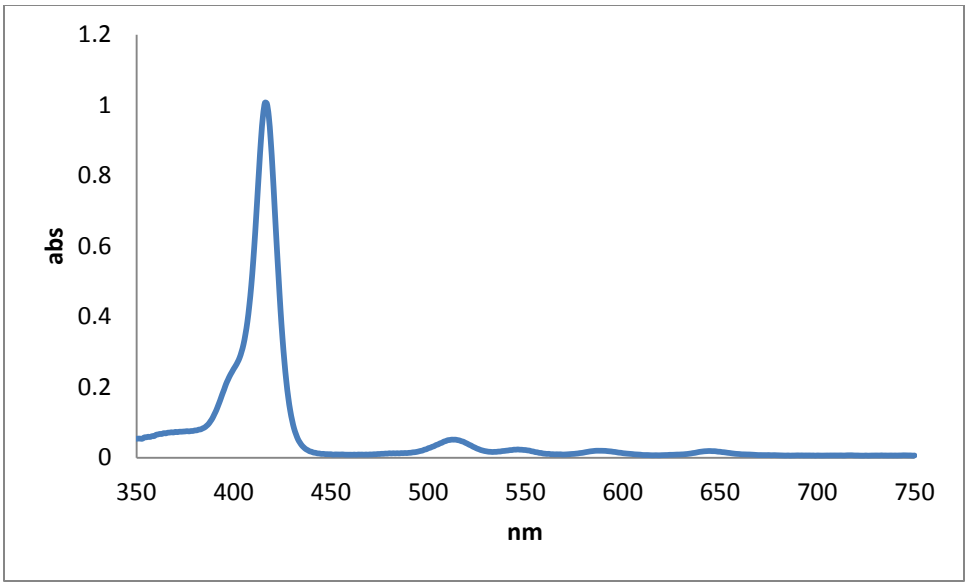

Figure 2-12. UV-Visible absorption of **10** in DCM.

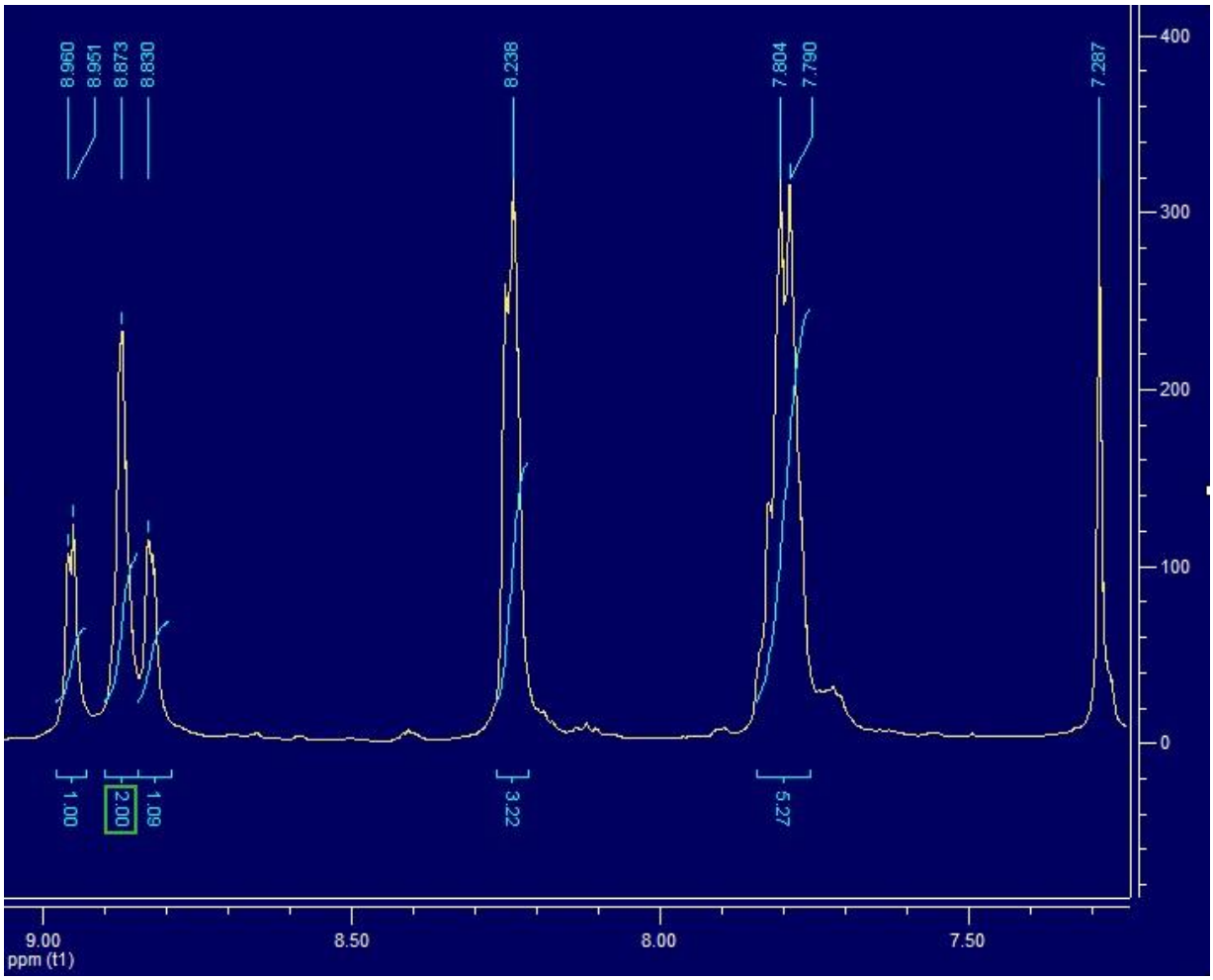

Figure 2-13. NMR of aromatic region of **10.**

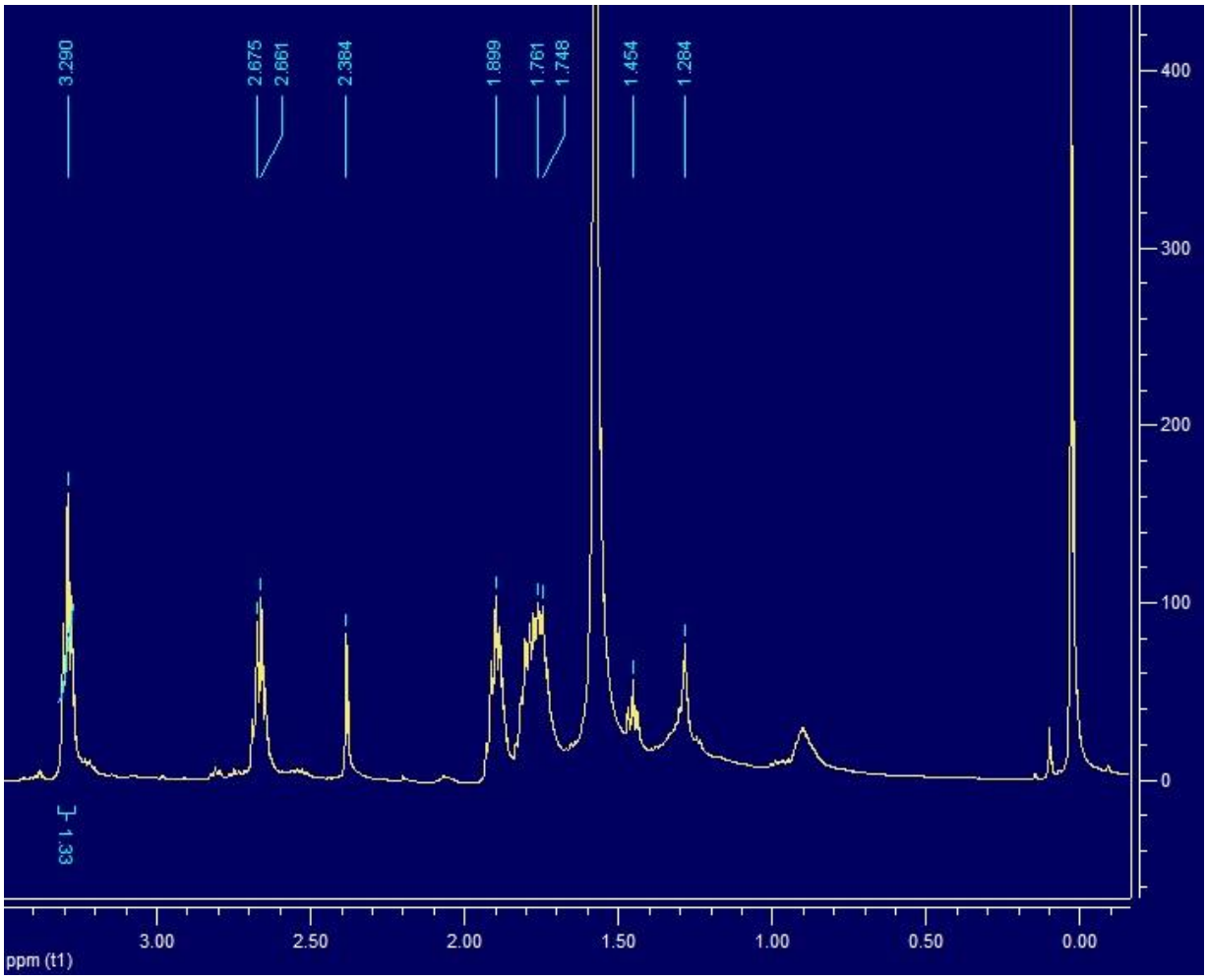

Figure 2-14. ^{1}H NMR of aliphatic region of **10.**

2.7 References

Adapted from "Porphyrins as molecular electronic components of functional devices." Jurow et al, Coordination Chemistry Reviews 254 (2010) 2297–2310

(1) Abruña, H. D.; Ratner, M. A.; Zee, R. D. v.; González, C. A.; Kagan, C. R.; Stewart, D. R.; Walker, A. V.; Batteas, J. D.; Chidsey, C. E. D.; Seideman, T. *Building Electronic Function into Nanoscale Molecular Architectures: Report of a National Science Foundation Workshop.*, National Science Foundation, 2007.

(2) Hille, B. *Ion Channels of Excitable Membranes*; 3 ed.; Sinauer Associates: Sunderland, 2001.

(3) Jin, Y.; Friedman, N.; Sheves, M.; He, T.; Cahen, D. *Proc. Natl. Acad. Sci. USA* **2006**, *103*, 8601.

(4) Hong, F. T. *Molecular Electronics. Biosensors and Biocomputers*; Springer: New York, 1990.

(5) Stoddart, J. F. *Chem. Soc. Rev.* **2009**, *38*, 1802.

(6) McCreery, R. L.; Bergren, A. J. *Adv. Mater.* **2009**, *21*, 1.

(7) Pognon, G.; Boudon, C.; Schenk, K. J.; Bonin, M.; Bach, B.; Weiss, J. *J. Am. Chem. Soc.* **2006**, *128*, 3488.

(8) Suslick, K. S.; Rakow, N. A.; Kosal, M. E.; Chou, J.-H. *J. Porphyrins Phthalocyanines* **2000**, *4*, 407.

(9) Fages, F.; Wytko, J. A.; Weiss, J. *Comptes Rendus Chimie* **2008**, *11*, 1241.

(10) Kubatkin, S.; Danilov, A.; Hjort, M.; Cornil, J.; Bredas, J.-L.; Stuhr-Hansen, N.; Hedegard, P.; Bjornholm, T. *Nature* **2003**, *425*, 698.

(11) Lafferentz, L.; Ample, F.; Yu, H.; Hecht, S.; Joachim, C.; Grill, L. *Science* **2009**, *323*, 1193.

(12) Ha, S.; Kaafarani, B.; Barlow, S.; Marder, S.; Kahn, A. *J. Phys. Chem. C* **2007**, *111*, 10493.

(13) Smith, R.; Lewis, P.; weiss, P. *Progr. Surf. Sci.* **2004**, *75*, 1.

(14) Hipps, K.; Scudiero, L.; Barlow, D.; Cooke, M. *J. Am. Chem. Soc.* **2002**, *124*, 2126.

(15) Li, J. Z.; Gryko, D.; Dabke, R. B.; Diers, J. R.; Bocian, D. F.; Kuhr, W. G.; Lindsey, J. S. *J. Org. Chem.* **2000**, *65*, 7379.

(16) Balakumar, A.; Lysenko, A. B.; Carcel, C.; Malinovskii, V. L.; Gryko, D. T.; Schweikart, K. H.; Loewe, R. S.; Yasseri, A. A.; Liu, Z. M.; Bocian, D. F.; Lindsey, J. S. *J. Org. Chem.* **2004**, *69*, 1435.

(17) Wei, L. Y.; Padmaja, K.; Youngblood, W. J.; Lysenko, A. B.; Lindsey, J. S.; Bocian, D. F. *Journal of Organic Chemistry* **2004**, *69*, 1461.

(18) Yasseri, A. A.; Syomin, D.; Malinovskii, V. L.; Loewe, R. S.; Lindsey, J. S.; Zaera, F.; Bocian, D. F. *Journal of the American Chemical Society* **2004**, *126*, 11944.

(19) Kang, B.; Aratani, N.; Lim, J. K.; Kim, D.; Osuka, A.; Yoo, K.-H. *Chem. Phys. Lett.* **2005**, *412*, 303.

(20) Vaughan, O. P. H.; Turner, M.; Williams, F. J.; Hille, A.; Sanders, J. K. M.; Lambert, R. M. *Journal of the American Chemical Society* **2006**, *128*, 9578.

(21) Chan, Y. H.; Schuckman, A. E.; Perez, L. M.; Vinodu, M.; Drain, C. M.; Batteas, J. D. *J. Phys. Chem. C* **2008**, *112*, 6110.
(22) Barlow, S.; Raval, R. *Surf. Sci. Rep* **2003**, *50*, 201.
(23) Forrest, S. *Chem. Rev.* **1997**, *97*, 1793.
(24) Garno, J. C.; Xu, C.; Bazzan, G.; Batteas, J. D.; Drain, C. M. In *Metal-Containing and Metallosupramolecular Polymers and Materials*; Schubert, U. S., Newkome, G. R., Manners, I., Eds.; American Chemical Society: 2006, p 168.
(25) Visser, J.; Katsonis, N.; Vicario, J.; Feringa, B. L. *Langmuir* **2009**, *25*, 5980.
(26) Liu, M.; Amro, N. A.; Liu, G.-y. *Annu. Rev. Phys. Chem.* **2008**, *59*, 367.
(27) Perrine, T. M.; Smith, R. G.; Marsh, C.; Dunietz, B. D. *J. Chem. Phys.* **2008**, *128*, 154706.
(28) Kang, B. K.; Aratani, N.; Lim, J. K.; Kim, D.; Osuka, A.; Yoo, K.-H. *Materials Science Engineering C* **2006**, *26*, 1023
(29) Sedghi, G.; Sawada, K.; Esdaile, L. J.; Hoffmann, M.; Anderson, H. L.; Bethell, D.; Haiss, W.; Higgins, S. J.; Nichols, R. J. *J. Am. Chem. Soc.* **2008**, *130*, 8582.
(30) Thanopulos, I.; Paspalakis, E.; Yannopapas, V. *Nanotech.* **2008**, *19*.
(31) Li, C.; Ly, J.; Lei, B.; Fan, W.; Zhang, D.; Han, J.; Meyyappan, M.; Thompson, M.; Zhou, C. *J. Phys. Chem. B* **2004**, *108*, 9646.
(32) Liu, H.; Duclairoir, F.; Fleury, B.; Dubois, L.; Chenavierb, Y.; Marchon, J.-C. *Dalton Trans.* **2009**, 3793.
(33) Roth, K. M.; Yasseri, A. A.; Liu, Z.; Dabke, R. B.; Malinovskii, V.; Schwelkart, K. H.; Yu, L.; Tiznado, H.; Zaera, F.; Lindsey, J. S.; Kuhr, W. G.; Bocain, D. F. *J. Am. Chem. Soc.*, **2003**, *125*, 505.
(34) Hipps, K. W.; Scudiero, L.; Barlow, D. E.; Cooke, M. P. *J. Am. Chem. Soc.* **2002**, *124*, 2126.
(35) Scudiero, L.; Barlow, D. E.; Hipps, K. W. *J. Phys. Chem. B* **2002**, *106*, 996.
(36) Scudiero, L.; Hipps, K. W.; Barlow, D. E. *J. Phys. Chem. B* **2003**, *107*, 2903.
(37) Ogunrinde, A.; Hipps, K. W.; Scudiero, L. *Langmuir* **2006**, *22*, 5697.
(38) Scudiero, L.; Hipps, K. W. *J. Phys. Chem. C* **2007**, *111*, 17516.
(39) Teague, L. C.; Boland, J. J. *J. Phys. Chem. B.* **2003**, *107*, 3820.
(40) Teague, L. C.; Chen, D.; Boland, J. J. *J. Phys. Chem. B.* **2004**, *108*, 7827.
(41) Teague, L. C.; Boland, J. J. *Thin Solid Films* **2004**, *464-465*, 1.
(42) Liu, Z.; Yasseri, A. A.; Lindsey, J. S.; Bocian, D. F. *Science* **2003**, *302*, 1543.
(43) Yerushalmi, R.; Scherz, A.; van der Boom, M. E. *J. Am. Chem. Soc.* **2004**, *126*, 2700.
(44) Muthukumaran, K.; Loewe, R. S.; Ambroise, A.; Tamaru, S.; Li, Q.; Mathur, G.; Bocain, D. F.; Misra, V.; Lindsey, J. S. *J. Org. Chem.* **2004**, *69*, 1444.
(45) Hurley, P. T.; Ribbe, A. E.; Buriak, J. M. *J. Am. Chem. Soc.* **2003**, *125*, 11334.
(46) Hacker, C. A.; Anderson, K. A.; Richter, L. J.; Richter, C. A. *Langmuir* **2005**, *21*, 882.
(47) Wiberg, J.; GUo, L.; Pettersson, K.; Nilsson, D.; Ljungdahl, T.; Martensson, J.; Albinsson, B. *J. Am. Chem. Soc.* **2006**, *129*.
(48) Ghirotti, M.; Chiorboli, C.; You, C.; Wurthner, F.; Scandola, F. *J. Phys. Chem. A* **2008**, *112*, 3376.
(49) D'Souza, F.; Chitta, R.; Gadde, S.; Islam, D.; Schumacher, A.; Zandler, M.; Araki, Y.; Ito, O. *J. Phys. Chem. B* **2006**, *110*, 25240.

(50) Campbell, W. M.; Burrell, A. K.; Officer, D. L.; Jolley, K. W. *Coord. Chem. Rev.* **2004**, *248*, 1363.
(51) Wasielewski, M. R. *J. Org. Chem.* **2006**, *71*, 5051.
(52) Albinsson, B.; Martensson, J. *J. Photochem. Photobio. C* **2008**, 138.
(53) Ozawa, H.; Kawao, M.; Tanaka, H.; Ogawa, T. *Chem. Lett.* **2009**, *38*.
(54) Sedghi, G.; Sawada, K.; Esdaile, L.; Hoffmann, M.; Anderson, H.; Bethell, D.; Haiss, W.; Higgins, S.; Nichols, R. *J. Am. Chem. Soc.* **2008**, *130*.
(55) Miyachi, M.; Ohta, M.; Nakai, M.; Kubota, Y.; Yamanoi, Y.; Yonezawa, T.; Nishihara, H. *Chem. Lett.* **2008**, *37*.
(56) Ambroise, A.; Kirmaier, C.; Wagner, R.; Loewe, R.; Bocian, D.; Holten, D.; Lindsey, J. *J. Org. Chem.* **2002**, *67*, 3811.
(57) Madru, R.; Guillaud, G.; Al Sadoun, M.; Maitrot, M.; André, J. J.; Simon, J.; Even, R. *Chemical Physics Letters* **1988**, *145*, 343.
(58) Ambroise, A.; Wagner, R. W.; Rao, P. D.; Riggs, J. A.; Hascoat, P.; Diers, J. R.; Seth, J.; Lammi, R. K.; Bocian, D. F.; Holten, D.; Lindsey, J. S. *Chem. Mater.* **2001**, *13*, 1023.
(59) Wagner, R.; Lindsey, J.; Seth, J.; Palaniappan, V.; Bocian, D. *J. Am. Chem. Soc.* **1996**, *118*, 3996.
(60) Noguchi, Y.; Kubota, T.; Mashiko, S.; Wakayama, Y. *J. Appl. Phys.* **2005**, *97*.
(61) Noguchi, Y.; Nagase, T.; Kubota, T.; Kamikado, T.; Mashiko, S. *Thin Solid Films* **2006**, *499*, 90.
(62) Noguchi, Y.; Ueda, R.; Kubota, T.; Kamikado, T.; Yokoyama, S.; Nagase, T. *Thin Solid Films* **2008**, *516*, 2762.
(63) Wakayama, Y.; Kubota, T.; Suzuki, H.; Kamikado, T.; Mashiko, S. *Journal of Applied Physics* **2003**, *94*, 4711.
(64) Wakayama, Y.; Kubota, T.; Suzuki, H.; Kamikado, T.; Mashiko, S. *Nanotechnology* **2004**, *15*, 1446.
(65) Wakayama, Y.; Ogawa, K.; Kubota, T.; Suzuki, H.; Kamikado, T.; Mashiko, S. *Appl. Phys. Lett.* **2004**, *85*, 329.

CHAPTER 3

Substituted Phthalocyanines for Photonic Devices

3.1 Introduction

A range of substituted phthalocyanines from a core platform function as the primary light absorbers in small molecule organic bulk heterojunction solar cells. In solution processed films the number and structure of the different exocyclic motifs significantly affect phase formation, hierarchical organization, and nanostructure, and so can be employed to tailor active layer morphology to enhance exciton dissociation and charge collection efficiencies in the bulk heterojunction photovoltaic devices. To elucidate the relationship between film nanomorphology and device function of solution-processed blends of phthalocyanines and fullerene in bulk heterojunction solar cells, we correlate grazing incidence small angle x-ray scattering structural data with solar cell performance using a standard, reproducible device architecture. Inclusion of a small amount of a *tert*-butylphthalocyanine dissrupts the otherwise homogenous alignment of chromophores in the active layer thereby greatly improving solar cell efficiency. The hierarchical organization of the donor and acceptor molecules in various blends has marked effects on the function, where a *more disordered film yields a more efficient device.*

Organic photovoltaic (OPV) devices have drawn tremendous research interest for their potential cost-effectiveness, lightweight flexible device form factors, and readily available components with low toxicity.[1-10] Semi-transparent OPV devices, which have reduce efficiencies *a prori*, may also find applications as functional window coatings; especially in urban settings where the surface is greater on the sides of buildings than the roofs.[1,5,11-13] Many state-of-the-art

OPV devices use a bulk heterojunction (BHJ) architecture, wherein an interpenetrating network of donor and acceptor materials are in contact with an anode and a cathode,[7,14-16] In an ideal BHJ system, a phase separated bicontinuous donor-acceptor network with optimized inter-domain distances and interfacial areas maximize exciton dissociation into free charge carriers and minimizing charge recombination during collection at electrodes.[2,17] Thus, the nanomorphology of the active layer is a key factor dictating device performance.[18-20] For example, in a system composed of a conducting polymer and a fullerene derivative, phenyl-C61-butyric acid methyl ester (PCBM), efficiencies nearly double to *ca.* 7% upon annealing because the internal morphology changes significantly.[21] Conversely, in some devices the addition of a small excess of sensitizer can alter the active layer nanostructure and decrease device efficiency.[17] Nanoparticles imbedded in the active layer can alter film morphology and serve as a photonic material to yield more efficient devices.[22] To correlate the changes in nanomorphology of the active layer to device performance, we have selected a simplified BHJ type solar cell architecture (Figure 3-1) which is easily fabricated in open air and easily reproduced in different laboratories without requiring the more complex OPV architectures necessary for greater efficiencies, e.g. using nanoimprinting or nanostructured electrodes.[23-26]

Small organic dye molecules show significant potential as efficient donor components in OPV devices.[7,27-30] Phthalocyanines (Pc) are tetra-isoindole macrocycles.[31] The HOMO-LUMO gap of Pc can be controlled by the number and electronic properties of substituents on the periphery of the macrocycle, thereby tuning the lowest energy Q absorption band from *ca.* 650 nm to *ca.* 750 nm where there is a high flux of solar photons.[32-35] The photonic properties of Pc make them good materials for OPV devices;[30] e.g. copper Pc,[36] and a blend of a zinc Pc and a C_{60} derivative[37] into conducting polymers in the heterojunction.[38-41] Blending PC dyes with

molecules exhibiting complementary absorption spectra to produce a mixture which better matches the incident solar spectrum results in substantial improvements in short circuit current densities.[9,17,42]

Established strategies for ensuring efficient charge migration and collection in OPV often include covalent linking of dyes[43] or layering by thermal evaporation in an effort to create more panchromatic devices.[44,45] Herein the devices are produced from a blended solution of Pc dyes with peak absorption and maximum efficiency in the 600-800 nm region and a functionalized fullerene electron acceptor incorporated into a simple and robust model device. We previously demonstrated that a blended active layer displays a marked improvement in efficiency over cells made of only one Pc.[35] This approach avoids strategies that compromise commercial viability, such as complex synthetic methods that link donors with acceptors or covalent multi-dye systems, and complex cell architectures, which can be difficult to fabricate and quantitatively reproduce.[27,46-48]

The present work investigates the relationships between PV performance in Pc blend/fullerene solution processed devices and the composition and hierarchical self-organization of the active layer quantified by grazing incidence small angle x-ray scattering (GISAXS). Similar methods have been used to look at the organization of poly(3-hexylthiophene) and a C_{60} derivative cast on poly(3,4-ethylenedioxythiophene)poly-(styrenesulfon-ate) (PEDOT:PSS),[49] evaporated CuPc on glass,[50] and other device designs.[51-53]

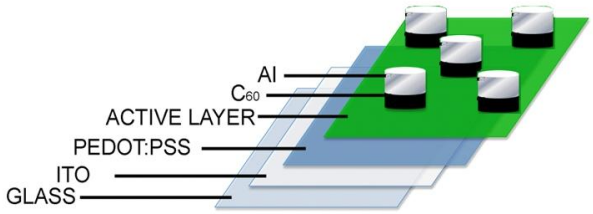

Figure 3-1. A scheme of device architecture; see abstract for picture. Samples for X-ray studies followed the same preparation excluding the C_{60} and Al electrodes. The evaporated C_{60} provides a better contact between the aluminum and active layer.

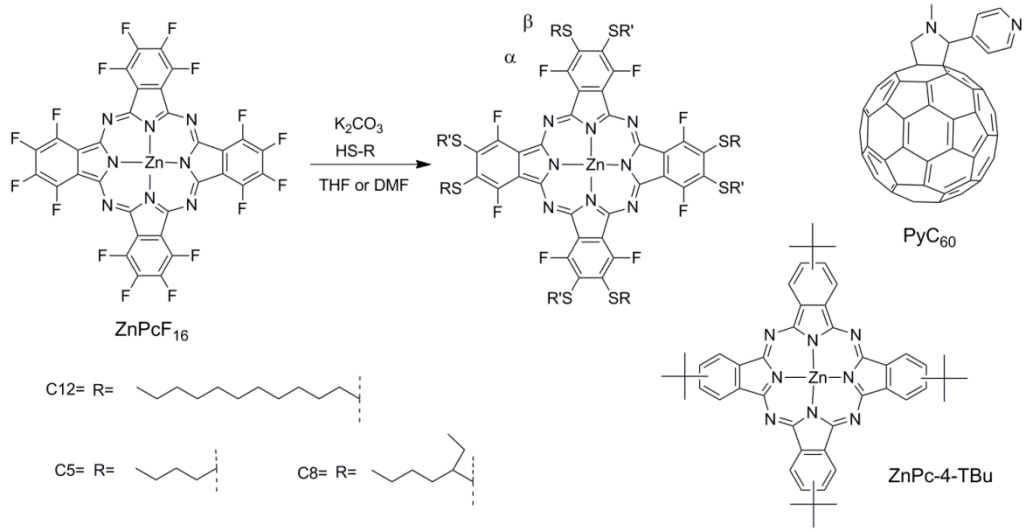

Figure 3-2. Compounds used, see Table 3-1 for specific reaction conditions.

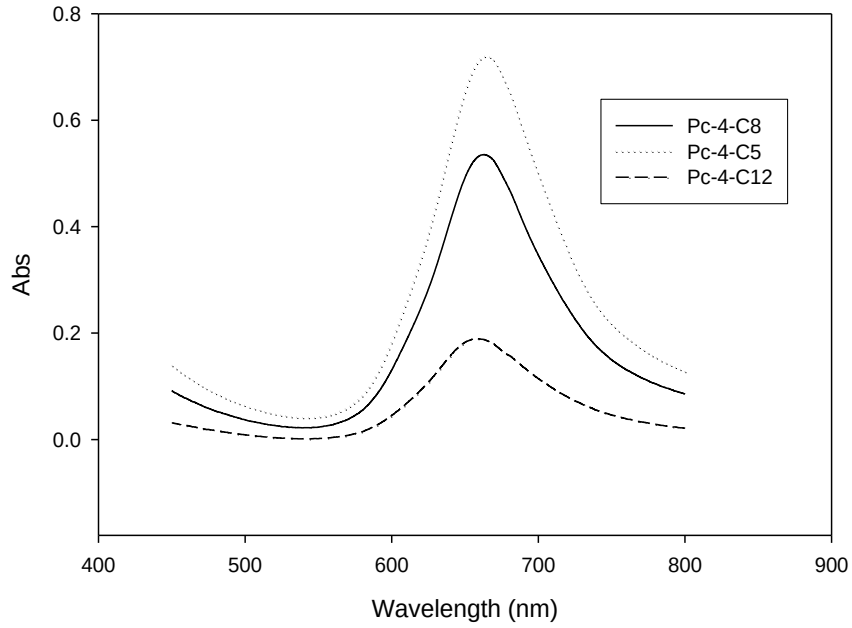

Figure 3-3. UV-visible spectra of the low energy Q band for the ZnPc tetra-substituted with three different alkanes shows that the absorbance increases as chain length decreases for the same thickness of the films.

Table 3-1. Compounds, reaction conditions, and strongest electronic absorption band. Use of the term "Pc-Cx Blend" where x is either 12, 5 or 8 denote a mixture of the 4 substituted molecule, the 8 substituted molecule and ZnPc-4-Tbu at 17:77:17 (w/w).

Compound[a]	Substituent[b]	# of thioalkanes	UV-visible λ_{max} (nm)	Reaction conditions[c]
ZnPc-4-C12 ●	R or R'=1-dodecanethiol	4 – 6	708	K_2CO_3, stir 24 h at RT in THF
ZnPc-8-C12 ○	R=R'=1-dodecanethiol	8 – 10	736	K_2CO_3, stir 8 h in refluxing THF
ZnPc-4-C5 ▲	R or R'=1-pentanethiol	3 – 5	708	K_2CO_3, stir 2 h at 50 C in THF
ZnPc-8-C5 Δ	R=R'=1-pentanethiol	8 – 10	733	K_2CO_3, stir 3h in refluxing THF
ZnPc-4-C8 ■	R or R'=2-ethyl-1-hexanethiol	4 – 6	711	K_2CO_3, stir 24 h at 50 C in THF
ZnPc-8-C8 □	R=R'= 2-ethyl-1-hexanethiol	8 – 10	726	K_2CO_3, stir 2 h in refluxing DMF
ZnPc-4-TBu ▼	tert-butyl	4	680	Sigma-Aldrich

[a] The middle number indicates degree of substitution, the symbols are used in the GISAXS data plots. [b] The major component; lesser amounts of other addition products are indicated in MALDI mass spectrometry and the range indicated in column 3. [c] All reactions used 100-fold excess thiol.

Materials and Methods

All solvents and reagents were purchased from Sigma-Aldrich and used without further purification unless otherwise stated. Fullerene C_{60} (99.5%) was obtained from BuckyUSA. A

Cary Bio-1 was used for UV-visible spectra, and an Asylum (MFP-3D, Asylum Research Corp.) was used for atomic force microscopy (AFM) measurements. All syntheses, device fabrications, and device measurements were performed multiple times by different researchers.

All device samples (Figure 3-1) were prepared by first spin coating a PEDOT:PSS hole conducting layer approximately 55 nm thick onto a pre-cleaned 140 nm thick indium tin oxide (ITO) coated glass substrate at 5,000 RPM from aqueous solution and baked at 140 °C for 10 minutes. An active layer was deposited by spin coating at 700 RPM for 45 seconds from toluene solutions of either an individual Pc derivative at 0.5% (w/w) (Pc-4-C5, Pc-8-C5, Pc-4-C8, Pc-8-C8, Pc-4-C12, Pc-8-C12, see Figure 3-2 and Table 3-1) or a blend of a four substituted, eight substituted, and *tert*-butyl Pc at relative ratios of 17:66:17 (w/w) at a total concentration of 0.25% (w/w) (Pc-C5 blend, Pc-C8 blend, Pc-C12 blend) to form a 75 nm thick film as measured by AFM. In all cases the Pc were mixed with 30% (w/w) of a pyridyl fullerene (PyC_{60})[54,55] (w/w) relative to the total dye content. These samples were investigated by grazing-incidence x-ray diffraction. For PV device characterization, ~40 nm thick fullerene (C_{60}) and 70 nm thick aluminum top contacts were sequentially deposited through a shadow mask (active device area: 3.14 mm^2) in vacuum by thermal evaporation on top of the active blend layer (Figure 3-1).

Synchrotron x-ray scattering measurements were made at the National Synchrotron Light Source at the Brookhaven National Labs. Data was collected at Beamline X6B using a Princeton Instruments CCD area detector and at Beamline X9A with a MARCCD detector. At X6B, measurements were made with an adjustable sample-detector distance of 16 to 50 cm, at wavelengths ranging from 0.65 Å to 1.2 Å to survey possible order on length scales from 3 Å to 40 Å. First-order diffraction peaks with d-spacings approximately 25-35 Å were the only ones detected for all samples. Incidence angles of 0.07, 0.12 and 0.20 degrees were compared, and

peak to background ratios found to be similar. All X6B data shown have the following configuration: detector distance 16 cm, wavelength 1.215 Å, and incident angle 0.12 degrees. At Beamline X9A measurements were made at a detector distance of 24.9 cm (+/- 2 mm) at a wavelength of 0.89 Å providing an accessible q-range from 0.13-2.89 $Å^{-1}$ corresponding to a length range of *ca.* 2-50 Å. Images taken using the X6B and X9A Beamlines were calibrated using powder standards (alumina and/or silver behenate) and analyzed using Datasqueeze [http://datasqueezesoftware.com] to integrate and plot the scattered x-ray intensity versus momentum transfer q and azimuthal angle χ around the incident beam direction. Fits from collected data sets were evaluated using FitYK [http://fityk.nieto.pl/]. Gaussian line shapes were used to quantify the peaks and extract full width at half maximum (FWHM) values.

PV parameters of fabricated devices were measured from device current-voltage (I-V) characteristics under simulated solar illumination. A custom-modified probe station equipped with Agilent 4156C precision semiconductor parameter analyzer was used to characterize dark and illuminated I-V characteristics, and an Oriel 9600 150 W solar simulator with an AM1.5G filter was used for solar illumination with 100 mW/cm^2 (1 SUN) condition (calibrated by Oriel 70268 thermopile detector).

All dyes were synthesized by similar procedures with minor modifications to yield a library of Pc having various degrees of peripheral thioalkane substitution, with tuned optical properties (Table 3-1).[35] All molecules, except for the tetra-*tert*-butyl Pc (ZnPc-4-Tbu) which was purchased from Aldrich and used as received, were fabricated from the same starting material, zinc 1,2,3,4,8,9,10,11,15,-16,17,18,22,23,24,25-hexadeca-fluoro-phthalocyaninato zinc(II), ($ZnPcF_{16}$), also obtained from Sigma.

3.2 Device Architecture

The device architecture is depicted in Figure 3-1. Active layers were spin cast from toluene solutions of either a single Pc, or a blend of multiple Pc, and a pyridyl functionalized fullerene acceptor, PyC_{60}. Contacts were then thermally evaporated. The degree of substitution of the phthalocyanine is controlled by variation of reaction conditions: temperature, duration, and solvent (see supporting information). The UV-visible absorption spectrum allows for easy tracking of the degree of peripheral substitution of the Pc by following the *ca.* 7 nm red shift of the strongly absorptive Q bands for each electron withdrawing fluorine substituted by an electron donating thioalkane. The substitution occurs initially at the more reactive β positions of the starting $ZnPcF_{16}$ (Figure 3-2), which has a strong absorption at 680 nm. Derivatives with one or two thioalkanes on the β positions of each isoindole have optical bands centered at 707 nm and 735 nm, respectively (Table 3-1). Using three thioalkanes with different chemical structures (Figure 3-2) produces a family of molecules that are chemically compatible but form films with marked morphological differences. The acceptor, PyC_{60}, was synthesized according to literature procedures.[54]

We focus on readily available, cost effective, and scalable materials that can be incorporated into simple devices with easily reproducible efficiencies. The layers are spin coated in ambient atmosphere from non-halogenated solvents to produce a stable device from which we can assess the effect of variations in active layer composition and nanomorphology. The active layer contains a blend of one or more Pc dye donors and PyC_{60}, which serves as an electron acceptor. The PyC_{60} allows the acceptor to coordinate to the Zn(II) center of the Pc molecules to facilitate charge transfer and exciton diffusion at the donor-acceptor interface.[56,57] Though modifications of the fullerene diminish its effectiveness as an electron acceptor, neither unfunctionalized C_{60} or

the commonly used phenyl-C_{61}-butyric-acid-methyl ester (PCBM) work well in this device architecture because C_{60} is not adequately soluble at the necessary concentration and PCBM creates poor quality cells that phase separate upon annealing.

Substitution of the F atoms on the periphery of the $ZnPcF_{16}$ core platform with thioalkanes is facile and systematically alters the HOMO-LUMO gap, as observed in the *ca.* 7 nm red shift in the UV-visible spectra per thioalkane added.[33,35] Thus, a blend of dyes built on this core platform can effectively use a greater part of the solar spectrum as evidenced by EQE measurements in our previous work (see supporting information).[35] The use of different thioalkanes preserves these chemical similarities and the advantages of blending multiple dyes while allowing for controlled variation of hierarchical organization and optical density (Figure 3-3). The shorter chains form films with greater optical density because the alkanes occupy less surface area in the active layer and allow for a higher packing density of the Pc cores.

3.3 Hydrocarbon Structure Dictates Hierarchical Order and Device Efficiency

Power conversion efficiencies depend on thioalkane chain length (Figure 3-4, Table 3-2). We hypothesized that the use of the ZnPc-C12 Blend within the active layer displayed low overall device power conversion efficiencies (PCE) due in part to the resistivity of the devices active layer. In order to decrease the device resistivity and simultaneously improve optical density by packing more chromophores into the same thickness of the cast layer, devices using ZnPc-C5 with short pentanethiol chains were evaluated. Devices made with a ZnPc-C5 blend exhibited nearly a 100% increase in PCE compared with devices containing the ZnPc-C12 blend, due in large part to a 60% increase in J_{SC}, a 25% increase in V_{OC}, and a ~40% decrease in device series resistance as determined from the tangential slope at $V_{OC.}$ Devices with only ZnPc-4-C5 in the active layer displayed nearly identical R_S but 20% lower PCE because of reduced V_{OC} and J_{SC}

compared to devices with the ZnPc-C5 blend. Thus for a given ZnPc core system, the thioalkane length is the main factor that determines device R_S rather than the number of attached thioalkanes. As discussed below, the dependence of R_S on the length of side thioalkane chain suggests that the molecular stacking of Pc occurs parallel to the film plane.

Table 3-2. PV cell parameters

	PCE%	Jsc mA cm^{-2}	Voc V	FF	Rs Ωcm^2
ZnPc-C12 blend	0.08	0.98	0.24	0.33	128
ZnPc-C5 blend	0.15	1.49	0.30	0.35	74
ZnPc-4-C5	0.12	1.43	0.25	0.35	76
ZnPc-C8 blend	0.06	0.64	0.31	0.30	281

Average of five devices, std. error <10%

Pc have disk shaped structures that are about 1.5 nm in diameter and can form discotic liquid crystal phases (DLC) when appended with appropriate, long-chain alkanes.[58-62] DLC can be induced to arrange themselves into columns stacked parallel to the substrate (homogeneous alignment) or perpendicular to the substrate (homeotropic alignment) as illustrated in Figure 3-6. DLC exhibit excellent electron transfer along the columnar axis and are used in a variety of

widely deployed technologies such as LCD screens and OPV.[58,63,64] A film of homeotropically aligned co-facially pi stacked Pc would be expected to rapidly transmit charge perpendicularly to the substrate and would be expected to approach the ideal bulk heterojunction architecture.[5,65-67]

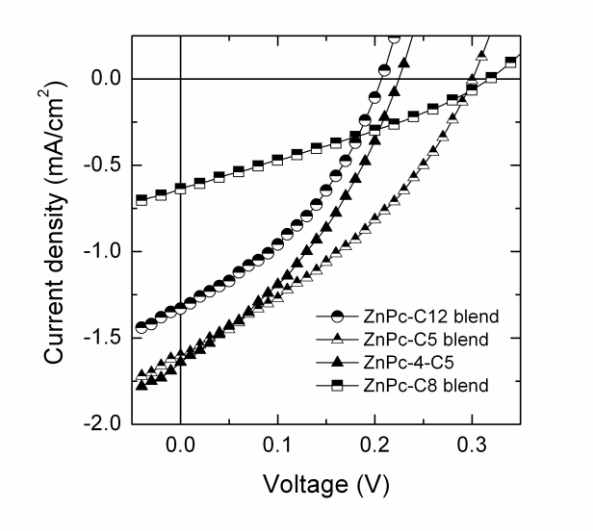

Figure 3-4. Current-voltage characteristics of solar cells under 1 sun AM 1.5G conditions. All devices contain 30% (w/w) PyC60 unless otherwise stated

In the case of a homogeneously aligned film, x-ray scattering measurements with the incident beam grazing the film surface exhibit hexagonal scattering patterns for well aligned films. For intermolecular spacing a (on the order of the molecular disk diameter), the spacing of diffracting planes $d = a(\sqrt{3}/2)$, yields diffraction spots with momentum transfer $q = 2\pi/d$, which is analyzed from the radial position of the diffracted beam. The six-fold symmetry creates three spots above the film horizon, as shown in the diffraction pattern of Pc-8-C12 (Figure 3-6c). The additional streak of intensity along the vertical axis arises from x-rays reflecting from the smooth film surface, and the dark shadows are from the beam stop. The magnitude of *q* and the width of the peak along *q* indicate the d-spacing and the distribution of d-spacings of the molecular columns.

The azimuthal angle χ provides information about film alignment. Figure 3-6d shows a graph of diffracted intensity, integrated over a small q interval at the diffracted peaks. The maxima at 30°, 90°, and 150° confirm hexagonal symmetry and homogeneous alignment for Pc-8-C12. The peak width in χ directly probes the orientations of the ordered grains. For example, small domains may be present whose hexagonal stacks do not lie parallel to the substrate, as depicted in Figure 3-6e. A distribution of crystalline regions will broaden the peaks along the χ direction. If the collection of grains has isotropic orientation, a diffraction ring with intensity independent of χ will be observed.

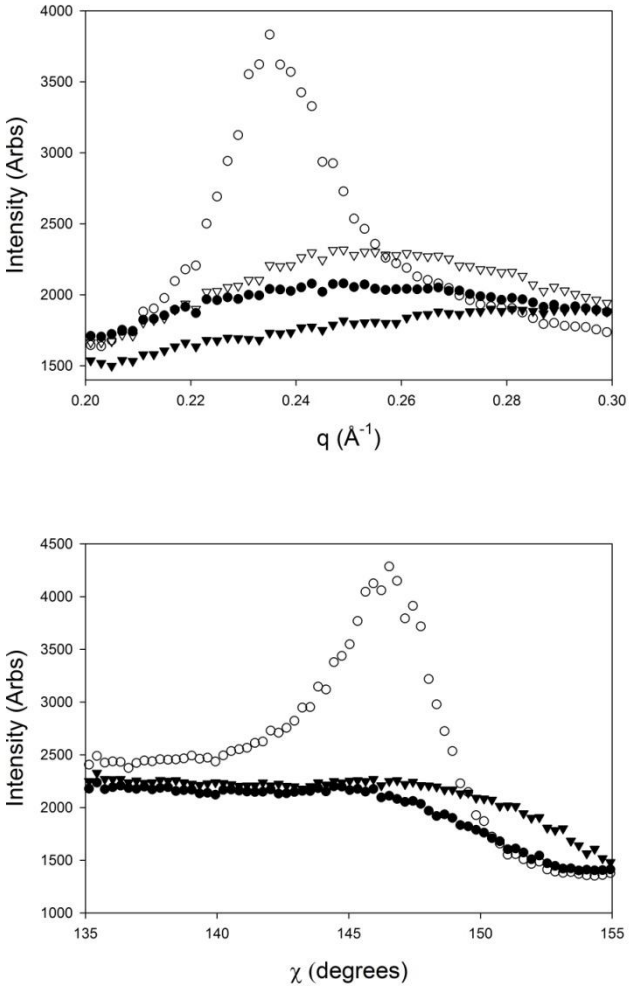

Figure 3-5. Comparison of GISAXS data for the alkylated ZnPc. ▼=ZnPc-4-TBu, ●=ZnPc-4-C12, ○=ZnPc-8-C12, ∇= blend of ZnPc-4-C12: ZnPc-8-C12: ZnPc-4-TBu (17:66:17 by weight). Top: plots of intensity versus q in the region where diffraction spots corresponding to a hexagonal lattice appear. A diffraction ring is present in all samples except ZnPc-4-Tbu. Bottom: plot of intensity versus χ.

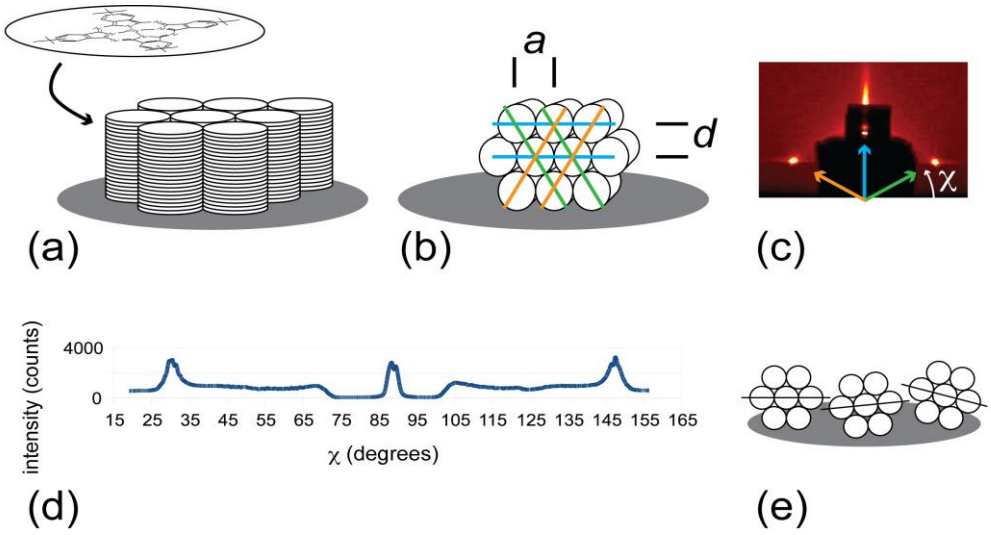

Figure 3-6. (a) Homeotropically aligned columns of Pc molecules; (b) Homogeneously aligned hexagonally packed columns, characterized by column spacing a and layer spacing d = $a\sqrt{3}/2$; (c) Representative GISAXS pattern of ZnPc-8-C12 showing diffraction peaks from the six fold-symmetric column layer planes. The azimuthal angle χ is referenced from a horizontal axis; (d) X-ray intensity integrated through a small q range containing the Bragg peaks as a function of χ, highlighting the 60° separation between peaks. Near χ =90°, flattened minima and irregular peak shape are due to transmission blocked by the beam stop; (e) Depiction of variation in packed-column orientation which causes diffracted peaks to broaden in the χ direction.

A range in q was surveyed to enable d-spacings from 3 Å to 40 Å to be detected, for all samples. No wide-angle peaks were observed, indicating insufficient diffraction contrast from long-range-ordered columnar pi-stacking of the molecules in any orientation. Instead, diffraction peaks were observed for columnar structures with hexagonal symmetry evident only in the detector plane. Thus, all diffracting dye molecules are oriented homogenously (Figure 3-6b, 5e).

Diffraction peaks were observed with q maxima ranging from 0.23 $Å^{-1}$ to 0.33 $Å^{-1}$, corresponding to column layer spacings of 19 Å to 27 Å, or inter-column distances of 22 Å to 31.5 Å, as expected for their molecular diameters with extended hydrocarbon chains of varying length. For active layer films, the diffraction peaks exhibited variations in widths of both q and χ among samples, and were never resolved into contributions from multiple peaks. This observation suggests that the samples, including the blends, consist of no more than one LC phase.

In samples displaying the most order, sharp spots are observed at the expected azimuthal angles indicative of a hexagonally packed homogeneously aligned film.[68] The peak corresponds to the (1,1) hexagonal column and indicates a center-to-center distance of 30.9 Å for the C_{12} film that is consistent with the molecular diameter of 25-35 Å with extended side chains.

3.4 Improving Device Performance by Frustrating Homogenous Order

Our previously work with the ZnPc-C12 Blend system demonstrated that the inclusion of a small percentage of ZnPc-4-TBu into a Pc mixture resulted in an increase in PCE which far exceeded the gain expected solely from the increased spectral coverage.[35] Because of the impact active layer nanostructure has on the photonic properties of these films, GISAXS measurements were made on devices to examine the effects of both the incorporation of the ZnPc-4-Tbu and the inclusion of dyes with different thioalkane side chains.

Films of ZnPc-8-C12 and ZnPc-4-C12 with PyC_{60} were found to exhibit homogeneous LC order, with diffraction patterns similar to that shown in Figure 3-6c (compare Figures 6 and 7). This observation is consistent with Pc molecules bearing long hydrocarbon chains stacking into liquid crystalline phases.[58-60,69-71] Charge transport in the normal direction in films with homogeneous alignment (Figure 3-6b) is intrinsically inhibited by charge hopping across

insulating side chains. Since the efficiency of inter-column charge hopping depends on the distance between macrocycle edges, the improved efficiencies observed in devices made from films containing domains of homogeneously aligned ZnPc-C5 arise from the shorter inter-column distances in addition to the increased optical cross sections.

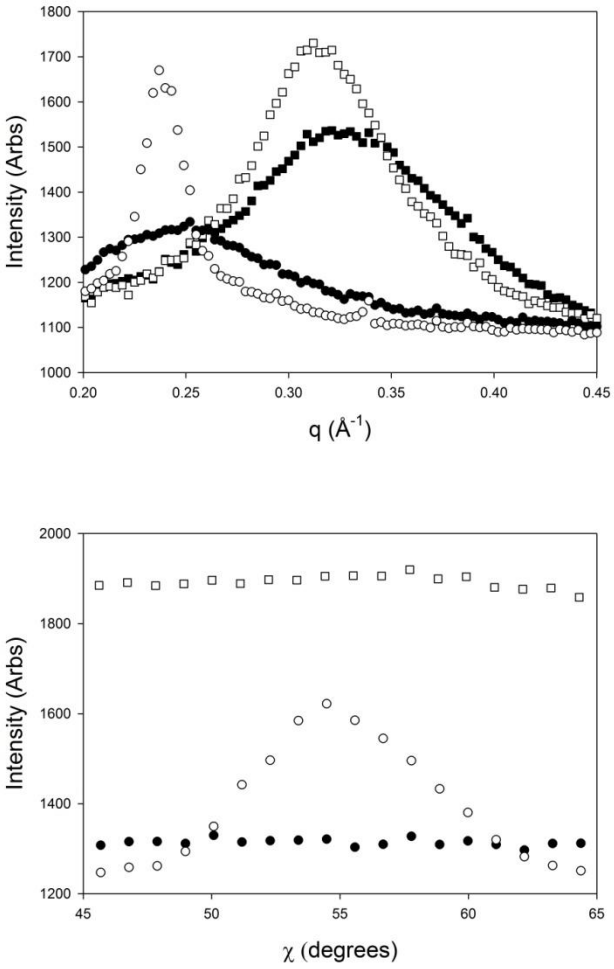

Figure 3-7. Integrated GISAXS diffraction peak intensities for selected –C8 and –C12 films; ■=ZnPc-4-C8, □=ZnPc-8-C8, ●=ZnPc-4-C12, ○=ZnPc-8-C12; Top: intensity versus q with χ integrated from 34.5-77.2; Bottom: Intensity versus χ with q integrated +/- 0.04 $Å^{-1}$ about the center position determined from fits in the top panel. All films contain 30% PyC_{60} by weight.

The ZnPc-C8 dyes with branched thioalkanes improved the optical cross section (Figure 3-3) relative to the Pc-C12 systems, but diminished the PV performance compared to the other devices. The absence of diffraction indicates a lack of domain separation between the donor an acceptor species in the ZnPc-C8/ PyC_{60} active layer, resulting in an increase of R_S by nearly twofold, and a ~35% decrease in J_{SC}, because of exciton recombination and poor charge collection.

Incorporating dyes with shorter alkyl chains increases the inter-domain conductivity between homogenously packed columns but also deters the formation of a homogenous mesophase. Blending with ZnPc-4-Tbu diminishes homogenous LC order in the same fashion and results in increased device efficiency. X-ray data (Figure 3-7) indicates that Pc with fewer and shorter side chains form films with less of the unfavorable homogeneous ordering observed in the Pc-C12 dye systems. GISAXS data from both ZnPc-4-C5 and ZnPc-8-C5 films exhibit a diffuse halo, centered at q=0.31 $Å^{-1}$ (a=23 Å). With 5% (w/w) ZnPc-4-TBu in the ZnPc-4-C5 and ZnPc-8-C5 films, no diffraction patterns are observed, indicating a complete disruption of repeating regions of homogenous order.

The ZnPc-C8 films exhibited narrower q peak widths than those with ZnPc-C5, though still broader than the ZnPc-C12 films. Diffraction patterns for ZnPc-C8 suggest that the branched alkanes allow for somewhat better side chain melting, liquid crystallinity, and blending with acceptor than the C5 dye (Figure 3-5, 7). Both an increased degree of alkyl substitution and an increased chain length result in larger regions of homogeneously ordered molecules that negatively impacted PV efficiencies.

The homogeneous alignment of the Pc arises from the greater affinity of the appended alkanes for the PDOT:PSS surface than the macrocycle core.[72,73] The lack of second order diffraction

peaks implies that the domains of homogeneously packed molecules are small, likely because the 70 nm layers contain non-periodic interruptions in molecular arrangements caused by roughness in the PEDOT layer. Broadening of these peaks into halos and rings arises from a randomization in the orientation of the ordered regions. At wide scattering angles no other information, such as a d-spacing corresponding to a pi-stacking length, is observed.

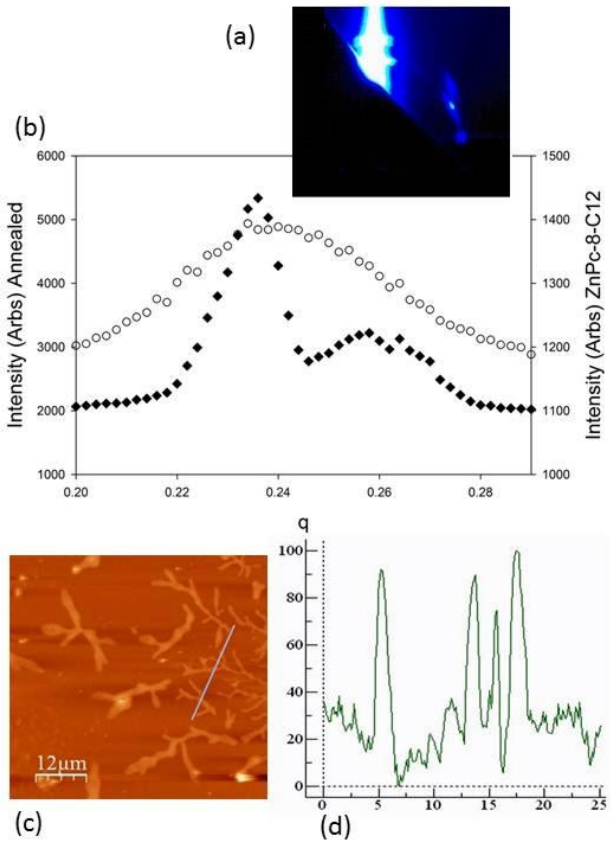

Figure 3-8. (a) False color image of diffraction pattern of the ZnPc-8-C12 after annealing at 140°; (b) χ-integrated intensity versus q prior to (○) and following the anneal (◆), showing the segregation into two LC phases with distinct column layer spacings; (c) AFM height image of an annealed sample of ZnPc-8-C12 showing dendritic regions not observed prior to anneal; (d) AFM height trace along line indicated in (c).

Since blends of Pc can exhibit enhanced performance relative to the individual dyes, studies were done to discern whether the dye molecules segregated into domains or mixed well on a molecular level. The organization of a film of ZnPc-C12 blend was compared to films of the individual C12 dyes alone. The GISAXS data from the blended films shows no clear evidence indicating the formation of domains composed of one of the dyes. The ZnPc-8-C12 film exhibits a bright, narrow diffraction peak, and the blends exhibit diffuse bands (Figure 3-5). This is consistent with earlier AFM friction studies, that demonstrated that the dyes are chemically similar (Table 3-1).

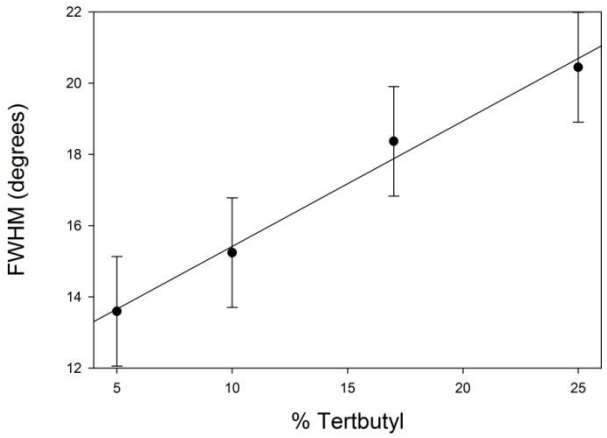

Figure 3- 9. Diminished LC order is shown by the increase of the FWHM of Gaussian fits to plots of the intensity versus χ integrated from q = 0 - 0.231 $Å^{-1}$ as the weight % of ZnPc-4-TBu increases in devices fabricated from 17:66 by weight blends of ZnPc-4-C12: ZnPc-8-C12.

The inclusion of 17% ZnPc-4-TBu into a mixture of ZnPc-4-C12 and ZnPc-8-C12 dyes increased the PCE by nearly 50%. A separate set of samples consisting of Pc-8-C12 blended with different ratios of ZnPc-4-TBu were prepared to quantify the effect of the latter on the morphology of the films and PCE. A blurred halo is observed in the GISAXS indicating the inclusion of the ZnPc-4-TBu disrupts the otherwise homogeneously ordered regions of the ZnPc-

8-C12 in the film or reorients ordered sections of dyes into random directions (Figure 3-9). This induced disorder contributes substantially toward the improvement in solar cell efficiency in the blended devices relative to the cells composed solely of the individual dyes. Taken together, it is likely that the devices made from the individual dyes feature large regions of Pc molecules oriented parallel to the surface thereby inhibiting charge migration to the electrodes, and allowing rates of geminate and intermolecular charge recombination to compete with rates of exciton diffusion to a requisite interface. A small percentage of ZnPc-4-TBu is sufficient to inhibit homogeneous alignment.

The concept that long range homogenous order is detrimental to device efficiencies is also supported by the near elimination of any detectable PCE upon annealing in a nitrogen atmosphere at 140 degrees for 15 minutes. The multiple peaks at various q values as well as the diffuse halos observed in the diffraction images suggest that annealing induces substantial phase separation of the device components (Figure 3-8). AFM data collected of the annealed films after the collection of the x-ray images shows phase separated finger-like domains on the order of 100 nm high (Figure 3-8).

3.5 Conclusion

Blended systems have clear advantages.[38] Devices using dye blends made from a core Pc platform display remarkable improvement in photovoltaic efficiency upon the integration of a small percentage of ZnPc-4-TBu because it disrupts the unfavorable homogenous packing of the dye molecules in the active layer.[74] The use of a core Pc platform also assures significant overlap of the HOMO-LUMO gaps of the dyes in the active layer, thereby facilitating charge transport. Shorter side chain substituents such as ZnPc-C5 reduce both the film resistivity and the liquid crystalline character of the dyes, while increasing the optical density of the active layer. Many

groups are investigating liquid crystalline molecules to serve as donors in organic bulk heterojunction solar cell devices.[58,60,69,75] Homeotropically aligned systems of dyes with interdigitated domains of electron acceptors may approach an ideal architecture for BHJ active layers;[1] however, difficulty in producing homeotropic packing remains an obstacle. The detrimental effect on cell performance resulting from the necessary alkyl substitution required to induce liquid crystallinity in Pc suggests that different methods of self-organization into favorable nanoarchitectures are needed. Understanding the effect of ZnPc-4-TBu in the ZnPc-C12 dye system, and the differences in nanostructure of films containing the three different thioalkane side chains, indicates disorder may be a better design principle for devices with blended active layers. Further investigations will explore the effect of substitution with conducting side chains as well as their effect on morphology.

Device Note

The solutions used to prepare the active layers were made at constant relative ratios of dye to solvent (w/w). The relative mole ratios of the dyes and C_{60} in the active layers ranged from 1:1 to 1:2.7 for the individual dye devices and 1.5:1 to 2:1 for the blended systems (Pc:Pyr C_{60}).

3.6 Synthesis

A variety of Pc for solar cell applications have been reported. [31,35,36,43,45,48,50,56,57,59,61,62,65,67,70,74-84] N-methyl-2-(4'-pyridyl)-3,4-fulleropyrrolidine was prepared as described in the literature. [54]

Pc-4-C12. To a stirring solution of 15 mL of freshly distilled THF under Ar was added $ZnPcF_{16}$ (50 mg, 0.0576 mmol), dodecanethiol (1.69 mL, 8.2 mmol) and potassium carbonate (50 mg) and the solution was stirred at room temperature for 24 hours. Reaction was mixture was poured into separatory funnel and washed with water, extracted into dichloromethane, and dried over Na_2SO_4. The solvent was removed under vacuum. Silica gel chromatography (4x15 cm)

with hexane followed by hexane/ethyl acetate 1:2 (v/v) yielded an emerald green solid. Formula $C_{80}H_{100}F_{12}N_8S_4Zn$, MALDI-MS calculated 1595.32, found: 1594.94 as the major component. UV-Vis. λ_{max} in CH_2Cl_2: 708 nm.

Pc-4-C5. To a stirring solution of 15 mL of freshly distilled THF under Ar was added $ZnPcF_{16}$ (50 mg, 8.2 mmol), pentanethiol (1.01 mL, 8.2 mmol) and potassium carbonate (50 mg). The resulting solution was stirred at 50 C for 2 hours and reaction progress monitored by UV-visible spectroscopy to determine the degree of substitution. The crude reaction mixture was washed with water, extracted into dichloromethane, and dried over Na_2SO_4. The solvent was removed under vacuum. Silica gel chromatography (4x15 cm) with hexane followed by hexane/ethyl acetate 1:2 (v/v) yielded an emerald green solid. Formula $C_{52}H_{44}F_{12}N_8S_4Zn$, MALDI-MS calculated mass 1202.58, found: 1202.09 as the major component. UV-Vis. λ_{max} in CH_2Cl_2: 708 nm.

Pc-4-C8. $ZnPcF_{16}$ (75 mg, 8.6 mmol) was stirred in 15 mL of freshly distilled THF under Ar for 10 minutes. 2-ethylhexanethiol (1.06 mL, 6.2 mmol) and potassium carbonate (150 mg) were added and the solution was stirred at 50 C for 24 hours and monitored by UV-visible spectroscopy to determine the degree of substitution. The crude product was washed with water, extracted into dichloromethane and dried over Na_2SO_4. The solvent was removed under vacuum. Silica gel chromatography (4x15 cm) with hexane followed by hexane/ethyl acetate 1:2 (v/v) yielded an emerald green solid. Formula, $C_{64}H_{68}F_{12}N_8S_4Zn$, MALDI-MS calculated 1370.89, found:1370.61 as the major component. UV-Vis. λ_{max} in CH_2Cl_2: 711 nm.

Pc-8-C12. To 15 mL of freshly distilled THF under Ar for 10 was added $ZnPcF_{16}$ (50 mg, 0.0576 mmol), dodecanethiol (1.69 mL, 8.2 mmol) and potassium carbonate (50 mg). The solution was stirred at reflux for 8 hours and monitored by UV-visible spectroscopy to determine

the degree of substitution. The crude reaction mixture was then was washed with water, extracted into dichloromethane and dried over Na_2SO_4. The solvent was removed under vacuum. Silica gel chromatography (4x15 cm) with hexane followed by hexane/ethyl acetate 1:2 (v/v) yielded an emerald green solid. Formula, $C_{128}H_{200}F_8N_8S_8Zn$, MALDI-MS calculated 2324.89, found: 2325.89 as the major component. UV-Vis. λ_{max} in CH_2Cl_2: 736 nm.

Pc-8-C5. To 15 mL of freshly distilled THF under Ar was added $ZnPcF_{16}$ (50 mg, 8.2 mmol), pentanethiol (1.01 mL, 8.2 mmol) and potassium carbonate (50 mg). The solution was stirred at reflux for 3 hours and monitored by UV-visible spectroscopy to determine the degree of substitution. The crude reaction mixture was washed with water, extracted into dichloromethane and dried over Na_2SO_4. The solvent was removed under vacuum. Silica gel chromatography (4x15 cm) with hexane followed by hexane/ethyl acetate 1:2 (v/v) yielded an emerald green solid. Formula, $C_{72}H_{88}F_8N_8S_8Zn$, MALDI-MS calculated 1539.4, found: 1538.71 as the major component. UV-Vis. λ_{max} in CH_2Cl_2: 733 nm.

Pc-8-C8. To 15 mL of freshly distilled DMF under Ar was added $ZnPcF_{16}$ (75 mg, 8.6 mmol), 2-ethylhexanethiol (1.06 mL, 6.2 mmol) and potassium carbonate (150 mg). The solution was stirred at reflux for 2 hours and monitored by UV-visible spectroscopy to determine the degree of substitution. The crude reaction mixture was then washed with water, extracted into dichloromethane and dried over Na_2SO_4. The solvent was removed under vacuum. Silica gel chromatography (4x15 cm) with hexane followed by hexane/ethyl acetate 1:2 (v/v) yielded an emerald green solid. Formula, $C_{104}H_{153}F_7N_8S_9Zn$ MALDI-MS calculated 2002.33, found: 2002.33 as the major component. UV-Vis. λ_{max} in CH_2Cl_2: 727 nm.

3.7 Surface Analysis

Samples were prepared by the same method used to prepare solar cells and x-ray samples. After spin coating the blend of dyes for the active layer, a razor blade was used to cut a line through the active layer and the underlying PEDOT:PSS layer, which is ca. 55 nm. Contact mode AFM was then used to determine the total thickness. Active layer thicknesses reported herein were calculated by subtracting the PEDOT:PSS thickness from the total AFM measured heights. Solutions used for all devices tested in this manuscript were prepared by weight percentage. To guarantee that the optical density differences observed arise from differences in molecular packing we diluted the lower molecular weight solutions and spin coated a series of samples from equimolar solutions all made to the concentration of the original Pc-4-C12 solution of 7.5 M. These samples demonstrated the reported trend. These cells are referred to as "Pc-X-CY dilute". Solutions used for all devices tested in this manuscript were prepared by weight percentage. To guarantee that the optical density differences observed arise from differences in molecular packing we diluted the lower molecular weight solutions and spin coated a series of samples from equimolar solutions all made to the concentration of the original Pc-4-C12 solution of 7.5 M. These samples demonstrated the reported trend. These cells are referred to as "Pc-X-CY dilute".

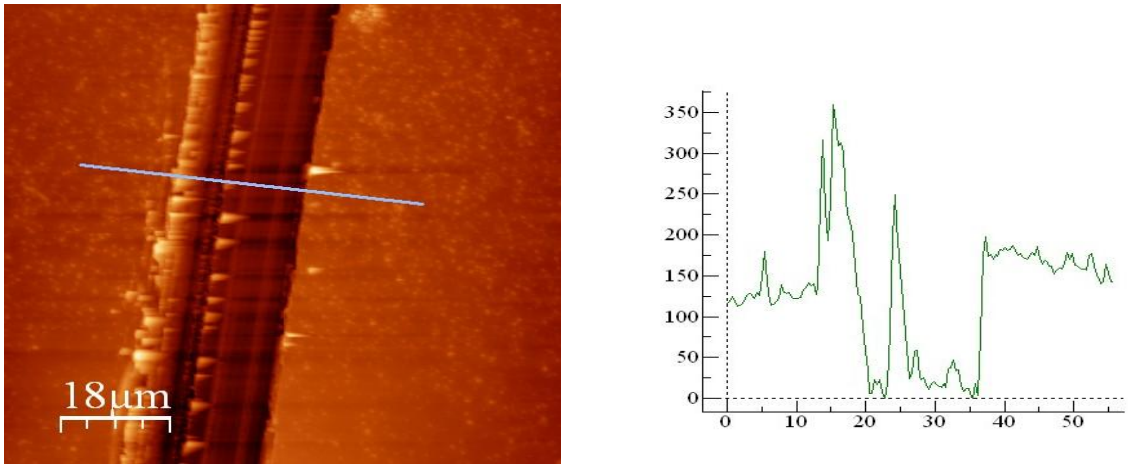

Figure 3-10. The 125 nm height measured by AFM of films of **Pc-4-C5** on PEDOT:PSS indicate an active layer thickness of ca.70 nm.

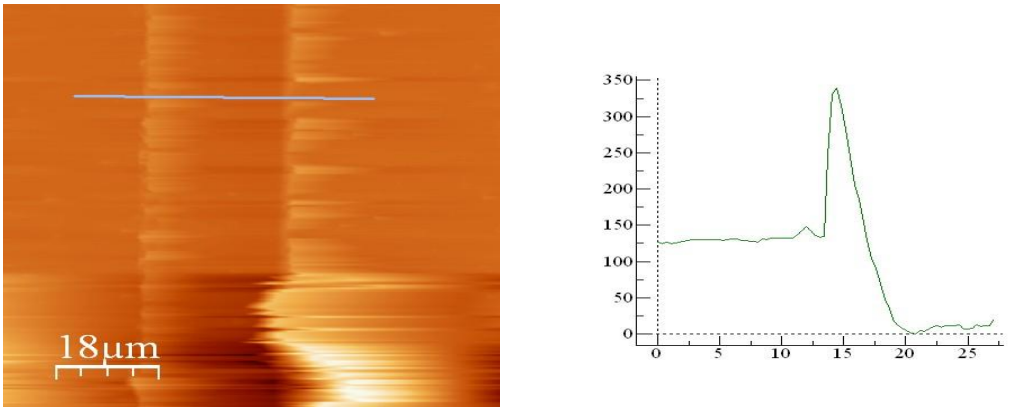

Figure 3-11. The 125 nm height measured by AFM of films of **Pc-4-C8** on PEDOT:PSS indicate an active layer thickness of ca.70 nm.

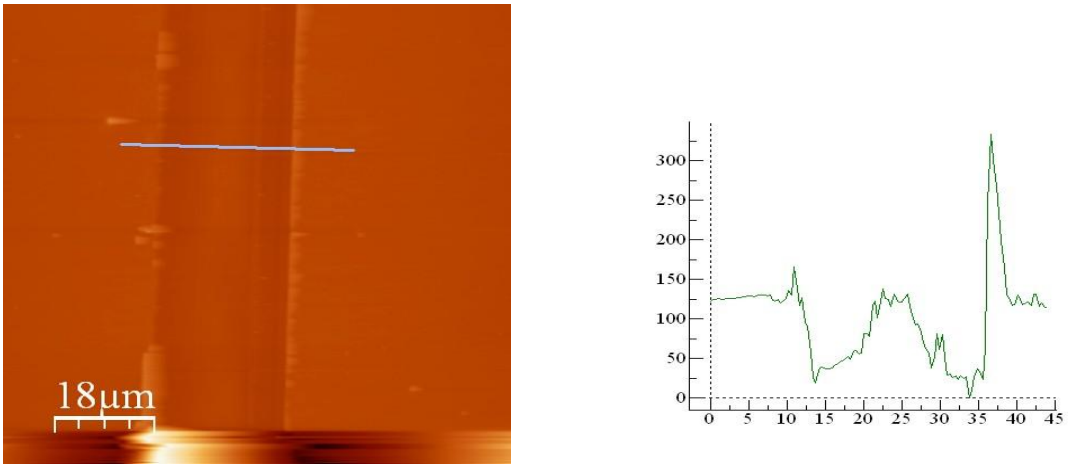

Figure 3-12. The 125 nm height measured by AFM of films of **Pc-4-C12** on PEDOT:PSS indicate an active layer thickness of ca.70 nm.

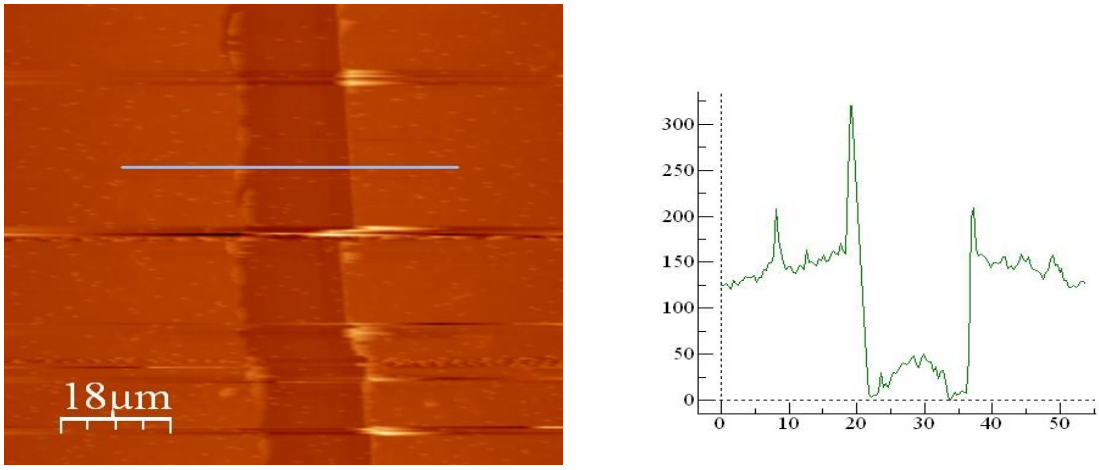

Figure 3-13. The 125 nm height measured by AFM of films of Pc-4-C5 on PEDOT:PSS indicate an active layer thickness of ca.70 nm. This sample was prepared from a dilute solution. Note that the film thicknesses are the same.

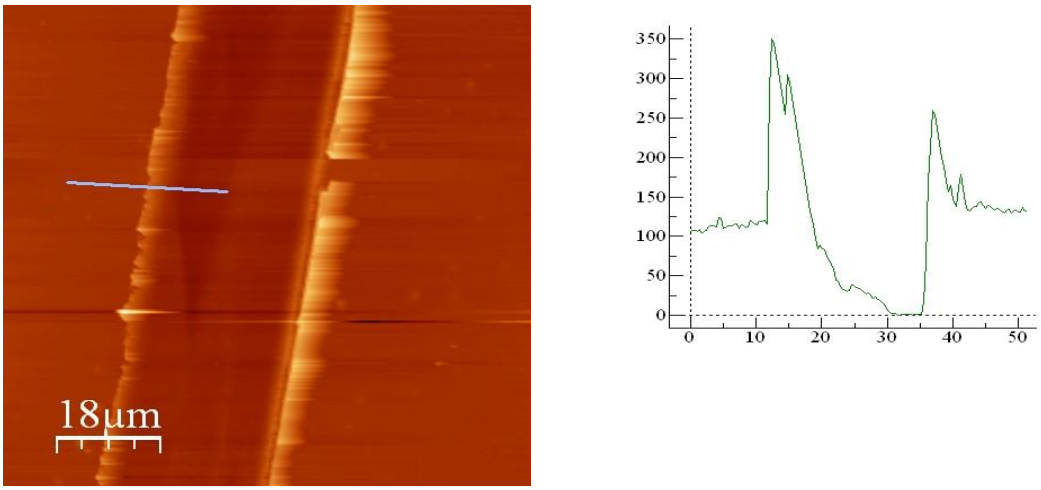

Figure 3-14. The 125 nm height measured by AFM of films of Pc-4-C8 on PEDOT:PSS indicate an active layer thickness of ca.70 nm. Prepared from a dilute solution.

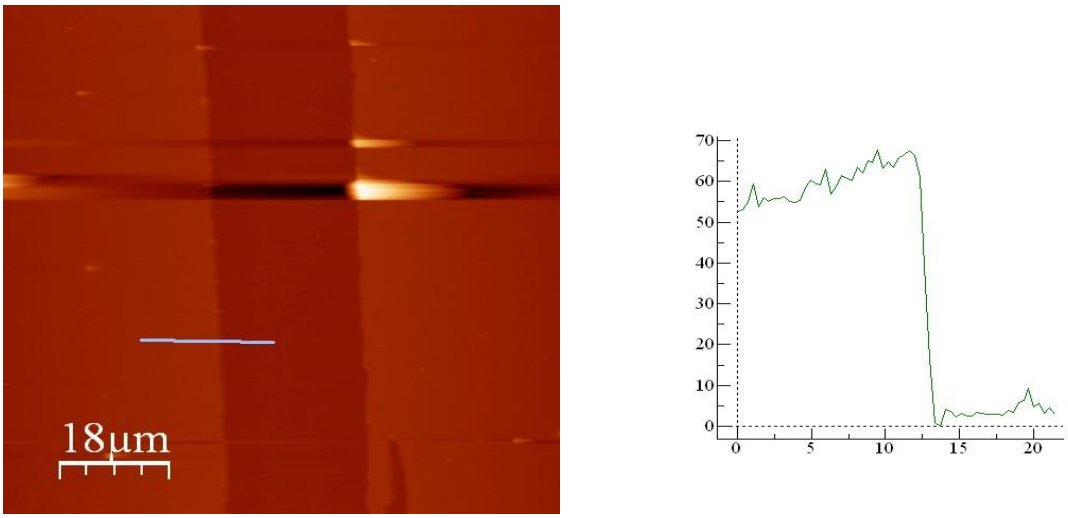

Figure 3-15. AFM indicating the thickness of the PEDOT:PSS film is 55nm.

3.8 MALDI Spectra

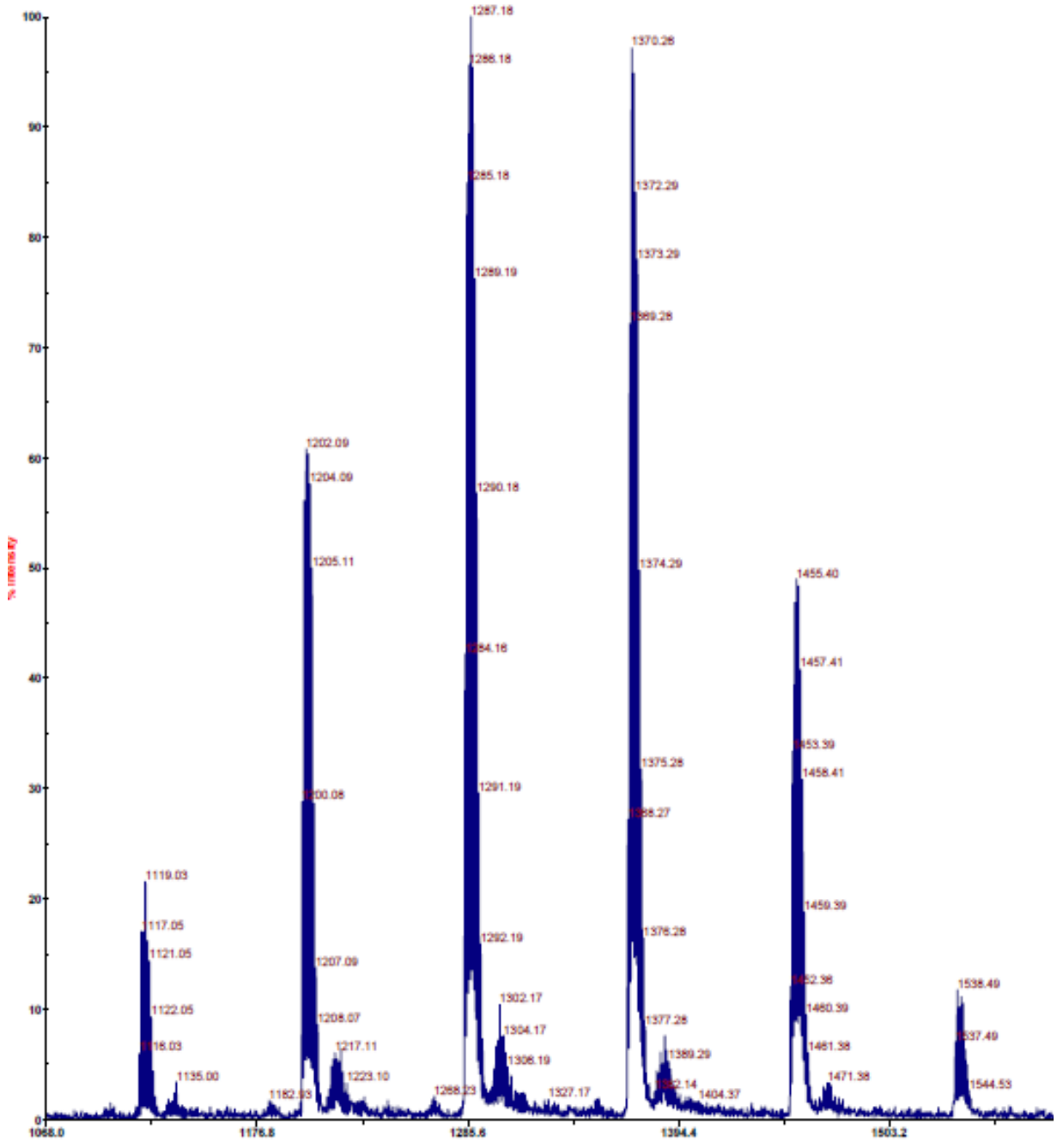

Figure 3-16. MALDI-MS of the **Pc-4-C5** used.

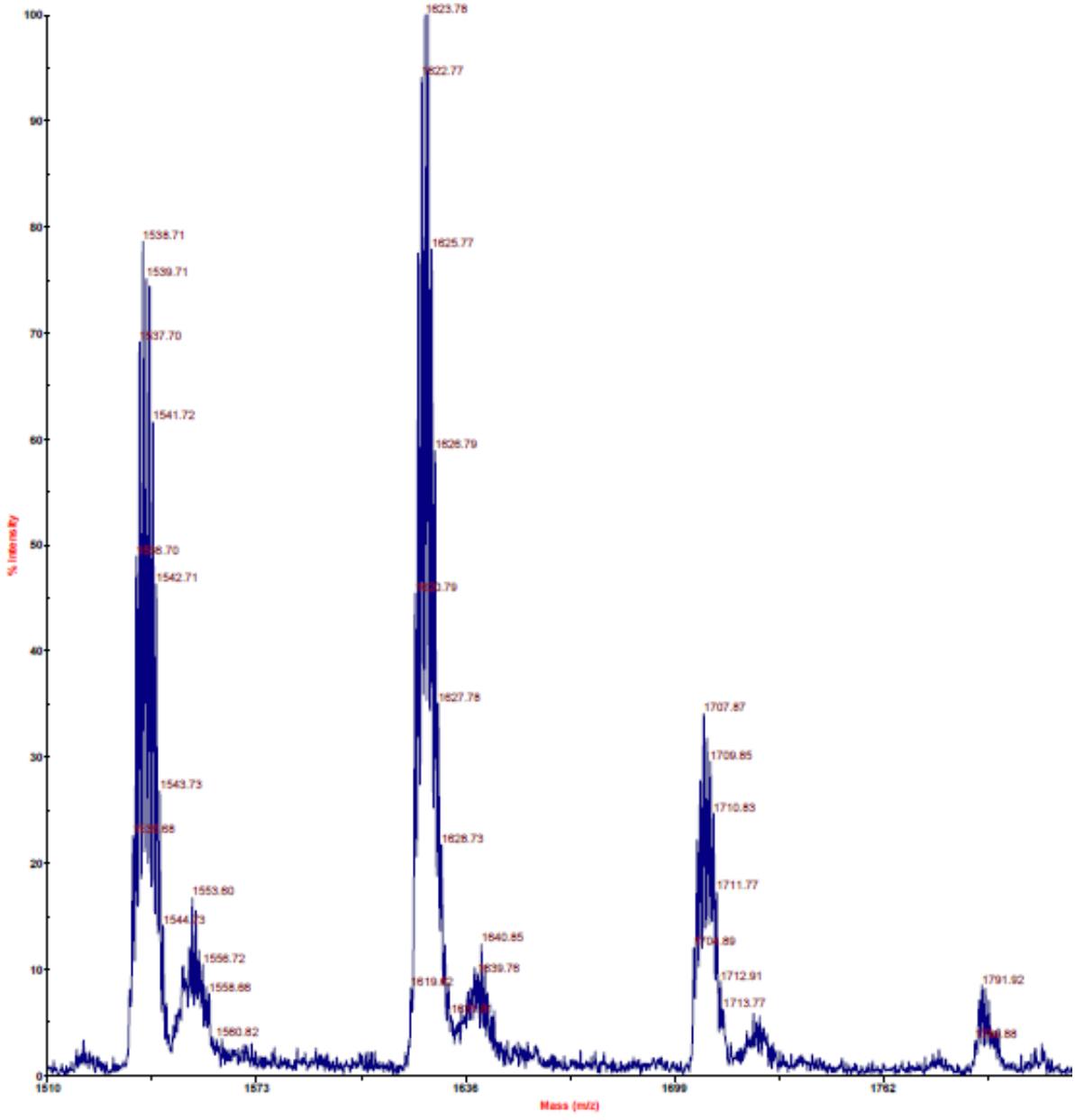

Figure 3-17. MALDI-MS of the **Pc-8-C5** used.

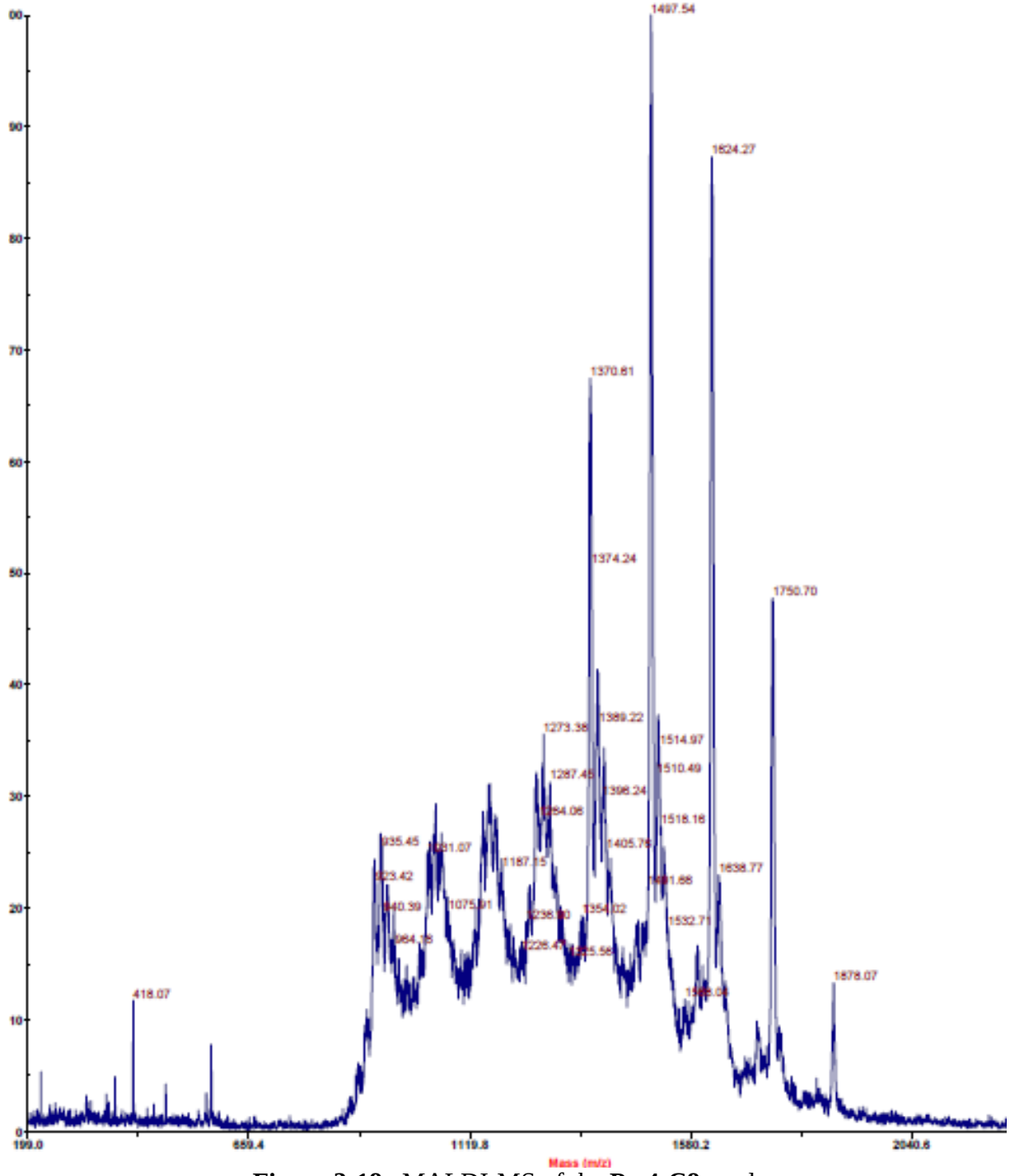

Figure 3-18. MALDI-MS of the **Pc-4-C8** used.

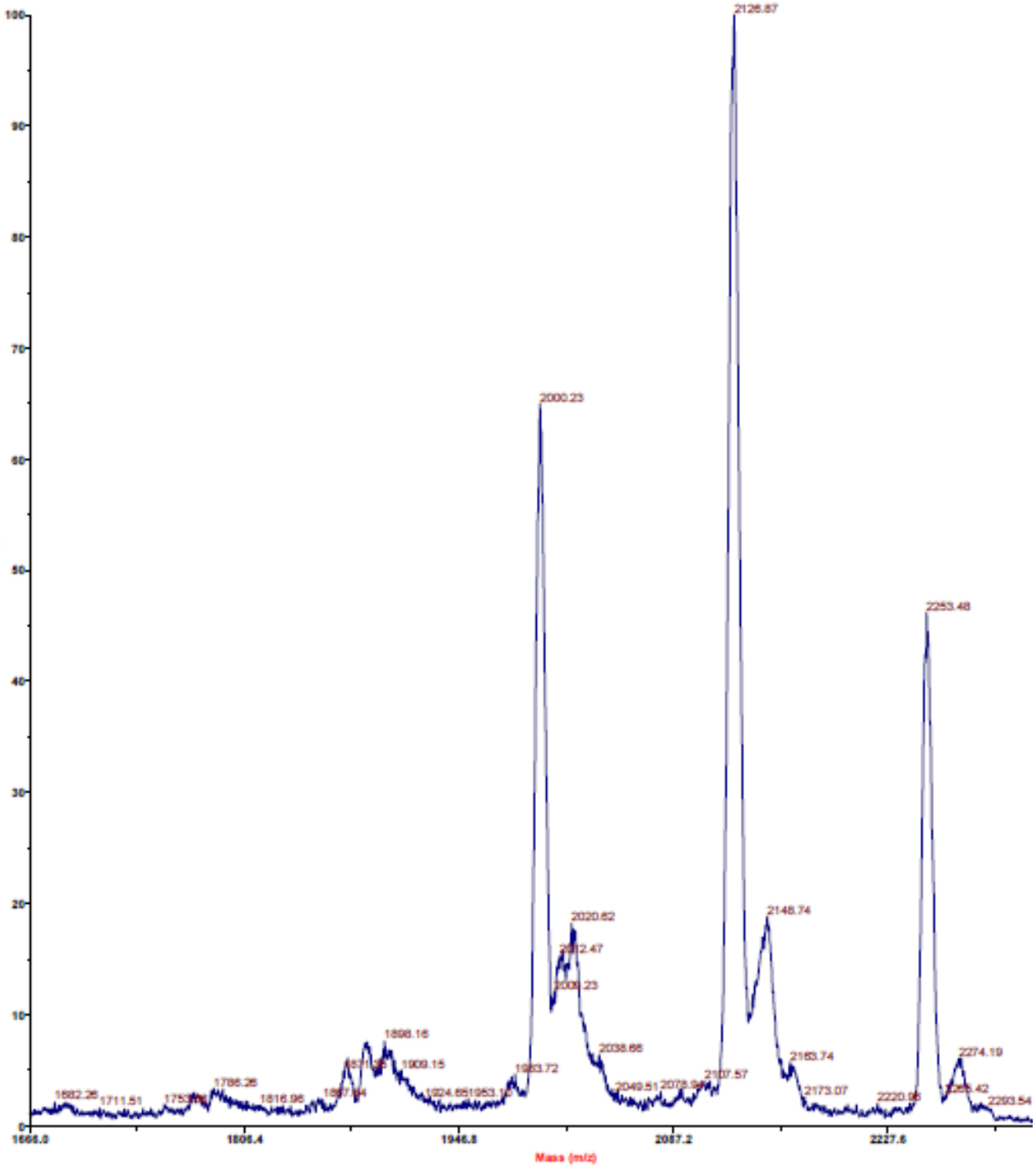

Figure 3-19. MALDI-MS of the **Pc-8-C8** used.

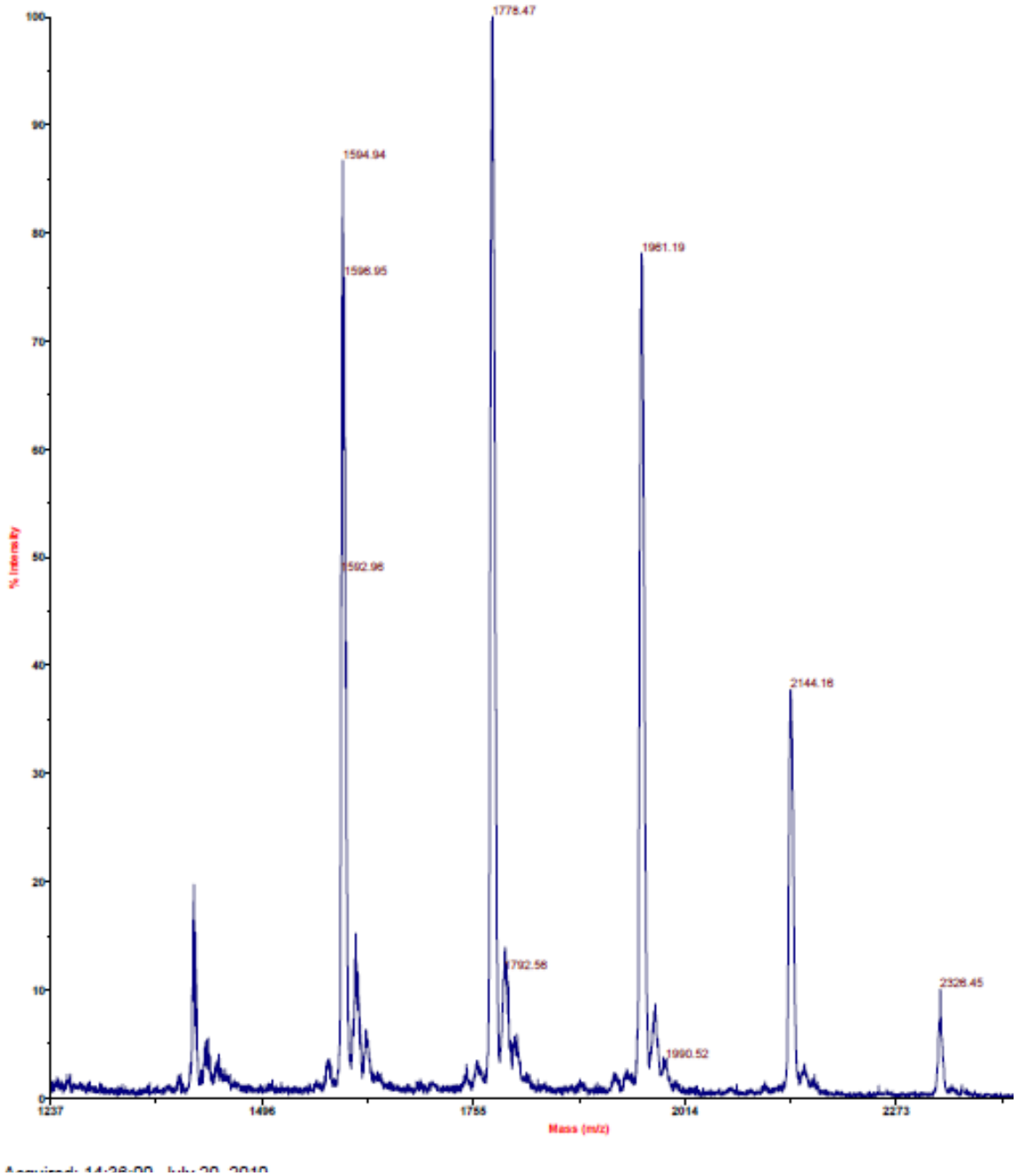

Figure 3-20. MALDI-MS of the **Pc-4-C12** used.

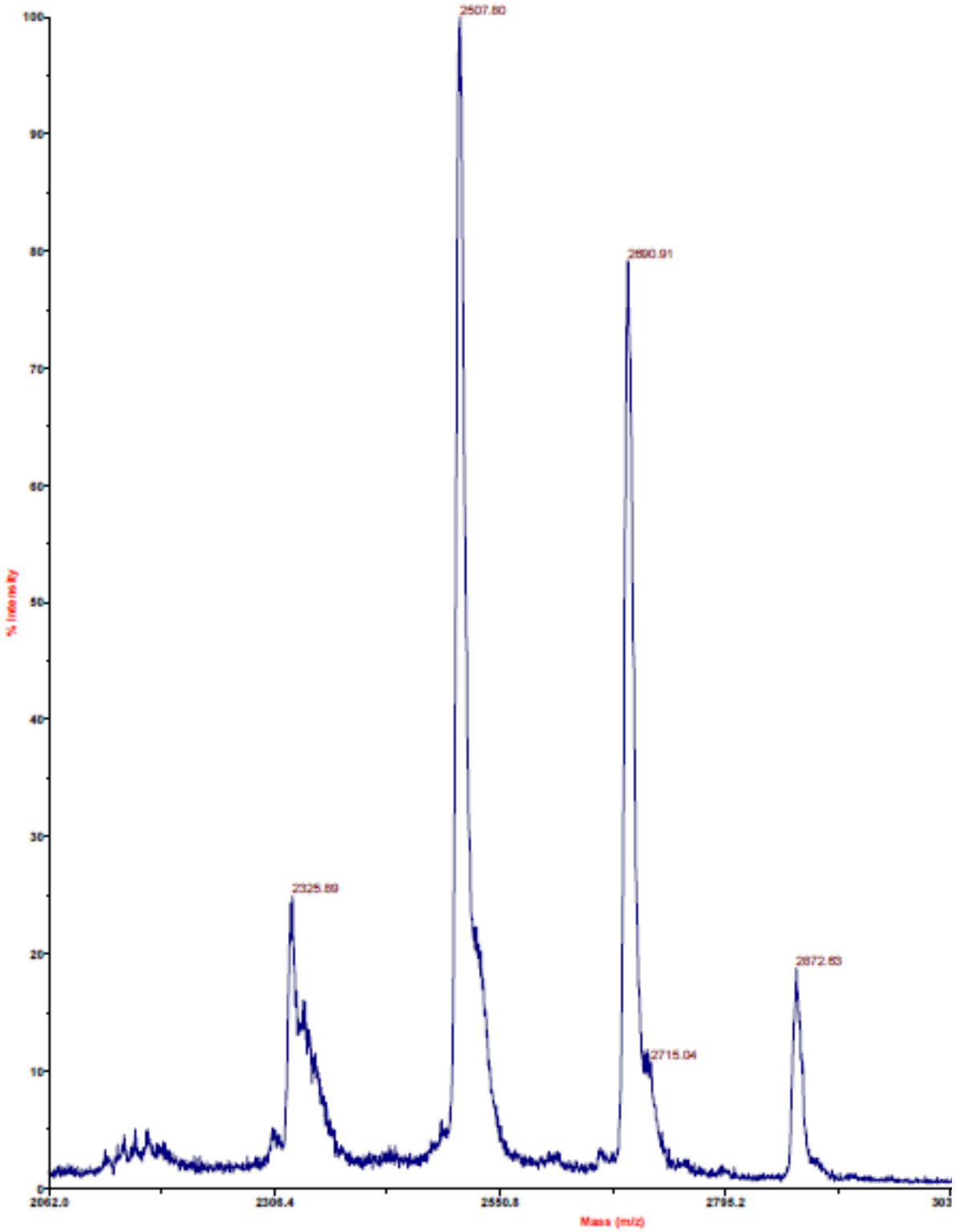

Figure 3-21. MALDI-MS of the **Pc-8-C12** used.

3.9 UV-visible Spectra

Data reported from dyes in solution were tested in dichloromethane at a concentration of 17 µM.

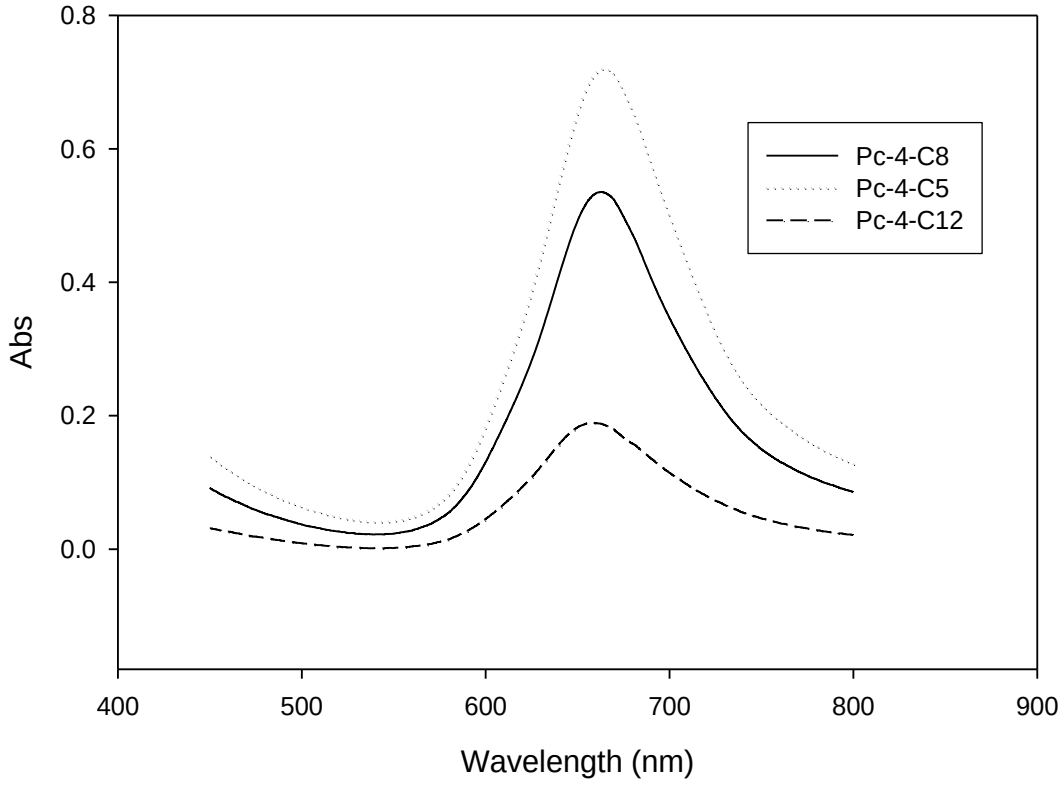

Figure 3-22. UV-visible spectra of the low energy Q band for the ZnPc tetra-substituted with three different alkanes shows that the absorbance increases as the chain length decreases for the same thickness of the films.

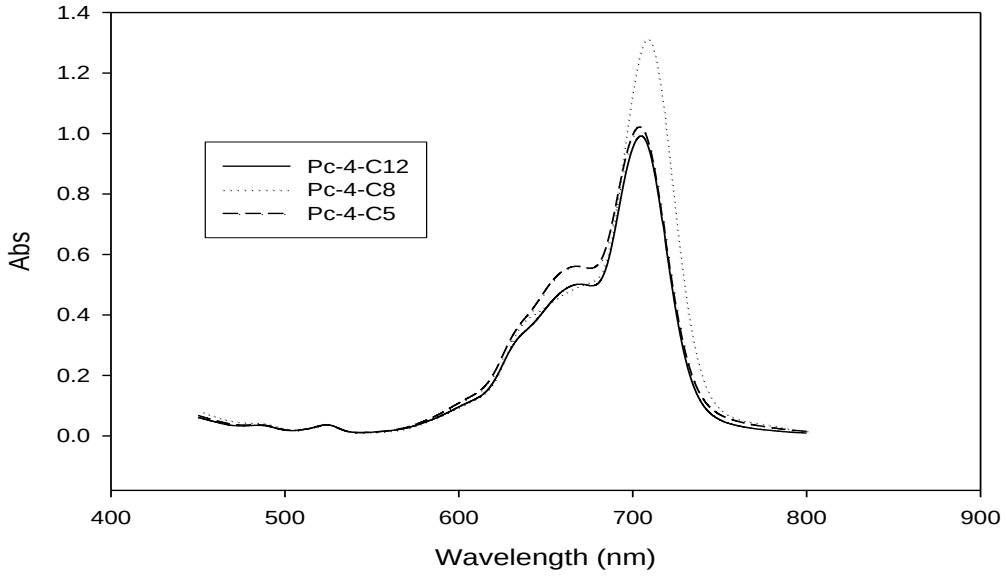

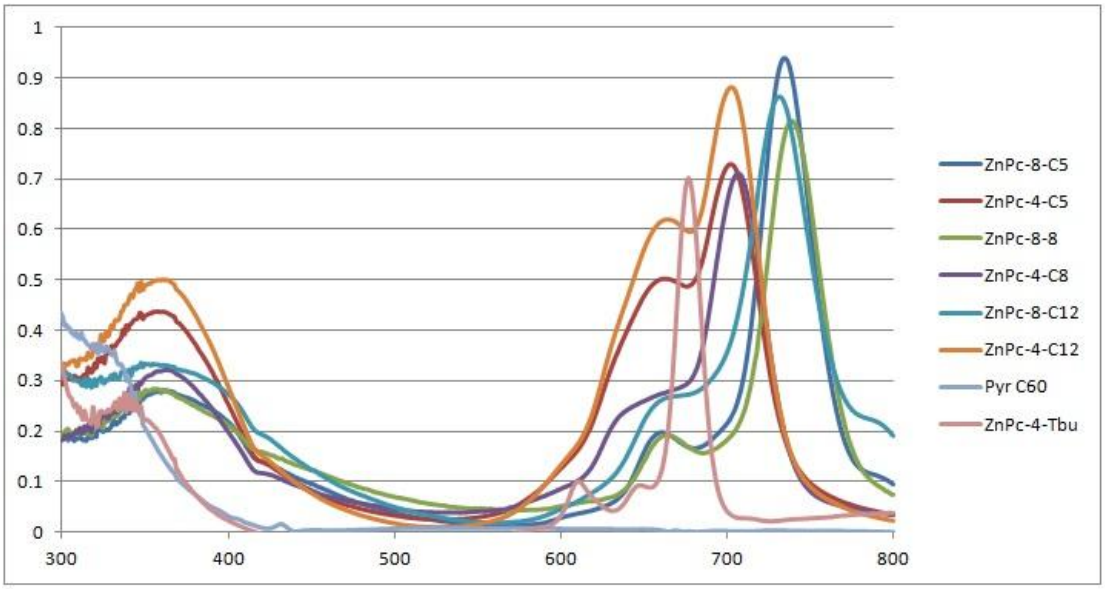

Figure 3-23. Top: UV-visible spectra of the low energy Q band for the ZnPc tetra-substituted with three different alkanes shows that the absorbance in solution are similar. Bottom: UV-visible spectra of all of the ZnPc used; note the red-shift and broadening of the low energy Q band with increasing substitution,

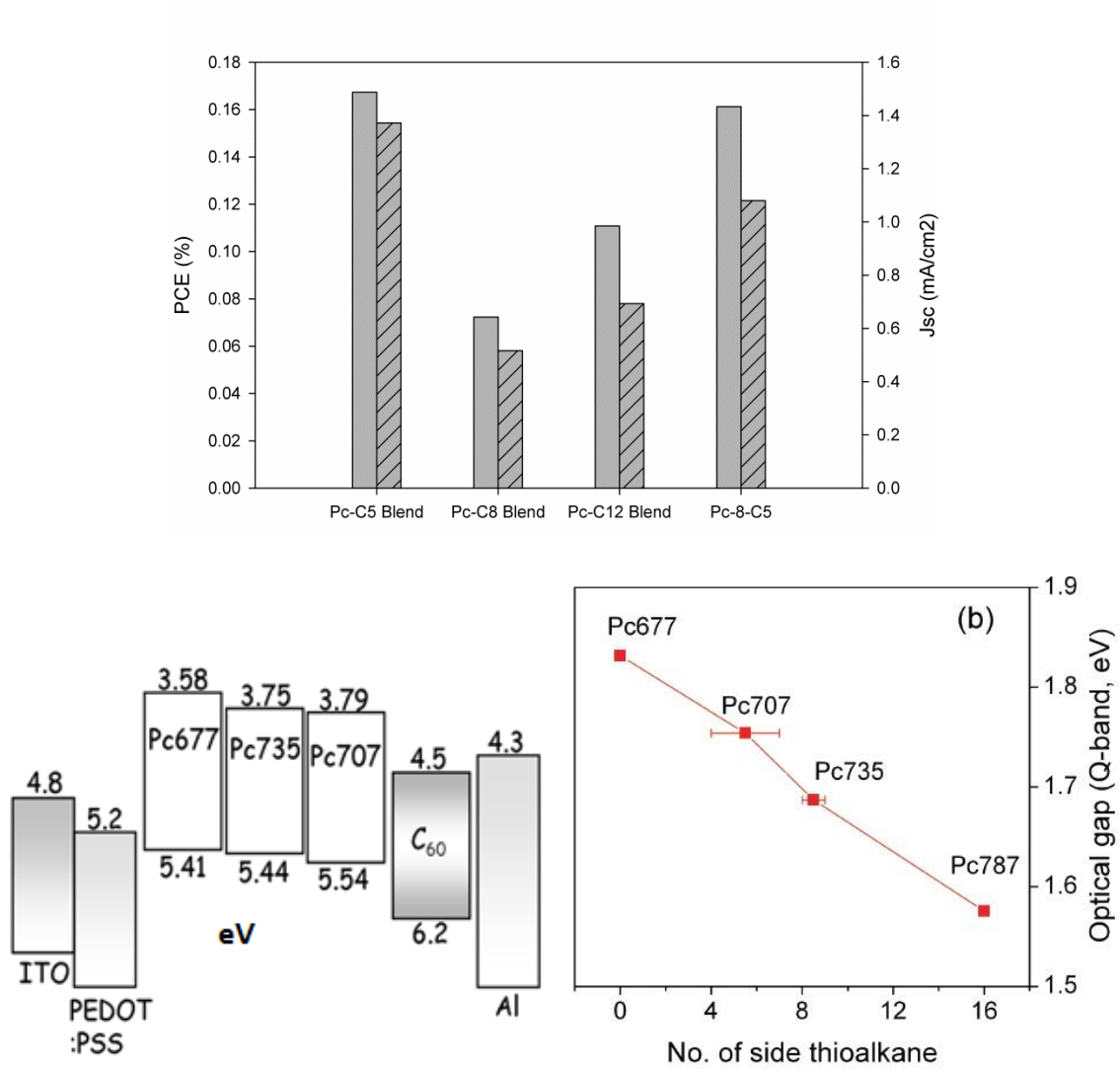

Figure 3-24. Top: Comparison of the key PV parameters for the different blended cells. Bottom: Band gaps and HOMO-LUMO gaps of some of the ZnPc dyes. Pc677=ZnPc-4-TBu; Pc707=ZnPc-4-C12; Pc735=ZnPc-8-C12. The number of F- and S-C12 substituents dictates the HOMO-LUMO gap. Figures taken from Varotto et al.[35]

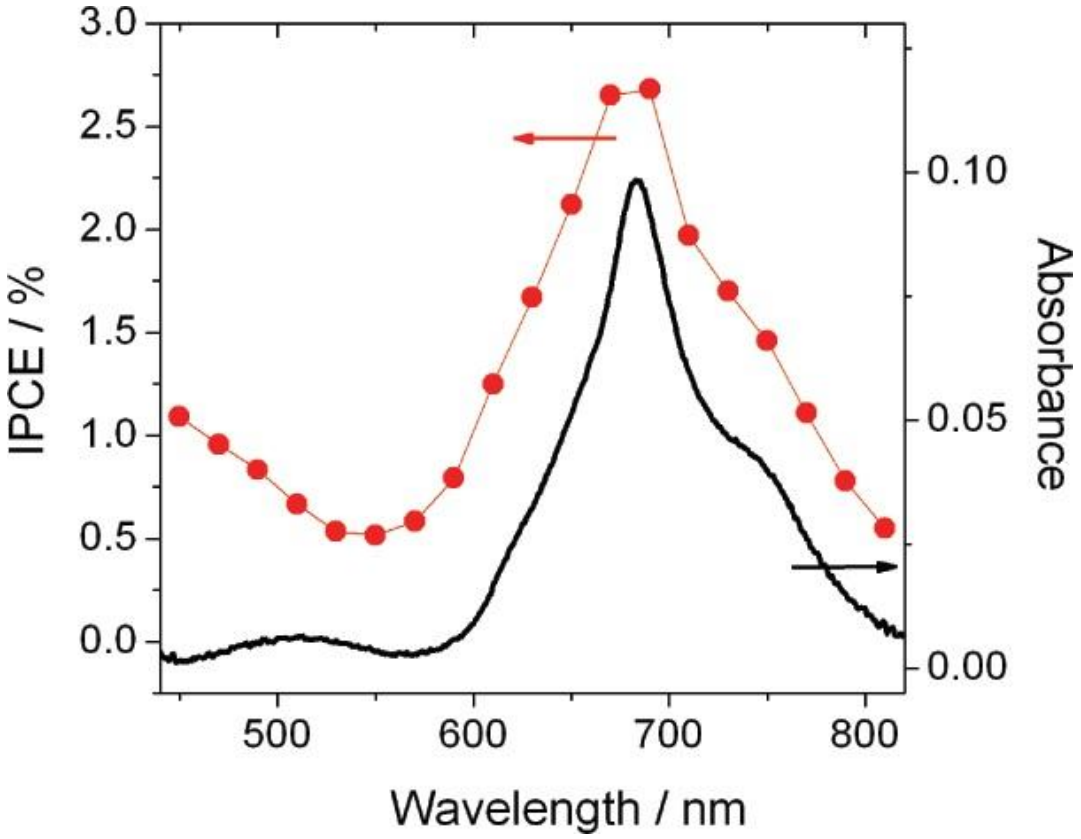

Figure 3-25. Comparison of the IPCE and the absorbance of a ZnPc-C12 Blend cell. Figure taken from Varotto et al.[35]

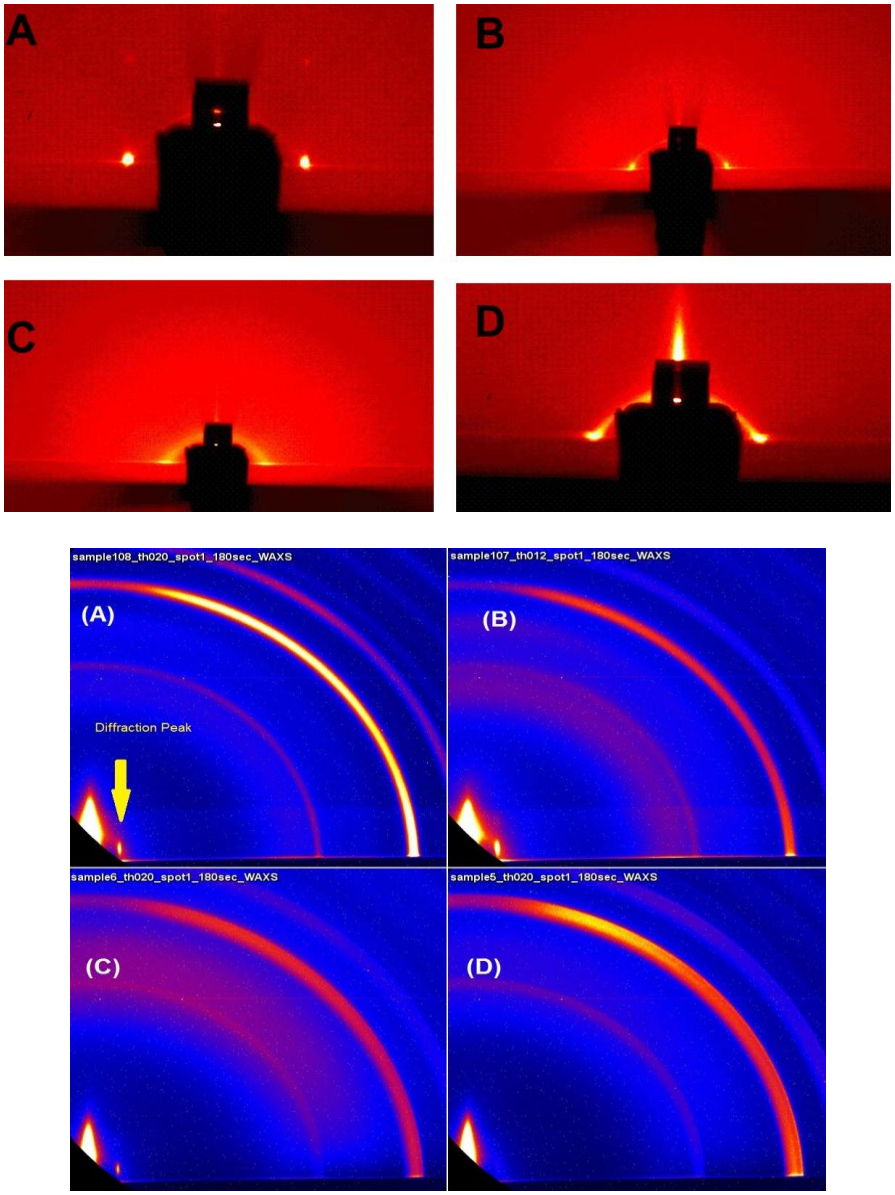

Figure 3-26. GISAXS false color images from X6B of ZnPc active layers on PEDOT:PSS on ITO (top) and mixtures of Pc-8-C12 devices with 5% (A), 10% (B), 15% (C), and 20% (D) Pc-4-Tbu on ITO from X9A (bottom). The patterns suggest short range hexagonal packing order on the ~35 Å scale. The addition of ZnPc-4-TBu diminishes the organization of the active layer. The lack of distinct separate, diffraction patterns suggests that there are no discrete domains of

individual dyes and instead there exists a blend. The ratio alkane subbed ZnPc: ZnPc-4-TBu was (A) 100:7.8, (B) 100:10.8, (C)100:19.29, and (D)is a blend of the three ZnPc with PyC_{60}.

3.10 Next Generation Compounds

The above studies demonstrated the importance of the alky chain in dictating the nanomorphology of the active layer in the BHJ solar cells. We thought that the exocyclic motifs can bring other functionality to the active layer, e.g. by enhancing charge migration, robustness, and hierarchical structure. We explored the synthesis of several heretofore unknown phthalocyanine dyes with functional side chains that were chosen because of known properties (Figure 3-27). Polyethylene glycols (PEG) have known ionic conductivity, there is some evidence that PEG material enhance charge migration, and the higher dieletric of films containing PEG appended dyes may enhance charge migration.[85-87] Para terphenyl moieties are robust to oxygen, light and temperature so are used in OLED and other photonic devices, thus have known photonic activity in addition to absorbing UV light.[88,89] The fluorous alkanes change the dielectric of the active layer film, are robust to oxidative degradation, and may facilitate charge separation.

In this regard, we further developed the click-type chemistry on the PcF_{16} and $TPPF_{20}$ core platforms where the condition of the reaction are somewhat modified to accound for the reactivity of primary versus aromatic thiols, solubility, and yield optimization. For the most part, solubility issues and chemical compatibility with the spin cast conducting polymer layers hampered the ability to incorporate these compounds into the BHJ solar cell described above.

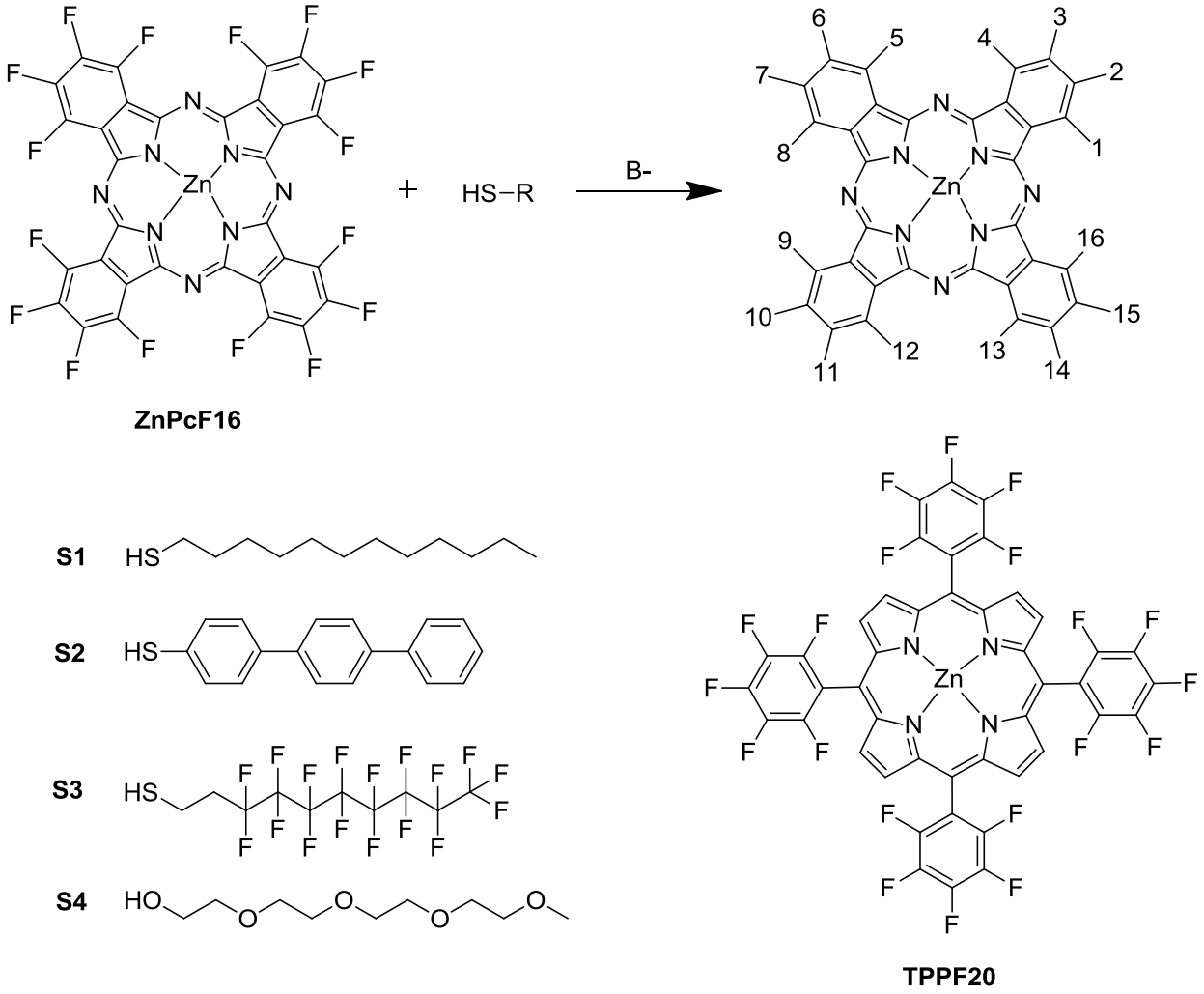

Figure 3-27. Basic synthetic scheme of substituted fluorous porphyrinoids with various alkane thiols.

Many of the materials used in our diverse projects shared a common basic synthetic framework (Figure 3-27). The standard procedure involves reacting a fluorous phthalocyanine or a fluorous porphyrin with any number of thiols or alcohols. The degree of substitution can be controlled by solvent choice and alteration of reaction conditions as well as concentration of the overall reaction mixture and duration of reaction. Reactions yield a distribution of substituted

products. Compound were purified by column unless demarked with an * in which case they were precipitated from methanol.

Table 3-3. Specific reaction conditions for various products.

Name Notebook	**Platform**	**Substituent**	**Molar Equivalents**	**Positions**	**Base**	**Solvent**	**Time**	**Temp**
1-424 8 Terphenyl Pc	$ZnPcF_{16}$	S2	10 eq	2 and 3, 6 and 7, 10 and 11, 14 and 15	K_2CO_3	DMF	24H	153
1-438 4 Terphenyl 4 alkyl Pc	ZnPc707	S2	4.1 eq	2 or 3, 6 or 7, 10 or 11, and 14 or 15; others are alkylatd	K_2CO_3	DMF	15H	153
1-422 4 PEG Pc	$ZnPcF_{16}$	S4	Excess	2 or 3, 6 or 7, 10 or 11, and 14 or 15	K_2CO_3	S4	16H	122
1-414 8 PEG Pc	$ZnPcF_{16}$	S4	Excess	2 and 3, 6 and 7, 10 and 11, 14 and 15	K_2CO_3	S4	26H	122

Table 3-3 continued. Specific reaction conditions for various products.

1-475* $ZnPcF_{136}$	$ZnPcF_{16}$	S3	10 eq	2 or 3, 6 or 7, 10 or 11, 14 or 15	K_2CO_3	DMF	16H	153
1-477* $ZnPcF_{264}$	$ZnPcF_{16}$	S3	50 eq	2 and 3, 6 and 7, 10 and 11, 14 and 15	K_2CO_3	DMF	16H	153
1-472 $ZnTPPF_{16}SF$	$TPPF_{20}$	S3	5 eq	Para	DIPEA	DMF	16H	153
1-281 4 alkyl $TPPF_{16}$	$TPPF_{20}$	S1	4.1 eq	Para	DIPEA	DMF	1H	153
1-262 8 terphenyl $TPPF_{12}$	$TPPF_{20}$	S1	8 eq	Para	DEA	DMF	16H	153

Because the absorption and photonic properties of perylenediimides are complementary to the Pc and Por dyes, several readily synthesized perylenediimides were prepared according to literature procedures.[90] Perylene diimides were syntehsised to be blneded into dye sytems for use in BHJ cells. Though synthesized in good yield they were not adquately soluble in solvents which form good films by spin casting to be effective in active devices. The synthetic procedure which produced afforded the best yield was not employed for the initial derrivatives.[90] The

synthetic procedure used is exemplified below. Different derivatives are made exactly the same way by altering the amine used.

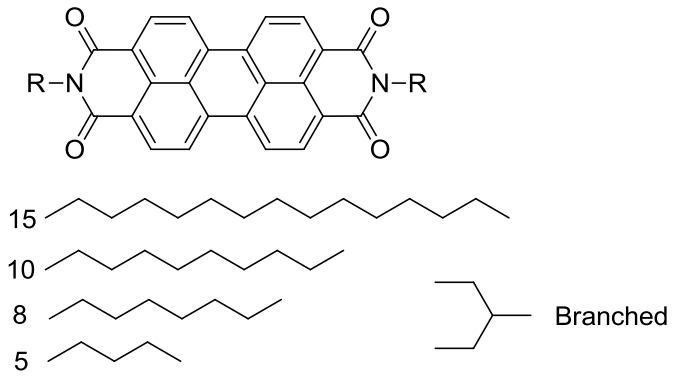

Figure 3-28. Perylene diimides with the featured alkyl substituents were synthesized in good yield. Detailed procedures for each derivative can be found in BH1-56-74.

Decylamino perylene bis-diimide

After flushing a three-neck round bottom, 2.93 g 3,4,9-10-tetracarboxylic perylene dianhydride, 02.938 g hexylamine (2.5 eq), and 4.04 g imidazole were heated to 180 C for 4 hours in 20 mL toluene. The mixture was cooled to room temperature, then 150 mL 2 N HCl and 75 mL ethanol were added. This was left to stir overnight. The resulting material was washed in a separation funnel with DI water and dichloromethane, concentrated via rotary evaporation and run through a silica gel column starting with pure dichloromethane and increasing MeOH to 5%. The product recrystallized from chloroform and methanol.

3.11 Perylene Spectra

Table 3-4. Perylene diimides

Substitution	**Calculated M/Z**	**Found M/z**
ethyl hexyl	530.6	530.0
C10	671.8	672.3
C6	558.2	558.2

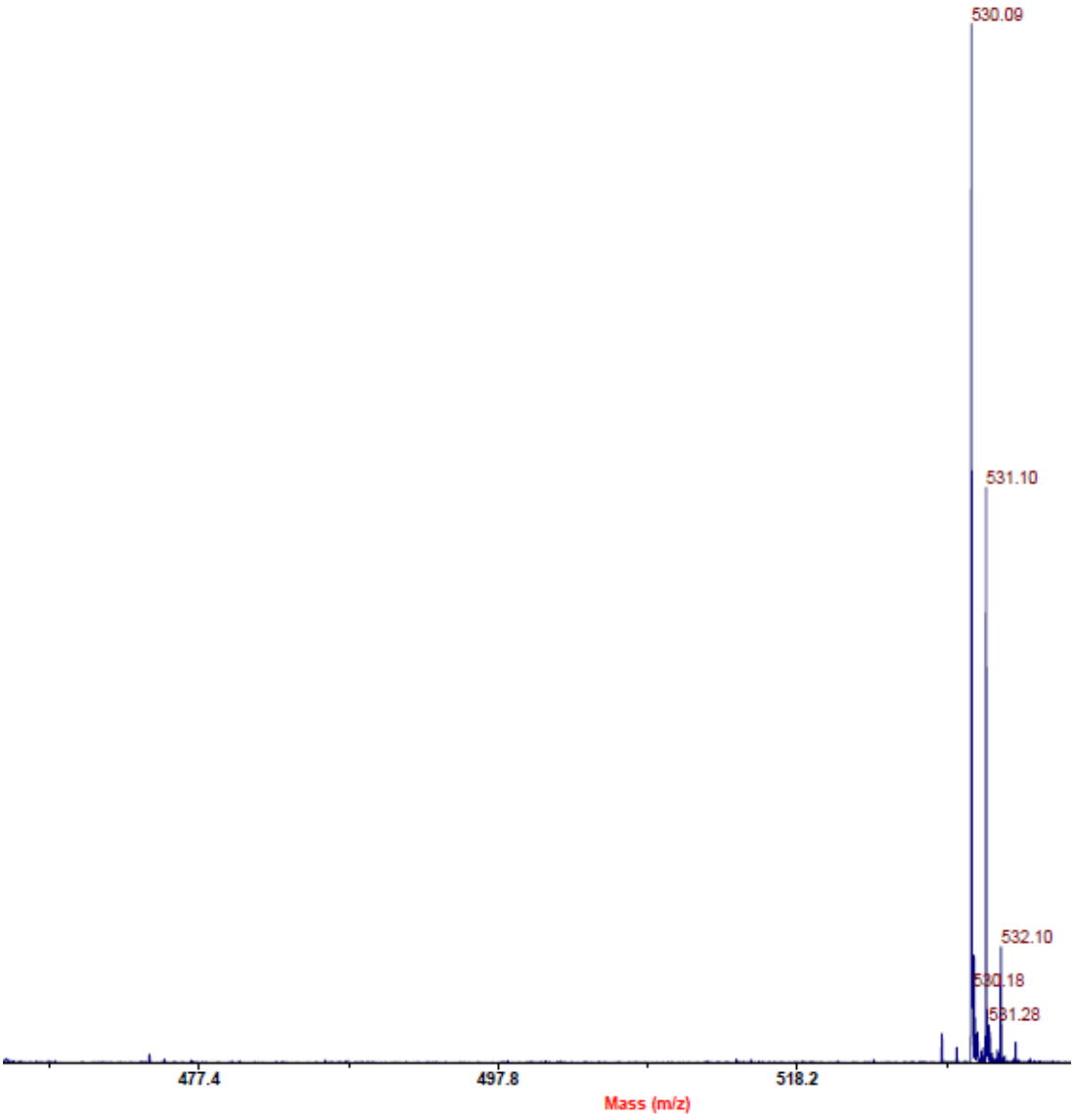

Figure 3-29. MALDI ethyl hexyl perylene

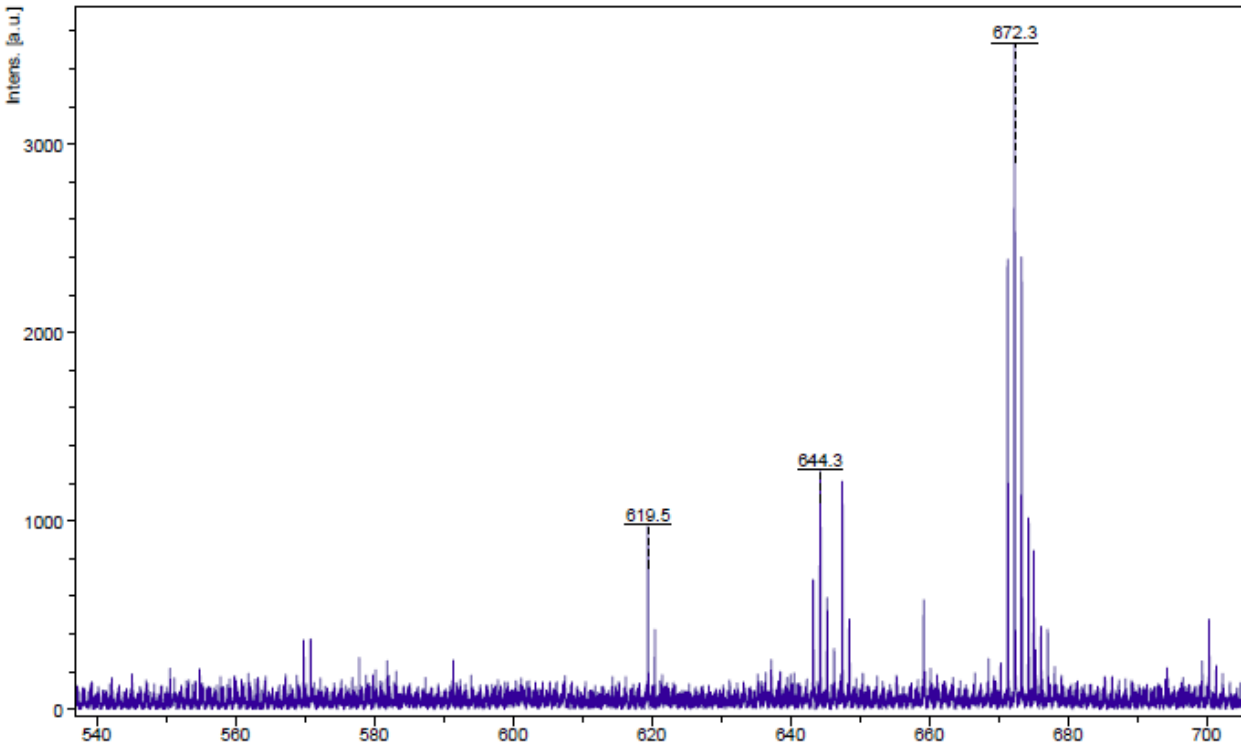

Figure 3-30. MALDI decyl perylene

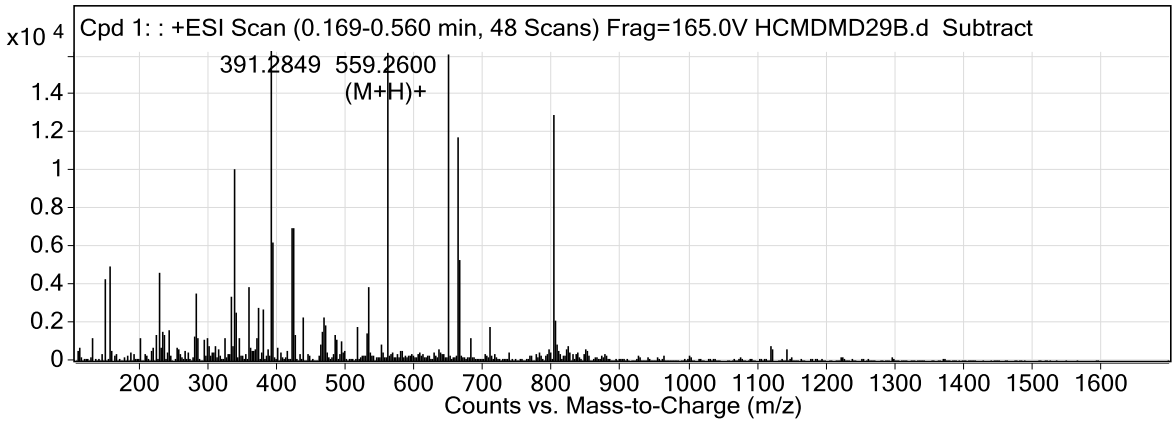

Figure 3-31. MALDI hexyl perylene

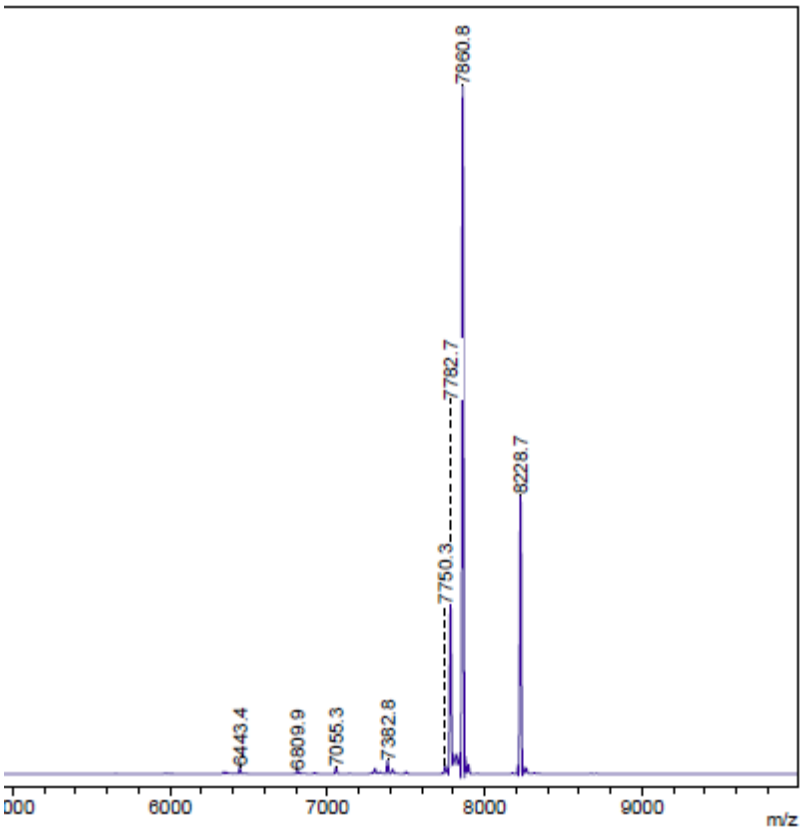

Figure 3-32. MALDI $ZnPcF_{264}$

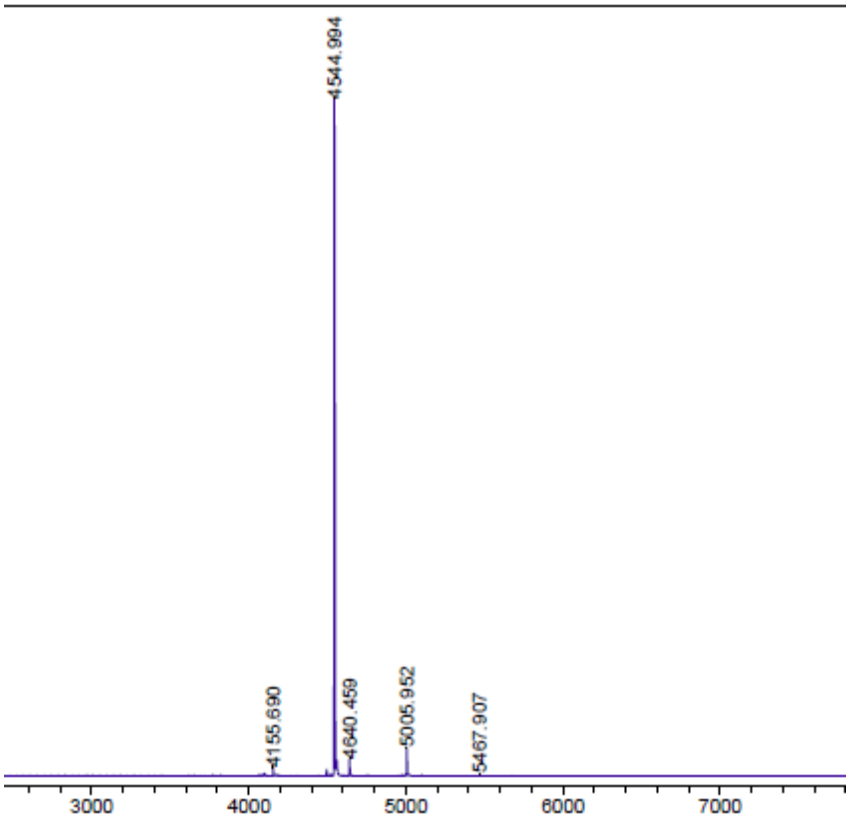

Figure 3-33. MALDI $ZnPcF_{136}$

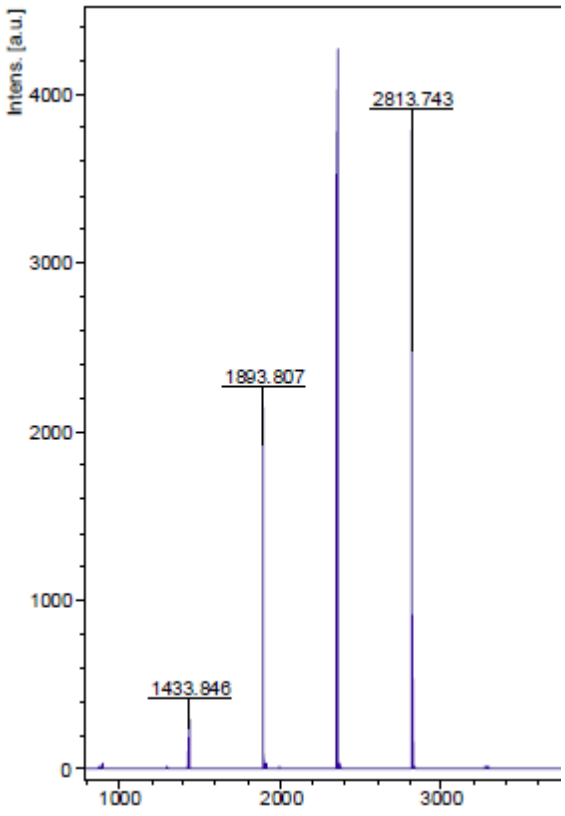

Figure 3-34. MALDI $TPPF_{84}$

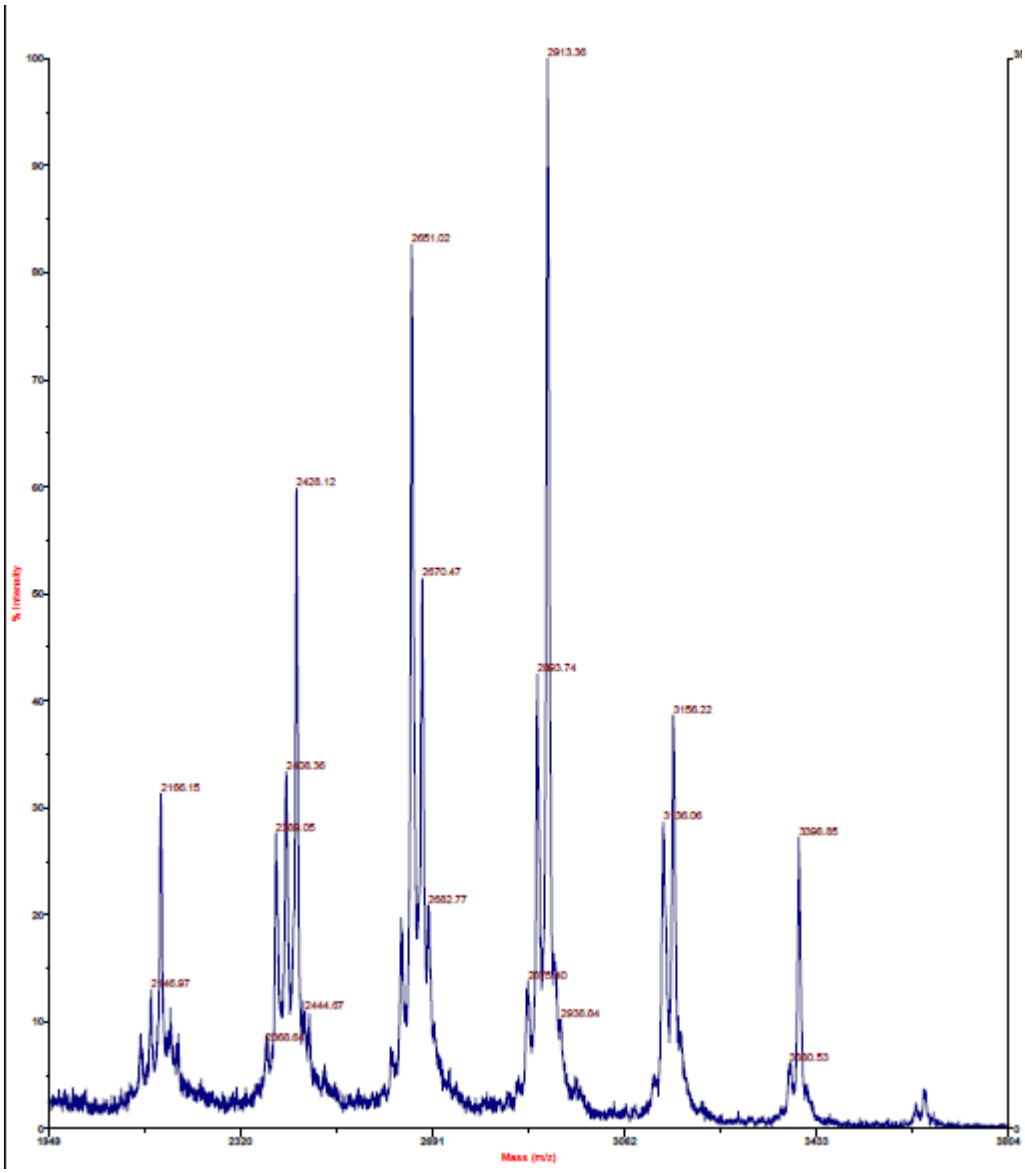

Figure 3-35. MALDI 1-262 8 terphenyl TPPF12

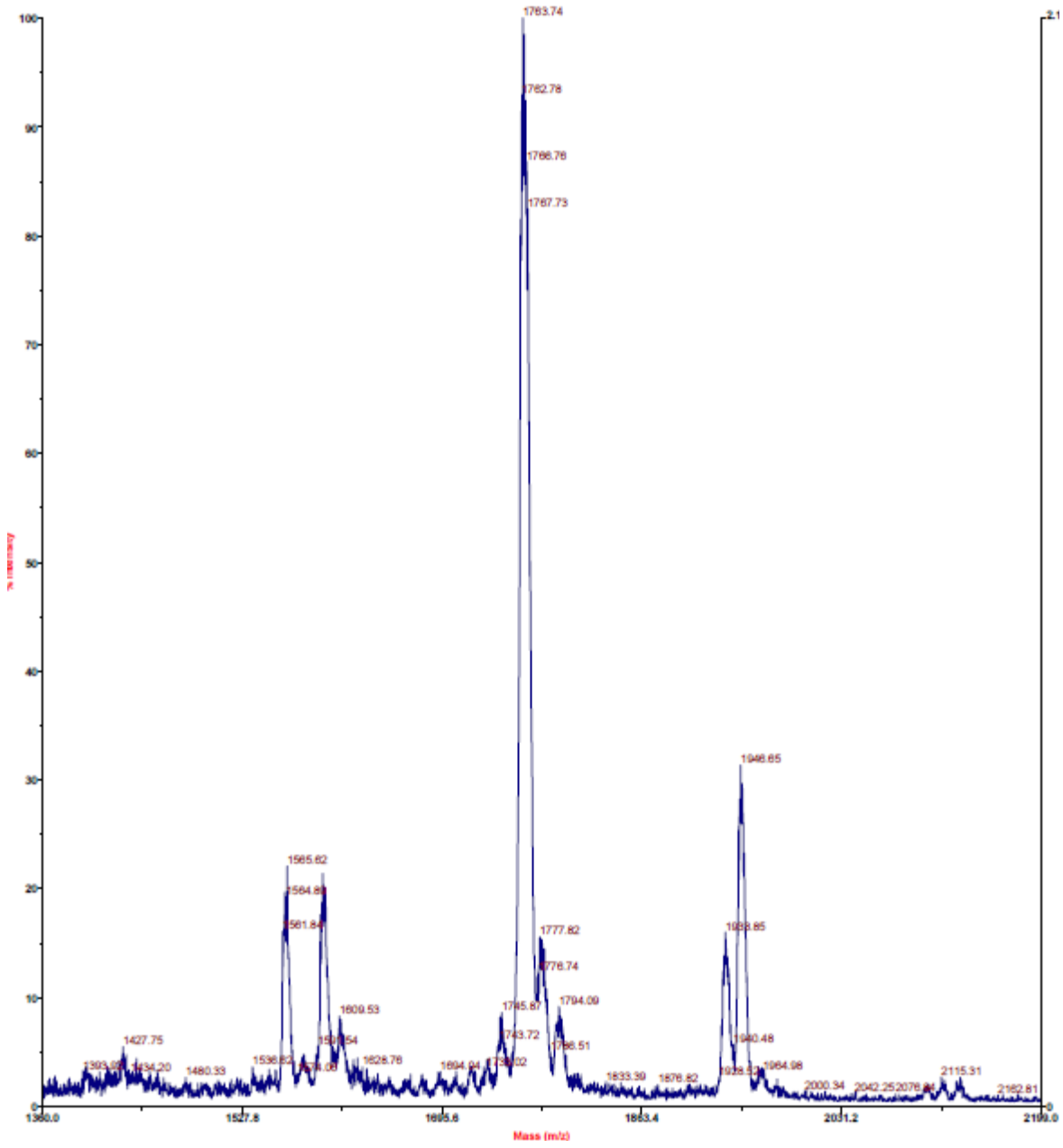

Figure 3-36. MALDI 1-281 4 alkyl TPPF16

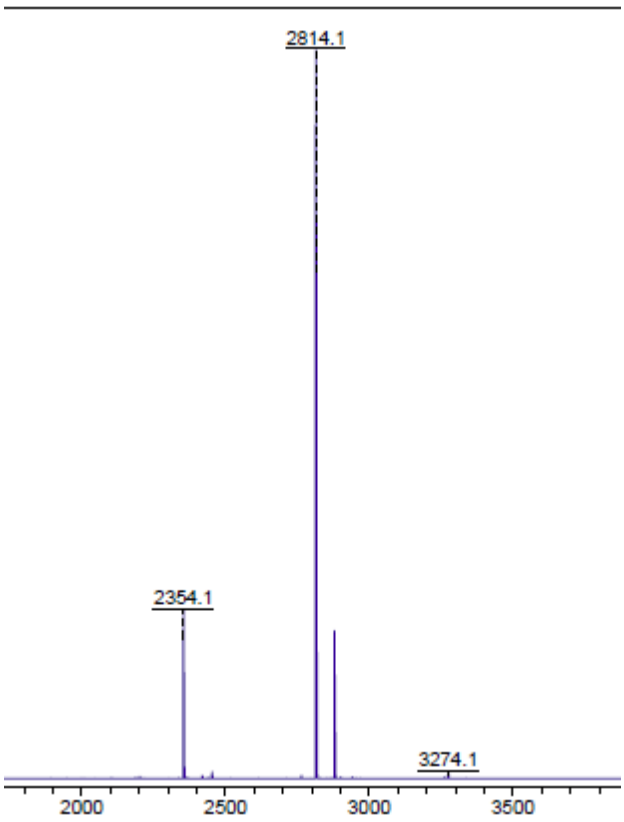

Figure 3-37. MALDI of 1-472 ZnTPPF16SF

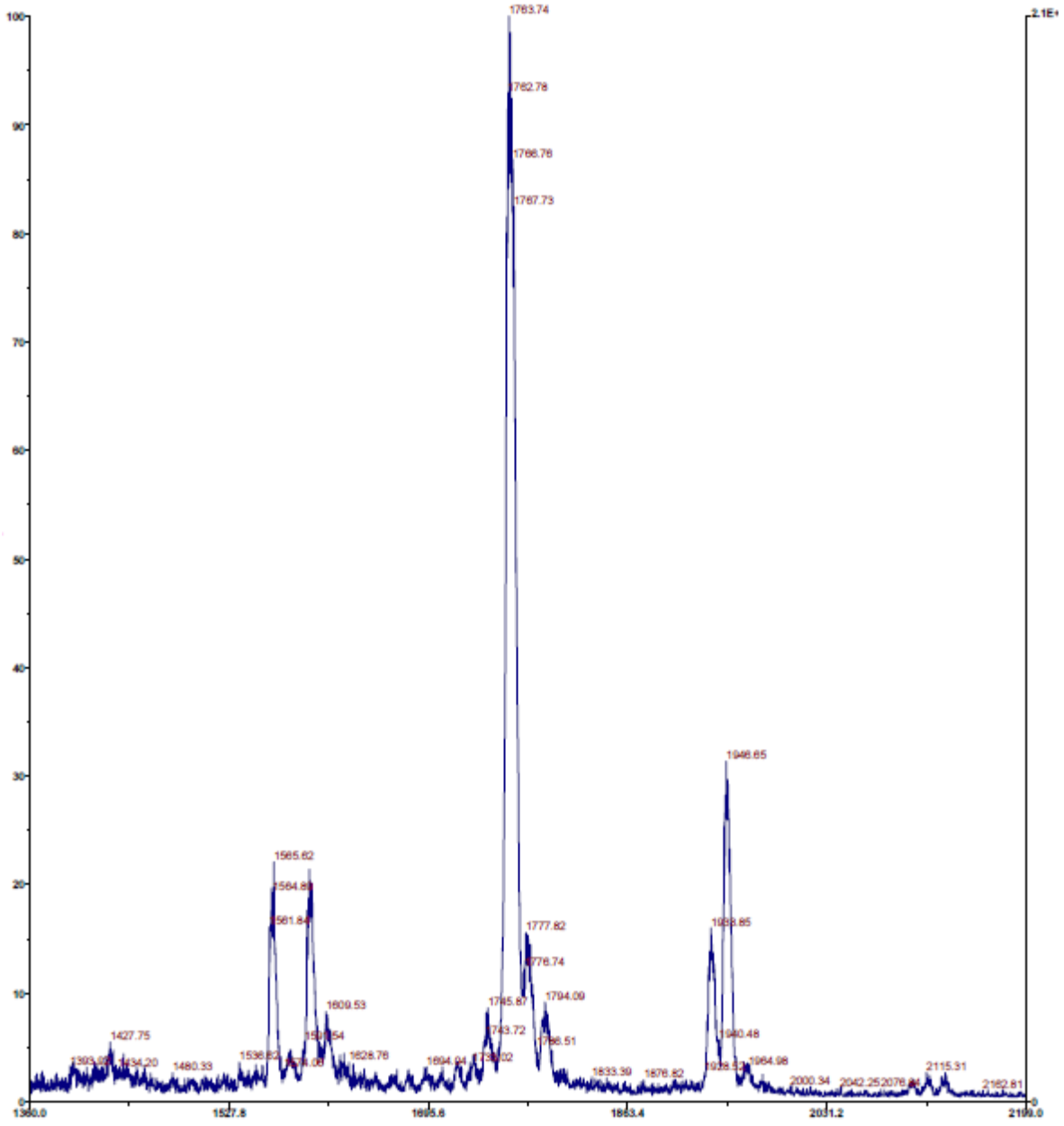

Figure 3-38. MALDI of TPPF16 4-C12 MJ 1-281

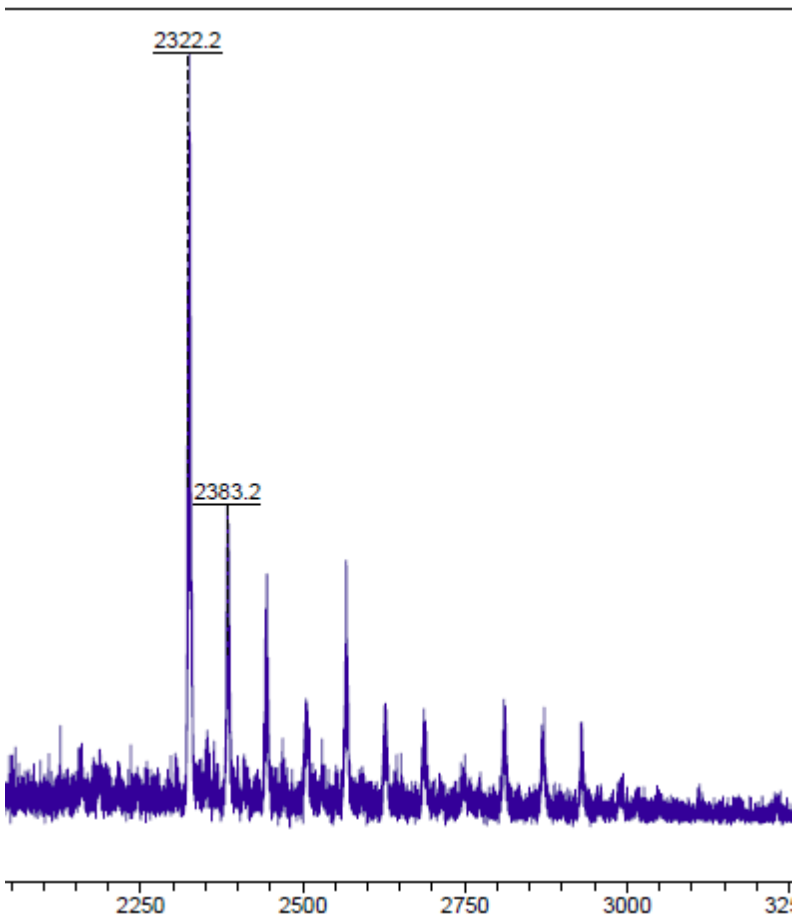

Figure 3-39. MALDI of 1-438 4 Terphenyl 4 alkyl Pc

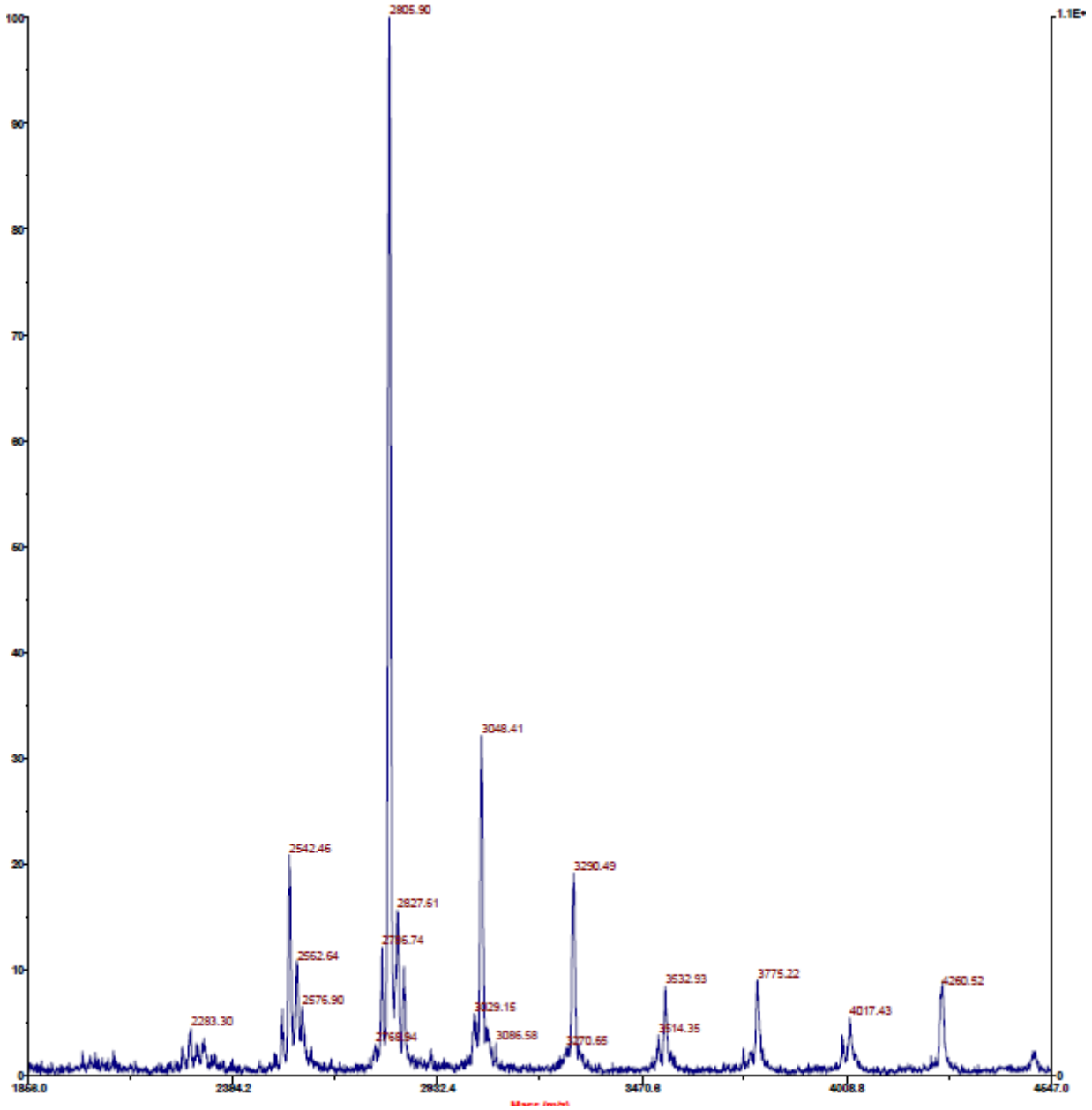

Figure 3-40. MALDI of 1-424 8 Terphenyl Pc

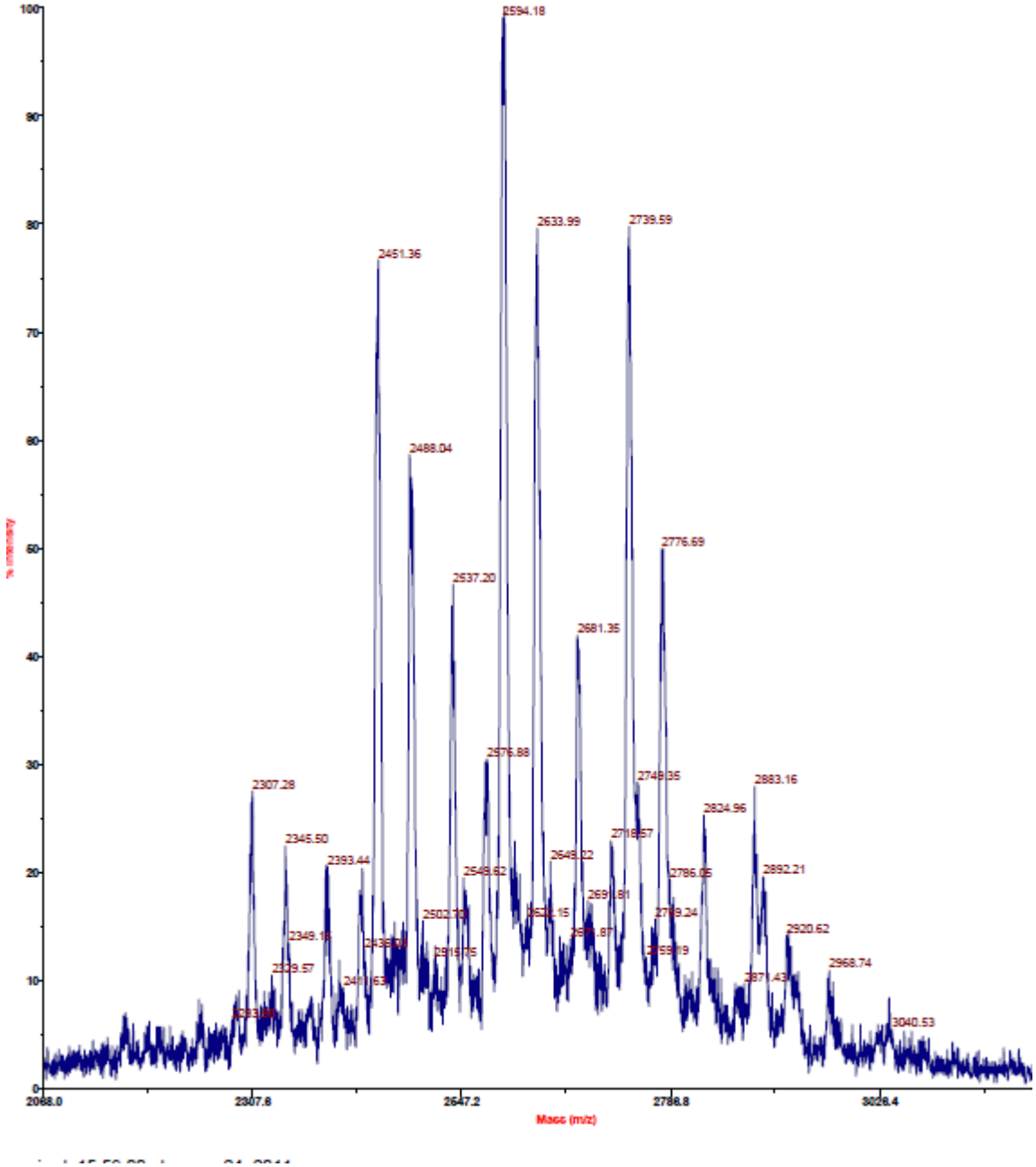

Figure 3-41. MALDI of 1-414 8 PEG Pc

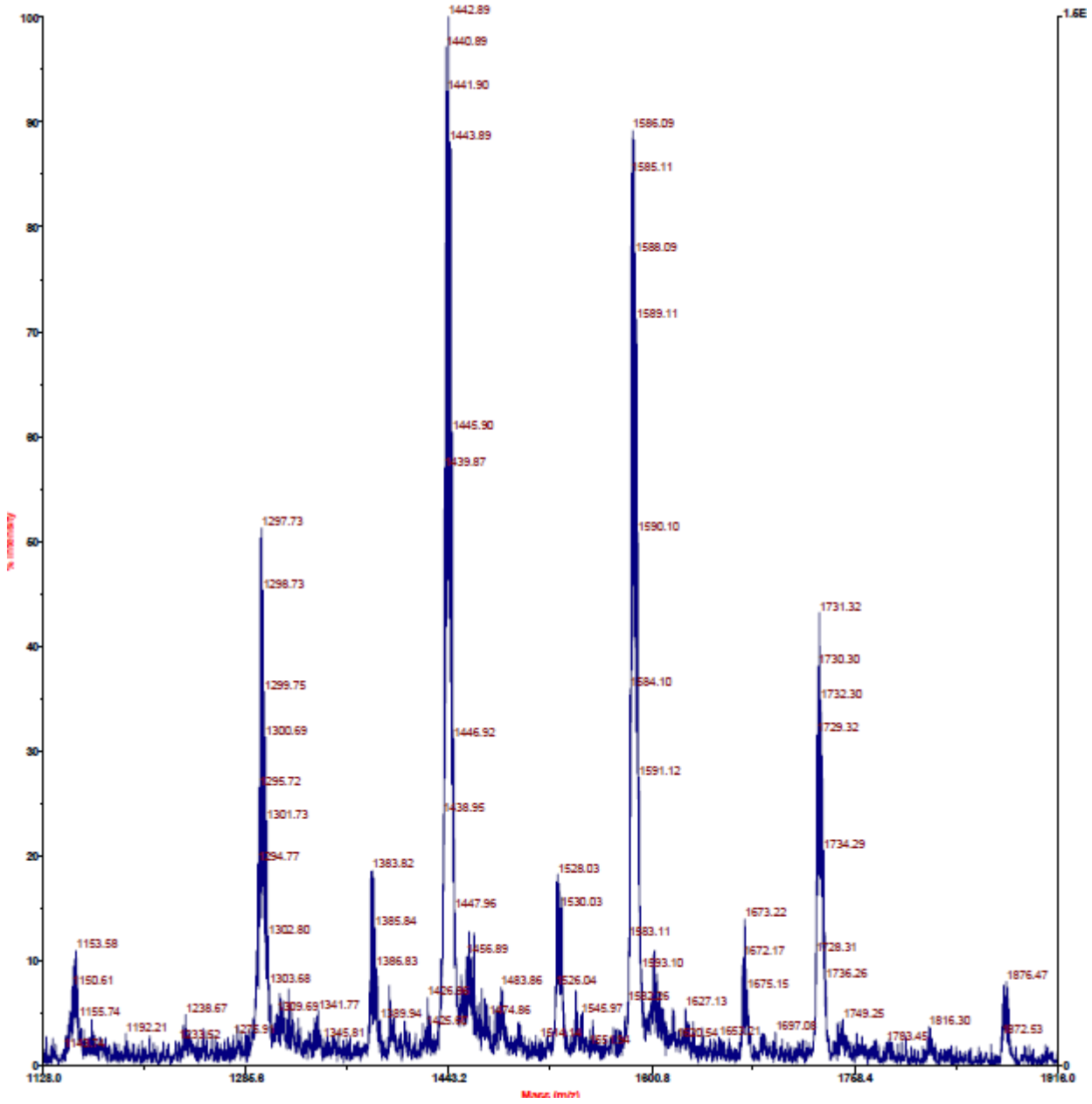

Figure 3-42. MALDI of 1-422 4 PEG Pc

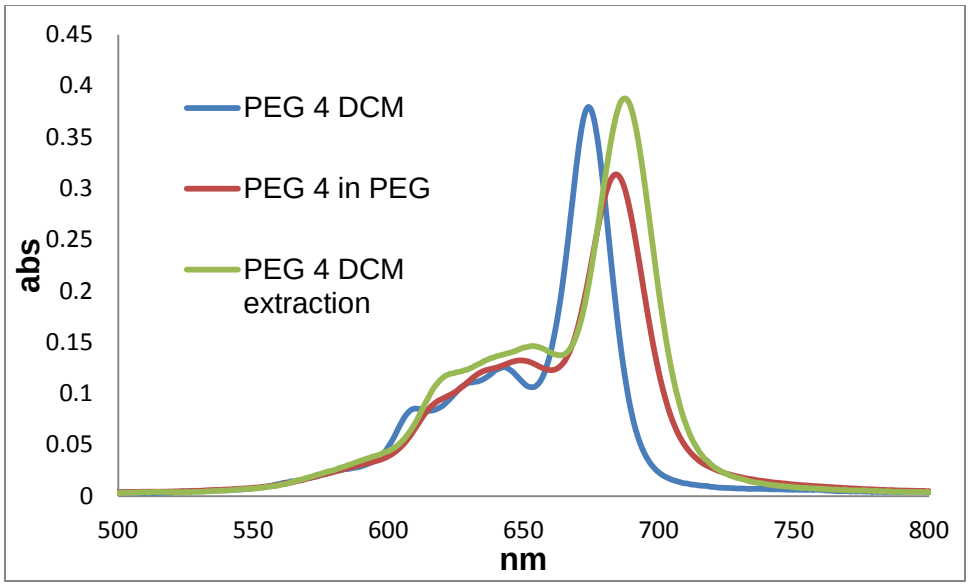

Figure 3-43. UV visible absorption spectrum of PEG substituted ZnPcF16 in various solvents from reaction mixture or after work up with water and extraction into DCM.

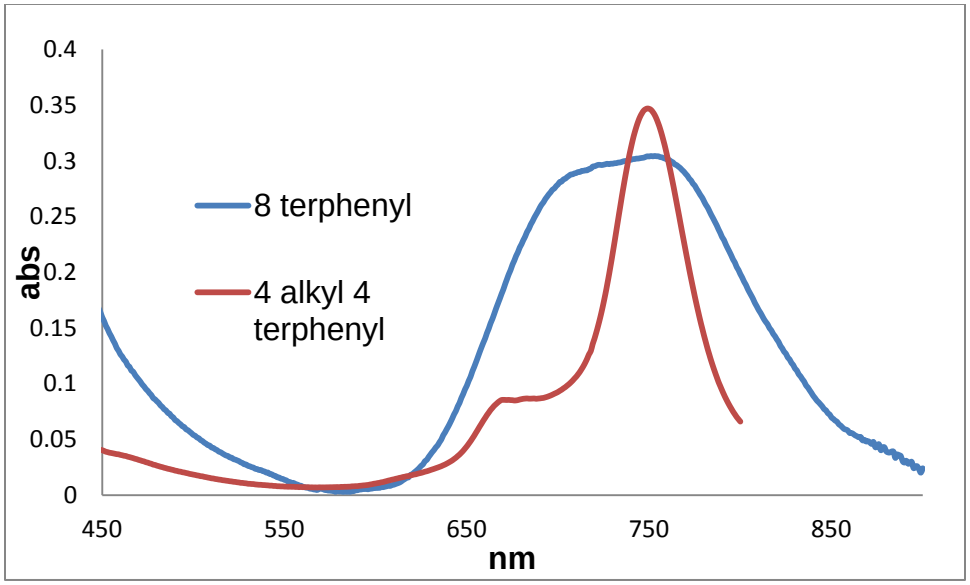

Figure 3-44. UV visible absorption spectrum of various terphneyl substituted ZnPcF16 species.

3.12 References

Adapted from "Controlling morphology and molecular packing of alkane substituted phthalocyanine blend bulk heterojunction solar cells"; Jurow et al., J Mater Chem A DOI: 10.1039/c2ta00415a

(1) Ameri, T.; Dennler, G.; Lungenschmied, C.; Brabec, C. J. *Energy Env. Sci.* **2009**, *2*, 347.

(2) Clarke, T. M.; Durrant, J. R. *Chem. Rev.* **2010**, *110*, 6736.

(3) Liang, Y.; Yu, L. *Poly. Rev.* **2010**, *50*, 454

(4) Zheng, Y.; Xue, J. *Poly. Rev.* **2010**, *50*, 420

(5) Ratcliff, E. L.; Zacher, B.; Armstrong, N. R. *J. Phys. Chem. Let.* **2011**, *2*, 1337.

(6) Krebs, F. C.; Fyenbo, J.; Tanenbaum, D. M.; Gevorgyan, S. A.; Andriessen, R.; van Remoortere, B.; Galagan, Y.; Jorgensen, M. *Energ. Envir. Sci.* **2011**, *4*, 4116.

(7) Walker, B.; Kim, C.; Nguyen, T.-Q. *Chem. Mater.* **2011**, *23*, 470.

(8) Ooyama, Y.; Harima, Y. *Eur. J. Org. Chem.* **2009**, *2009*, 2903.

(9) Lee, H. J.; Leventis, H. C.; Haque, S. A.; Torres, T.; Grätzel, M.; Nazeeruddin, M. K. *J. Power Sources* **2011**, *196*, 596.

(10) Brabec, C. J.; Sariciftci, N. S.; Hummelen, J. C. *Adv. Funct. Mater.* **2001**, *11*, 15.

(11) Liao, K.-S.; Yambem, S. D.; Haldar, A.; Alley, N. J.; Curran, S. A. *Energies* **2010**, *3*, 1212.

(12) He, F.; Yu, L. *J. Phys. Chem. Lett.* **2011**, *2*, 3102.

(13) Bailey-Salzman, R. F.; Rand, B. P.; Forrest, S. R. *Appl. Phys. Lett.* **2006**, *88*, 233502.

(14) Peumans, P.; Uchida, S.; Forrest, S. R. *Nature* **2003**, *425*, 158.

(15) Scharber, M. C.; Mühlbacher, D.; Koppe, M.; Denk, P.; Waldauf, C.; Heeger, A. J.; Brabec, C. J. *Adv. Mat.* **2006**, *18*, 789.

(16) Khan, S. M.; Kaur, M.; Heflin, J. R.; Sayyad, M. H. *J. Phys. Chem. Solids* **2011**, *72*, 1430.

(17) Said, A. J.; Poize, G.; Martini, C.; Ferry, D.; Marine, W.; Giorgio, S.; Fages, F.; Hocq, J.; Bouclé, J.; Nelson, J.; Durrant, J. R.; Ackermann, J. *J. Phys. Chem. C* **2010**, *114*, 11273.

(18) Sun, Y.; Welch, G. C.; Leong, W. L.; Takacs, C. J.; Bazan, G. C.; Heeger, A. J. *Nat. Mater.* **2012**, *11*, 44.

(19) Chu, T.-Y.; Lu, J.; Beaupré, S.; Zhang, Y.; Pouliot, J.-R. m.; Wakim, S.; Zhou, J.; Leclerc, M.; Li, Z.; Ding, J.; Tao, Y. *J. Am. Chem. Soc.* **2011**, *133*, 4250.

(20) Zhu, Y.; Xu, X.; Zhang, L.; Chen, J.; Cao, Y. *Solar Energy Materials Solar Cells* **2012**, *97*, 83.

(21) Brabec, C. J.; Gowrisanker, S.; Halls, J. J. M.; Laird, D.; Jia, S.; Williams, S. P. *Adv. Materials* **2010**, *22*, 3839.

(22) Wang, D. H.; Kim, D. Y.; Choi, K. W.; Seo, J. H.; Im, S. H.; Park, J. H.; Park, O. O.; Heeger, A. J. *Angew. Chem. Int. Ed.* **2011**, *50*, 5519.

(23) Allen, J. E.; Yager, K. G.; Hlaing, H.; Nam, C.-Y.; Ocko, B. M.; Black, C. T. *Appl. Phys. Lett.* **2011**, *99*, 163301.

(24) Hlaing, H.; Lu, X.; Hofmann, T.; Yager, K. G.; Black, C. T.; Ocko, B. M. *ACS Nano* **2011**, *5*, 7532.
(25) Allen, J. E.; Black, C. T. *ACS Nano* **2011**, *5*, 7986.
(26) Wu, W.-R.; Jeng, U. S.; Su, C.-J.; Wei, K.-H.; Su, M.-S.; Chiu, M.-Y.; Chen, C.-Y.; Su, W.-B.; Su, C.-H.; Su, A.-C. *ACS Nano* **2011**, *5*, 6233.
(27) Loser, S.; Bruns, C. J.; Miyauchi, H.; Ortiz, R. o. P.; Facchetti, A.; Stupp, S. I.; Marks, T. J. *J. Am. Chem. Soc.* **2011**, *133*, 8142.
(28) Lee, C. Y.; She, C.; Jeong, N. C.; Hupp, J. T. *Chem. Commun.* **2010**, *46*, 6090.
(29) Ning, Z.; Fu, Y.; Tian, H. *Energy Environ. Sci.* **2010**, *3*, 1170.
(30) Walter, M. G.; Rudine, A. B.; Wamser, C. C. *J. Porphyrins Phthalocyanines* **2010**, *14*, 759.
(31) de la Torre, G.; Claessens, C. G.; Torres, T. *Chem. Com.* **2007**, 2000.
(32) Blankenship, R. E.; Tiede, D. M.; Barber, J.; Brudvig, G. W.; Fleming, G.; Ghirardi, M.; Gunner, M. R.; Junge, W.; Kramer, D. M.; Melis, A.; Moore, T. A.; Moser, C. C.; Nocera, D. G.; Nozik, A. J.; Ort, D. R.; Parson, W. W.; Prince, R. C.; Sayre, R. T. *Science* **2011**, *332*, 805.
(33) Radivojevic, I.; Varotto, A.; Farley, C.; Drain, C. M. *Energ. Envir. Sci.* **2010**, *3*, 1897.
(34) Rand, B. P.; Genoe, J.; Heremans, P.; Poortmans, J. *Progress in Photovoltaics: Research and Applications* **2007**, *15*, 659.
(35) Varotto, A.; Nam, C.-Y.; Radivojevic, I.; P. C. Tomé, J.; Cavaleiro, J. A. S.; Black, C. T.; Drain, C. M. *J. Am. Chem. Soc.* **2010**, *132*, 2552.
(36) Schumann, S.; Hatton, R. A.; Jones, T. S. *J. Phys. Chem. C* **2011**, *115*, 4916.
(37) D'Souza, F.; Ito, O. *Chem. Soc. Rev.* **2012**, *41*, 86.
(38) Honda, S.; Ohkita, H.; Benten, H.; Ito, S. *Adv. Energy Mater.* **2011**, *1*, 588.
(39) Zeng, W.; Yong, K. S.; Kam, Z. M.; Zhu, F.; Li, Y. *Appl. Phys. Let.* **2010**, *97*, 133304.
(40) Honda, S.; Yokoya, S.; Ohkita, H.; Benten, H.; Ito, S. *J. Phys. Chem. C* **2011**, *115*, 11306.
(41) Honda, S.; Ohkita, H.; Benten, H.; Ito, S. *Chem. Com.* **2010**, *46*, 6596.
(42) Moon, S.-J.; Baranoff, E.; Zakeeruddin, S. M.; Yeh, C.-Y.; Diau, E. W.-G.; Gratzel, M.; Sivula, K. *Chem. Comm.* **2011**, *47*, 8244.
(43) Bartelmess, J.; Ballesteros, B.; de la Torre, G.; Kiessling, D.; Campidelli, S.; Prato, M.; Torres, T.; Guldi, D. M. *J. Am. Chem. Soc.* **2010**, *132*, 16202.
(44) Schlenker, C. W.; Barlier, V. S.; Chin, S. W.; Whited, M. T.; McAnally, R. E.; Forrest, S. R.; Thompson, M. E. *Chem. Mater.* **2011**, *23*, 4132.
(45) Kim, J. Y.; Bard, A. J. *Chem. Phys. Let.* **2004**, *383*, 11.
(46) de la Torre, G.; Giacalone, F.; Segura, J. L.; Martín, N.; Guldi, D. M. *Chem. Eur. J.* **2005**, *11*, 1267.
(47) Fukuzumi, S.; Ohkubo, K.; Imahori, H.; Shao, J.; Ou, Z.; Zheng, G.; Chen, Y.; Pandey, R. K.; Fujitsuka, M.; Ito, O.; Kadish, K. M. *J. Am. Chem. Soc.* **2001**, *123*, 10676.
(48) Quintiliani, M.; Kahnt, A.; Vazquez, P.; Guldi, D. M.; Torres, T. *J. Matr. Chem.* **2008**, *18*, 1542.
(49) Gomez, E. D.; Barteau, K. P.; Wang, H.; Toney, M. F.; Loo, Y.-L. *Chem. Com.* **2011**, *47*, 436.

(50) Kim, H. J.; Kim, J. W.; Lee, H. H.; Kim, T.-M.; Jang, J.; Kim, J.-J. *J. Phys. Chem. Let.* **2011**, *2*, 1710.
(51) Beaujuge, P. M.; Frechet, J. M. J. *J. Am. Chem. Soc.* **2011**, *133*, 20009.
(52) Li, S.-S.; Chang, C.-P.; Lin, C.-C.; Lin, Y.-Y.; Chang, C.-H.; Yang, J.-R.; Chu, M.-W.; Chen, C.-W. *J. Am. Chem. Soc.* **2011**, *133*, 11614.
(53) Liao, H.-C.; Tsao, C.-S.; Lin, T.-H.; Chuang, C.-M.; Chen, C.-Y.; Jeng, U. S.; Su, C.-H.; Chen, Y.-F.; Su, W.-F. *J. Am. Chem. Soc.* **2011**, *133*, 13064.
(54) Prato, M.; Maggini, M.; Giacometti, C.; Scorrano, G.; Sandona, G.; Farnia, G. *Tetrahedron* **1996**, *52*, 5221.
(55) Bottari, G.; Suanzes, J. A.; Trukhina, O.; Torres, T. *J. Phys. Chem. Let.* **2011**, *2*, 905.
(56) Rodríguez-Cordoba, W.; Noria, R.; Guarín, C. A.; Peon, J. *J. Am. Chem. Soc.* **2011**, *133*, 4698.
(57) Troshin, P. A.; Koeppe, R.; Peregudov, A. S.; Peregudova, S. M.; Egginger, M.; Lyubovskaya, R. N.; Sariciftci, N. S. *Chem. Mater.* **2007**, *19*, 5363.
(58) Kaafarani, B. R. *Chem. Mater.* **2010**, *23*, 378.
(59) Lee, J.-K.; Jang, S.-I.; Kim, Y.-G.; Jang, Y.-W.; Jeong, B.-H.; Kim, J.-U.; Jung, K.-S.; Kim, M.-R. *Molecular Crystals Liquid Crystals* **2008**, *491*, 307
(60) Roussel, O.; Kestemont, G.; Tant, J.; De Halleux, V.; Aspe, R. G.; Levin, J.; Remacle, A.; Gearba, I. R.; Ivanov, D.; Lehmann, M.; Geerts, Y. *Molecular Crystals and Liquid Crystals* **2003**, *396*, 35
(61) Hori, T.; Miyake, Y.; Yamasaki, N.; Yoshida, H.; Fujii, A.; Shimizu, Y.; Ozaki, M. *Appl. Phys. Express* **2010**, *3*, 101602.
(62) Sakamoto, K.; Ohno-Okumura, E. *Materials* **2009**, *2*, 1127.
(63) Service, R. F. *Science* **2011**, *332*, 293.
(64) Hayashi, H.; Nihashi, W.; Umeyama, T.; Matano, Y.; Seki, S.; Shimizu, Y.; Imahori, H. *J. Am. Chem. Soc.* **2011**, *133*, 10736.
(65) Lei, S.; Yang, Y.; Zeng, Q.; Wang, C. *Langmuir* **2011**, *27*, 3496.
(66) Zhu, F.; Grobosch, M.; Treske, U.; Huang, L.; Chen, W.; Yang, J.; Yan, D.; Knupfer, M. *ACS Appl. Mater. Interfaces* **2011**, *3*, 2195.
(67) Placencia, D.; Wang, W.; Gantz, J.; Jenkins, J. L.; Armstrong, N. R. *J. Phys. Chem. C* **2011**, *115*, 18873.
(68) Bramble, J. P.; Tate, D. J.; Revill, D. J.; Sheikh, K. H.; Henderson, J. R.; Liu, F.; Zeng, X.; Ungar, G.; Bushby, R. J.; Evans, S. D. *Adv. Func. Mater.* **2010**, *20*, 914.
(69) Laschat, S.; Baro, A.; Steinke, N.; Giesselmann, F.; Hägele, C.; Scalia, G.; Judele, R.; Kapatsina, E.; Sauer, S.; Schreivogel, A.; Tosoni, M. *Angew. Chem. Int. Ed.* **2007**, *46*, 4832.
(70) Lux, A.; Rozenberg, G. G.; Petritsch, K.; Moratti, S. C.; Holmes, A. B.; Friend, R. H. *Synthetic Metals* **1999**, *102*, 1527.
(71) Schmidt-Mende, L.; Fechtenkötter, A.; Müllen, K.; Moons, E.; Friend, R. H.; MacKenzie, J. D. *Science* **2001**, *293*, 1119.
(72) Milic, T.; Garno, J. C.; Batteas, J. D.; Smeureanu, G.; Drain, C. M. *Langmuir* **2004**, *20*, 3974.
(73) Milic, T. N.; Chi, N.; Yablon, D. G.; Flynn, G. W.; Batteas, J. D.; Drain, C. M. *Angew. Chem. Int. Ed.* **2002**, *41*, 2117.
(74) Petritsch, K.; Dittmer, J. J.; Marseglia, E. A.; Friend, R. H.; Lux, A.; Rozenberg, G. G.; Moratti, S. C.; Holmes, A. B. *Solar Energy Materials and Solar Cells* **2000**, *61*, 63.

(75) Gearba, R. I.; Bondar, A. I.; Goderis, B.; Bras, W.; Ivanov, D. A. *Chem. Mater.* **2005**, *17*, 2825.
(76) Kang, H.-J.; Kang, E.-H.; Park, S.-W.; Lee, J.-W.; Lee, J.-K. *Macromolecular Symposia* **2006**, *235*, 195.
(77) Singh, T. B.; Erten, S.; Günes, S.; Zafer, C.; Turkmen, G.; Kuban, B.; Teoman, Y.; Sariciftci, N. S.; Icli, S. *Organic Electronics* **2006**, *7*, 480.
(78) Alzeer, J.; Roth, P. J. C.; Luedtke, N. W. *Chem. Com.* **2009**, 1970.
(79) Bilgiçli, A. T.; Yarasir, M. N.; Kandaz, M.; Riza Özkaya, A. *Polyhedron* **2010**, *29*, 2498.
(80) Hirade, M.; Nakanotani, H.; Yahiro, M.; Adachi, C. *ACS Appl. Mater. Interfaces* **2010**, *3*, 80.
(81) Liang, F.; Shi, F.; Fu, Y.; Wang, L.; Zhang, X.; Xie, Z.; Su, Z. *Solar Energy Materials and Solar Cells* **2010**, *94*, 1803.
(82) Bottari, G.; Suanzes, J. A.; Trukhina, O.; Torres, T. *J. Phys. Chem. Let.* **2011**, *2*, 905.
(83) Honda, S.; Yokoya, S.; Ohkita, H.; Benten, H.; Ito, S. *J. Phys. Chem. C* **2011**, *115*, 11306.
(84) Zhang, S.; Sakai, R.; Abe, T.; Iyoda, T.; Norimatsu, T.; Nagai, K. *ACS Appl. Mater. Interfaces* **2011**, *3*, 1902.
(85) Bendler*, J. T.; Fontanella, J. J.; Shlesinger, M. F.; Wintersgill, M. C. *Electrochimica Acta* **2001**, *46*, 1615.
(86) Wen, T.-C.; Wang, Y.-J.; Cheng, T.-T.; Yang, C.-H. *Polymer* **1999**, *40*, 3979.
(87) Wieczorek, W.; Lipka, P.; Żukowska, G.; Wyciślik, H. *The Journal of Physical Chemistry B* **1998**, *102*, 6968.
(88) Belhadj, F.; Moissette, A.; Brémard, C.; Hureau, M.; Derriche, Z. *ChemPhysChem* **2011**, *12*, 1378.
(89) Grundmann, M.; Springer Berlin Heidelberg: 2010, p 451.
(90) Antunes, P. A.; Constantino, C. J. L.; Aroca, R. F.; Duff, J. *Langmuir* **2001**, *17*, 2958.

CHAPTER 4

Porphyrin Dimers as Higher Fullerene Tweezers

4.1 Introduction

Porphyrins are known to closely associate with the curved surface of fullerenes both in solution and as co-crystals.[1] These systems are used extensively in the creation of donor-acceptor materials to study charge separated states as part of artificial photosynthetic materials. The chemical stability and tuneable photonic properties of the p-type porphyrins couple well with the electronic properties of the n-type fullerenes to form nearly ideal donor-acceptor systems.

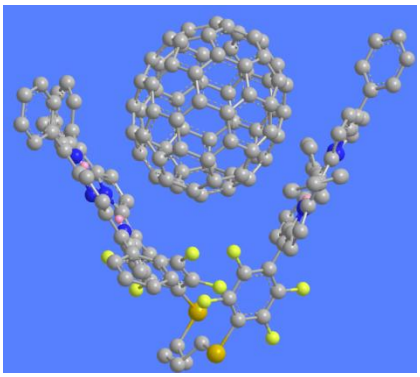

Figure 4-1. MM2 calculated structure of **1**H and C_{70} where grey=C, blue=N, yellow=F, and orange=S, and H are left out for clarity.

Covalently linked porphyrin/fullerene donor-acceptor systems have also served as model systems for the study of electron transfer for over 20 years.[2] Many groups have synthesized covalently linked porphyrin/fullerene systems with diverse architectures that demonstrated functionalities that can be potentially used in the development of optoelectronic devices.[3-10] In general, as the architectural complexity and added functional entities of the donor-acceptor target increases, the synthetic yield decreases. Rigorously synthesized and carefully designed systems

with rigid tethers are examples.[11,12] High yield coupling and click-type reactions provide access to some porphyrin/fullerene systems with better yields.[13] Supramolecular approaches can mitigate synthetic complications, but one drawback of molecular designs with covalent, coordination,[14] hydrogen bonding,[15] and electrostatic[16] tethers is that derivatives of fullerenes are usually not as good acceptor motifs as the parent fullerene.[17]

4.2 Porphyrin Dimer

Supramolecular approaches to porphyrin systems that bind the underivatized fullerene can result in materials with similar or better photonic functionalities.[18-23] Synthesis of the fullerene hosts range from simple to complex, but the former have greater commercial potential. The porphyrin dimer described in this investigation is synthesized by a simple two-step procedure in high yield (Scheme 1).

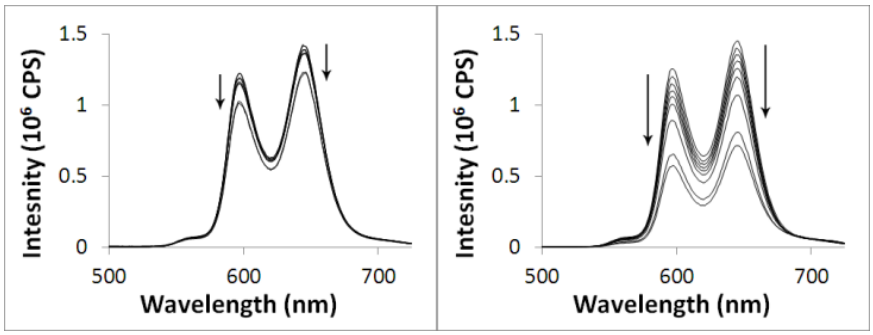

Figure 4-2. Fluorescence emission spectra of a titration of (left) C60 and (right) C70 into 10 µM 1Zn solution in toluene. Both graphs show quenching of the porphyrin excited state, but the effect due to C70 is much more significant. The solutions were excited at 417 nm.

The free base (**1**H) and Zinc(II) (**1**Zn) dimers are designed with a flexible α,ω-dithiol alkane linker to allow for an induced-fit, sandwich type binding of fullerenes such as C_{60}, C_{70} (Figure 4-

1), and single wall carbon nanotubes. The inclusion of the perfluorophenyl linker allows for easy dimerization by simple click-type substitution reactions with thioalkanes and may help promote interaction with the conjugated pi system of the chosen fullerene molecule.[24] The modular design allows the length of the linker to be easily varied by substituting the pentane dithiol with any of the numerous commercially available dithioalkanes.

In toluene, the **1**H and **1**Zn dimers complex fullerene C_{70} greater than 10-fold better than C_{60}

Table 4-1. Binding constants for **1**H, **1**Zn and for several reported fullerene binding porphyrinic compounds in toluene.

Host	K_{C60} (M^{-1})	K_{C70} (M^{-1})	K_{C70}/K_{C60}	Ref.
MPF	5.0×10^{2}	3.7×10^{3}	7.4	this work
1H	7.1×10^{2}	8.9×10^{3}	12.5	this work
1Zn	8.0×10^{2}	1.1×10^{4}	13.8	this work
cyclic H_2Por	7.94×10^{5}	1.58×10^{7}	19.9	1[a]
cyclic ZnPor	6.31×10^{5}	2.00×10^{7}	31.7	1[a]
jaws H_2Por	5.20×10^{3}	-	-	1[a]
jaws ZnPor	1.95×10^{3}	-	-	1[a]
calix. H_2Por	4.92×10^{3}	2.11×10^{4}	4.29	11
calix. ZnPor	8.6×10^{3}	2.80×10^{4}	3.26	11

[a] and references therein, see supporting information for structures

Table 4-1. UV-visible and fluorescence titrations of the fullerenes into solutions of the dimers reveal systematic red shifts in the former and quenching in the latter. Values for K in Table 4-1 were calculated from the slope of Stern-Volmer plots (e.g. fluorescence data in Figure 4-2), and competition experiments, wherein the dimers were titrated with a ~1:1 mixture of C_{60}:C_{70}, indicate that the dimer preferentially binds C_{70} more than 10-fold better than C_{60}. **1Zn** demonstrated a binding constant of 1.1×10^{4} M^{-1}, which is competitive with much more

synthetically demanding molecules.

The UV-visible absorption spectra (Figures 4-4 - 4-9) of both **1**H and **1**Zn show a small but real ground state interaction with C_{70} indicated by a decrease and slight redshift of the Soret peak. This is illustrated in the insets to figures 4-4 - 4-9, which plot the difference between the predicted and observed absorbance of the combined solutions as a function of fullerene concentration. For the monomeric compounds and the titration of C_{60} for the dimer, no such effect is observed.

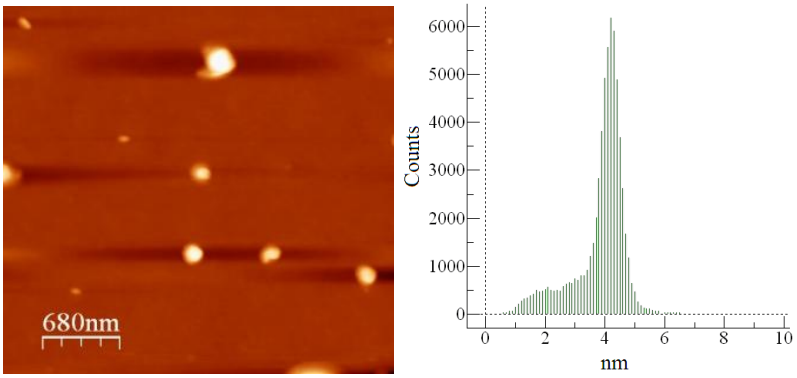

Figure 4-3. Left: AFM of a 1:1 1Zn : C70 (10 µM each in toluene) cast onto ozone cleaned glass shows a ~4 nm thick film with larger 10-25 nm high islands of the fullerene complexed by the dimer. Right: Histogram of particle sizes.

Steady state fluorescence measurements demonstrate fullerene quenching of the porphyrin excited state (Figure 4-1, S7, S8). Stern-Volmer plots (Figure 4-12) show greater quenching by C_{70} than by C_{60} for all species studied. The porphyrin fluorescence lifetimes measured by time correlated single photon counting experiments show virtually no change (9 ns for **1**H and 2 ns for **1**Zn in toluene excited at 425 nm), and a static quenching mechanism is indicated. Assuming there is no significant difference in the nature of energy transfer from the various fluorophore species, and expecting that complexation behaviour is driven by van der Waals forces with small

contributions from electrostatics and coordinate bonding, we conclude that the greater quenching observed in the case of the C_{70} can be attributed to a stronger interaction due to the larger, flatter surface in the equatorial region of the fullerene molecule.[25] We have done these studies in toluene to compare to published data, but solvation of both the dimer and the fullerenes diminish the intermolecular interactions, and more polar solvents may enhance complexation.[26]

To study the system in the solid state, films were prepared on ozone cleaned glass by drop casting from toluene solutions of fullerene, fullerene and **1**H, fullerene plus **1**Zn, or pure **1.** The resulting films were examined by atomic force microscopy (AFM), and transmission electron microscopy (TEM). Solutions of **1** and C_{70} form 3-5 nm films of the supramolecular material when cast on clean glass surfaces (Figure 4-3). A few islands of larger aggregates of the materials are also observed. Monomeric porphyrins form simple aggregates on the glass surface. Pure 0.5 mM C_{70} solutions cast on the glass form large nanoaggregates, while solutions of pure C_{60} form long narrow rods. Lower concentrations form sparse films. When combined with **1,** the dimensions of the C_{60} aggregates remain constant but are more uniformly dispersed aggregates. The self-organized films demonstrate the increased affinity of **1** to C_{70} but the architecture of the molecules in the films may be different than in solution. TEM studies of the films show similar morphologies and the energy dispersive x-ray microanalysis clearly shows the Zn in films of **1**Zn:C_{70}. There are three possible supramolecular structures consistent with the AFM heights: the sandwich-type complex shown in Figure 4-1, the C_{70} sitting on top of a closed dimer where the porphyrins are cofacially pi-stacked, and two open dimers sandwiching two C_{70} (see supporting information).

Carbon nanotubes share many of the interesting properties of fullerenes and have also been extensively used in porphyrin based D/A systems.[27-29] When THF solutions of **1** were incubated

with large excess of single walled carbon nanotubes (SWCNT), sonicated for 10 minutes and centrifuged at 8,000 RPM for 10 minutes. UV-visible spectra show small red shifts in the dimer. The supernatant demonstrated similar fluorescence quenching and UV spectral changes to the experiments with the fullerene C_{70}, indicating that the dimer interacts favourably with the larger SWCNT.

4.3 Conclusions

Simple porphyrin dimers with flexible linkers can bind fullerenes, and this molecular design allows rapid synthesis of molecules with different tethers to evaluate other supramolecular design principles. Future studies will include synthesis of differently tethered dimers, and characterization of the dimer interaction with SWCNT. These synthetically scalable dimers may be used as a means for purifying crude fullerene mixtures. The photophysical data indicates electron transfer from the porphyrin donor to the C_{70} acceptor. Nanoscale films of the supramolecular complex are similarly quenched. If porphyrin-fullerene films are to reach potential applications,[30-38] scalability is a central issue.

4.4 Synthesis and Materials

^{1}H and ^{13}C NMR spectra were recorded in a Bruker Avance 500 MHz spectrometer. Electrospray ionization mass spectrometric analyses were performed at the CUNY Mass Spectrometry Facility at Hunter College using an Agilent Technologies HP-1100 LCMSD instrument. MALDI-MS spectra were recorded as a service by the University of Illinois with a Bruker UltrafleXtreme MALDI TOF mass spectrometer purchased in part with a grant from the National Center for Research Resources, National Institutes of Health (S10 RR027109 A). All

reagents were obtained from commercial sources and used without further purification. Atomic force microscopy (AFM) measurements were conducted with an Asylum AFM (MFP-3D, Asylum Research Corp.) Transmission electron microscopy uses a Jeol 200kV instrument. Calculations were done on ChemOffice Chem 3D (2011) software using MM2 by cycling through molecular dynamics and minimizing the energy.

5,10,15-triphenyl-20-(2,3,4,5,6-pentafluorophenyl)porphyrin (MPF)

To a mixture of propionic acid (0.6 L) and nitrobenzene (6 mL) was added benzaldehyde (21.34 mmol, 2.17 mL) and pentafluorobenzaldehyde (7.0 mmol, 0.875 mL) with stirring. The mixture was heated to 100 ºC and pyrrole (28.3 mmol, 1.94 mL) was added slowly. The reaction was refluxed for three hours in the dark and allowed to cool. 300 mL silica was added to the reaction flask and the propionic acid was evaporated. The silica gel was washed with dichloromethane and acetone until no more color eluted. The solution was evaporated to 100 mL and washed with sodium bicarbonate and water, dried over anhydrous sodium sulfate and evaporated to dryness. The organic layer was then recrystallized from hexanes to yield a purple powder. The porphyrin mixture was filtered, dissolved in dichloromethane, loaded onto a 600 mL silica gel column and separated with an eluent of 30:70 toluene:petroleum ether (v/v). The fifth of the six bands was collected, evaporated and recrystallized from hexanes to yield 360 mg (0.511 mmol, 7.22% yield) of product *MPF*.

*5,10,15-triphenyl-20-(2,3,4,5,6-pentafluorophenyl)porphyrinato zinc(II), ZnMPF***.**

MPF (0.511 mmol, 0.360 g) was added to 20 mL of chloroform. Zinc acetate dihydrate (4.09 mmol, 0.897 g) was added to eight mL methanol. The methanol solution was added to the *MPF* in chloroform, and the mixture was refluxed for three hours. The mixture was washed with

water, extracted into dichloromethane, dried over sodium sulfate, and evaporated to dry to yield mg 276 mg *ZnMPF* (76.67% yield).

Dimer of 5,10,15-tripheynl-20-(4-perfluorophenyl)porphyrinato zinc(II) (1Zn)

ZnMPF (116 mg, 0.151 mmol) was added to dry DMF (16.6 mL) under a nitrogen atmosphere. To the stirring solution, 1,5-pentane-dithiol (0.23 ml, 1.7 mmol) was added followed by diisopropylethylamine (2.914 mL, 16.73 mmol). The reaction mixture was stirred at 80 ºC for 12 hours, cooled to room temperature, washed with water, extracted into dichloromethane, dried over sodium sulfate, and evaporated to dryness under reduced pressure. The crude product was purified by column chromatography to remove starting materials and recrystallized from hexanes to yield 95.37mg of *1Zn* (yield 82.19%).

Dimer of 5,10,15-triphenyl-20-(2,3,4,5,6-pentafluorophenyl)porphyrin free base (1H)

1Zn (80 mg, 0.091 mmol) was added to dry chloroform (5 mL) under a nitrogen atmosphere. To the stirring solution concentrated HCl (0.5 mL, 20.43 mmol) was added dropwise. The mixture was stirred at room temperature for three hours. The reaction mixture was then washed with water, extracted into dichloromethane, dried over sodium sulfate, and evaporated to dry under reduced pressure. The crude product was recrystallized from hexanes to yield 75 mg of product *1H* (yield 93.75%).

MALDI: calculated 1505.6423 found 1505.4

NMR (500 MHz, $CDCl_3$): 9.02(d),4H, β pyrrole; 9.96(m), 12H, β pyrrole; 8.20(m),12H, *ortho* phenyl; 7.77(m), 18H, *meta/para* phenyl; 3.39(t), 2H, S-CH_2 tether; 3.15(m), 2H, HS-CH_2 tether; 2.05(m), 2H, tether; 1.86(m),4H, tether.

4.5 Photophysics

UV-visible absorption spectroscopy was performed on a Cary 1-Bio UV-Visible spectrometer. Steady state fluorescence spectra were obtained on a HORIBA Jobin-Yvon FluoroLog-3 fluorometer, and singlet state lifetimes were taken using the SPEX-IBH TCSPC add-on component to the same system using a pulsed NanoLED laser at 425 nm. In order to minimize secondary absorption and emission, 1 mm path length quartz or optical glass cuvettes were used for all spectroscopic studies. The emission spectra and lifetimes were taken using a front-face configuration, which also helped to minimize these inner-filter effects. All photophysical studies were carried out in spectrophotometric grade 99.99% toluene, used as purchased. Solutions of diporphyrin species were prepared at one half the molar concentrations of the monomer controls in order to yield the equivalent macrocycle concentration for comparison.

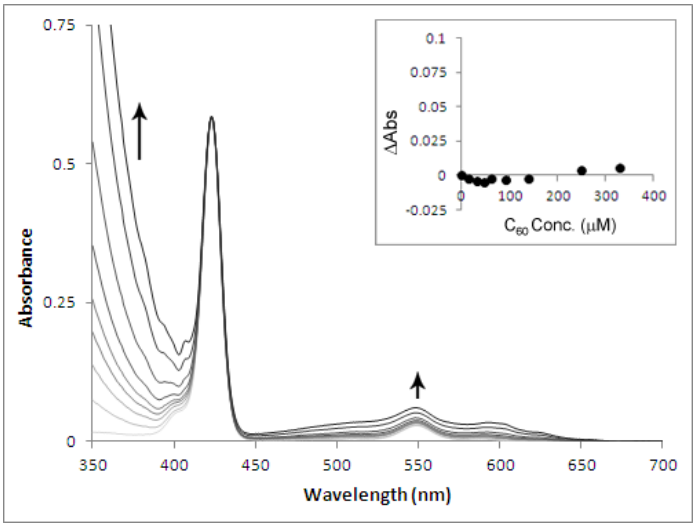

Figure 4-4: UV-visible spectrophotometric titration of C_{60} into **1Zn** solution. The inset shows the difference between the calculated sum of the absorbance of the two components at 423 nm and the experimentally observed absorbance for the mixed solutions, as function of the quencher concentration. [**1Zn**] = 10.0 μM; [C_{60}] = 0–0.33 mM.

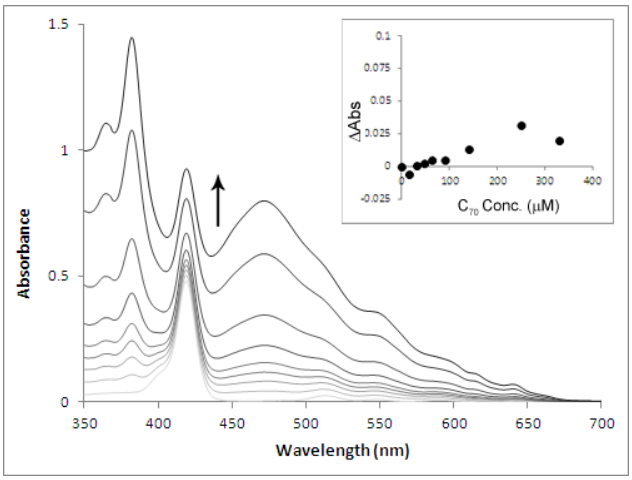

Figure 4-5: UV-visible spectrophotometric titration of C_{70} into **1H** solution. The inset shows the difference between the calculated sum of the absorbance of the two components at 419 nm and the experimentally observed absorbance for the mixed solutions, as function of the quencher concentration. [**1H**] = 10.0 μM; [C_{70}] = 0–0.33 mM.

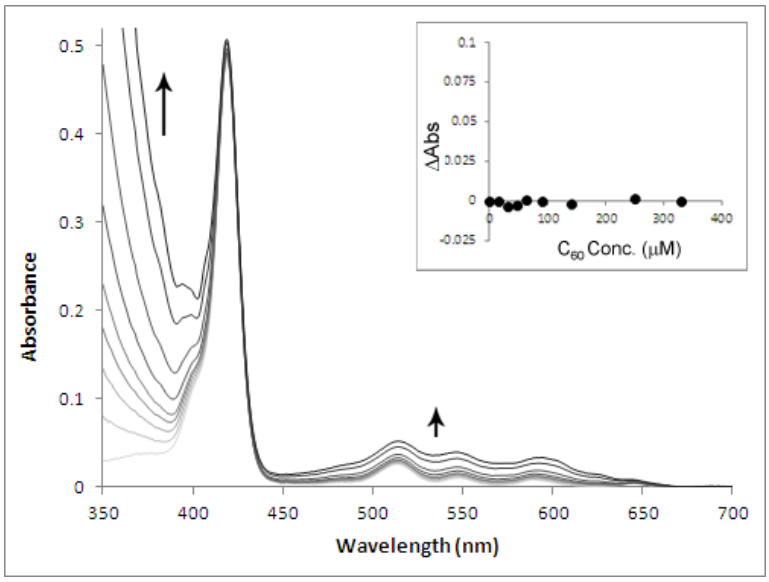

Figure 4-6: UV-Visible spectrophotometric titration of C_{60} into **1H** solution. The inset shows the difference between the calculated sum of the absorbance of the two components at 419 nm and the experimentally observed absorbance for the mixed solutions, as function of the quencher concentration. [**1H**] = 10.0 μM; [C_{60}] = 0–0.33 mM.

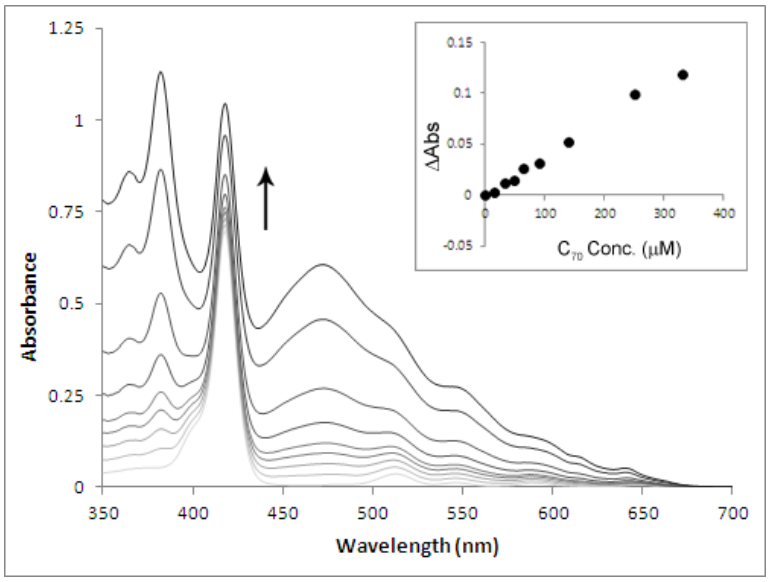

Figure 4-7: UV-Visible spectrophotometric titration of C_{70} into **MPF** solution. The inset shows the difference between the calculated sum of the absorbance of the two components at 418 nm and the experimentally observed absorbance for the mixed solutions, as function of the quencher concentration. [**MPF**] = 20.0 μM; [C_{70}] = 0–0.33 mM.

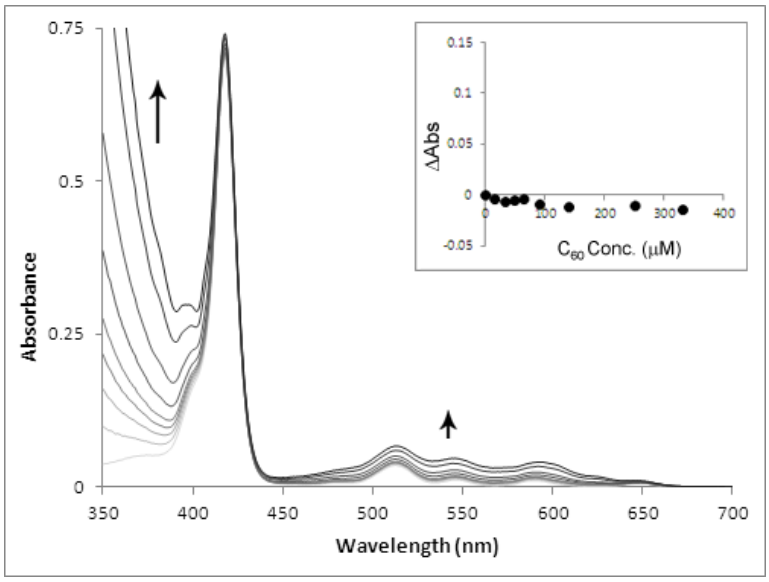

Figure 4-8: UV-Visible spectrophotometric titration of C_{60} into **MPF** solution. The inset shows the difference between the calculated sum of the absorbance of the two components at 418 nm and the experimentally observed absorbance for the mixed solutions, as function of the quencher concentration. [**MPF**] = 20.0 μM; [C_{60}] = 0–0.33 mM.

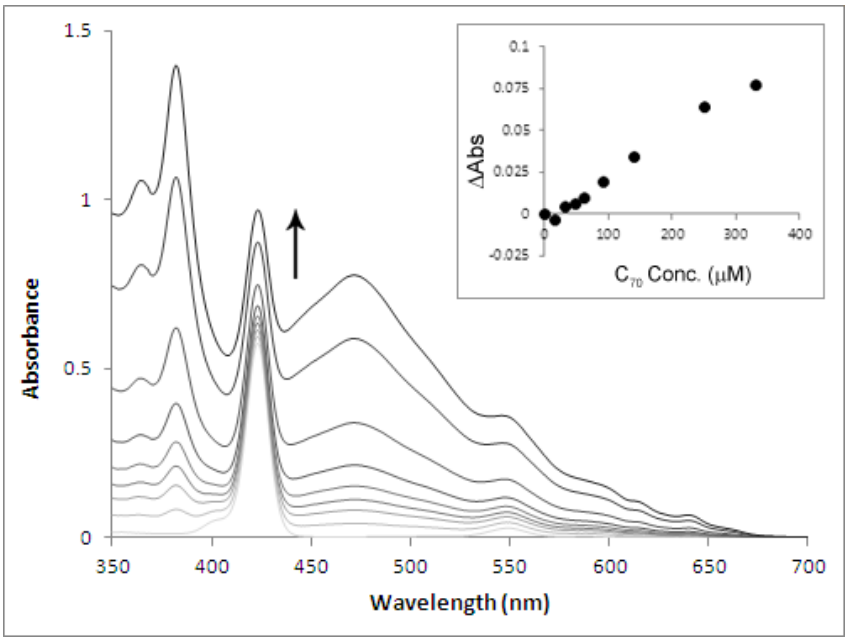

Figure 4-9. UV-Visible spectrophotometric titration of C_{70} into **1Zn** solution. The inset shows the difference between the calculated sum of the absorbance of the two components at 419 nm and the experimentally observed absorbance for the mixed solutions, as function of the quencher concentration. [**1Zn**] = 10.0 μM; [C_{70}] = 0–0.33 mM.

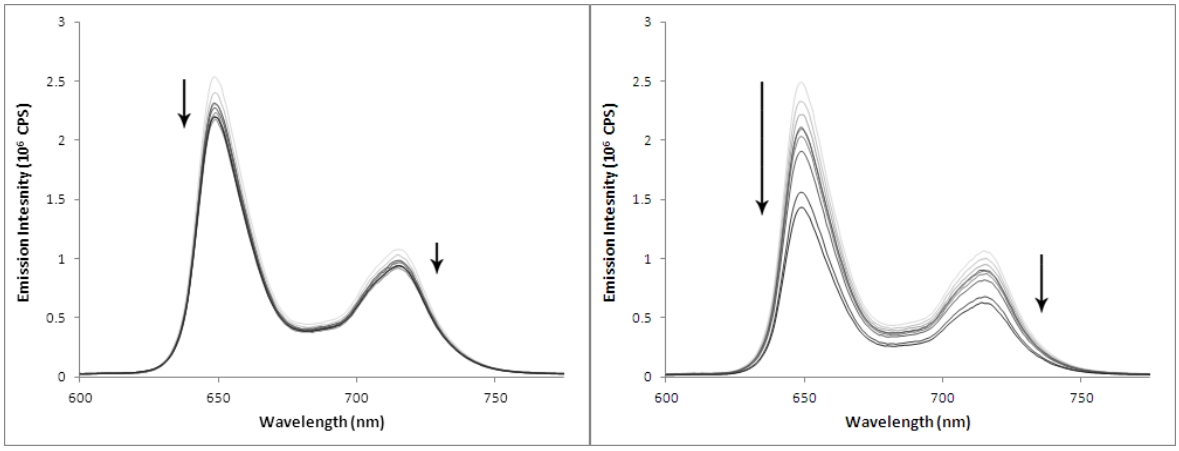

Figure 4-10: Fluorescence emission spectra of a titration of (left) C_{60} and (right) C_{70} into a **1H** solution. Both graphs show quenching, but the effect of C_{70} is again more pronounced. The solutions were excited at a wavelength of 414 nm, a near-isosbestic point. Emissions were corrected for the increase in absorbance at the excitation wavelength. [**1H**] = 10.0 µM; [C_{60}] or [C_{70}] = 0–0.33 mM.

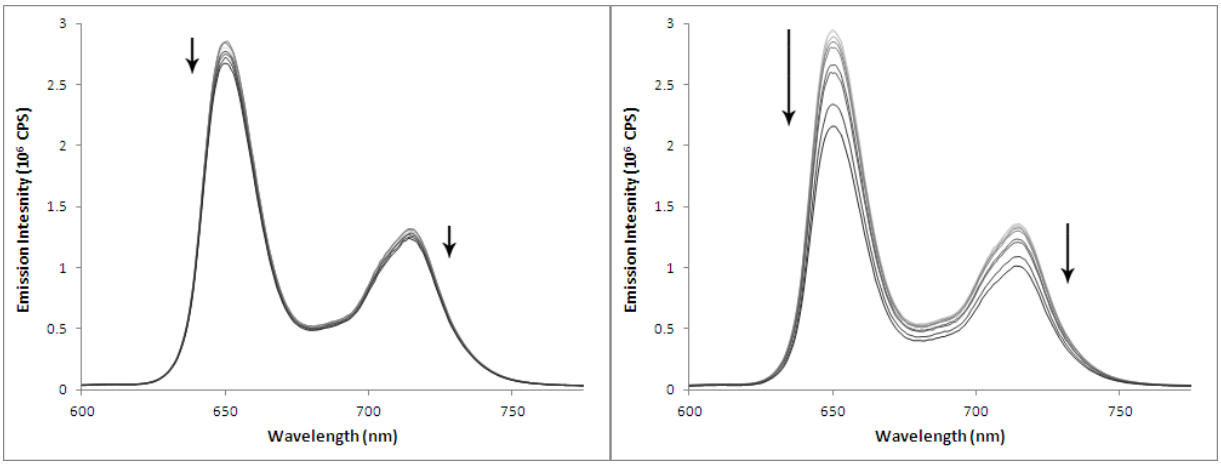

Figure 4-11: Fluorescence emission spectra of a titration of (left) C_{60} and (right) C_{70} into a **MPF** solution. Both graphs show quenching, but the effect of C_{70} is again more pronounced. The solutions were excited at a wavelength of 414 nm, a near-isosbestic point. Emissions were corrected for the increase in absorbance at the excitation wavelength. [**MPF**] = 20.0 µM; [C_{60}] or [C_{70}] = 0–0.33 mM.

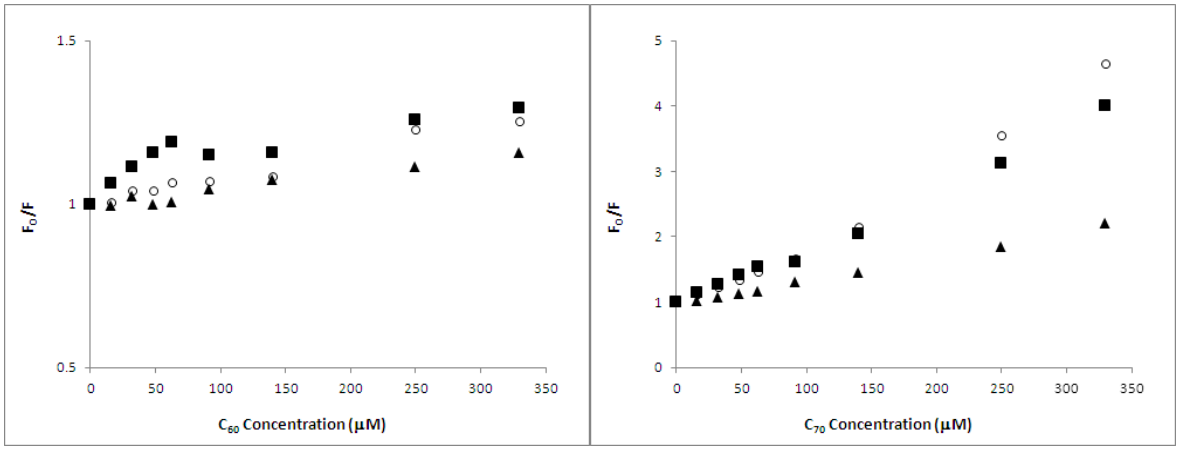

Figure 4-12: Stern-Volmer plots for each species discussed. The ratio of unquenched to quenched fluorescence as C60 (left) and C70 (right) are titrated into solutions of **1Zn** (○), **1H** (■) and **MPF** (▲) is plotted as a function of quencher concentration. Note the difference in scale between the left and right graphs. The molar concentration of the **MPF** control was twice that of the dimers in order to maintain equivalent macrocycle concentrations for comparison. There is thus a clear enhancement of the dimer quenching over the monomer. The slopes of the best fit lines to these plots are the binding constants collected in Table 4-1 below. Similar binding constants were obtained from fluorescence data corresponding to two different excitation wavelengths.

4.6 Carbon Nanotube Studies

3ml aliquots of 85 μM solution of **1Zn** in THF were sonicated with 1 mg single walled carbon nanotubes (SWCNT) for 10 minutes. Solutions were centrifuged to remove insoluble SWCNT and its complexes with the dimer. The supernatants were then analyzed by fluorescence and UV-Visible spectroscopy.

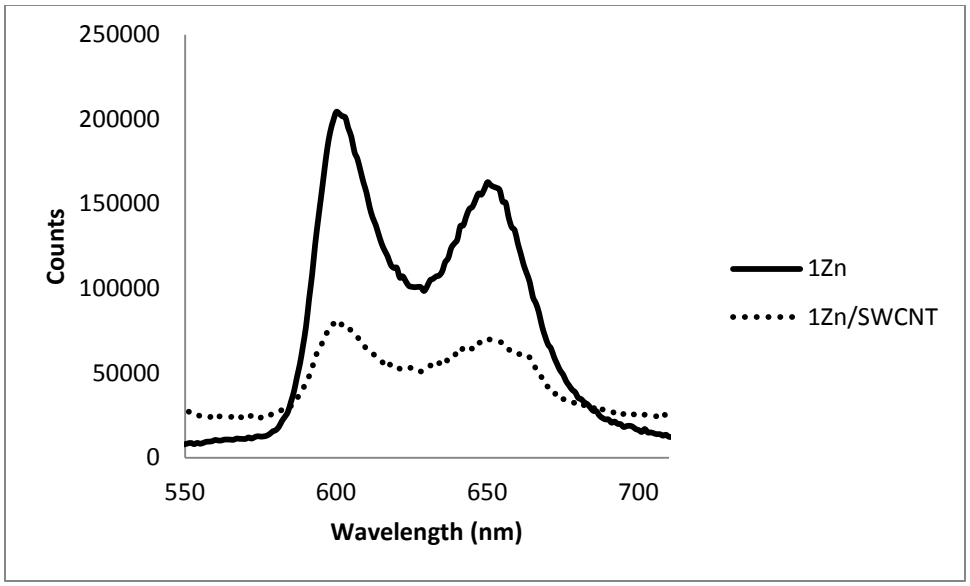

Figure 4-13. Fluorescence spectrum of typical nanotube experiment. 10 µM **1Zn** solution before and after treatment with nanotubes. Excitation at 425 nm in right angle mode demonstrates 60% quenching without baseline correction.

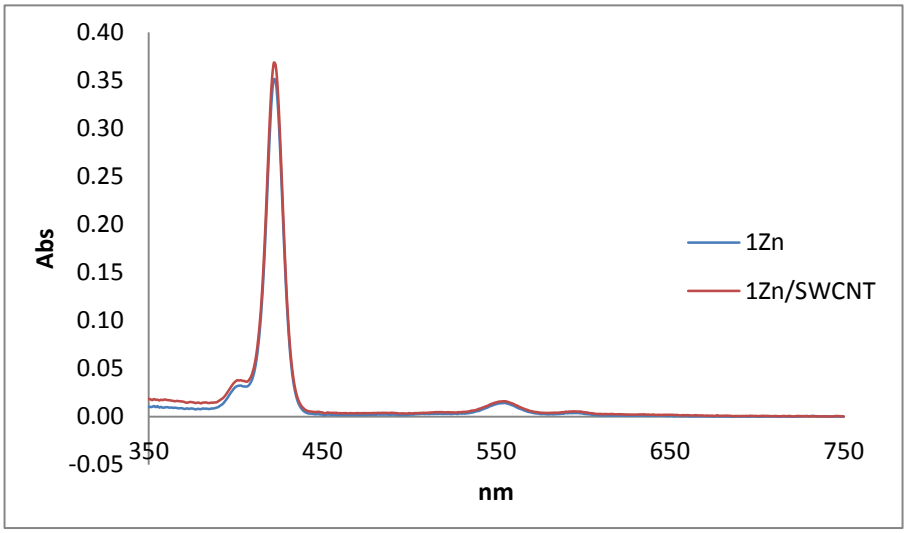

Figure 4-14. Uv-Vis spectrum of typical nanotube 10 µM **1Zn** solution before and after treatment with nanotubes. Baselines corrected at 750 nm.

4.7 Surface Analysis

Samples for atomic force microscopy were prepared by drop casting toluene solutions onto ozone cleaned glass slides and letting the solutions evaporate in air.

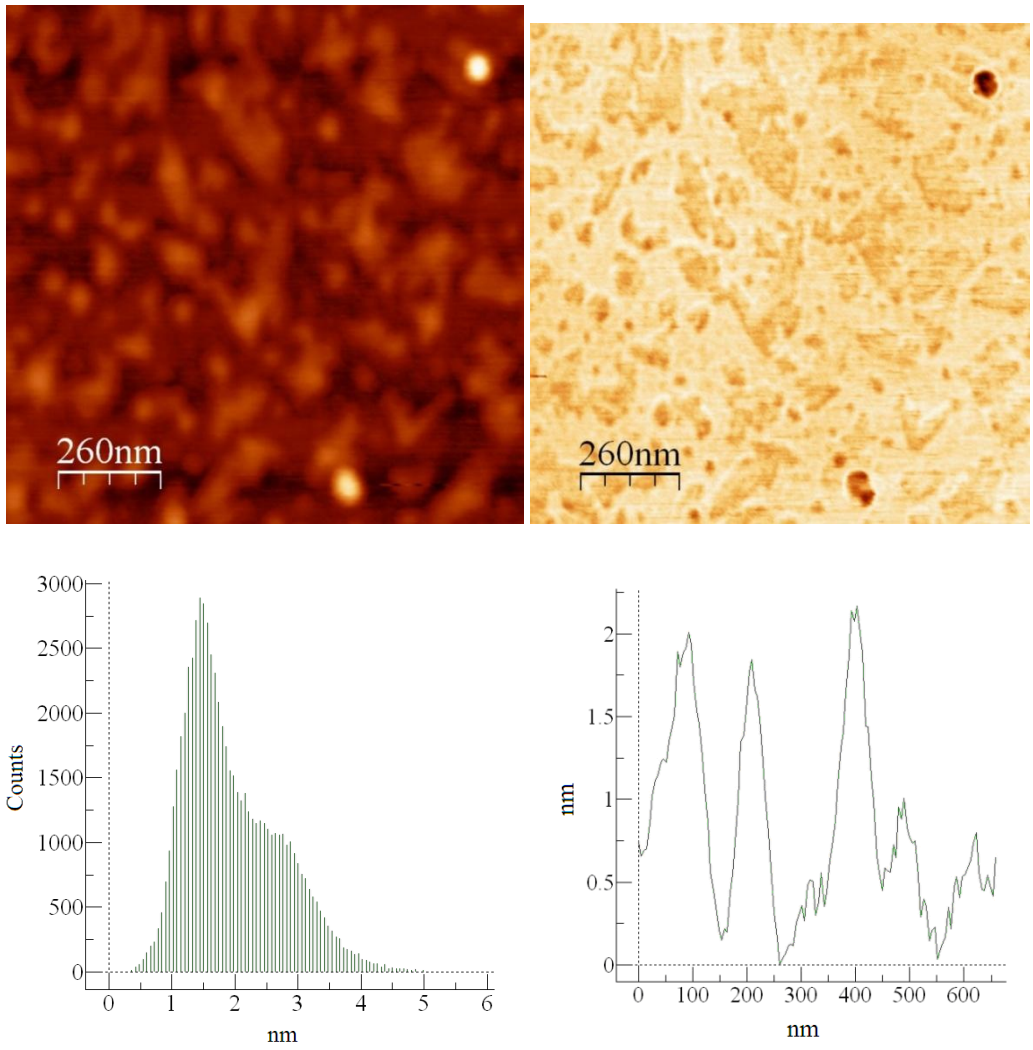

Figure 4-15. AFM of films deposited from 1 mM solution of C_{70}. Top: (left) height image, (right) phase image. Bottom: (left) histogram of particle sizes; ~1.1 nm corresponds to diameter of C_{70},[39,40] (right) height profile.

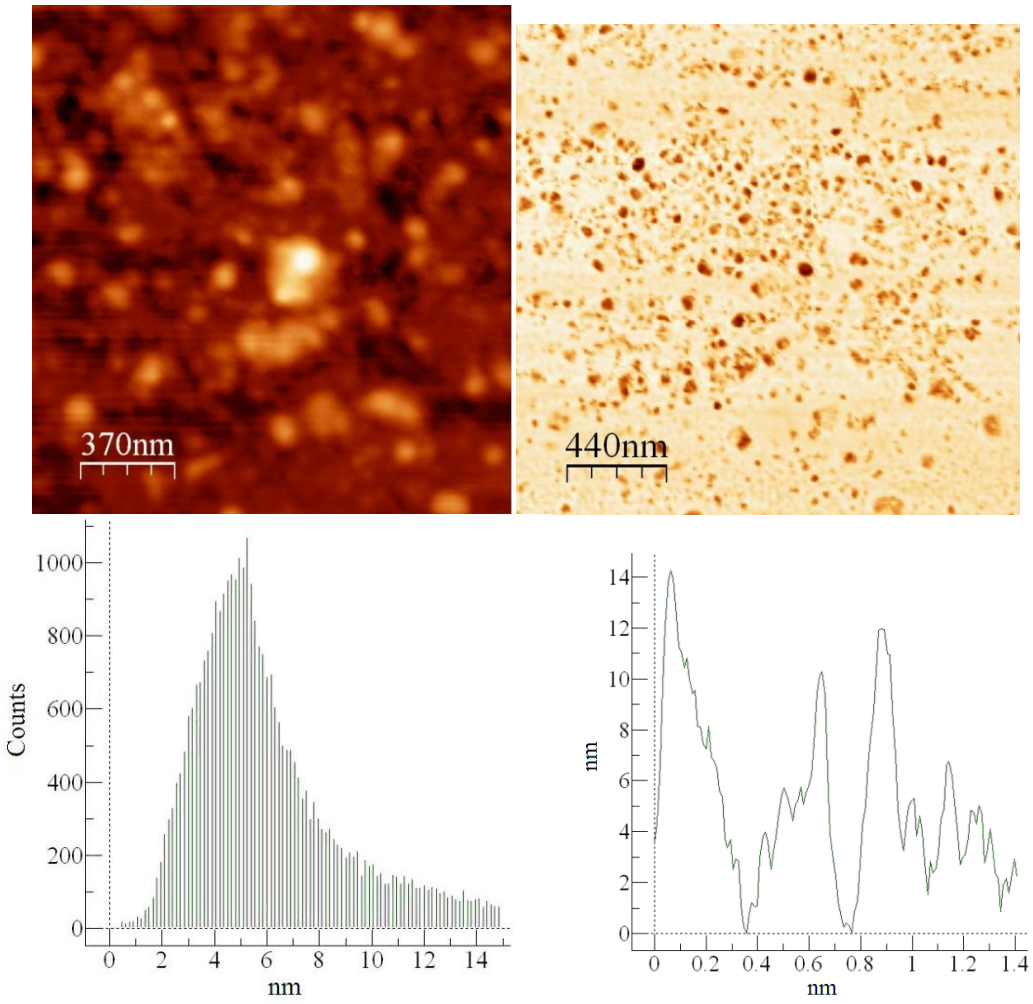

Figure 4-16. Films deposited from 10 µM solution of **1H**. Top: (left) height image, (right) phase image. Bottom: (left) histogram of particle sizes; mean ~5 nm, (right) is height profile of larger aggregates.

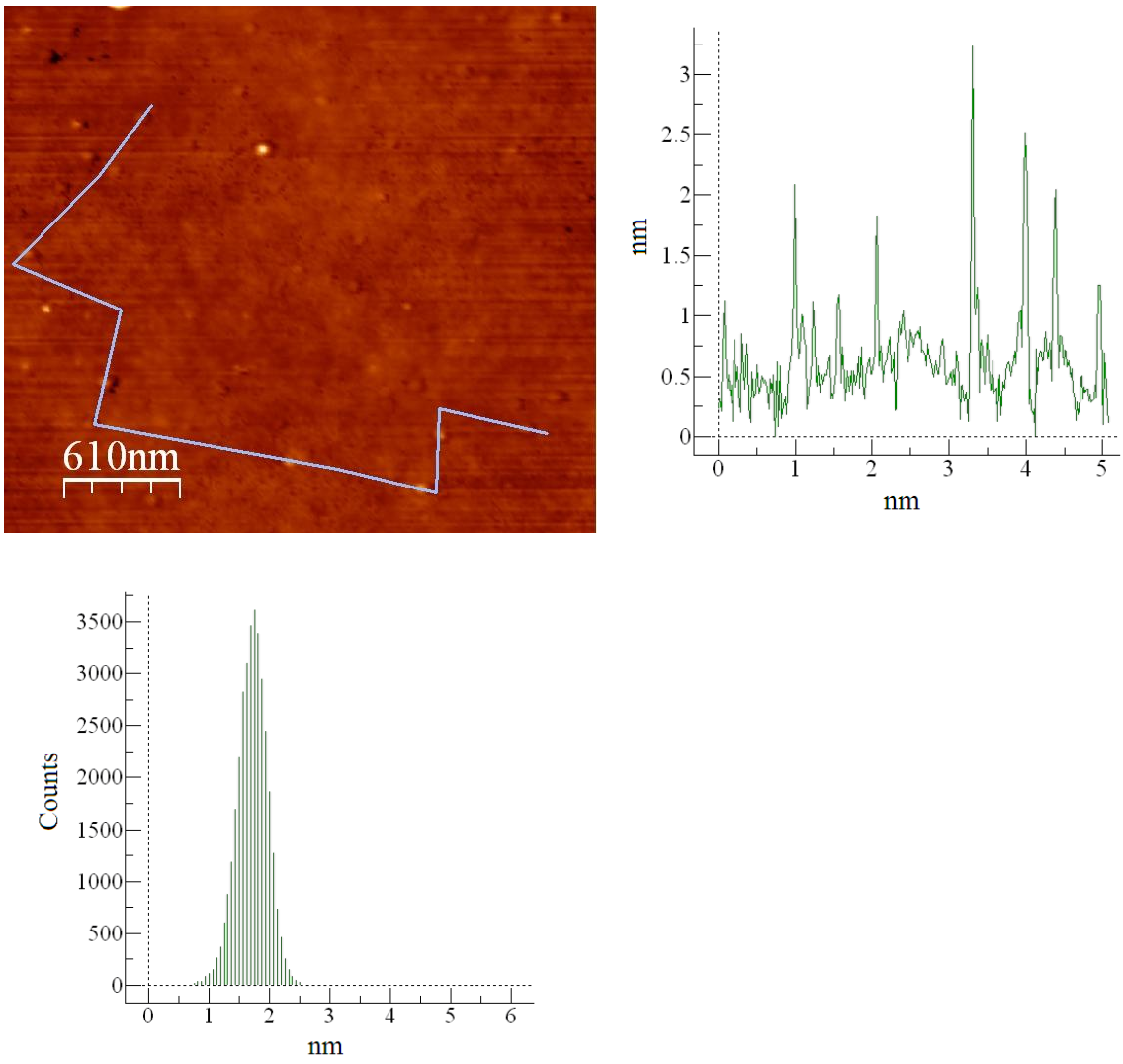

Figure 4-17. Films deposited from 10 µM solutions of C_{70}.Top: (left) height image, (right) height profile trace. Bottom: (left) histogram of particle sizes; ~1.1 nm corresponds to diameter of C_{70}.

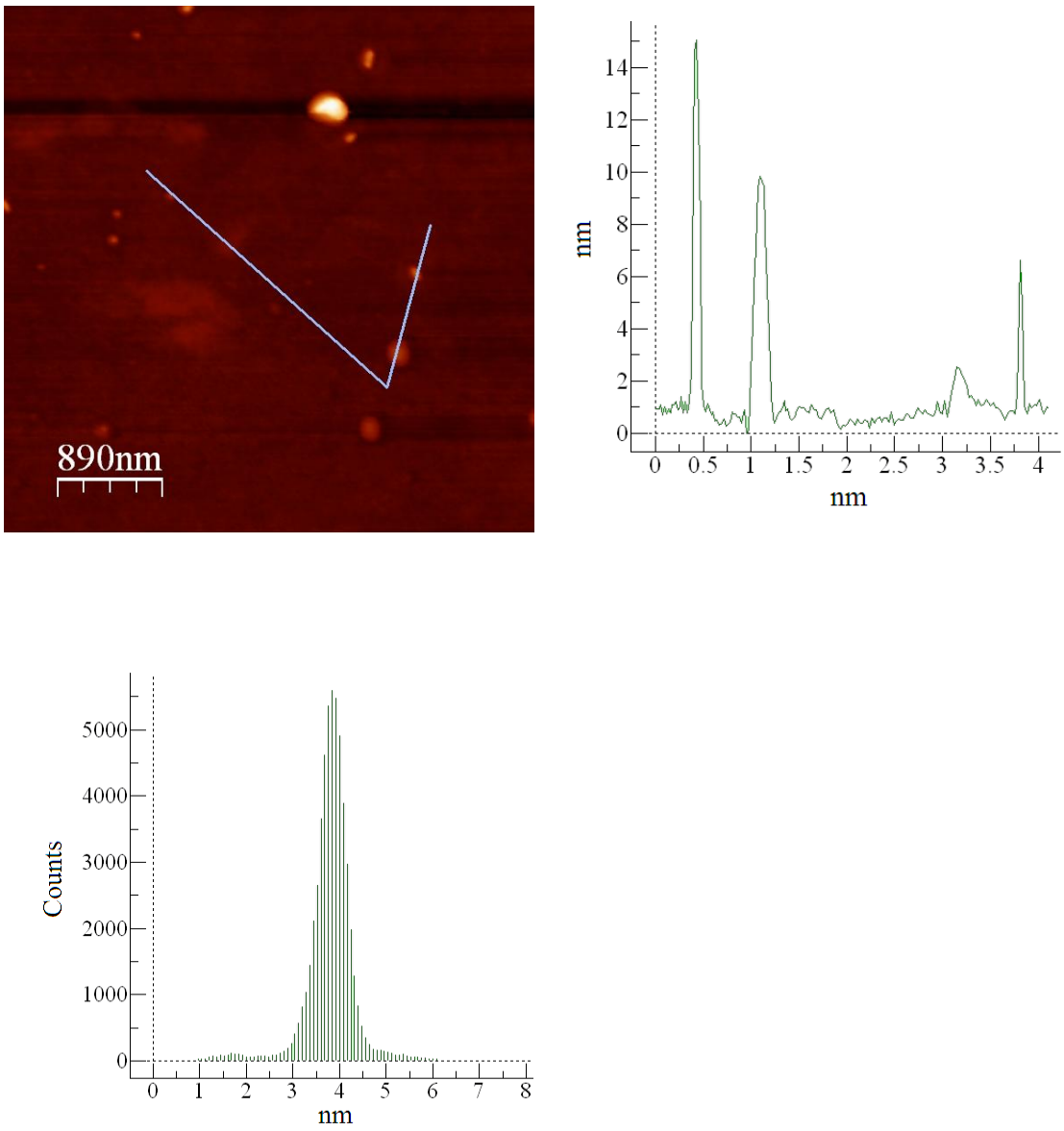

Figure 4-18. Films deposited from equimolar solutions of C_{70} and dimer **1H**, 10 μM each. Top: (left) height image, (right) height profile trace. Bottom: histogram of particle sizes; mean of ~3.8 nm corresponds to diameter of C_{70} complexed with two porphyrins ~1.1 nm for the C_{70} and ~1.4 nm for each porphyrin.

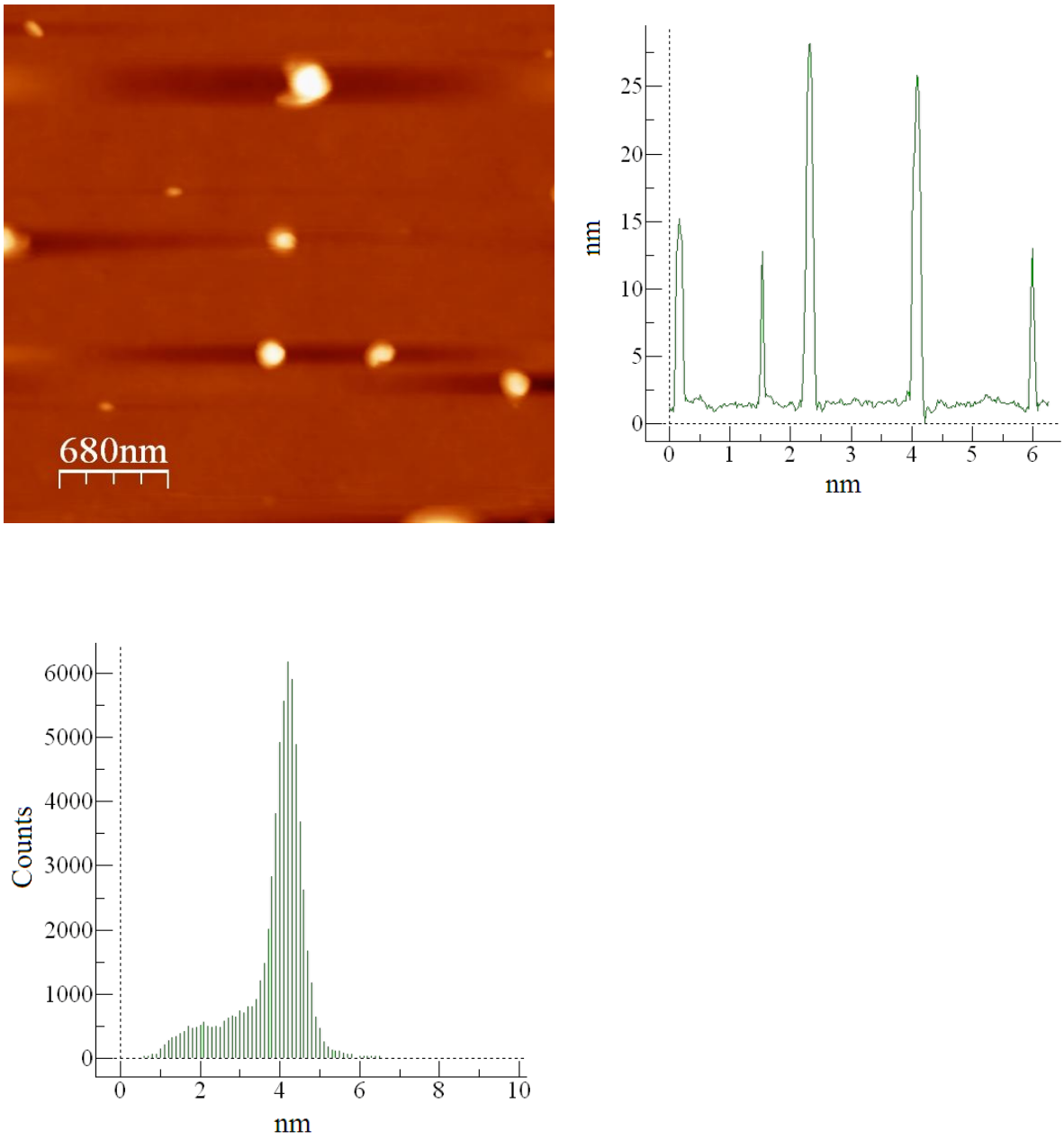

Figure 4-19. Films deposited from equimolar solutions of C_{70} and dimer **1Zn**, 10 µM each. Top: (left) height image showing a few large islands interspersed in the ~ 4 nm thick film, (right) height profile trace. Bottom: histogram of particle sizes in the films; a mean of ~4 nm corresponds to diameter of C_{70} complexed with two porphyrins.

4.8 TEM

All data were collected at 200 kV on a Jeol 2100 Transmission Electron Microscope equipped with EDAX at the eucentric height to ensure reproducibility of measurements. An 8 μL drop of the solution was placed on a 300 mesh carbon coated copper grid, (TED Pella Inc., Redding, California, USA), and allowed to dry for 1 minute. Since a carbon coated grid was used and carbon from C70 is present in the mixture, the Netcounts method (sample area minus control area)* (Jacopo Samson et *al*. ***Nanomaterials*** **2011**, ***1***, 64-78) was not used so the x-ray scattered lines from the carbon coated copper grid and other metals in the background, show up in the spectrum (indicated by the Cu and W peaks).

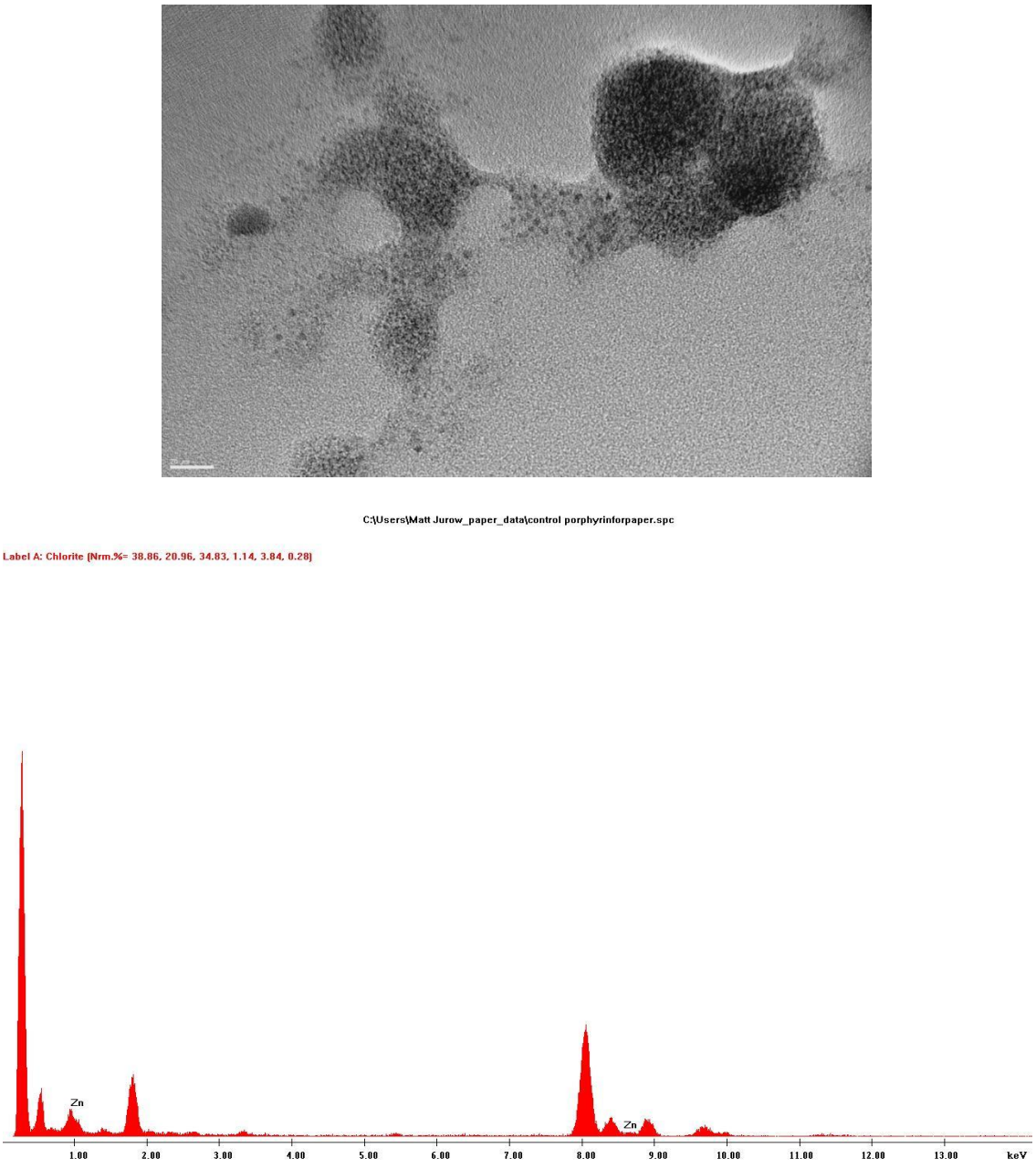

Figure 4-20. Top: Image from a solution of 10 µM **1Zn.** No larger aggregates were observed. The scale bar is 20 nm. Bottom: Corresponding EDAX spectrum with slight Zn signature from the metallic core of the porphyrin.

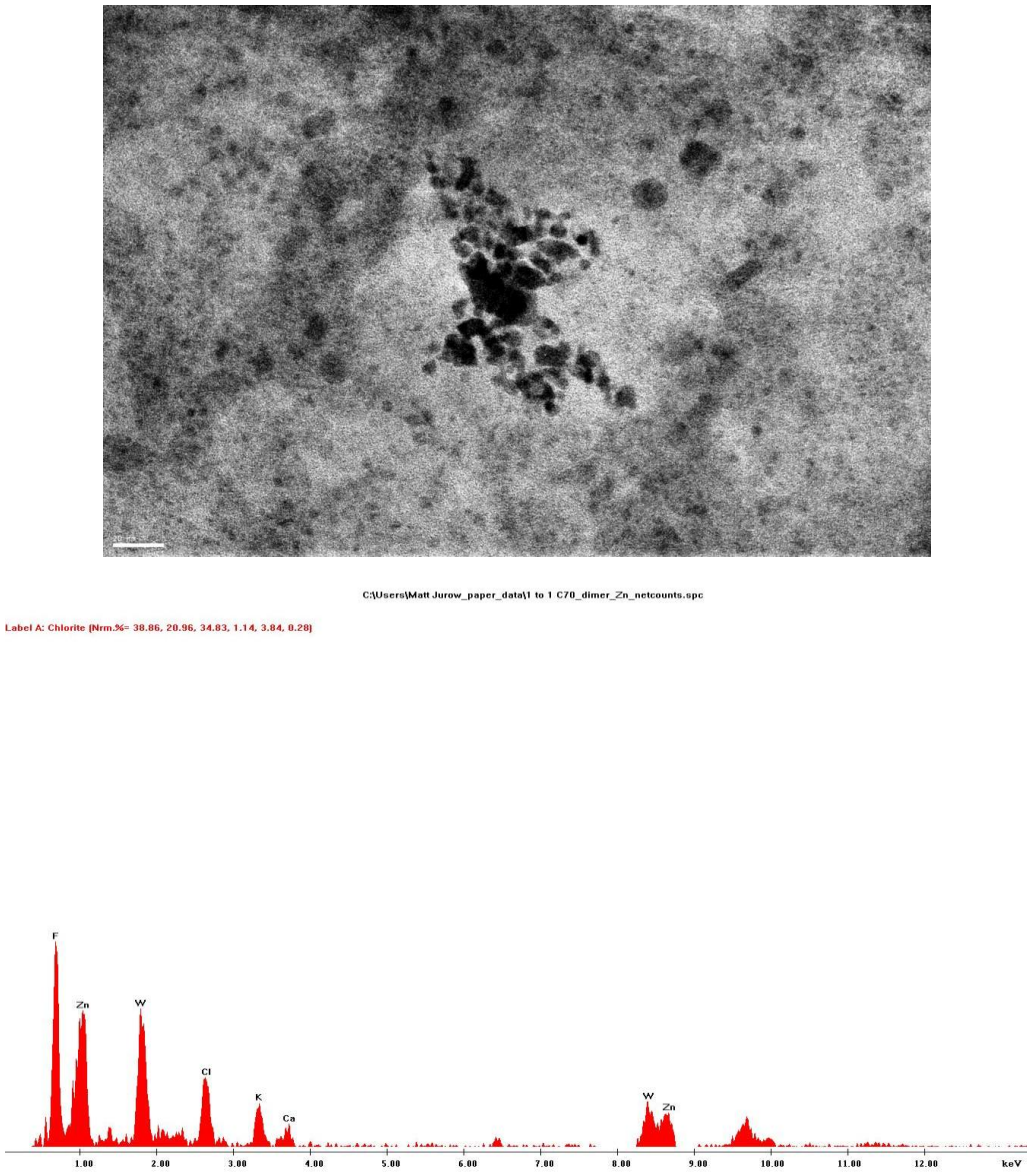

Figure 4-21. Top: Image from a mixture of fullerene and **1Zn,** 10 μM in each. Aggregates were observed throughout the sample. The scale bar is 20 nm. Bottom: Corresponding EDAX spectrum with Zn signature from the metallic core of the porphyrin demonstrates that aggregates are not phase separated fullerene.

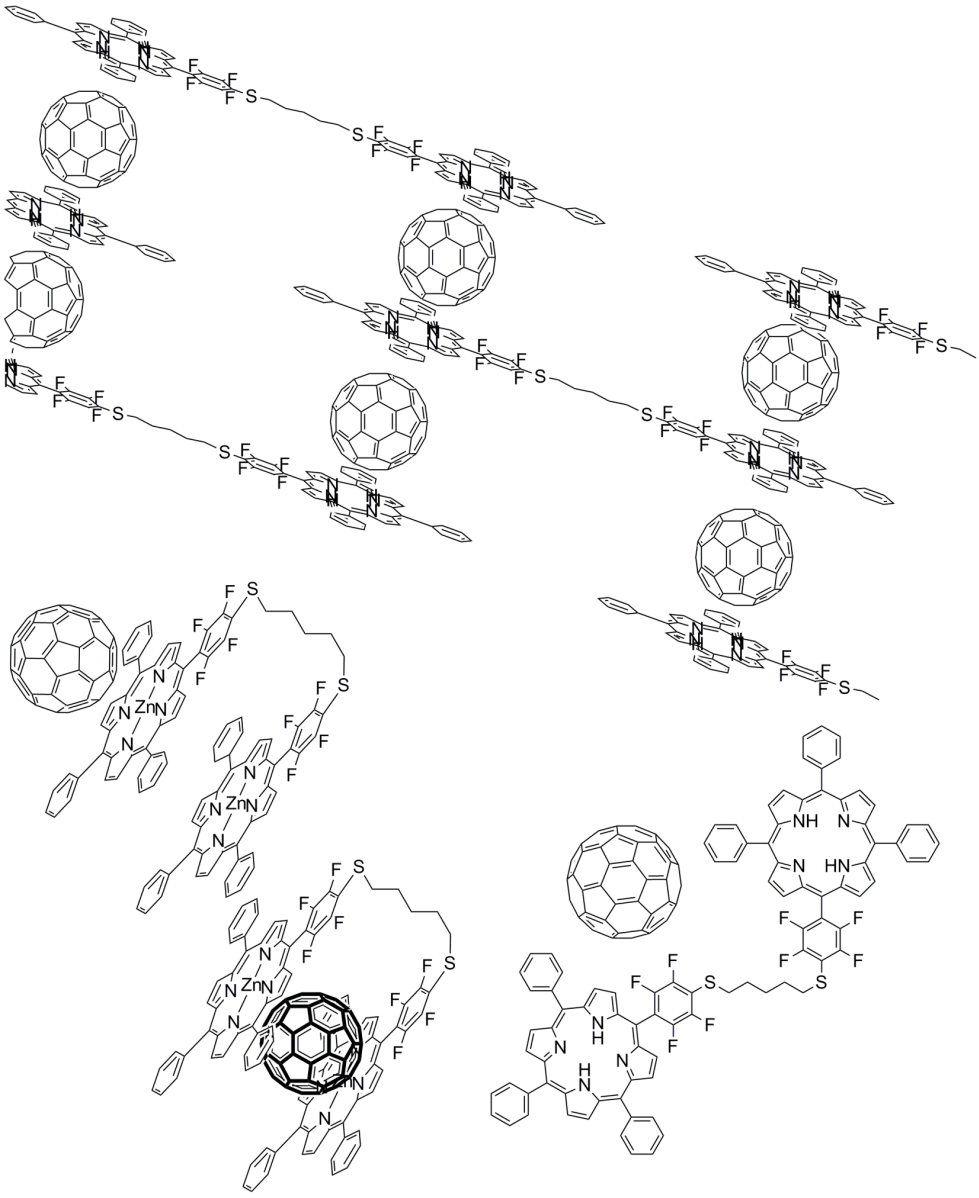

Figure 4-22. Possible supramolecular architectures of the fullerenes and the tethered dimer.

4.9 References

Adapted from "Facile synthesis of a flexible tethered porphyrin dimer that preferentially complexes fullerene C70." Jurow et al, DOI: 10.1039/c2cc31340e

(1) Boyd, P. D. W.; Reed, C. A. *Acc. Chem. Res.* **2005**, *38*, 235.

(2) Baran, P. S.; Monaco, R. R.; Khan, A. U.; Schuster, D. I.; Wilson, S. R. *J. Am. Chem. Soc.* **1997**, *119*, 8363.

(3) Bhattacharya, S.; Tominaga, K.; Kimura, T.; Uno, H.; Komatsu, N. *Chem. Phys. Let.* **2007**, *433*, 395.

(4) He, L.; Zhu, Y.-Z.; Zheng, J.-Y.; Ma, Y.-F.; Chen, Y.-S. *J. Photochem. Photobio. A: Chem.* **2010**, *216*, 15.

(5) Liddell, P. A.; Kodis, G.; Kuciauskas, D.; Andreasson, J.; Moore, A. L.; Moore, T. A.; Gust, D. *Phys. Chem. Chem. Phys.* **2004**, *6*, 5509.

(6) Mukherjee, S.; Bauri, A. K.; Bhattacharya, S. *Chem. Phys. Let.* **2010**, *500*, 128.

(7) Tamaki, K.; Imahori, H.; Sakata, Y.; Nishimura, Y.; Yamazaki, I. *Chem. Commun.* **1999**, 625.

(8) Umeyama, T.; Tezuka, N.; Kawashima, F.; Seki, S.; Matano, Y.; Nakao, Y.; Shishido, T.; Nishi, M.; Hirao, K.; Lehtivuori, H.; Tkachenko, N. V.; Lemmetyinen, H.; Imahori, H. *Angew. Chem. Int. Ed.* **2011**, *50*, 4615.

(9) Zhang, Y.; Yu, Y.; Jiang, Z.; Xu, H.; Wang, Z.; Zhang, X.; Oda, M.; Ishizuka, T.; Jiang, D.; Chi, L.; Fuchs, H. *Langmuir* **2009**, *25*, 6627.

(10) Wu, Z.-Q.; Shao, X.-B.; Li, C.; Hou, J.-L.; Wang, K.; Jiang, X.-K.; Li, Z.-T. *J. Am. Chem. Soc.* **2005**, *127*, 17460.

(11) Dudic, M.; Lhotak, P.; Stibor, I.; Petrickova, H.; Lang, K. *New J. Chem.* **2004**, *28*, 85.

(12) Shoji, Y.; Tashiro, K.; Aida, T. *J. Am. Chem. Soc.* **2004**, *126*, 6570.

(13) Jakob, M.; Berg, A.; Levanon, H.; Schuster, D. I.; Megiatto, J. D. *J. Phys. Chem. C* **2011**, *115*, 24555.

(14) Wilson, S. R.; MacMahon, S.; Tat, F. T.; Jarowski, P. D.; Schuster, D. I. *Chem. Commun.* **2003**, 226.

(15) Sessler, J. L.; Jayawickramarajah, J.; Gouloumis, A.; Torres, T.; Guldi, D. M.; Maldonado, S.; Stevenson, K. J. *Chem. Commun.* **2005**, 1892.

(16) D'Souza, F.; Chitta, R.; Gadde, S.; Zandler, M. E.; Sandanayaka, A. S. D.; Araki, Y.; Ito, O. *Chem. Commun.* **2005**, 1279.

(17) Echegoyen, L.; Echegoyen, L. E. *Acc. Chem. Res.* **1998**, *31*, 593.

(18) D'Souza, F.; Ito, O. *Chem. Commun.* **2009**, 4913.

(19) Drain, C. M.; Nifiatis, F.; Vasenko, A.; Batteas, J. D. *Angew. Chem. Int. Ed.* **1998**, *37*, 2344.

(20) Varotto, A.; Todaro, L.; Vinodu, M.; Koehne, J.; Liu, G.-y.; Drain, C. M. *Chem. Commun.* **2008**, 4921.

(21) Drain, C. M.; Varotto, A.; Radivojevic, I. *Chem. Rev.* **2009**, *109*, 1630.

(22) Mulholland, A. R.; Woodward, C. P.; Langford, S. J. *Chem. Commun.* **2011**, *47*, 1494.

(23) Babu, S. S.; Mohwald, H.; Nakanishi, T. *Chem. Soc. Rev.* **2010**, *39*, 4021.

(24) Coates, G. W.; Dunn, A. R.; Henling, L. M.; Ziller, J. W.; Lobkovsky, E. B.; Grubbs, R. H. *J. Am. Chem. Soc.* **1998**, *120*, 3641.

(25) Vilmercati, P.; Cudia, C. C.; Larciprete, R.; Cepek, C.; Zampieri, G.; Sangaletti, L.; Pagliara, S.; Verdini, A.; Cossaro, A.; Floreano, L.; Morgante, A.; Petaccia, L.; Lizzit, S.; Battocchio, C.; Polzonetti, G.; Goldoni, A. *Surf. Sci.* **2006**, *600*, 4018.

(26) Boyd, P. D. W.; Hodgson, M. C.; Rickard, C. E. F.; Oliver, A. G.; Chaker, L.; Brothers, P. J.; Bolskar, R. D.; Tham, F. S.; Reed, C. A. *J. Am. Chem. Soc.* **1999**, *121*, 10487.

(27) Li, H.; Zhou, B.; Lin, Y.; Gu, L.; Wang, W.; Fernando, K. A. S.; Kumar, S.; Allard, L. F.; Sun, Y.-P. *J. Am. Chem. Soc.* **2004**, *126*, 1014.

(28) Sgobba, V.; Rahman, G. M. A.; Guldi, D. M.; Jux, N.; Campidelli, S.; Prato, M. *Adv. Mat.* **2006**, *18*, 2264.

(29) Tasis, D.; Tagmatarchis, N.; Bianco, A.; Prato, M. *Chem. Rev.* **2006**, *106*, 1105.

(30) Ariga, K.; Hill, J. P.; Ji, Q. *Phys. Chem. Chem. Phys.* **2007**, *9*, 2319.

(31) Ariga, K.; Sakakibara, K.; Richards, G. J.; Hill, J. P. *Supramolecular Chem.* **2011**, *23*, 183.

(32) Sakakibara, K.; Hill, J. P.; Ariga, K. *Small* **2011**, *7*, 1288.

(33) Kim, D. *Multiporphyrin Arrays: Fundamentals and Applications*; CRC Press: Boca Raton, 2012.

(34) Radivojevic, I.; Varotto, A.; Farley, C.; Drain, C. M. *Energy & Environmental Science* **2010**, *3*, 1897.

(35) Jurow, M.; Schuckman, A. E.; Batteas, J. D.; Drain, C. M. *Coordination Chemistry Reviews* **2010**, *254*, 2297.

(36) Drain, C. M.; Smeureanu, G.; Patel, S.; Gong, X. C.; Garno, J.; Arijeloye, J. *New Journal of Chemistry* **2006**, *30*, 1834.

(37) Drain, C. M.; Bazzan, G.; Milic, T.; Vinodu, M.; Goeltz, J. C. *Israel Journal of Chemistry* **2005**, *45*, 255.

(38) Drain, C. M.; Batteas, J. D.; Flynn, G. W.; Milic, T.; Chi, N.; Yablon, D. G.; Sommers, H. *Proceedings of the National Academy of Sciences of the United States of America* **2002**, *99*, 6498.

(39) Deak, D. S.; Porfyrakis, K.; Castell, M. R. *Chem. Commun.* **2007**, 2941.

(40) Dietz, P.; Fostiropoulos, K.; Krätschmer, W.; Hansma, P. K. *Citation: Appl. Phys. Lett.* **1992**, *60*, 62.

CHAPTER 5

Zr(IV) Porphyrinoids on Graphene Oxide by Axial Ligation

5.1 Abstract

$Zr^{(IV)}$ porphyrinoids were reacted at room temperature with graphene oxide (GO) as a dispersion in THF and as films on glass. Axial coordination of the protruding oxophylic central metal ion of the chromophore to the oxygen bearing functional groups on the GO surface results in a new hybrid material with high dye loading. The photophysical properties of the material are derived from both the chromophores and the GO.

The unique properties of graphene oxide (GO) have driven research on using GO in functional materials for diverse applications.[1] GO can be produced by a variety of scalable methods that result in similar, but not identical, products.[2] Theories about the exact structure of GO have continuously evolved because of the non-homogenous nature of the material. The most commonly accepted (Lerf-Klinowski) model describes a surface composed of a substituted network of sp2 and sp3 hybridized carbon atoms. Alcohol and epoxide functionalities are present on the basal planes with carboxylic groups along the edges and larger defect sites of the flakes, which range between tens of nanometers and tens of microns in edge length and 0.8-1.5 nm in thickness if fully exfoliated depending on the method of production.[3]

Interest in GO has focused on properties arising from its non-stoichiometric nature resulting in regions of variable oxyphilicity, controllable dispersability in water and organic solvents,[4] interesting photonic properties, and potential for use in biological systems such as for photodynamic therapeutics and for drug delivery.[1,5-8] Recent reports demonstrate GO

applications in nonlinear optics,[9] as p or n type materials,[10,11] as a functional surfactant,[12] and antennae complexes to collect solar energy.

Free base and metallo tetraphenylporphyrins can be covalently bound to GO via amides[13,14] and esters[15] to yield photonic materials. Cationic porphyrins electrostatically associate with GO and rGO, and GO can be appended with polyethylene glycols to make biocompatible materials.[6,7] The large, planar phthalocyanines and their metalo derivatives associate with graphene areas in rGO via pi-pi interactions.[16,17] Sensitized hybrid GO materials may serve as components of solar cell devices.[18]

We report herein the efficient preparation and photonic properties of materials composed of 5,10,15,20-tetraphenylporphyrinato Zr^{IV}, Zr^{IV}(TPP), or phthalocyaninato Zr^{IV} , Zr^{IV}(Pc) (Figure 5-2) coordinated directly to the oxygen containing functional groups on the surfaces and edges of GO via coordination to the protruding oxyphilic metal ion. The starting materials, with acetates as auxiliary ligands, $ZrTPP(ac)_2$ and $ZrPc(ac)_2$, are easily synthesized in good yield from commercially available precursors and have electronic spectra typical of porphyrins and phthalocyanines respectively.[19,20] The Zr(IV) metal ion, ionic radius 0.72 Å, is displaced 0.9 Å to 1 Å from the mean plane of the macrocycle nitrogens.[19] Group IV metalloporphryrinoids have demonstrated similar binding modes to defects in polyoxometalates and to TiO_2 surfaces for use in dye sensitized solar cells.[20,21] Direct attachment of the chromophore to the GO surface via the protruding metal ion results in a coplanar orientation of the chromophores relative to the GO surface and at an angle on the edges and large defects (Figure 5-1). The Zr^{IV} serves as a direct conduit for electronic coupling of the dye and GO systems because of the mixing of the metal ion and chromophore orbitals.[9,22] Thus, the photonic properties of this new hybrid material can be exploited and tuned.

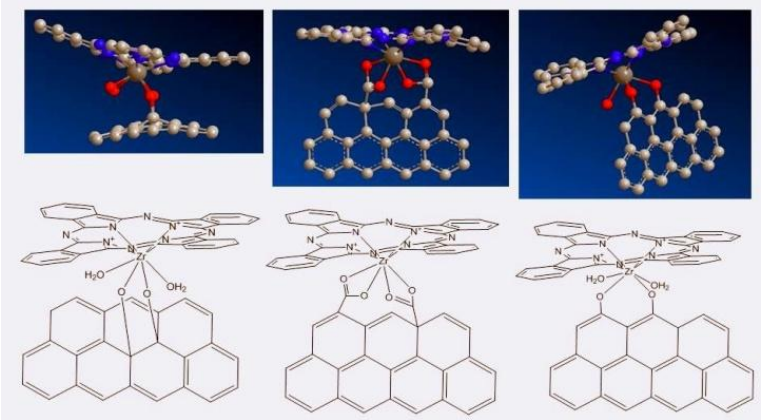

Figure 5-1. Three of several possible binding modes for Zr^{IV}(Pc) on GO. MM2 calculations (top, left to right) for internal diol, side carboxylates, and side diols; grey=C, blue=N, red=O, dark grey=Zr^{IV}, H left out for clarity.

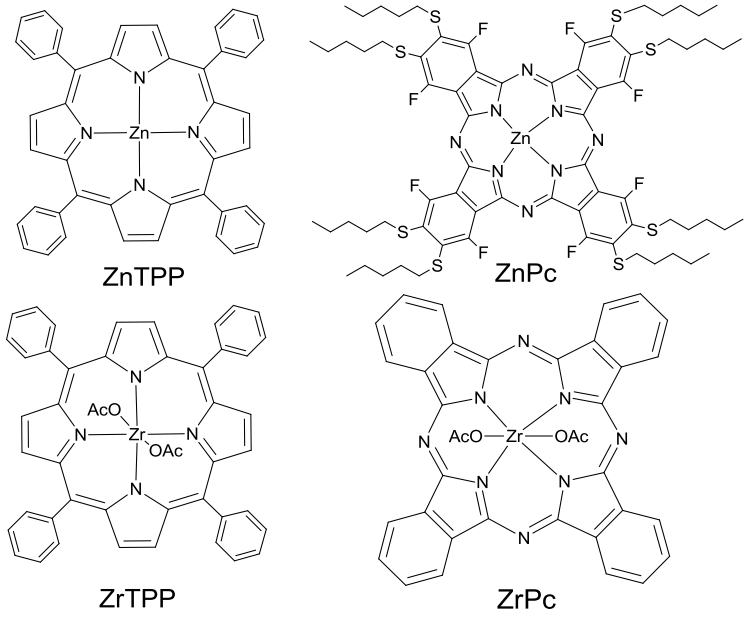

Figure 5-2. Structure of porphyrins and phthalocyanines used. Zn(Pc) is made by simple click type substitution of peripheral fluorine atoms of a commercially available precursor with thioalkanes to improve solubility.[23] Synthetic details of Zr^{IV} compounds are reported elsewhere.[20]

5.2 Experimental Procedures

Titration Spectra: A dispersion of 0.1mg/mL GO in THF made by sonicating single layer GO flakes (purchased from ACS material LLC; 99% single layer, 99% pure, 40.78% oxygen by weight) in freshly distilled THF was titrated into solutions of porphyrin (2 μM) or phthalocyanine (3 μM) in THF. Fluorescence emission spectra were excited at: Zn(Pc)/655nm, Zr^{IV}(Pc)/633nm, Zn(TPP)/422nm and Zr^{IV}(TPP)/417nm.

AFM measurements were conducted with an Asylum AFM (MFP-3D, Asylum Research Corp.) UV-visible absorption spectroscopy was performed on a Cary 1-Bio UV-Visible spectrometer. Steady state fluorescence spectra were obtained on a HORIBA Jobin-Yvon FluoroLog-3 fluorometer. Quartz or optical glass cuvettes were used for all spectroscopic studies. All photophysical studies were carried out in distilled solvents. Experiments have been repeated multiple times by at least three different researchers.

Solid Films: Graphene oxide in aqueous suspension (3 mg/mL) was spin coated onto piranha cleaned quartz slides and dried in an oven to make 3 nm thick continuous films. Films were then soaked in 0.1 mM solutions of dyes in CH_2Cl_2 for 3 days at room temperature in the dark to ensure equilibration. Coated films were rinsed extensively with clean CH_2Cl_2 to remove any unbound dye, backs of slides were cleaned repeatedly with MeOH and spectra were recorded.

Nanocomposites: 100 μM solutions of both Zr^{IV}(Pc) and Zn(Pc) in THF were prepared to a GO concentration of 0.1mg/mL. Solutions were sonicated for 5 minutes to ensure good dispersion. After allowing 48 H for equilibration at room temperature, samples were centrifuged

at 13,000 RPM for 15 minutes and washed with fresh THF to remove unbound molecules. Procedure was repeated twice to ensure complete removal of unbound dye.

TEM: All data were collected at 200 kV on a Jeol 2100 transmission electron microscope equipped with EDAX at the eucentric height to ensure reproducibility of the measurements. An 8 µL drop of the above described nanocomposite dispersion was placed on a 300 mesh carbon coated copper grid (TED Pella Inc.) and allowed to dry for 1 minute before imaging.

AFM: Samples for AFM were prepared either by dip coating ozone cleaned glass into the nanocomposites THF suspensions described above or by centrifuging the suspension, dispersing the pellet into nanopure water by sonication and spin coating onto ozone cleaned glass.

Probe Measurements: Devices were made by spin coating layers of GO (of 8 nm or 15 nm) onto ozone cleaned glass from an aqueous suspension. Sheet resistance was measured by Van der Pauw technique of the pristine GO layers, of an 8 nm GO film soaked in Zr^{IV}(Pc) or Zr^{IV}(TPP) (0.1 mM in methylene chloride), or of an 8 nm GO film spin coated on top of a ca. 40 nm thick layer of Zr^{IV}(TPP) or Zr^{IV}(Pc) spin cast from chlorobenzene on ozone cleaned glass. Measurements were taken in the dark and under illumination.

5.3 Results and Discussion

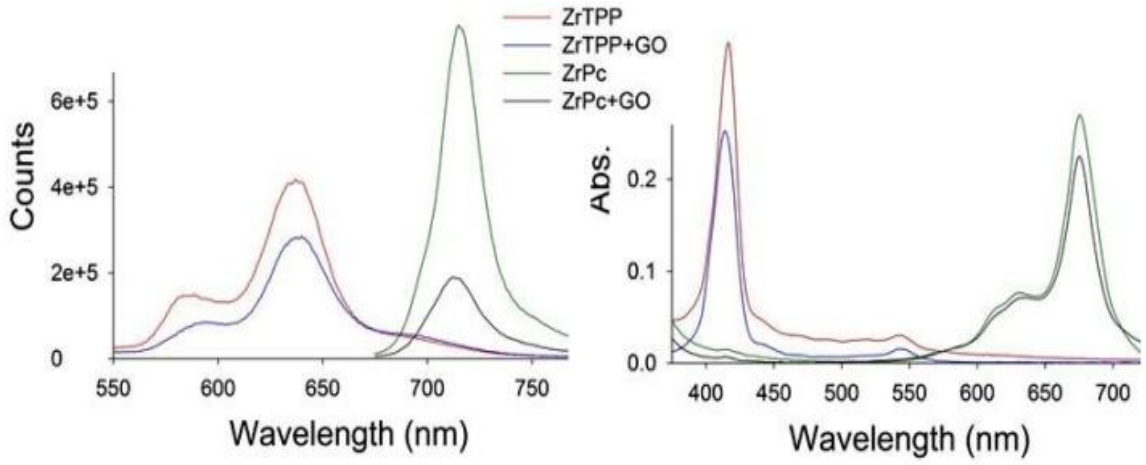

Figure 5-3. UV-visible (right) and fluorescence (left) spectra of a $Zr^{IV}(Pc)(ac)_2$ or $Zr^{IV}(TPP)(ac)_2$ solution and after addition of 120 µL of 0.1 mg/mL GO dispersed in THF. (λ_{ex} = 417 nm for $Zr^{IV}(TPP)$ and 633 nm for $Zr^{IV}(Pc)$)

GO was dispersed by brief sonication in THF at a concentration of 0.1 mg/mL.[24] This solution was then slowly titrated in 40 µL aliquots into a THF solution of 3 µM $Zr^{IV}(Pc)ac_2$ or 2 µM $Zr^{IV}(TPP)ac_2$ while monitoring the UV-visible and fluorescence emission spectra (Figure 5-3). The solution was allowed to equilibrate for 24 hours to allow the displacement reaction to occur. Upon completion of the titration, the UV-visible spectra of the hybrid materials with Zr(Pc) and Zr(TPP) attached to GO monotonically decreases as the solution is diluted, thus indicating that the solution is homogeneously dissolved. The spectral shifts and decreased intensity in the $Zr^{IV}(Pc)$ Q band (676 nm) and $Zr^{IV}(TPP)$ Soret (421 nm) are consistent with displacement of the acetate ligands by the oxygen functional groups on the GO and formation of the hybrid material.[25]

Significant fluorescence quenching indicates energy transfer or charge injection from the chromophore excited state into the GO.[13,26] When binding is complete, the emission is quenched by 70% for the Zr^{IV}(Pc) and 30% for the Zr^{IV} (TPP), respectively. For Zn(TPP) and Zn(Pc) controls, the electronic absorption and emission spectra are unchanged by addition of the GO dispersion. The orthogonal phenyl moieties on Zr^{IV}(TPP) likely reduce binding to the surfaces of GO by steric hindrance.

To investigate the properties of the material in the solid state, films of GO were spin cast onto quartz substrates from dispersions in water, soaked in 0.1 mM dye solutions in CH_2Cl_2 for 72 h, and rinsed thoroughly with clean solvent. An aqueous GO dispersion of 3 mg/mL was found to yield a 15 nm thick film while a 1 mg/mL dispersion yielded an 8 nm continuous film. After soaking, similar fluorescence quenching by charge transfer from dye to GO is observed for these adsorbed films.[27] UV-visible and fluorescence spectra (Figure 5-4) demonstrate the presence of the dyes by the absorbance from the Zr^{IV}(TPP) Soret (420 nm) and Zr^{IV}(Pc) Q (693 nm) bands.

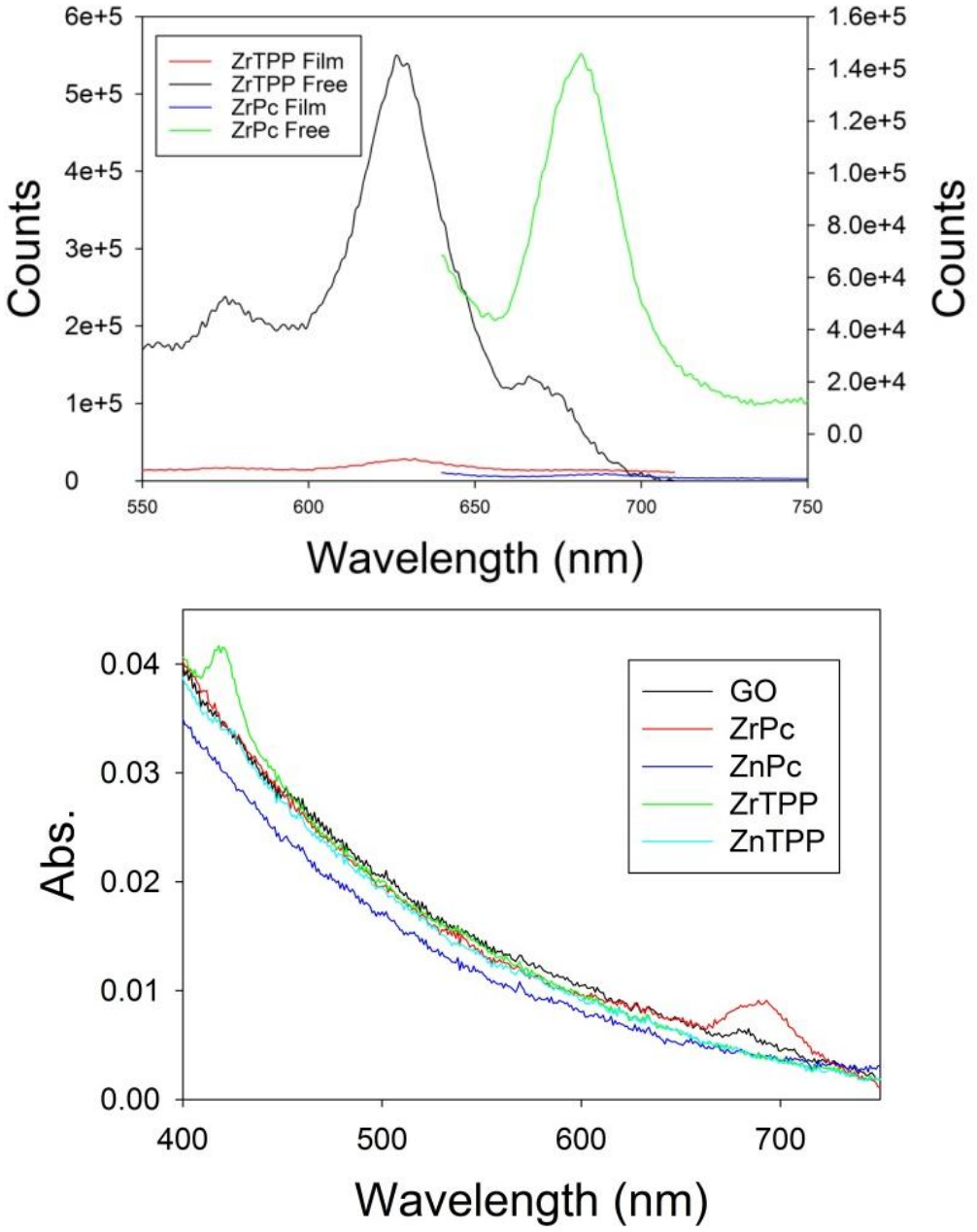

Figure 5-4. Top: comparison of fluorescence of dyes bound to GO and unbound dyes. Bottom: UV-visible spectra of GO films treated with Zr^{IV} dye solutions.

The absence of significant shifts in the optical spectra indicate that the dye molecules are not aggregated. The small peaks from the control Zn^{II} complexes are likely the result of dye molecules interacting with the GO in graphene like regions through pi-pi interactions. Optical data on the films suggests a surface density of ca. one chromophore per five nanometers square,[28] assuming average flakes of 1 μm^2 and dyes bind to only one face. The 40% oxygen content of the GO material used facilitates high surface coverage. The distribution of the dyes is likely greater on the flake edges where there is greater oxygen content.

In a separate experiment, GO was dispersed in THF to make 100 µM Zr^{IV}(Pc) solution with 0.1mg/mL GO suspended to ensure saturation of GO surfaces with chromophores. Suspensions were allowed to react until equilibrium was reached, whereupon the mixture was centrifuged, rinsed with clean THF to remove unbound dye, and dispersed again in THF by brief sonication to form bound nanocomposites of GO and dye.

Ozone cleaned glass slides were dip coated into these dispersions and rinsed well with clean THF. Samples were then examined by atomic force microscopy (AFM) (Figure 5-5). The 40% oxygen by weight of the GO used allows for high surface density of the bound chromophores and the formation of a nearly complete monolayer bound to the GO surfaces. Previous work characterized a single layer of GO as ca. 1.0 nm thick.[29 30] Single layer flakes of GO coated on both sides with Zr^{IV}(Pc) are visible (Figure 5-4) with a height of ca. 1.8-2 Å. The total heights of the Zr^{IV}(Pc)/GO composite correspond well to those predicted by combining the heights of the GO with those of the crystal structures of the chromophores. Control samples were prepared by identical methods both in the clean THF and in solutions of Zn(Pc) and Zn(TPP). In each case individual flakes of 1.2-1.4 Å are observed without the zinc dyes.

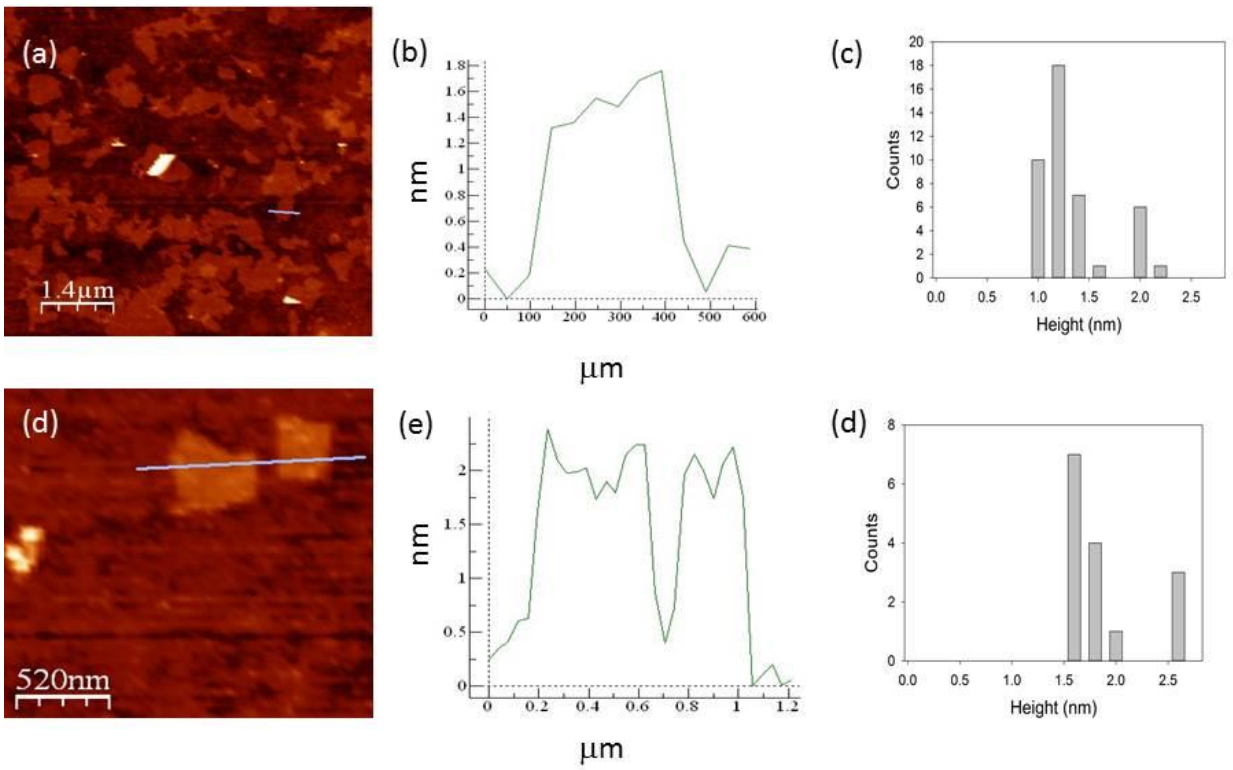

Figure 5-5. A GO dispersion of 0.1mg/mL was cast onto ozone cleaned glass, with the resulting control AFM image (a), corresponding height trace (b) and histogram (c). A 5 mg/mL aqueous GO dispersion was added to a Zr^{IV}(Pc) solution in THF to make a 0.1 mg/mL GO dispersion in 0.1 mM Zr^{IV}(Pc) solution. System was allowed to equilibrate for 3 days. Solutions were twice rinsed by centrifuging at 13k RPM for 10 minutes, decanting supernatant and dispersing in fresh THF by 10 minute sonication. Glass slides were dipped into resulting GO/Zr^{IV}(Pc) suspension and rinsed again with fresh THF to remove any unbound Zr^{IV}(Pc). The resulting AFM image (d), height trace (e) and histogram (d) of a representative sample are shown. Flake heights are 1.8 nm on average which corresponds well to the thickness of the GO flake bound on both sides by Zr^{IV}(Pc) molecules.

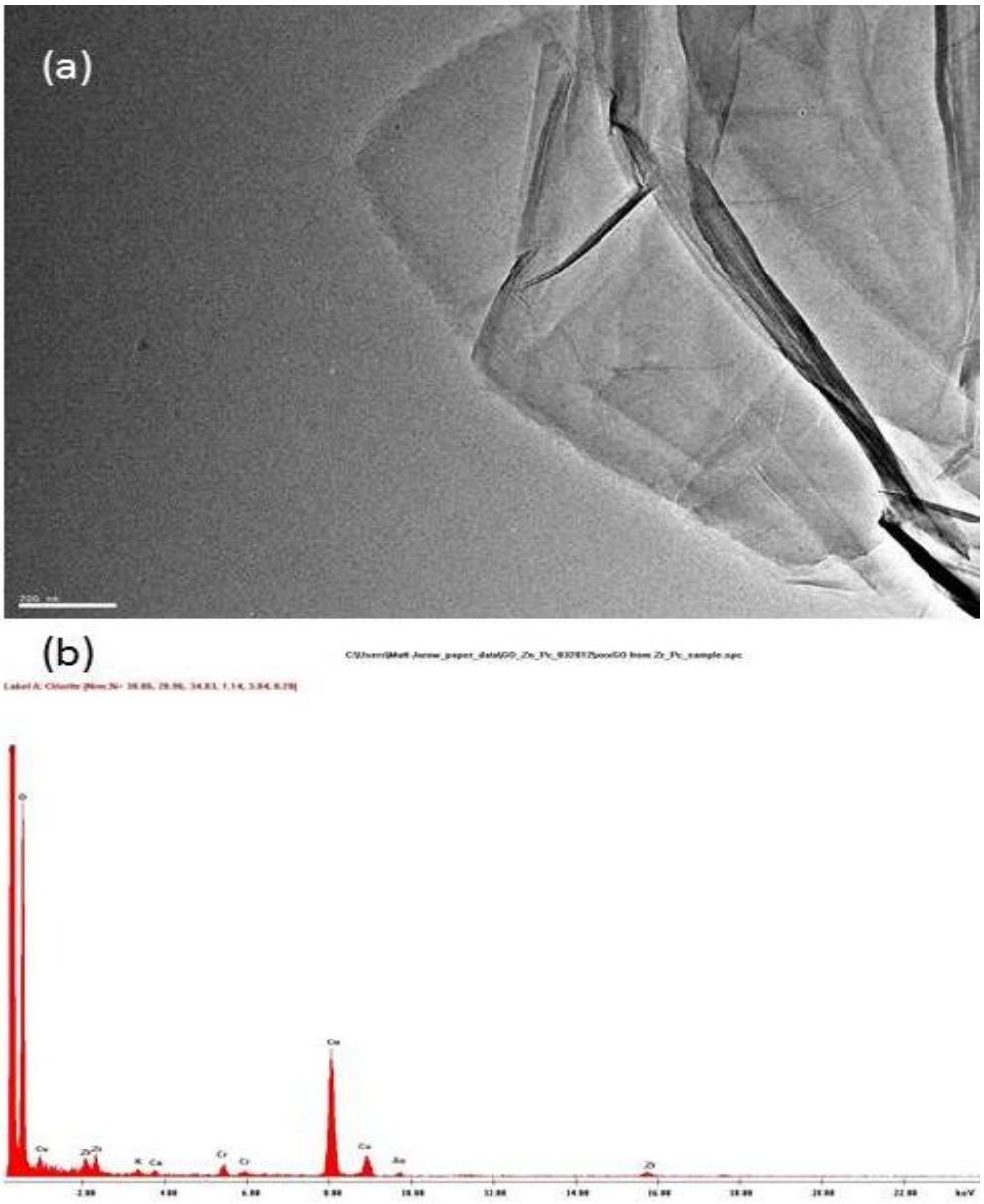

Figure 5-6. TEM image of Zr^{IV}(Pc) coated GO flakes (a) and EDAX spectrum (b). Overlapping layers are visible. Rough edges are likely bound porphyrin aggregates. Scale bar is 200 nm. EDAX indicates presence of oxygen from the GO as well as Zr from the Zr^{IV}(Pc). The EDAX spectrum is reproducible along entire area demonstrating even coating of the GO surface with Pc. No zinc peaks are observed in the EDAX spectra of the control systems treated with Zn^{II}(Pc), see appendix.

TEM images of the same nanocomposites indicate a uniform coating of the GO surface with Zr^{IV}(Pc) and EDAX spectra display characteristic bands for the presence of Zr (Figure 5-6). No evidence of Zn is observed when GO is mixed with Zn^{II}(Pc) under the same conditions.

When the same nanocomposites dispersions were again centrifuged and dispersed in water the Zr^{IV}(Pc)/GO nanocomposites are less stable and precipitate rapidly while the unfunctionalized GO remains suspended. This indicates a significantly increased hydrophobicity of the hybrid material relative to GO. AFM analysis of films prepared by spin casting of sonicated samples (60 W, 30 minutes) display perforations of the graphene flakes resultant from removal of the oxophillic Zr (IV) species. The perforation/degradation of the GO sheets also eliminates the observed fluorescence of the pristine GO flakes. No fluorescence was observed upon excitation at 633 nm indicating removal of the bound Pc dye. Control experiments with Zn(Pc) and GO displays the characteristic UV-visible spectrum and broad fluorescence of GO without perforations.

As a separate control experiment GO dispersion in THF were reacted with $ZrCl_4$. Large aggregates of metal linked GO sheets precipitate immediately. When dispersed by sonication into water no perforation or changes to the flakes are observed.

Four point probe measurements (Table 5-1) yielded sheet resistance values of 2.9×10^{10} and 3.6×10^{9} Ω/□ for 8 nm and 15 nm thick GO films, respectively. For dye/GO composite films, made by spin casting the dye treated GO or dipping the cast GO into Zr^{IV}(Pc) or Zr^{IV}(TPP) solutions, the sheet resistance of 8 nm films decreased by ca. 50%. This indicates the Zr^{IV} dyes can bridge some of the defects in the GO material. Future work will investigate the properties of the dye/substrate interface as well as anticipated doping and photoconductivity applications.[4,10,31,32]

	DARK			LIGHT		
	R_{ave}	S_{dev}	R_{sheet}	R_{ave}	S_{dev}	R_{sheet}
8nm GO	6.3E+09	0.00	**2.9E+10**	6.5E+09	0.02	**2.9E+10**
15nm GO	8.0E+08	0.05	**3.6E+09**	7.9E+08	0.06	**3.6E+09**
Por/GO	2.5E+09	0.03	**1.1E+10**	2.5E+09	0.02	**1.1E+10**
Pc/GO	6.0E+09	0.30	**2.7E+10**	6.0E+09	0.28	**2.7E+10**
GO/Por	3.4E+09	0.01	**1.5E+10**	3.4E+09	0.01	**1.5E+10**
GO/Pc	3.3E+09	0.04	**1.5E+10**	3.3E+09	0.04	**1.5E+10**

Table 5-1. Sheet resistance (Rs) values in Ω/mm^2 of GO layers on glass, GO layers deposited on top of dye layers, and GO layers with dyes attached by soaking. The high standard deviation of the Pc/GO species is the result of an observed anisotropy in the measurement.

5.4 Layer by Layer Systems

Layer by layer systems were made by sequential dipping of cleaned quartz slides in solutions of Zn(Pc), Zr^{IV}(Pc) or $ZrCl_4$ after initial deposition of an 8 nm GO layer made by spin casting (Figure 5-7). Layer by layer assembly is a valuable and simple technique to create functional materials with controlled size, morphology, and physical properties on any number of substrates. Initially, free hydroxyl groups on the GO flakes associate, likely by hydrogen bonding, with the quartz substrate(Figure 5-8 and 5-9).[33] The nonstoichiometric nature of the GO flakes in the initial layer lead to imperfect and varied results as the systems grow. Zn(Pc)

adheres to the hydrophobic basal plane regions of unoxidized sp^2 hybridized carbon allowing for layer growth while $Zr^{IV}(Pc)$ and $ZrCl_4$ both bind to the oxygenated regions of the GO.[4] Binding of the chromophore and the addition of GO is evidenced by increased absorbance at the UV absorption maxima for the dyes and across the entire spectrum for the GO (Figure 5-10). In each case the bound molecules serve as nucleation points for the formation of microcrystals of dye which then promote aggregation of GO flakes creating uneven films in the latter layers decorated with dye aggregates.

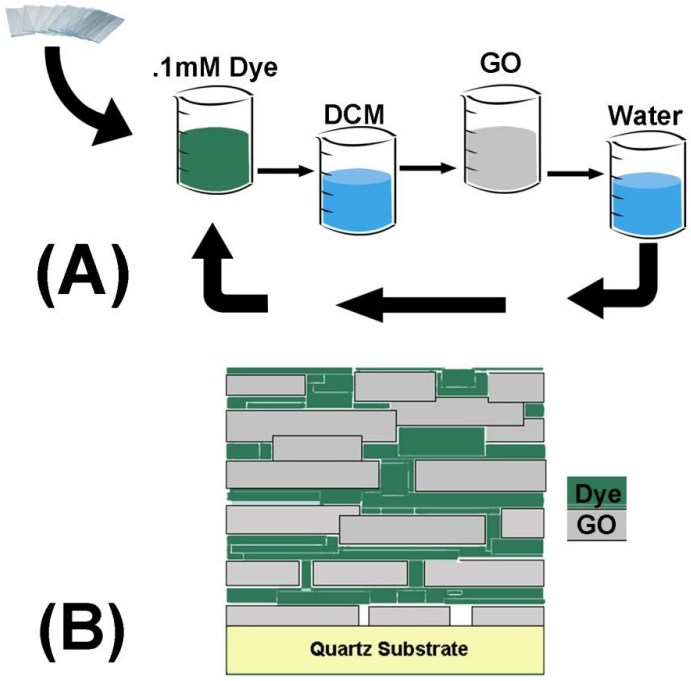

Figure 5-7. Depiction of layer by layer process (top) and result (bottom).

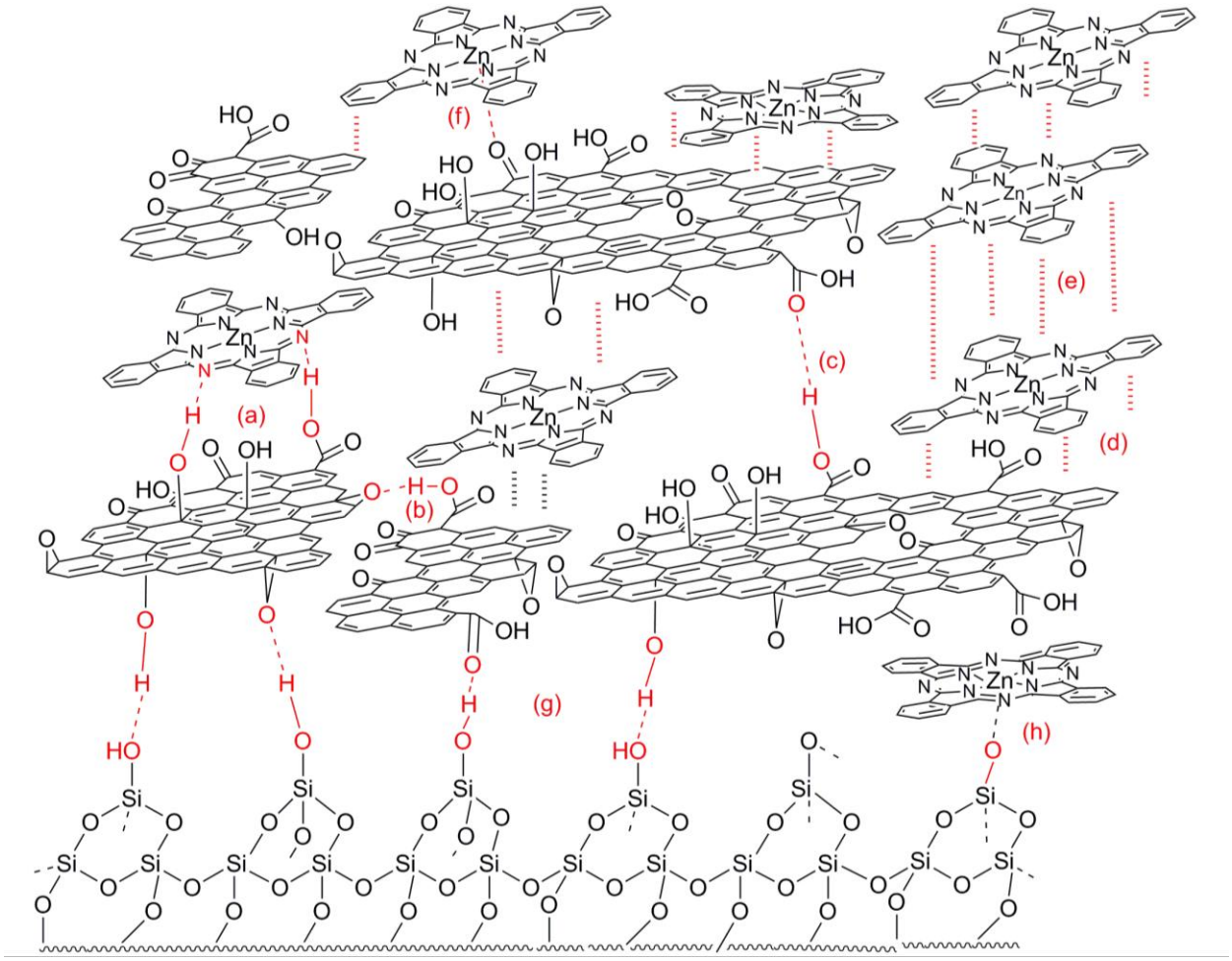

Figure 5-8. The layers are incomplete, thus there are interactions between GO sheets and between the dyes. Schematic representation of possible intermolecular interactions between the Zn(Pc) dye and GO include: (a) H-bond interactions between the GO and *meso* nitrogens on the dye, (b) H-bond interactions between neighboring GO in the same layer, (c) H-bond interactions between layers of GO, (d) pi-pi interactions between the dye and GO, (e) pi-pi interactions between dyes, (f) coordination of an oxygen on GO to the Zn(II) center of the dye, (g) H-bond interactions between GO and the quartz substrate, (h) coordination of the quartz oxygen into the ZnPc. There are other configurations of these interactions.

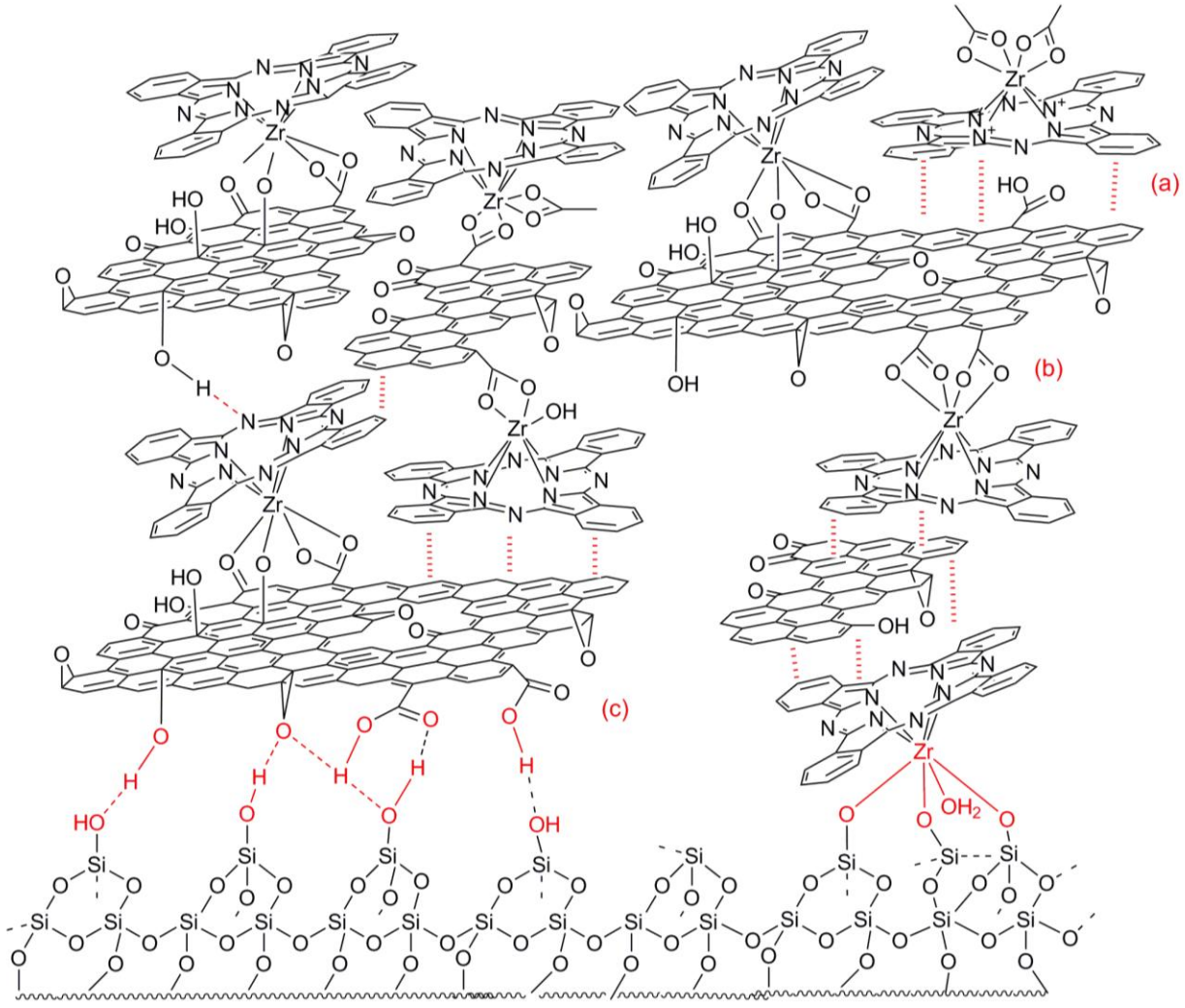

Figure 5-9. Schematic representation of the possible intermolecular interactions between GO, $Zr^{IV}(Pc)$ and the quartz substrate include: (a) pi-pi interactions between the starting $Zr^{IV}(Pc)(ac)_2$, (b) coordination of the protruding Zr(IV) ion of the Pc to the oxygen groups on GO, (c) H-bonds between the substrate and the GO. Other variations of these interactions are also present, and see Figure 8-8.

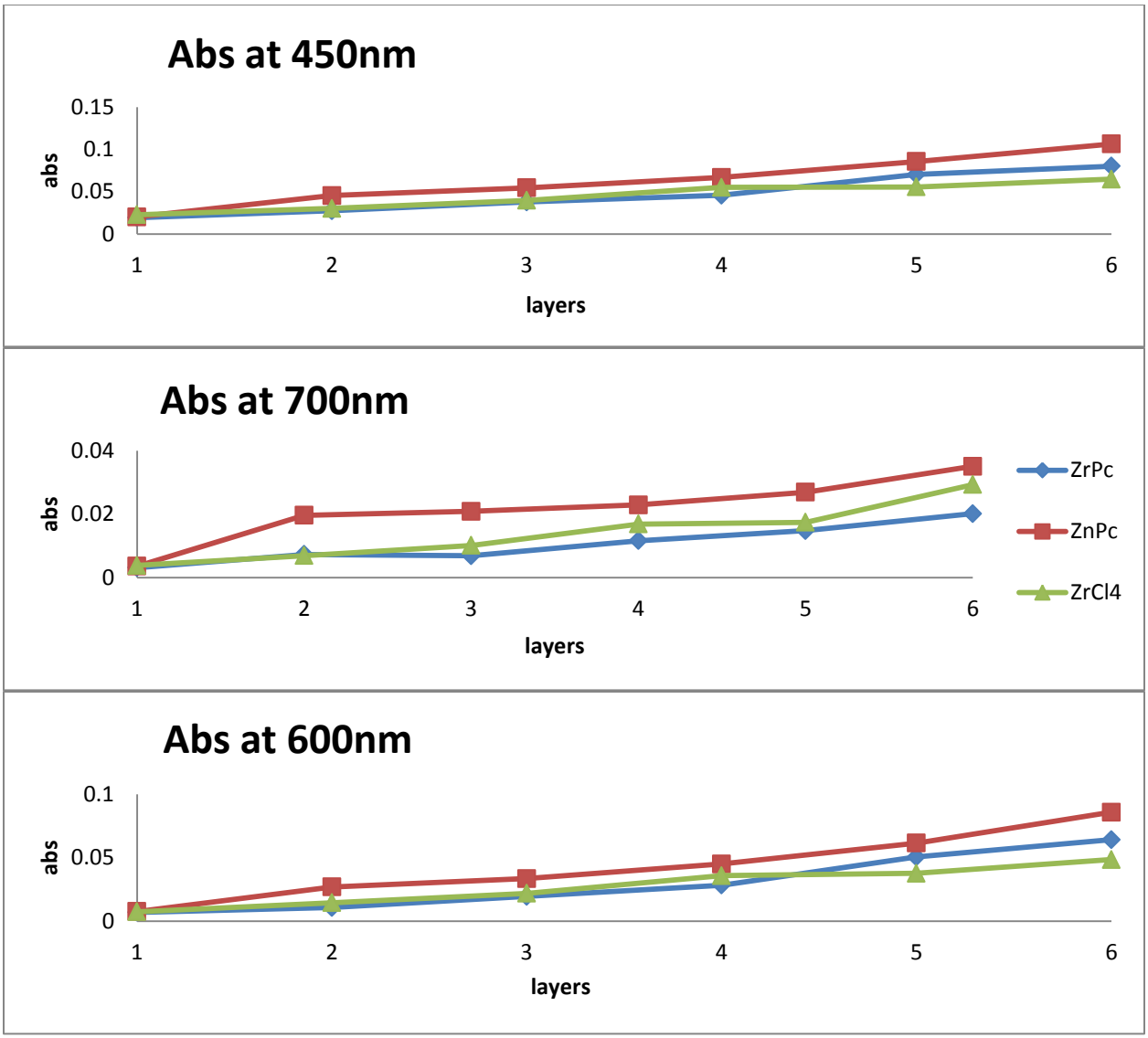

Figure 5-10. Plots of absorbance of layer by layer samples at specified wavelengths and layers.

The highly varied composition of the GO affords many possible binding modes and binding sites for the Zr^{IV} dyes, for interactions between flakes of the GO, and for interactions with the substrate. Similarly, the hydrophobic dye can interact with grapheme like areas of the GO, while the oxophylic metal center can interact with oxygen functional groups on the GO and with the substrate. Though the initial layers are incomplete, sequential dipping of the substrate

into the GO and Zr^{IV} dye solutions builds nanofilms with controlled thickness, controlled optical density, and controlled coverage.

5.5 Conclusions

A composite film composed of Zr^{IV} porphyrins or phthalocyanines appended to a GO substrate with high surface coverage displays photonic properties derived from both components. These properties are enabled by the concomitant binding of the metal center to both the porphyrinoid and the carboxylate groups decorating the edges of the GO sheets and the OH groups on the planar surfaces. The fluorescence of the bound dyes is quenched.

The fluorescence emission spectra observed from GO in water solution, is altered once chromophores are attached to the functionalized regions of GO, thus the dyes changed electronic dynamics of the substrate.[8] Reduced GO has enhanced electronic properties and the Zr^{IV} dyes should bind to remaining oxygen containing defect sites.[34] This type of direct sensitization will broaden the applications of GO and foster the creation of novel composite systems and new functional materials.

5.6 References

(1) Loh, K. P.; Bao, Q.; Eda, G.; Chhowalla, M. *Nat Chem* **2010**, *2*, 1015.
(2) Dreyer, D. R.; Park, S.; Bielawski, C. W.; Ruoff, R. S. *Chemical Society Reviews* **2010**, *39*, 228.
(3) Lerf, A.; He, H.; Forster, M.; Klinowski, J. *The Journal of Physical Chemistry B* **1998**, *102*, 4477.
(4) Kim, J.; Cote, L. J.; Kim, F.; Yuan, W.; Shull, K. R.; Huang, J. *Journal of the American Chemical Society* **2010**, *132*, 8180.
(5) Shih, C.-J.; Lin, S.; Sharma, R.; Strano, M. S.; Blankschtein, D. *Langmuir* **2011**, *28*, 235.
(6) Liu, Z.; Robinson, J. T.; Sun, X.; Dai, H. *Journal of the American Chemical Society* **2008**, *130*, 10876.
(7) Sun, X.; Liu, Z.; Welsher, K.; Robinson, J.; Goodwin, A.; Zaric, S.; Dai, H. *Nano Research* **2008**, *1*, 203.
(8) Luo, Z.; Vora, P. M.; Mele, E. J.; Johnson, A. T. C.; Kikkawa, J. M. *Applied Physics Letters* **2009**, *94*, 111909.
(9) Yao, C.; Yan, L.-K.; Guan, W.; Liu, C.-G.; Song, P.; Su, Z.-M. *Dalton Trans.* **2010**, *39*, 7645.
(10) Arnold, M. S.; Zimmerman, J. D.; Renshaw, C. K.; Xu, X.; Lunt, R. R.; Austin, C. M.; Forrest, S. R. *Nano Letters* **2009**, *9*, 3354.
(11) Tung, V. C.; Huang, J.-H.; Tevis, I.; Kim, F.; Kim, J.; Chu, C.-W.; Stupp, S. I.; Huang, J. *Journal of the American Chemical Society* **2011**, *133*, 4940.
(12) Tung, V. C.; Kim, J.; Cote, L. J.; Huang, J. *Journal of the American Chemical Society* **2011**, *133*, 9262.
(13) Xu, Y.; Liu, Z.; Zhang, X.; Wang, Y.; Tian, J.; Huang, Y.; Ma, Y.; Zhang, X.; Chen, Y. *Advanced Materials* **2009**, *21*, 1275.
(14) Karousis, N.; Sandanayaka, A. S. D.; Hasobe, T.; Economopoulos, S. P.; Sarantopoulou, E.; Tagmatarchis, N. *Journal of Materials Chemistry* **2011**, *21*, 109.
(15) Bala Murali Krishna, M.; Venkatramaiah, N.; Venkatesan, R.; Narayana Rao, D. *Journal of Materials Chemistry* **2012**, *22*, 3059.
(16) Chunder, A.; Pal, T.; Khondaker, S. I.; Zhai, L. *The Journal of Physical Chemistry C* **2010**, *114*, 15129.
(17) Malig, J.; Jux, N.; Kiessling, D.; Cid, J.-J.; Vázquez, P.; Torres, T.; Guldi, D. M. *Angewandte Chemie International Edition* **2011**, *50*, 3561.
(18) Wang, X.; Zhi, L.; Mullen, K. *Nano Letters* **2007**, *8*, 323.
(19) Brand, H.; Arnold, J. *Coordination Chemistry Reviews* **1995**, *140*, 137.
(20) Falber, A.; Burton-Pye, B. P.; Radivojevic, I.; Todaro, L.; Saleh, R.; Francesconi, L. C.; Drain, C. M. *European Journal of Inorganic Chemistry* **2009**, *2009*, 2459.
(21) Radivojevic, I.; Bazzan, G.; Burton-Pye, B. P.; Ithisuphalap, K.; Saleh, R.; Durstock, M. F.; Francesconi, L. C.; Drain, C. M. *J. Phys. Chem. C* **2012**, *ASAP*, dx.doi.org/10.1021/jp301853d.
(22) Liao, M.-S.; Scheiner, S. *J. Chem. Phys.* **2002**, *117*.
(23) Varotto, A.; Nam, C.-Y.; Radivojevic, I.; P. C. Tomé, J.; Cavaleiro, J. A. S.; Black, C. T.; Drain, C. M. *Journal of the American Chemical Society* **2010**, *132*, 2552.

(24) Paredes, J. I.; Villar-Rodil, S.; Martínez-Alonso, A.; Tascón, J. M. D. *Langmuir* **2008**, *24*, 10560.
(25) Beletskaya, I.; Tyurin, V. S.; Tsivadze, A. Y.; Guilard, R.; Stern, C. *Chemical Reviews* **2009**, *109*, 1659.
(26) Zhang, L.; Xia, J.; Zhao, Q.; Liu, L.; Zhang, Z. *Small* **2010**, *6*, 537.
(27) Treossi, E.; Melucci, M.; Liscio, A.; Gazzano, M.; Samorì, P.; Palermo, V. *J. Am. Chem. Soc.* **2009**, *131*, 15576.
(28) Bazzan, G.; Smith, W.; Francesconi, L. C.; Drain, C. M. *Langmuir* **2008**, *24*, 3244.
(29) Becerril, H. A.; Mao, J.; Liu, Z.; Stoltenberg, R. M.; Bao, Z.; Chen, Y. *ACS Nano* **2008**, *2*, 463.
(30) Li, D.; Muller, M. B.; Gilje, S.; Kaner, R. B.; Wallace, G. G. *Nat Nano* **2008**, *3*, 101.
(31) Jin, M.; Jeong, H.-K.; Yu, W. J.; Bae, D. J.; Kang, B. R.; Lee, Y. H. *Journal of Physics D: Applied Physics* **2009**, *42*, 135109.
(32) Chang, C.-H.; Fan, X.; Li, L.-J.; Kuo, J.-L. *The Journal of Physical Chemistry C* **2012**.
(33) Zhao, X.; Zhang, Q.; Hao, Y.; Li, Y.; Fang, Y.; Chen, D. *Macromolecules* **2010**, *43*, 9411.
(34) Luo, D.; Zhang, G.; Liu, J.; Sun, X. *The Journal of Physical Chemistry C* **2011**, *115*, 11327.

Appendix

5A.1 Titration Spectra

Whereas the addition of the GO dispersion or benzoic acid produces an immediate increase in fluorescence intensity in Zr^{IV}(Pc) and Zr^{IV}(TPP) species (excited at their absorption maxima, Figure S4, S5) because of the disaggregation of pi stacked dye molecules. Once sample are allowed to equilibrate for >24 hours fluorescence intensity decreases to values displayed in Figures S1, S2 and S3.

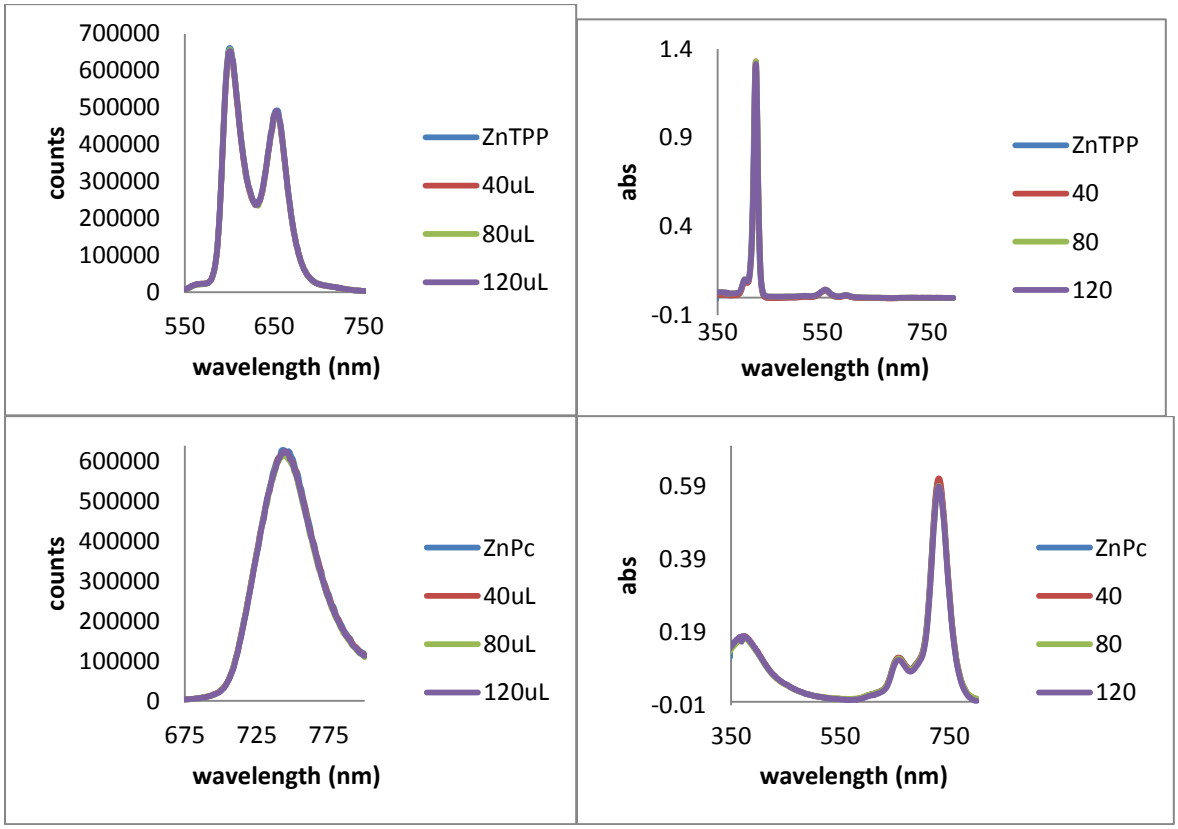

Figure 5A-1. Fluorescence spectra (left) and UV-visible spectra (right) of Zn(TPP) (top, excitation at 422nm) and Zn(Pc) (bottom, excited at 655nm) 24 hours after addition of 0.1 mg/mL GO solution demonstrating the lack of interaction between the fluorophore and the GO substrate.

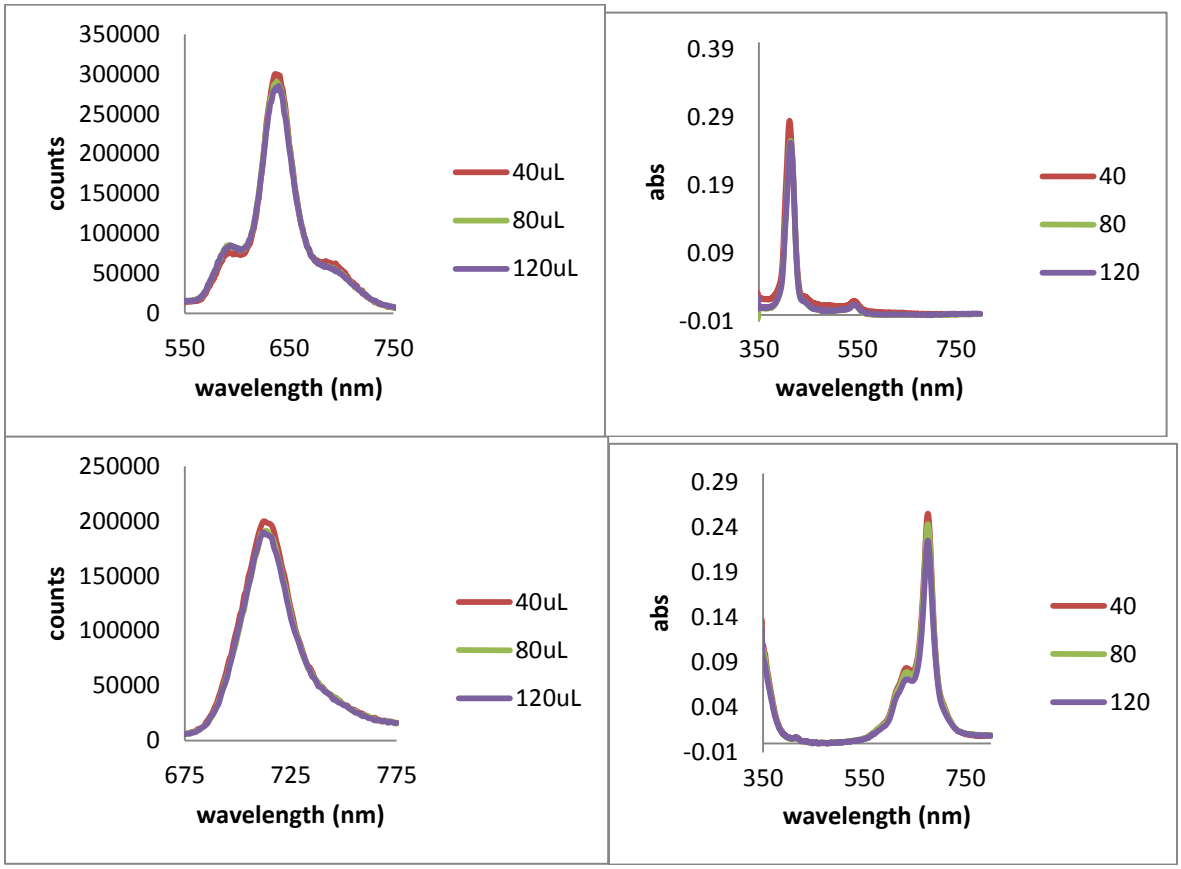

Figure 5A-2. Fluorescence spectra (left) and UV-visible spectra (right) of Zr^{IV}(TPP) (top, excited at 417nm) and Zr^{IV}(Pc) (bottom, excited at 633 nm) 24 hours after addition of 0.1 mg/mL GO solution demonstrating saturation of the GO surface.

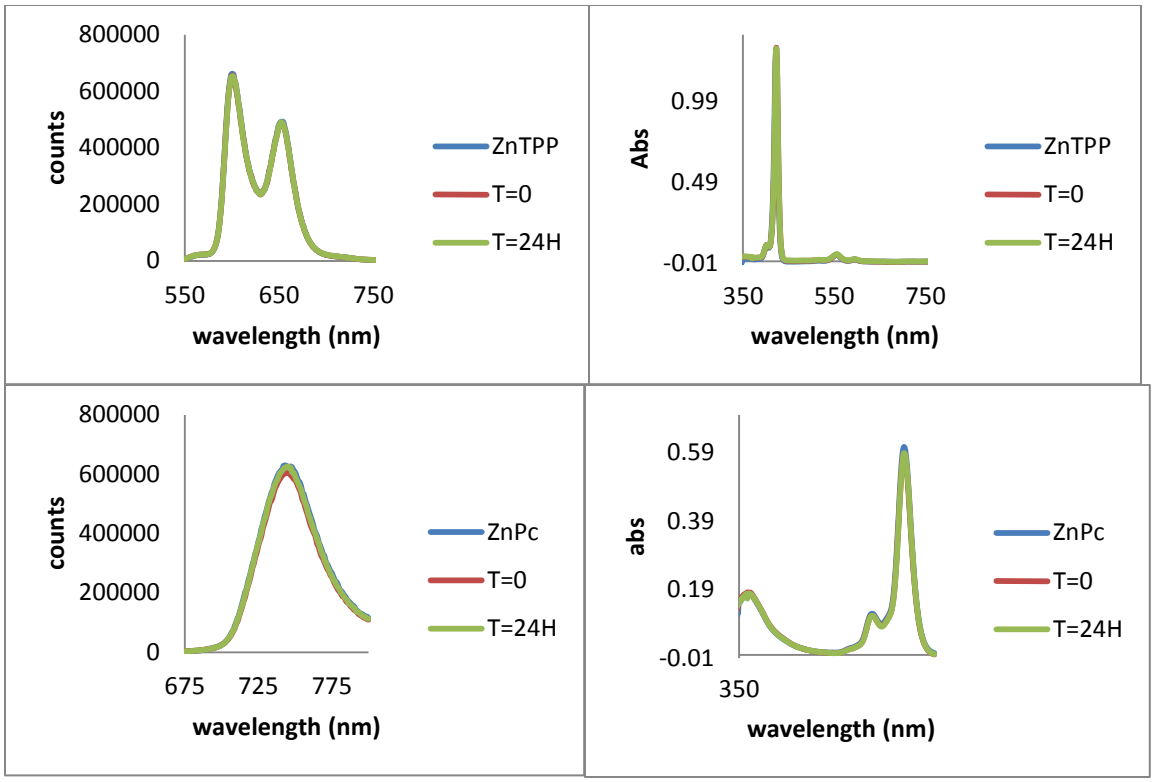

Figure 5A-3. Fluorescence spectra (left) and UV-visible spectra (right) of Zn(TPP) (top, excited at 422 nm) and Zn(Pc) (bottom, excited at 655nm) after addition of 120 µL of 0.1mg/mL GO solution at time of addition and after allowing 24 hours for equilibration demonstrating no interaction in either case.

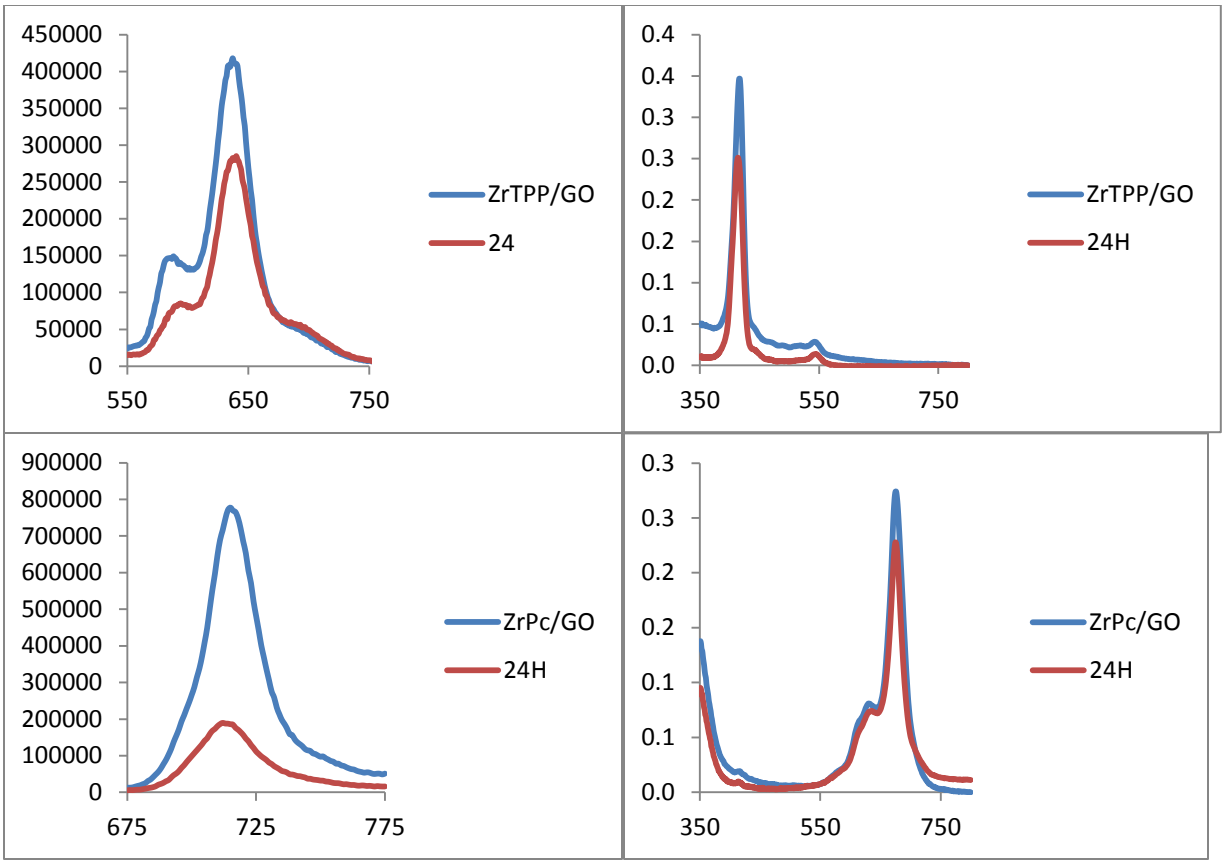

Figure 5A-4. Fluorescence spectra (left) and UV-visible spectra (right) of Zr^{IV}(TPP) (top, excited at 417 nm) and Zr^{IV}(Pc) (bottom, excited at 633 nm) after addition of 120 µL 0.1mg/mL GO solution at time of addition and after allowing 24 hours to equilibrate. The substantial increase in fluorescence intensity upon addition of GO is due to disaggregation of the chromophores as they complex with GO. The smaller increase in the fluorescence intensity of the porphyrin (*ca.* 20%) relative to the phthalocyanine (*ca.* 200%) corresponds well with the aggregation behavior of porphyrins and phthalocyanines. Lifetime measurements indicate no new species formed at any time during addition and equilibration. Total fluorescence quenching of 76% and 32% observed for Zr^{IV}(Pc) and Zr^{IV}(TPP) respectively.

5A.2 Nanocomposites

100 µM solutions of both Zr^{IV}(Pc) and Zn(Pc) in CH_2Cl_2 were prepared. GO was added to these solutions to reach a final concentration of 0.1mg/mL. Solutions were sonicated for 15 minutes. After incubating at room temperature for 48 H samples were centrifuged at 13,000 RPM and washed with fresh THF to remove unbound molecules. The procedure was repeated to ensure complete removal of unbound dye. Once clean, mixtures were centrifuged and THF removed. Pellet was then dispersed in nanopure water or THF for measurements.

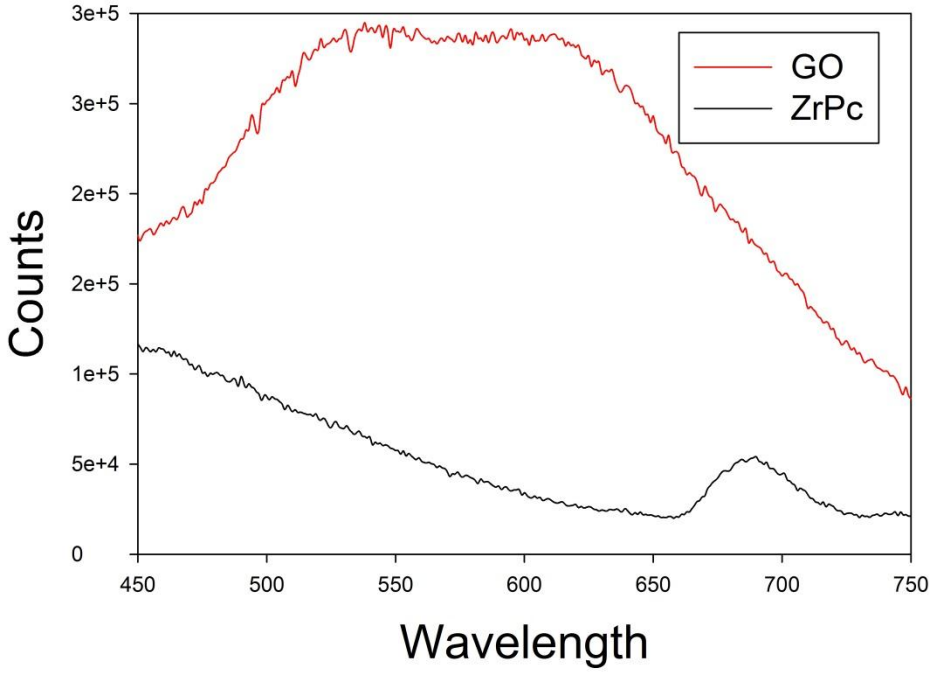

Figure 5A-5. GO nanocomposites were dispersed in THF. Comparison of unfunctionalized GO fluorescence and the Zr^{IV}(Pc)/GO system.

5A.3 TEM Images

All data were collected at 200 kV on a Jeol 2100 Transmission Electron Microscope equipped with EDAX at the eucentric height to ensure reproducibility of measurements. An 8 μL drop of above dispersions was placed on a 300 mesh carbon coated copper grid, (TED Pella Inc., Redding, California, USA), and allowed to dry for 1 minute before imagining.

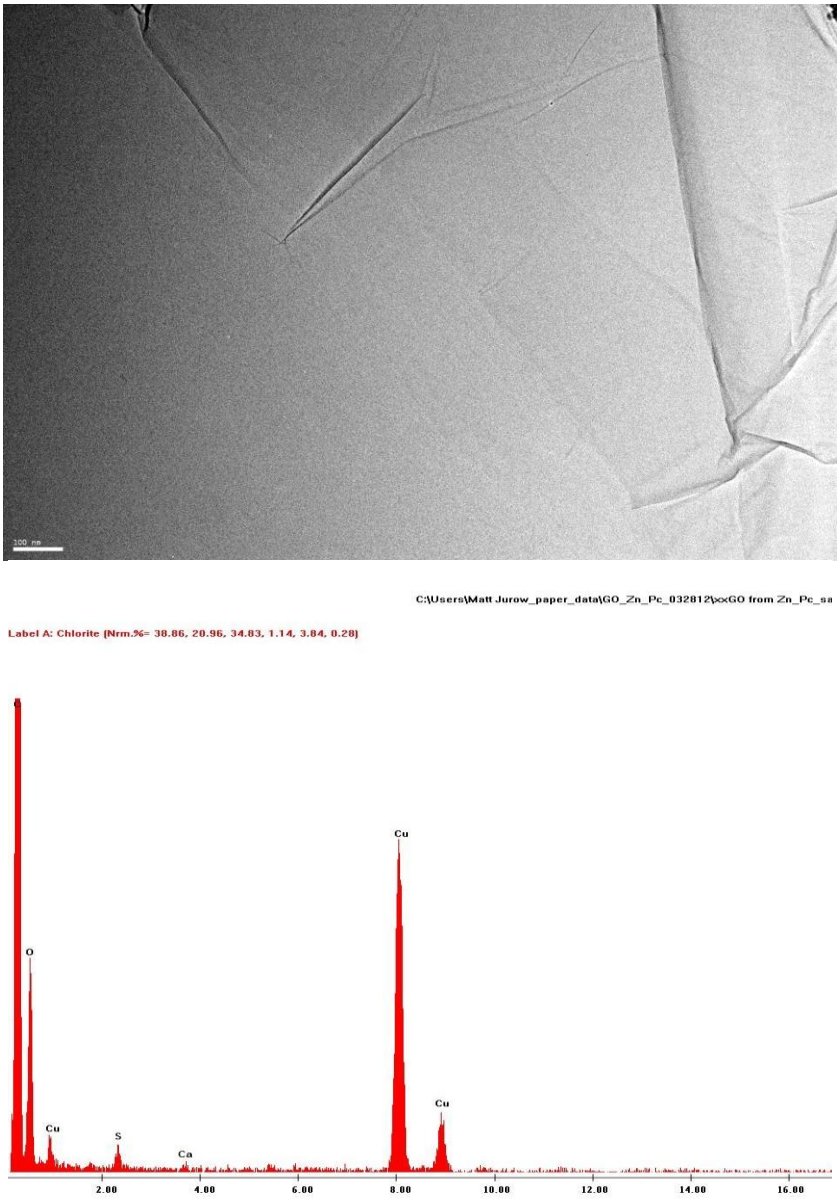

Figure 5A-6. TEM image of Zn(Pc) on GO (top) and EDAX spectrum (bottom). Creases, folds and layer overlaps are visible. Scale bar is 100 nm. EDAX indicates presence of oxygen from the GO. C and Cu peaks are from the underlying grids. No Zn peaks are detected.

5A.4 AFM Images

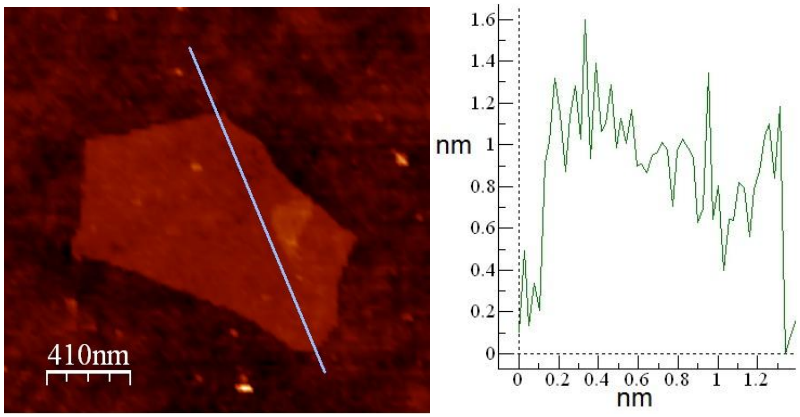

Figure 5A-7. AFM height image (left) and line trace (right) of GO dispersion incubated with Zn(Pc), thoroughly rinsed and cast on glass slides. A single layer flake is clearly seen with thickness of ca. 8 Å.

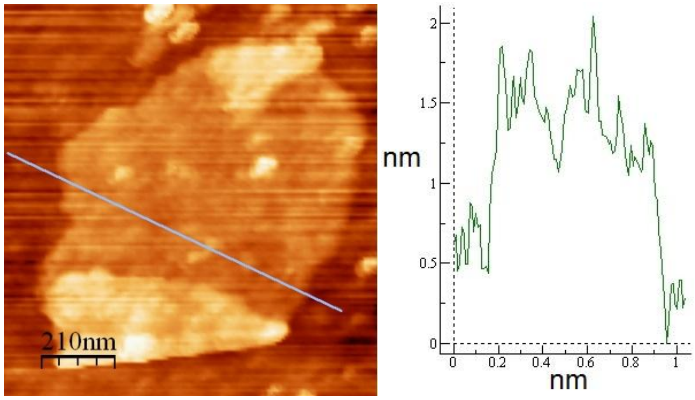

Figure 5A-8. AFM height image (left) and line trace (right) of GO dispersion incubated with $Zr^{IV}PC$, thoroughly rinsed and cast on glass slides. A flake is depicted with height of ca. 1nm.

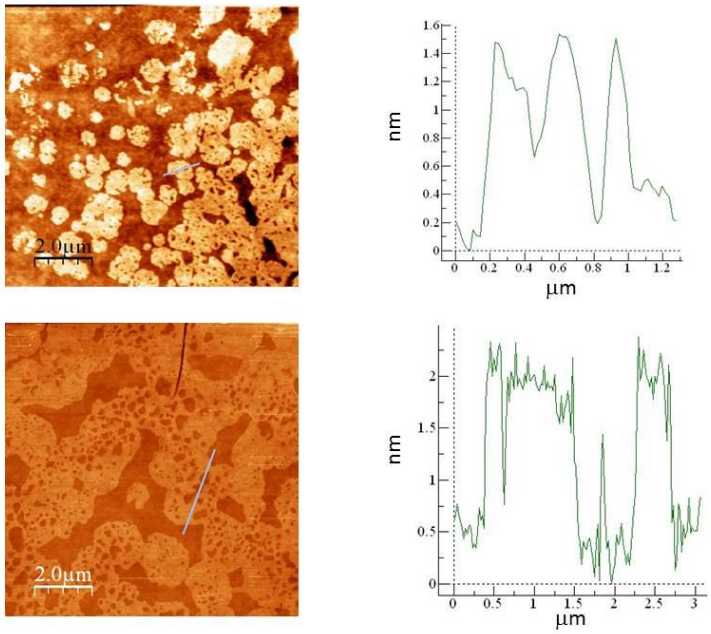

Figure 5A-9. 5mg/mL aqueous GO dispersion was added to Zr^{IV}(Pc) in THF to make a 0.1mg/mL GO solution in 0.1 mM dye. System was allowed to equilibrate for 2 days. Solutions were centrifuged at 13K RPM for 10 minutes, excess dye was decanted and pellet was re-dispersed in THF by sonicating for 10 minutes. This rinsing was repeated twice and then solutions were centrifuged again and dispersed in water and spin coated onto ozone cleaned glass slides. Holes in the graphene sheets are likely from the desorption of the Zr^{IV}(Pc) upon sonication in water (top). The same process was done using Zr^{IV}(TPP) with similar results (bottom).

5A.5 Film Studies

Graphene oxide solution (3 mg/mL in water) was spin coated onto piranha cleaned quartz slides and dried in an oven to make 3nm thick continuous films. Films were then soaked in 0.1 mM solutions of dyes in CH_2Cl_2 for 3 days at room temperature in the dark to ensure equilibration. Coated films were rinsed extensively with clean CH_2Cl_2 to remove any unbound dye, backs of slides were wiped repeatedly with MeOH and spectra were recorded. No appreciable fluorescence was observed at any excitation wavelength.

5A.6 Other Spectra

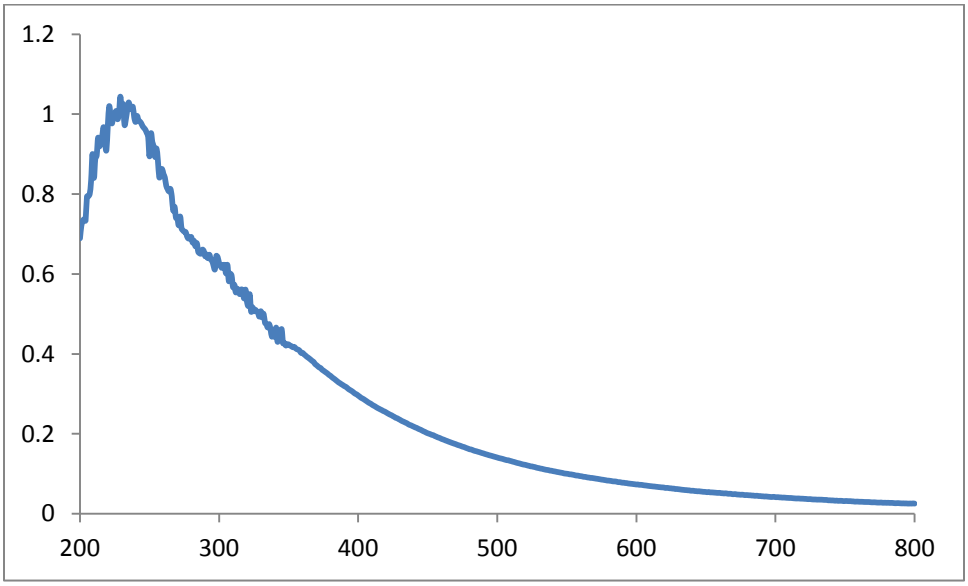

Figure 5A-10. Absorption spectrum of GO in water

5A.7 Probe Measurements

Devices were made by spin coating layers (of 8nm or 15nm) onto ozone cleaned glass. Sheet resistance was measured by Van der Pauw technique of the pristine GO layers, of an 8nm

GO film soaked in Zr^{IV}(Pc) or Zr^{IV}(TPP) (0.1mM in CH_2Cl_2), or of an 8nm GO film spin coated on top of a ca. 40nm thick layer of Zr^{IV}(TPP) or Zr^{IV}(Pc) spin cast from chlorobenzene on ozone cleaned glass. Measurements were taken in the dark and under illumination.

BIBLIOGRAPHY

1. Introduction and Background

(1) Committee on Challenges for the Chemical Sciences in the 21st Century Beyond the Molecular Frontier: Challenges for Chemistry and Chemical Engineering; The National Academies Press: Washington, DC, 2003.

(2) Whitesides, G. M.; Deutch, J. Nature 2011, 469, 21.

(3) Service, R. F. Science 2005, 309, 548.

(4) Service, R. F. Science 2005, 309, 95.

(5) Casey, C. P. Chem. International 2005, 27, 8.

(6) Roco, M. C.; Hersam, M. C.; Mirkin, C. A.; Hersam, M.; Weiss, P. S. 2011, 1, 467.

(7) Radivojevic, I.; Bazzan, G.; Burton-Pye, B. P.; Ithisuphalap, K.; Saleh, R.; Durstock, M. F.; Francesconi, L. C.; Drain, C. M. J. Phy. Chem. C 2012, 116, 15867.

(8) Jurow, M.; Farley, C.; Pabon, C.; Hageman, B.; Dolor, A.; Drain, C. M. Chem. Comm. 2012, 48, 4731.

(9) Aggarwal, A.; Singh, S.; Samson, J.; Drain, C. M. Macromol Rapid Comm. 2012, 33, 1220.

(10) Varotto, A.; Smeureanu, G.; Aggarwal, A.; Drain, C. M. In ACS Symposium Series: Fluorine-related Nanoscience with Energy Applications; American Chemical Society: Washington, 2011; Vol. 1064, p 55.

(11) Singh, S.; Aggarwal, A.; Farley, C.; Hageman, B. A.; Batteas, J. D.; Drain, C. M. Chem. Comm. 2011, 47, 7134.

(12) Samson, J.; Piscopo, I.; Yampolski, A.; Nahirney, P.; Parpas, A.; Aggarwal, A.; Saleh, R.; Drain, C. M. Nanomaterials 2011, 1, 64.

(13) Samson, J.; Nahirney, P. C.; Drain, C. M.; Piscopo, I. Microscopy Today 2011, 19, 38.

(14) Sahar-Halbany, A.; Vance, J. M.; Drain, C. M. J. Chem. Ed. 2011, 88, 615.

(15) Bazzan, G.; Aggarwal, A.; Drain, C. M. In ACS Symposium Series, Interfaces and Interphases in Analytical Chemistry; Helburn, R., Vitha, M. F., Eds.; American Chemical Society: Washington, 2011, p 167.

(16) Aggarwal, A.; Singh, S.; Zhang, Y.; Anthes, M.; Samaroo, D.; Gao, R.; Drain, C. M. Tetrahedron Lett. 2011, 52, 5456.

(17) Aggarwal, A.; Singh, S.; Drain, C. M. J. Porphyrins Phthalocyanines 2011, 15, 1.

(18) Aggarwal, A.; Qureshy, M.; Johnson, J.; Batteas, J. D.; Drain, C. M.; Samaroo, D. J. Porphyrins Phthalocyanines 2011, 15, 338.

(19) Varotto, A.; Nam, C. Y.; Radivojevic, I.; Tome, J. P. C.; Cavaleiro, J. A. S.; Black, C. T.; Drain, C. M. J. Am. Chem. Soc. 2010, 132, 2552.

(20) Toschi, A.; Lee, E.; Thompson, S.; Gadir, N.; Yellen, P.; Drain, C. M.; Ohh, M.; Foster, D. A. Cancer Lett. 2010, 299, 72.

(21) Singh, S.; Aggarwal, A.; Thompson, S.; Tome, J. P. C.; Zhu, X. C.; Samaroo, D.; Vinodu, M.; Gao, R. M.; Drain, C. M. Bioconjugate Chem. 2010, 21, 2136.

(22) Radivojevic, I.; Varotto, A.; Farley, C.; Drain, C. M. Energy Environm. Sci. 2010, 3, 1897.

(23) Radivojevic, I.; Sfeir, M.; Nam, C.-Y.; Burton-Pye, B. P.; Falber, A.; Black, C. T.; Drain, C. M. Proc. IEEE: Solar Energ 2010, 003280.

(24) Radivojevic, I.; Likhtina, I.; Shi, X.; Singh, S.; Drain, C. M. Chem. Comm. 2010, 46, 1643.

(25) Nia, S.; Gong, X. C.; Drain, C. M.; Jurow, M.; Rizvi, W.; Qureshy, M. J. Porphyrins Phthalocyanines 2010, 14, 621.

(26) Jurow, M.; Schuckman, A. E.; Batteas, J. D.; Drain, C. M. Coord. Chem. Rev. 2010, 254, 2297.

(27) Drain, C. M.; Singh, S. In The Handbook of Porphyrin Science with Applications to Chemistry, Physics, Materials Science, Engineering, Biology and Medicine; Kadish, K. M., Smith, K. M., Guilard, R., Eds.; World Scientific Publishers: Singapore, 2010; Vol. 3, p 485.

(28) Smeureanu, G.; Aggarwal, A.; Soll, C. E.; Arijeloye, J.; Malave, E.; Drain, C. M. Chem. Eur. J. 2009, 15, 12133.

(29) Samson, J.; Varotto, A.; Nahirney, P. C.; Toschi, A.; Piscopo, I.; Drain, C. M. Acs Nano 2009, 3, 339.

(30) Falber, A.; Burton-Pye, B. P.; Radivojevic, I.; Todaro, L.; Saleh, R.; Francesconi, L. C.; Drain, C. M. Eur. J. Inorg. Chem. 2009, 2459.

(31) Drain, C. M.; Varotto, A.; Radivojevic, I. Chem. Rev. 2009, 109, 1630.

(32) de la Rica, R.; Thompson, S.; Baldi, A.; Fernandez-Sanchez, C.; Drain, C. M.; Matsui, H. Anal. Chem. 2009, 81, 10167.

(33) Varotto, A.; Todaro, L.; Vinodu, M.; Koehne, J.; Liu, G. Y.; Drain, C. M. Chem. Comm. 2008, 4921.

(34) Stevens, N.; O'Connor, N.; Vishwasrao, H.; Samaroo, D.; Kandel, E. R.; Akins, D. L.; Drain, C. M.; Turro, N. J. J. Am. Chem. Soc. 2008, 130, 7182.

(35) Serem, W. K.; Varotto, A.; Castro, G.; Drain, C. M.; Garno, J. C. NOBCChE Proceedings 2008.

(36) Falber, A.; L.Todaro; Goldberg, I.; Favilla, M. V.; Drain, C. M. Inorg. Chem. 2008, 47, 454.

(37) Chan, Y.-H.; Schuckman, A. E.; Perez, L. M.; Vinodu, M.; Drain, C. M.; Batteas, J. D. J. Phys. Chem. C 2008, 112, 6110.

(38) Bazzan, G.; Smith, W.; Francesconi, L. C.; Drain, C. M. Langmuir 2008, 24, 3244.

(39) Samaroo, D.; Vinodu, M.; Chen, X.; Drain, C. M. J. Combi. Chem. 2007, 9, 998.

(40) Balaban, T. S.; Berova, N.; Drain, C. M.; Hauschild, R.; Kalt, H.; Lebedkin, S.; Lehn, J.-M.; Huang, X.; Nifaitis, F.; Pescitelli, G.; Prokhorenko, V. I.; Riedel, G.; Smeureanu, G.; Zeller, J. Chem. Eur. J. 2007, 13, 8411.

(41) Xu, C.; Wu, T.; Drain, C. M.; Batteas, J. D.; Fasolka, M. J.; Beers, K. L. Macromolecules 2006, 39, 3359.

(42) Xu, C.; Wu, T.; Batteas, J. D.; Drain, C. M.; Beers, K. L.; Fasolka, M. J. Applied Surface Science 2006, 252, 2529.

(43) Vittadello, M.; Stallworth, P. E.; Alamgir, F. M.; Suarez, S.; Abbrent, S.; Drain, C. M.; Noto, V. D.; Greenbaum, S. G. Inorg. Chim. Acta 2006, 339, 2513.

(44) Samaroo, D.; Soll, C. E.; Todaro, L. J.; Drain, C. M. Org. Lett. 2006, 8, 4985

(45) Helt, J. M.; Drain, C. M.; Bazzan, G. J. Am. Chem. Soc. 2006, 128, 9371.

(46) Garno, J. C.; Xu, C.; Bazzan, G.; Batteas, J. D.; Drain, C. M. In ACS Symposium series: Metal-Containing and Metallo-Supramolecular Polymers and Materials; Schubert, U. S.,

Newcome, G. R., Manners, I., Eds.; American Chemical Society: Washington, DC., 2006; Vol. 928, p 168.

(47) Drain, C. M.; Smeureanu, G.; Patel, S.; Gong, X.; Garno, J.; Arijeloye, J. New J. Chem. 2006, 30, 1834.

(48) Cheng, K. F.; Thai, N. A.; Grohmann, K.; Teague, L. C.; Drain, C. M. Inorg. Chem. 2006, 45, 6928.

(49) Xu, C.; Wu, T.; Mei, Y.; Drain, C. M.; Batteas, J. D.; Beers, K. L. Langmuir 2005, 21, 11136.

(50) Xu, C.; Wu, T.; Drain, C. M.; Batteas, J. D.; Beers, K. L. Macromolecules 2005, 38, 6.

(51) Drain, C. M.; Goldberg, I.; Sylvain, I.; Falber, A. Topics in Current Chemistry 2005, 245, 55.

(52) Drain, C. M.; Bazzan, G.; Milic, T.; Vinodu, M.; Goeltz, J. C. Israel J. Chem. 2005, 45, 255.

(53) Cheng, K. F.; Thai, N. A.; Teague, L. C.; Grohmann, K.; Drain, C. M. Chem. Commun. 2005, 4678.

(54) Xu, C.; Wu, T.; Drain, C. M.; Batteas, J. D.; Beers, K. L. ACS Polymer Reprints 2004, 45, 667.

(55) Milic, T.; Garno, J. C.; Batteas, J. D.; Smeureanu, G.; Drain, C. M. Langmuir 2004, 20, 3974.

(56) Helt, J. M.; Drain, C. M.; Batteas, J. D. J. Am. Chem. Soc. 2004, 136, 628.

(57) Drain, C. M.; Smeareanu, G.; Batteas, J.; Patel, S. In Dekker Encyclopedia of Nanoscience and Nanotechnology; Schwartz, J. A., Contescu, C. I., Putyera, K., Eds.; Marcel Dekker, Inc.: New York, 2004; Vol. 5, p 3481.

(58) Drain, C. M.; Milic, T.; Garno, J. C.; Smeureanu, G.; Batteas, J. D. ACS Polymer Reprints 2004, 45, 346.

(59) Drain, C. M.; Chen., X. In Encyclopedia of Nanoscience & Nanotechnology; Nalwa, H. S., Ed.; American Scientific Press: New York, 2004; Vol. 9, p 593.

(60) Chen, X.; Hui, L.; Foster, D. A.; Drain, C. M. Biochem. 2004, 43, 10918.

(61) Chen, X.; Drain, C. M. Drug Design Review - Online 2004, 1, 215.

(62) Peng, X.; Huang, Y.; Gao, C.; Peng, J.; Komatsu, N.; Osuka, A.; Cao, Y. J. Phys. Chem. C 2010, 114, 18449.

(63) Tanoue, R.; Higuchi, R.; Enoki, N.; Miyasato, Y.; Uemura, S.; Kimizuka, N.; Stieg, A. Z.; Gimzewski, J. K.; Kunitake, M. ACS Nano 2011, 5, 3923.

(64) Rojas, G.; Simpson, S.; Chen, X.; Kunkel, D. A.; Nitz, J.; Xiao, J.; Dowben, P. A.; Zurek, E.; Enders, A. Phys. Chem. Chem. Phys. 2012, 14, 4971.

(65) Bai, F.; Sun, Z.; Wu, H.; Haddad, R. E.; Coker, E. N.; Huang, J. Y.; Rodriguez, M. A.; Fan, H. Nano Letters 2011, 11, 5196.

(66) Li, L.-L.; Fu, X.-F.; Ren, Z.; Zhao, Y.-G.; Feng, W.; Yan, C.-H. Langmuir 2010, 26, 15730.

(67) Qiu, Y.; Chen, P.; Liu, M. J. Am. Chem. Soc. 2010, 132, 9644.

(68) Nam, Y. S.; Shin, T.; Park, H.; Magyar, A. P.; Choi, K.; Fantner, G.; Nelson, K. A.; Belcher, A. M. J. Am. Chem. Soc. 2010, 132, 1462.

(69) Börjesson, K.; Wiberg, J.; El-Sagheer, A. H.; Ljungdahl, T.; Mårtensson, J.; Brown, T.; Nordén, B.; Albinsson, B. ACS Nano 2010, 4, 5037.

(70) Ariga, K.; Hill, J. P.; Lee, M. V.; Vinu, A.; Charvet, R.; Acharya, S. Sci. Tech. Adv. Mat. 2008, 9, 014109.
(71) Li, M.; Ishihara, S.; Ji, Q.; Akada, M.; Hill, J. P.; Ariga, K. Sci. Tech. Adv. Mat. 2012, 13, 053001.
(72) Drain, C. M. Proc. Natl. Acad. Sci., USA 2002, 99, 5178.
(73) Whitesides, G. M.; Grzybowski, B. Science 2002, 295, 2418.
(74) Ruthard, C.; Schmidt, M.; Gröhn, F. Macromol. Rapid Comm. 2011, 32, 706.
(75) Lehn, J.-M. Science 2002, 2400.
(76) Drain, C. M.; Christensen, B.; Mauzerall, D. C. Proc. Natl. Acad. Sci. USA 1989, 86, 6959.
(77) Webb, M. J.; Bampos, N. Chem. Sci. 2012, 3, 2351.
(78) Trapani, M.; Plutino, M. R.; Sabatino, G.; Occhiuto, I.; Borriello, A.; De Luca, G.; Scolaro, L. M. Chem. Comm. 2012, 48, 5136.
(79) Subbaiyan, N. K.; D'Souza, F. Chem. Comm. 2012, 48, 3641.
(80) Sakuma, T.; Sakai, H.; Hasobe, T. Chem. Comm. 2012, 48, 4441.
(81) Menting, R.; Ng, D. K. P.; Roder, B.; Ermilov, E. A. Phys. Chem. Chem. Phys. 2012.
(82) Menting, R.; Lau, J. T. F.; Xu, H.; Ng, D. K. P.; Roder, B.; Ermilov, E. A. Chem. Comm. 2012, 48, 4597.
(83) Ishizuka, T.; Sankar, M.; Yamada, Y.; Fukuzumi, S.; Kojima, T. Chem. Comm. 2012, 48, 6481.
(84) Guo, P.; Chen, P.; Ma, W.; Liu, M. J. Mater. Chem. 2012, 22, 20243.
(85) D'Urso, A.; Fragala, M. E.; Purrello, R. Chem. Comm. 2012, 48, 8165.
(86) Hill, J. P.; D'Souza, F.; Ariga, K. In Supramol. Chem.; John Wiley & Sons, Ltd: 2012.
(87) Kadish, K.; Smith, K.; Guilard, R. The Porphryin Handbook; Academic Press: New York, 2003; Vol. 1-20.
(88) Kadish, K. M.; Smith, K. M.; Guilard, R. The Handbook of Porphyrin Science with Applications to Chemistry, Physics, Materials Science, Engineering, Biology and Medicine; World Scientific Publishers: Singapore, 2010; Vol. 1-10.
(89) Akhigbe, J.; Zeller, M.; Brückner, C. Organic Letters 2011, 13, 1322.
(90) Diev, V. V.; Schlenker, C. W.; Hanson, K.; Zhong, Q.; Zimmerman, J. D.; Forrest, S. R.; Thompson, M. E. J. Org. Chem. 2011, 77, 143.
(91) Lee, C. Y.; Farha, O. K.; Hong, B. J.; Sarjeant, A. A.; Nguyen, S. T.; Hupp, J. T. J. Am. Chem. Soc. 2011, 133, 15858.
(92) Lindsey, J. S.; Bocian, D. F. Acc. Chem. Res. 2011, 44, 638.
(93) Seol, M.-L.; Choi, S.-J.; Kim, C.-H.; Moon, D.-I.; Choi, Y.-K. ACS Nano 2011, 6, 183.
(94) Takagi, S.; Shimada, T.; Masui, D.; Tachibana, H.; Ishida, Y.; Tryk, D. A.; Inoue, H. Langmuir 2010, 26, 4639.
(95) Feese, E.; Sadeghifar, H.; Gracz, H. S.; Argyropoulos, D. S.; Ghiladi, R. A. Biomacromol. 2011, 12, 3528.
(96) Larsen, R. W.; Wojtas, L.; Perman, J.; Musselman, R. L.; Zaworotko, M. J.; Vetromile, C. M. J. Am. Chem. Soc. 2011, 133, 10356.
(97) Megiatto, J. D.; Schuster, D. I. Org. Lett. 2011, 13, 1808.

(98) Brancatelli, G.; De Zorzi, R.; Hickey, N.; Siega, P.; Zingone, G.; Geremia, S. Crystal Growth Design 2012.

(99) Fry, H. C.; Garcia, J. M.; Medina, M. J.; Ricoy, U. M.; Gosztola, D. J.; Nikiforov, M. P.; Palmer, L. C.; Stupp, S. I. J. Am. Chem. Soc. 2012, 134, 14646.

(100) Sivalingam, Y.; Martinelli, E.; Catini, A.; Magna, G.; Pomarico, G.; Basoli, F.; Paolesse, R.; Di Natale, C. J. Phys. Chem. C 2012, 116, 9151.

(101) D'Souza, F.; Sandanayaka, A. S. D.; Ito, O. J. Phys. Chem. Lett. 2010, 1, 2586.

(102) Maligaspe, E.; Sandanayaka, A. S. D.; Hasobe, T.; Ito, O.; D'Souza, F. J. Am. Chem. Soc. 2010, 132, 8158.

(103) Cho, W. J.; Cho, Y.; Min, S. K.; Kim, W. Y.; Kim, K. S. J. Am. Chem. Soc. 2011, 133, 9364.

(104) Farha, O. K.; Shultz, A. M.; Sarjeant, A. A.; Nguyen, S. T.; Hupp, J. T. J. Am. Chem. Soc. 2011, 133, 5652.

(105) Fateeva, A.; Devautour-Vinot, S.; Heymans, N.; Devic, T.; Grenèche, J.-M.; Wuttke, S.; Miller, S.; Lago, A.; Serre, C.; De Weireld, G.; Maurin, G.; Vimont, A.; Férey, G. Chem. Mater. 2011, 23, 4641.

(106) Zhan, H.; Lamare, S.; Ng, A.; Kenny, T.; Guernon, H.; Chan, W.-K.; Djurišić, A. B.; Harvey, P. D.; Wong, W.-Y. Macromol. 2011, 44, 5155.

(107) Tian, Y.; Shumway, B. R.; Meldrum, D. R. Chem. Mater. 2010, 22, 2069.

(108) Morris, W.; Volosskiy, B.; Demir, S.; Gándara, F.; McGrier, P. L.; Furukawa, H.; Cascio, D.; Stoddart, J. F.; Yaghi, O. M. Inorg. Chem. 2012, 51, 6443−6445.

(109) Fathalla, M.; Neuberger, A.; Li, S.-C.; Schmehl, R.; Diebold, U.; Jayawickramarajah, J. J. Am. Chem. Soc. 2010, 132, 9966.

(110) Koepf, M.; Conradt, J.; Szmytkowski, J. d.; Wytko, J. A.; Allouche, L.; Kalt, H.; Balaban, T. S.; Weiss, J. Inorg. Chem. 2011, 50, 6073.

(111) Liu, Z.; Yasseri, A. A.; Lindsey, J. S.; Bocian, D. F. Science 2003, 302, 1543.

(112) Peet, J.; Heeger, A. J.; Bazan, G. C. Acc. Chem. Res. 2009, 42, 1700.

(113) Frischmann, P. D.; Mahata, K.; Wurthner, F. Chem. Soc. Rev. 2013.

(114) Schmittel, M.; Kalsani, V.; Bats, J. W. Inorg. Chem. 2005, 44, 4115.

(115) Lehn, J.-M. Supramolecular Chemistry: Concepts and Perspectives; Wiley VCH: Weinheim, 1995.

(116) Lerouge, F.; Cerveau, G.; Corriu, R. J. P.; C., S.; Guilard, R. Chem. Comm. 2007, 2007, 1553.

(117) Drain, C. M.; Batteas, J. D.; Flynn, G. W.; Milic, T.; Chi, N.; Yablon, D. G.; Sommers, H. Proc. Natl. Acad. Sci., USA 2002, 99, 6498.

(118) Laget, V.; Hornick, C.; Rabu, P.; Drillon, M.; Ziessel, R. Coord. Chem. Rev. 1998, 178-180, 1533.

(119) Ishikawa, N.; Sugita, M.; Ishikawa, T.; Koshihara, S.-y.; Kaizu, Y. J. Phys. Chem. B 2004, 108, 11265.

(120) Zhao, M.; Zhong, C.; Stern, C.; Barrett, A. G. M.; Hoffman, B. M. J. Am. Chem. Soc. 2005, 127, 9769.

(121) Zhao, M.; Zhong, C.; Stern, C.; Barrett, A. G. M.; Hoffman, B. M. Inorg. Chem. 2004, 43, 3377.

(122) Miller, J. S. Polyhedron 2001, 20, 1723.

(123) Ishikawa, N.; Sugita, M.; Ishikawa, T.; Koshihara, S.-Y.; Kaizu, Y. J. Am. Chem. Soc. 2003, 125, 8694.

(124) Muthukumaran, K.; Loewe, R. S.; Ambroise, A.; Tamaru, S. i.; Li, Q.; Mathur, G.; Bocian, D. F.; Misra, V.; Lindsey, J. S. J. Org. Chem. 2004, 69, 1444.

(125) Gong, X.; Milic, T.; Xu, C.; Batteas, J. D.; Drain, C. M. J. Am. Chem. Soc. 2002, 124, 14290.

(126) Pasetto, P.; Chen, X.; Drain, C. M.; Franck, R. W. Chem. Commun. 2001, 81.

(127) Drain, C. M.; Nifiatis, F.; Vasenko, A.; Batteas, J. D. Angew. Chem. Int. Ed. 1998, 37, 2344.

(128) Lee, S. J.; Malliakas, C. D.; Kanatzidis, M. G.; Hupp, J. T.; Nguyen, S. T. Adv. Mater. 2008, 20, 3543.

(129) Shi, N.; Yin, G.; Han, M.; Jiang, L.; Xu, Z. Chem. Eur. J. 2008, 14, 6255.

(130) Zhang, X.; Takeuchi, M. Angew. Chem. Inter. Ed. 2009, 48, 9646.

(131) Medforth, C. J.; Wang, Z.; Martin, K. E.; Song, Y.; Jacobsen, J. L.; Shelnutt, J. A. Chem. Comm. 2009, 7261.

(132) Tian, Y.; Martin, K. E.; Shelnutt, J. Y. T.; Evans, L.; Busani, T.; Miller, J. E.; Medforth, C. J.; Shelnutt, J. A. Chem. Comm. 2011, 47, 6069.

(133) Tian, Y.; Busani, T.; Uyeda, G. H.; Martin, K. E.; van Swol, F.; Medforth, C. J.; Montano, G. A.; Shelnutt, J. A. Chem. Comm. 2012, 48, 4863.

(134) Zaytsev, D. V.; Xie, F.; Mukherjee, M.; Bludin, A.; Demeler, B.; Breece, R. M.; Tierney, D. L.; Ogawa, M. Y. Biomacromol. 2010, 11, 2602.

(135) Wang, C.-L.; Lan, C.-M.; Hong, S.-H.; Wang, Y.-F.; Pan, T.-Y.; Chang, C.-W.; Kuo, H.-H.; Kuo, M.-Y.; Diau, E. W.-G.; Lin, C.-Y. Energy Environ. Sci. 2012, 5, 6933.

(136) Alessio, E.; Casanova, M.; Zangrando, E.; Iengo, E. Chem. Comm. 2012, 48, 5112.

(137) Martinez-Diaz, M. V.; de la Torre, G.; Torres, T. Chem. Comm. 2010, 46, 7090.

(138) Beletskaya, I.; Tyurin, V. S.; Tsivadze, A. Y.; Guilard, R.; Stern, C. Chem. Rev. 2009, 109, 1659.

(139) Pietrangeli, D.; Ricciardi, G. Tetrahedron Let. 2011, 52, 1105.

(140) Imahori, H.; Umeyama, T.; Kurotobi, K.; Takano, Y. Chem. Comm. 2012, 48, 4032.

(141) Pereira, A. M. V. M.; Soares, A. R. M.; Hausmann, A.; Neves, M. G. P. M. S.; Tome, A. C.; Silva, A. M. S.; Cavaleiro, J. A. S.; Guldi, D. M.; Torres, T. Phys. Chem. Chem. Phys. 2011, 13, 11858.

(142) Pereira, A. M. V. M.; Hausmann, A.; Tomé, J. P. C.; Trukhina, O.; Urbani, M.; Neves, M. G. P. M. S.; Cavaleiro, J. A. S.; Guldi, D. M.; Torres, T. Chem. Eur. J. 2012, 18, 3210.

(143) Ngo, T. H.; Nastasi, F.; Puntoriero, F.; Campagna, S.; Dehaen, W.; Maes, W. Eur. J. Org. Chem. 2012, 2012, 5605.

(144) Panda, D. K.; Goodson, F. S.; Ray, S.; Lowell, R.; Saha, S. Chem. Comm. 2012, 48, 8775.

(145) Kan, J.; Chen, Y.; Gao, J.; Wan, L.; Lei, T.; Ma, P.; Jiang, J. Mater. Chem. 2012, 22, 15695.

(146) Milic, T. N.; Chi, N.; Yablon, D. G.; Flynn, G. W.; Batteas, J. D.; Drain, C. M. Angew. Chem., Int. Ed. 2002, 41, 2117.

(147) De Luca, G.; Romeo, A.; Villari, V.; Micali, N.; Foltran, I.; Foresti, E.; Lesci, I. G.; Roveri, N.; Zuccheri, T.; Scolaro, L. M. J. Am. Chem. Soc. 2009, 131, 6920.

(148) Teixeira, R.; Andrade, S. M.; Vaz Serra, V.; Paulo, P. M. R.; Sánchez-Coronilla, A.; Neves, M. G. P. M. S.; Cavaleiro, J. A. S.; Costa, S. M. B. J. Phys. Chem. B 2012, 116, 2396.

(149) Wakahara, T.; D'Angelo, P.; Miyazawa, K. i.; Nemoto, Y.; Ito, O.; Tanigaki, N.; Bradley, D. D. C.; Anthopoulos, T. D. J. Am. Chem. Soc. 2012, 134, 7204.

(150) Takai, A.; Chkounda, M.; Eggenspiller, A.; Gros, C. P.; Lachkar, M.; Barbe, J.-M.; Fukuzumi, S. J. Am. Chem. Soc. 2010, 132, 4477.

(151) Yang, Y.; Zhang, Y.-M.; Chen, Y.; Zhao, D.; Chen, J.-T.; Liu, Y. Chem. Eur. J. 2012, 18, 4208.

(152) Pagona, G.; Zervaki, G. E.; Sandanayaka, A. S. D.; Ito, O.; Charalambidis, G.; Hasobe, T.; Coutsolelos, A. G.; Tagmatarchis, N. J. Phys. Chem. C 2012, 116, 9439.

(153) Kim, D. Multiporphyrin Arrays: Fundamentals and Applications; Pan Stanford Publishing: Singapore, 2012.

(154) Sessler, J. L.; Karnas, E.; Sedenberg, E. In Supramolecular Chemistry: From Molecules to Nanomaterials.; Gale, P. A., Steed, J. W., Eds.; John Wiley & Sons: Hoboken, 2012.

2. **Asymmetric Porphyrins as Molecular Electronic Device Components**

(1) Abruña, H. D.; Ratner, M. A.; Zee, R. D. v.; González, C. A.; Kagan, C. R.; Stewart, D. R.; Walker, A. V.; Batteas, J. D.; Chidsey, C. E. D.; Seideman, T. Building Electronic Function into Nanoscale Molecular Architectures: Report of a National Science Foundation Workshop., National Science Foundation, 2007.

(2) Hille, B. Ion Channels of Excitable Membranes; 3 ed.; Sinauer Associates: Sunderland, 2001.

(3) Jin, Y.; Friedman, N.; Sheves, M.; He, T.; Cahen, D. Proc. Natl. Acad. Sci. USA 2006, 103, 8601.

(4) Hong, F. T. Molecular Electronics. Biosensors and Biocomputers; Springer: New York, 1990.

(5) Stoddart, J. F. Chem. Soc. Rev. 2009, 38, 1802.

(6) McCreery, R. L.; Bergren, A. J. Adv. Mater. 2009, 21, 1.

(7) Pognon, G.; Boudon, C.; Schenk, K. J.; Bonin, M.; Bach, B.; Weiss, J. J. Am. Chem. Soc. 2006, 128, 3488.

(8) Suslick, K. S.; Rakow, N. A.; Kosal, M. E.; Chou, J.-H. J. Porphyrins Phthalocyanines 2000, 4, 407.

(9) Fages, F.; Wytko, J. A.; Weiss, J. Comptes Rendus Chimie 2008, 11, 1241.

(10) Kubatkin, S.; Danilov, A.; Hjort, M.; Cornil, J.; Bredas, J.-L.; Stuhr-Hansen, N.; Hedegard, P.; Bjornholm, T. Nature 2003, 425, 698.

(11) Lafferentz, L.; Ample, F.; Yu, H.; Hecht, S.; Joachim, C.; Grill, L. Science 2009, 323, 1193.

(12) Ha, S.; Kaafarani, B.; Barlow, S.; Marder, S.; Kahn, A. J. Phys. Chem. C 2007, 111, 10493.

(13) Smith, R.; Lewis, P.; weiss, P. Progr. Surf. Sci. 2004, 75, 1.

(14) Hipps, K.; Scudiero, L.; Barlow, D.; Cooke, M. J. Am. Chem. Soc. 2002, 124, 2126.

(15) Li, J. Z.; Gryko, D.; Dabke, R. B.; Diers, J. R.; Bocian, D. F.; Kuhr, W. G.; Lindsey, J. S. J. Org. Chem. 2000, 65, 7379.

(16) Balakumar, A.; Lysenko, A. B.; Carcel, C.; Malinovskii, V. L.; Gryko, D. T.; Schweikart, K. H.; Loewe, R. S.; Yasseri, A. A.; Liu, Z. M.; Bocian, D. F.; Lindsey, J. S. J. Org. Chem. 2004, 69, 1435.

(17) Wei, L. Y.; Padmaja, K.; Youngblood, W. J.; Lysenko, A. B.; Lindsey, J. S.; Bocian, D. F. Journal of Organic Chemistry 2004, 69, 1461.

(18) Yasseri, A. A.; Syomin, D.; Malinovskii, V. L.; Loewe, R. S.; Lindsey, J. S.; Zaera, F.; Bocian, D. F. Journal of the American Chemical Society 2004, 126, 11944.

(19) Kang, B.; Aratani, N.; Lim, J. K.; Kim, D.; Osuka, A.; Yoo, K.-H. Chem. Phys. Lett. 2005, 412, 303.

(20) Vaughan, O. P. H.; Turner, M.; Williams, F. J.; Hille, A.; Sanders, J. K. M.; Lambert, R. M. Journal of the American Chemical Society 2006, 128, 9578.

(21) Chan, Y. H.; Schuckman, A. E.; Perez, L. M.; Vinodu, M.; Drain, C. M.; Batteas, J. D. J. Phys. Chem. C 2008, 112, 6110.

(22) Barlow, S.; Raval, R. Surf. Sci. Rep 2003, 50, 201.

(23) Forrest, S. Chem. Rev. 1997, 97, 1793.

(24) Garno, J. C.; Xu, C.; Bazzan, G.; Batteas, J. D.; Drain, C. M. In Metal-Containing and Metallosupramolecular Polymers and Materials; Schubert, U. S., Newkome, G. R., Manners, I., Eds.; American Chemical Society: 2006, p 168.

(25) Visser, J.; Katsonis, N.; Vicario, J.; Feringa, B. L. Langmuir 2009, 25, 5980.

(26) Liu, M.; Amro, N. A.; Liu, G.-y. Annu. Rev. Phys. Chem. 2008, 59, 367.

(27) Perrine, T. M.; Smith, R. G.; Marsh, C.; Dunietz, B. D. J. Chem. Phys. 2008, 128, 154706.

(28) Kang, B. K.; Aratani, N.; Lim, J. K.; Kim, D.; Osuka, A.; Yoo, K.-H. Materials Science Engineering C 2006, 26, 1023

(29) Sedghi, G.; Sawada, K.; Esdaile, L. J.; Hoffmann, M.; Anderson, H. L.; Bethell, D.; Haiss, W.; Higgins, S. J.; Nichols, R. J. J. Am. Chem. Soc. 2008, 130, 8582.

(30) Thanopulos, I.; Paspalakis, E.; Yannopapas, V. Nanotech. 2008, 19.

(31) Li, C.; Ly, J.; Lei, B.; Fan, W.; Zhang, D.; Han, J.; Meyyappan, M.; Thompson, M.; Zhou, C. J. Phys. Chem. B 2004, 108, 9646.

(32) Liu, H.; Duclairoir, F.; Fleury, B.; Dubois, L.; Chenavierb, Y.; Marchon, J.-C. Dalton Trans. 2009, 3793.

(33) Roth, K. M.; Yasseri, A. A.; Liu, Z.; Dabke, R. B.; Malinovskii, V.; Schwelkart, K. H.; Yu, L.; Tiznado, H.; Zaera, F.; Lindsey, J. S.; Kuhr, W. G.; Bocain, D. F. J. Am. Chem. Soc., 2003, 125, 505.

(34) Hipps, K. W.; Scudiero, L.; Barlow, D. E.; Cooke, M. P. J. Am. Chem. Soc. 2002, 124, 2126.

(35) Scudiero, L.; Barlow, D. E.; Hipps, K. W. J. Phys. Chem. B 2002, 106, 996.

(36) Scudiero, L.; Hipps, K. W.; Barlow, D. E. J. Phys. Chem. B 2003, 107, 2903.

(37) Ogunrinde, A.; Hipps, K. W.; Scudiero, L. Langmuir 2006, 22, 5697.
(38) Scudiero, L.; Hipps, K. W. J. Phys. Chem. C 2007, 111, 17516.
(39) Teague, L. C.; Boland, J. J. J. Phys. Chem. B. 2003, 107, 3820.
(40) Teague, L. C.; Chen, D.; Boland, J. J. J. Phys. Chem. B. 2004, 108, 7827.
(41) Teague, L. C.; Boland, J. J. Thin Solid Films 2004, 464-465, 1.
(42) Liu, Z.; Yasseri, A. A.; Lindsey, J. S.; Bocian, D. F. Science 2003, 302, 1543.
(43) Yerushalmi, R.; Scherz, A.; van der Boom, M. E. J. Am. Chem. Soc. 2004, 126, 2700.
(44) Muthukumaran, K.; Loewe, R. S.; Ambroise, A.; Tamaru, S.; Li, Q.; Mathur, G.; Bocain, D. F.; Misra, V.; Lindsey, J. S. J. Org. Chem. 2004, 69, 1444.
(45) Hurley, P. T.; Ribbe, A. E.; Buriak, J. M. J. Am. Chem. Soc. 2003, 125, 11334.
(46) Hacker, C. A.; Anderson, K. A.; Richter, L. J.; Richter, C. A. Langmuir 2005, 21, 882.
(47) Wiberg, J.; GUo, L.; Pettersson, K.; Nilsson, D.; Ljungdahl, T.; Martensson, J.; Albinsson, B. J. Am. Chem. Soc. 2006, 129.
(48) Ghirotti, M.; Chiorboli, C.; You, C.; Wurthner, F.; Scandola, F. J. Phys. Chem. A 2008, 112, 3376.
(49) D'Souza, F.; Chitta, R.; Gadde, S.; Islam, D.; Schumacher, A.; Zandler, M.; Araki, Y.; Ito, O. J. Phys. Chem. B 2006, 110, 25240.
(50) Campbell, W. M.; Burrell, A. K.; Officer, D. L.; Jolley, K. W. Coord. Chem. Rev. 2004, 248, 1363.
(51) Wasielewski, M. R. J. Org. Chem. 2006, 71, 5051.
(52) Albinsson, B.; Martensson, J. J. Photochem. Photobio. C 2008, 138.
(53) Ozawa, H.; Kawao, M.; Tanaka, H.; Ogawa, T. Chem. Lett. 2009, 38.
(54) Sedghi, G.; Sawada, K.; Esdaile, L.; Hoffmann, M.; Anderson, H.; Bethell, D.; Haiss, W.; Higgins, S.; Nichols, R. J. Am. Chem. Soc. 2008, 130.
(55) Miyachi, M.; Ohta, M.; Nakai, M.; Kubota, Y.; Yamanoi, Y.; Yonezawa, T.; Nishihara, H. Chem. Lett. 2008, 37.
(56) Ambroise, A.; Kirmaier, C.; Wagner, R.; Loewe, R.; Bocian, D.; Holten, D.; Lindsey, J. J. Org. Chem. 2002, 67, 3811.
(57) Madru, R.; Guillaud, G.; Al Sadoun, M.; Maitrot, M.; André, J. J.; Simon, J.; Even, R. Chemical Physics Letters 1988, 145, 343.
(58) Ambroise, A.; Wagner, R. W.; Rao, P. D.; Riggs, J. A.; Hascoat, P.; Diers, J. R.; Seth, J.; Lammi, R. K.; Bocian, D. F.; Holten, D.; Lindsey, J. S. Chem. Mater. 2001, 13, 1023.
(59) Wagner, R.; Lindsey, J.; Seth, J.; Palaniappan, V.; Bocian, D. J. Am. Chem. Soc. 1996, 118, 3996.
(60) Noguchi, Y.; Kubota, T.; Mashiko, S.; Wakayama, Y. J. Appl. Phys. 2005, 97.
(61) Noguchi, Y.; Nagase, T.; Kubota, T.; Kamikado, T.; Mashiko, S. Thin Solid Films 2006, 499, 90.
(62) Noguchi, Y.; Ueda, R.; Kubota, T.; Kamikado, T.; Yokoyama, S.; Nagase, T. Thin Solid Films 2008, 516, 2762.

(63) Wakayama, Y.; Kubota, T.; Suzuki, H.; Kamikado, T.; Mashiko, S. Journal of Applied Physics 2003, 94, 4711.

(64) Wakayama, Y.; Kubota, T.; Suzuki, H.; Kamikado, T.; Mashiko, S. Nanotechnology 2004, 15, 1446.

(65) Wakayama, Y.; Ogawa, K.; Kubota, T.; Suzuki, H.; Kamikado, T.; Mashiko, S. Appl. Phys. Lett. 2004, 85, 329.

3. Substituted Phthalocyanines for Photonic Devices

(1) Ameri, T.; Dennler, G.; Lungenschmied, C.; Brabec, C. J. Energy Env. Sci. 2009, 2, 347.

(2) Clarke, T. M.; Durrant, J. R. Chem. Rev. 2010, 110, 6736.

(3) Liang, Y.; Yu, L. Poly. Rev. 2010, 50, 454

(4) Zheng, Y.; Xue, J. Poly. Rev. 2010, 50, 420

(5) Ratcliff, E. L.; Zacher, B.; Armstrong, N. R. J. Phys. Chem. Let. 2011, 2, 1337.

(6) Krebs, F. C.; Fyenbo, J.; Tanenbaum, D. M.; Gevorgyan, S. A.; Andriessen, R.; van Remoortere, B.; Galagan, Y.; Jorgensen, M. Energ. Envir. Sci. 2011, 4, 4116.

(7) Walker, B.; Kim, C.; Nguyen, T.-Q. Chem. Mater. 2011, 23, 470.

(8) Ooyama, Y.; Harima, Y. Eur. J. Org. Chem. 2009, 2009, 2903.

(9) Lee, H. J.; Leventis, H. C.; Haque, S. A.; Torres, T.; Grätzel, M.; Nazeeruddin, M. K. J. Power Sources 2011, 196, 596.

(10) Brabec, C. J.; Sariciftci, N. S.; Hummelen, J. C. Adv. Funct. Mater. 2001, 11, 15.

(11) Liao, K.-S.; Yambem, S. D.; Haldar, A.; Alley, N. J.; Curran, S. A. Energies 2010, 3, 1212.

(12) He, F.; Yu, L. J. Phys. Chem. Lett. 2011, 2, 3102.

(13) Bailey-Salzman, R. F.; Rand, B. P.; Forrest, S. R. Appl. Phys. Lett. 2006, 88, 233502.

(14) Peumans, P.; Uchida, S.; Forrest, S. R. Nature 2003, 425, 158.

(15) Scharber, M. C.; Mühlbacher, D.; Koppe, M.; Denk, P.; Waldauf, C.; Heeger, A. J.; Brabec, C. J. Adv. Mat. 2006, 18, 789.

(16) Khan, S. M.; Kaur, M.; Heflin, J. R.; Sayyad, M. H. J. Phys. Chem. Solids 2011, 72, 1430.

(17) Said, A. J.; Poize, G.; Martini, C.; Ferry, D.; Marine, W.; Giorgio, S.; Fages, F.; Hocq, J.; Bouclé, J.; Nelson, J.; Durrant, J. R.; Ackermann, J. J. Phys. Chem. C 2010, 114, 11273.

(18) Sun, Y.; Welch, G. C.; Leong, W. L.; Takacs, C. J.; Bazan, G. C.; Heeger, A. J. Nat. Mater. 2012, 11, 44.

(19) Chu, T.-Y.; Lu, J.; Beaupré, S.; Zhang, Y.; Pouliot, J.-R. m.; Wakim, S.; Zhou, J.; Leclerc, M.; Li, Z.; Ding, J.; Tao, Y. J. Am. Chem. Soc. 2011, 133, 4250.

(20) Zhu, Y.; Xu, X.; Zhang, L.; Chen, J.; Cao, Y. Solar Energy Materials Solar Cells 2012, 97, 83.

(21) Brabec, C. J.; Gowrisanker, S.; Halls, J. J. M.; Laird, D.; Jia, S.; Williams, S. P. Adv. Materials 2010, 22, 3839.

(22) Wang, D. H.; Kim, D. Y.; Choi, K. W.; Seo, J. H.; Im, S. H.; Park, J. H.; Park, O. O.; Heeger, A. J. Angew. Chem. Int. Ed. 2011, 50, 5519.

(23) Allen, J. E.; Yager, K. G.; Hlaing, H.; Nam, C.-Y.; Ocko, B. M.; Black, C. T. Appl. Phys. Lett. 2011, 99, 163301.

(24) Hlaing, H.; Lu, X.; Hofmann, T.; Yager, K. G.; Black, C. T.; Ocko, B. M. ACS Nano 2011, 5, 7532.

(25) Allen, J. E.; Black, C. T. ACS Nano 2011, 5, 7986.

(26) Wu, W.-R.; Jeng, U. S.; Su, C.-J.; Wei, K.-H.; Su, M.-S.; Chiu, M.-Y.; Chen, C.-Y.; Su, W.-B.; Su, C.-H.; Su, A.-C. ACS Nano 2011, 5, 6233.

(27) Loser, S.; Bruns, C. J.; Miyauchi, H.; Ortiz, R. o. P.; Facchetti, A.; Stupp, S. I.; Marks, T. J. J. Am. Chem. Soc. 2011, 133, 8142.

(28) Lee, C. Y.; She, C.; Jeong, N. C.; Hupp, J. T. Chem. Commun. 2010, 46, 6090.

(29) Ning, Z.; Fu, Y.; Tian, H. Energy Environ. Sci. 2010, 3, 1170.

(30) Walter, M. G.; Rudine, A. B.; Wamser, C. C. J. Porphyrins Phthalocyanines 2010, 14, 759.

(31) de la Torre, G.; Claessens, C. G.; Torres, T. Chem. Com. 2007, 2000.

(32) Blankenship, R. E.; Tiede, D. M.; Barber, J.; Brudvig, G. W.; Fleming, G.; Ghirardi, M.; Gunner, M. R.; Junge, W.; Kramer, D. M.; Melis, A.; Moore, T. A.; Moser, C. C.; Nocera, D. G.; Nozik, A. J.; Ort, D. R.; Parson, W. W.; Prince, R. C.; Sayre, R. T. Science 2011, 332, 805.

(33) Radivojevic, I.; Varotto, A.; Farley, C.; Drain, C. M. Energ. Envir. Sci. 2010, 3, 1897.

(34) Rand, B. P.; Genoe, J.; Heremans, P.; Poortmans, J. Progress in Photovoltaics: Research and Applications 2007, 15, 659.

(35) Varotto, A.; Nam, C.-Y.; Radivojevic, I.; P. C. Tomé, J.; Cavaleiro, J. A. S.; Black, C. T.; Drain, C. M. J. Am. Chem. Soc. 2010, 132, 2552.

(36) Schumann, S.; Hatton, R. A.; Jones, T. S. J. Phys. Chem. C 2011, 115, 4916.

(37) D'Souza, F.; Ito, O. Chem. Soc. Rev. 2012, 41, 86.

(38) Honda, S.; Ohkita, H.; Benten, H.; Ito, S. Adv. Energy Mater. 2011, 1, 588.

(39) Zeng, W.; Yong, K. S.; Kam, Z. M.; Zhu, F.; Li, Y. Appl. Phys. Let. 2010, 97, 133304.

(40) Honda, S.; Yokoya, S.; Ohkita, H.; Benten, H.; Ito, S. J. Phys. Chem. C 2011, 115, 11306.

(41) Honda, S.; Ohkita, H.; Benten, H.; Ito, S. Chem. Com. 2010, 46, 6596.

(42) Moon, S.-J.; Baranoff, E.; Zakeeruddin, S. M.; Yeh, C.-Y.; Diau, E. W.-G.; Gratzel, M.; Sivula, K. Chem. Comm. 2011, 47, 8244.

(43) Bartelmess, J.; Ballesteros, B.; de la Torre, G.; Kiessling, D.; Campidelli, S.; Prato, M.; Torres, T.; Guldi, D. M. J. Am. Chem. Soc. 2010, 132, 16202.

(44) Schlenker, C. W.; Barlier, V. S.; Chin, S. W.; Whited, M. T.; McAnally, R. E.; Forrest, S. R.; Thompson, M. E. Chem. Mater. 2011, 23, 4132.

(45) Kim, J. Y.; Bard, A. J. Chem. Phys. Let. 2004, 383, 11.

(46) de la Torre, G.; Giacalone, F.; Segura, J. L.; Martín, N.; Guldi, D. M. Chem. Eur. J. 2005, 11, 1267.

(47) Fukuzumi, S.; Ohkubo, K.; Imahori, H.; Shao, J.; Ou, Z.; Zheng, G.; Chen, Y.; Pandey, R. K.; Fujitsuka, M.; Ito, O.; Kadish, K. M. J. Am. Chem. Soc. 2001, 123, 10676.

(48) Quintiliani, M.; Kahnt, A.; Vazquez, P.; Guldi, D. M.; Torres, T. J. Matr. Chem. 2008, 18, 1542.

(49) Gomez, E. D.; Barteau, K. P.; Wang, H.; Toney, M. F.; Loo, Y.-L. Chem. Com. 2011, 47, 436.

(50) Kim, H. J.; Kim, J. W.; Lee, H. H.; Kim, T.-M.; Jang, J.; Kim, J.-J. J. Phys. Chem. Let. 2011, 2, 1710.

(51) Beaujuge, P. M.; Frechet, J. M. J. J. Am. Chem. Soc. 2011, 133, 20009.

(52) Li, S.-S.; Chang, C.-P.; Lin, C.-C.; Lin, Y.-Y.; Chang, C.-H.; Yang, J.-R.; Chu, M.-W.; Chen, C.-W. J. Am. Chem. Soc. 2011, 133, 11614.

(53) Liao, H.-C.; Tsao, C.-S.; Lin, T.-H.; Chuang, C.-M.; Chen, C.-Y.; Jeng, U. S.; Su, C.-H.; Chen, Y.-F.; Su, W.-F. J. Am. Chem. Soc. 2011, 133, 13064.

(54) Prato, M.; Maggini, M.; Giacometti, C.; Scorrano, G.; Sandona, G.; Farnia, G. Tetrahedron 1996, 52, 5221.

(55) Bottari, G.; Suanzes, J. A.; Trukhina, O.; Torres, T. J. Phys. Chem. Let. 2011, 2, 905.

(56) Rodríguez-Cordoba, W.; Noria, R.; Guarín, C. A.; Peon, J. J. Am. Chem. Soc. 2011, 133, 4698.

(57) Troshin, P. A.; Koeppe, R.; Peregudov, A. S.; Peregudova, S. M.; Egginger, M.; Lyubovskaya, R. N.; Sariciftci, N. S. Chem. Mater. 2007, 19, 5363.

(58) Kaafarani, B. R. Chem. Mater. 2010, 23, 378.

(59) Lee, J.-K.; Jang, S.-I.; Kim, Y.-G.; Jang, Y.-W.; Jeong, B.-H.; Kim, J.-U.; Jung, K.-S.; Kim, M.-R. Molecular Crystals Liquid Crystals 2008, 491, 307

(60) Roussel, O.; Kestemont, G.; Tant, J.; De Halleux, V.; Aspe, R. G.; Levin, J.; Remacle, A.; Gearba, I. R.; Ivanov, D.; Lehmann, M.; Geerts, Y. Molecular Crystals and Liquid Crystals 2003, 396, 35

(61) Hori, T.; Miyake, Y.; Yamasaki, N.; Yoshida, H.; Fujii, A.; Shimizu, Y.; Ozaki, M. Appl. Phys. Express 2010, 3, 101602.

(62) Sakamoto, K.; Ohno-Okumura, E. Materials 2009, 2, 1127.

(63) Service, R. F. Science 2011, 332, 293.

(64) Hayashi, H.; Nihashi, W.; Umeyama, T.; Matano, Y.; Seki, S.; Shimizu, Y.; Imahori, H. J. Am. Chem. Soc. 2011, 133, 10736.

(65) Lei, S.; Yang, Y.; Zeng, Q.; Wang, C. Langmuir 2011, 27, 3496.

(66) Zhu, F.; Grobosch, M.; Treske, U.; Huang, L.; Chen, W.; Yang, J.; Yan, D.; Knupfer, M. ACS Appl. Mater. Interfaces 2011, 3, 2195.

(67) Placencia, D.; Wang, W.; Gantz, J.; Jenkins, J. L.; Armstrong, N. R. J. Phys. Chem. C 2011, 115, 18873.

(68) Bramble, J. P.; Tate, D. J.; Revill, D. J.; Sheikh, K. H.; Henderson, J. R.; Liu, F.; Zeng, X.; Ungar, G.; Bushby, R. J.; Evans, S. D. Adv. Func. Mater. 2010, 20, 914.

(69) Laschat, S.; Baro, A.; Steinke, N.; Giesselmann, F.; Hägele, C.; Scalia, G.; Judele, R.; Kapatsina, E.; Sauer, S.; Schreivogel, A.; Tosoni, M. Angew. Chem. Int. Ed. 2007, 46, 4832.

(70) Lux, A.; Rozenberg, G. G.; Petritsch, K.; Moratti, S. C.; Holmes, A. B.; Friend, R. H. Synthetic Metals 1999, 102, 1527.

(71) Schmidt-Mende, L.; Fechtenkötter, A.; Müllen, K.; Moons, E.; Friend, R. H.; MacKenzie, J. D. Science 2001, 293, 1119.

(72) Milic, T.; Garno, J. C.; Batteas, J. D.; Smeureanu, G.; Drain, C. M. Langmuir 2004, 20, 3974.

(73) Milic, T. N.; Chi, N.; Yablon, D. G.; Flynn, G. W.; Batteas, J. D.; Drain, C. M. Angew. Chem. Int. Ed. 2002, 41, 2117.

(74) Petritsch, K.; Dittmer, J. J.; Marseglia, E. A.; Friend, R. H.; Lux, A.; Rozenberg, G. G.; Moratti, S. C.; Holmes, A. B. Solar Energy Materials and Solar Cells 2000, 61, 63.

(75) Gearba, R. I.; Bondar, A. I.; Goderis, B.; Bras, W.; Ivanov, D. A. Chem. Mater. 2005, 17, 2825.

(76) Kang, H.-J.; Kang, E.-H.; Park, S.-W.; Lee, J.-W.; Lee, J.-K. Macromolecular Symposia 2006, 235, 195.

(77) Singh, T. B.; Erten, S.; Günes, S.; Zafer, C.; Turkmen, G.; Kuban, B.; Teoman, Y.; Sariciftci, N. S.; Icli, S. Organic Electronics 2006, 7, 480.

(78) Alzeer, J.; Roth, P. J. C.; Luedtke, N. W. Chem. Com. 2009, 1970.

(79) Bilgiçli, A. T.; Yarasir, M. N.; Kandaz, M.; Riza Özkaya, A. Polyhedron 2010, 29, 2498.

(80) Hirade, M.; Nakanotani, H.; Yahiro, M.; Adachi, C. ACS Appl. Mater. Interfaces 2010, 3, 80.

(81) Liang, F.; Shi, F.; Fu, Y.; Wang, L.; Zhang, X.; Xie, Z.; Su, Z. Solar Energy Materials and Solar Cells 2010, 94, 1803.

(82) Bottari, G.; Suanzes, J. A.; Trukhina, O.; Torres, T. J. Phys. Chem. Let. 2011, 2, 905.

(83) Honda, S.; Yokoya, S.; Ohkita, H.; Benten, H.; Ito, S. J. Phys. Chem. C 2011, 115, 11306.

(84) Zhang, S.; Sakai, R.; Abe, T.; Iyoda, T.; Norimatsu, T.; Nagai, K. ACS Appl. Mater. Interfaces 2011, 3, 1902.

(85) Bendler*, J. T.; Fontanella, J. J.; Shlesinger, M. F.; Wintersgill, M. C. Electrochimica Acta 2001, 46, 1615.

(86) Wen, T.-C.; Wang, Y.-J.; Cheng, T.-T.; Yang, C.-H. Polymer 1999, 40, 3979.

(87) Wieczorek, W.; Lipka, P.; Żukowska, G.; Wyciślik, H. The Journal of Physical Chemistry B 1998, 102, 6968.

(88) Belhadj, F.; Moissette, A.; Brémard, C.; Hureau, M.; Derriche, Z. ChemPhysChem 2011, 12, 1378.

(89) Grundmann, M.; Springer Berlin Heidelberg: 2010, p 451.

(90) Antunes, P. A.; Constantino, C. J. L.; Aroca, R. F.; Duff, J. Langmuir 2001, 17, 2958.

4. Porphyrin Dimers as Higher Fullerene Tweezers

(1) Boyd, P. D. W.; Reed, C. A. Acc. Chem. Res. 2005, 38, 235.

(2) Baran, P. S.; Monaco, R. R.; Khan, A. U.; Schuster, D. I.; Wilson, S. R. J. Am. Chem. Soc. 1997, 119, 8363.
(3) Bhattacharya, S.; Tominaga, K.; Kimura, T.; Uno, H.; Komatsu, N. Chem. Phys. Let. 2007, 433, 395.
(4) He, L.; Zhu, Y.-Z.; Zheng, J.-Y.; Ma, Y.-F.; Chen, Y.-S. J. Photochem. Photobio. A: Chem. 2010, 216, 15.
(5) Liddell, P. A.; Kodis, G.; Kuciauskas, D.; Andreasson, J.; Moore, A. L.; Moore, T. A.; Gust, D. Phys. Chem. Chem. Phys. 2004, 6, 5509.
(6) Mukherjee, S.; Bauri, A. K.; Bhattacharya, S. Chem. Phys. Let. 2010, 500, 128.
(7) Tamaki, K.; Imahori, H.; Sakata, Y.; Nishimura, Y.; Yamazaki, I. Chem. Commun. 1999, 625.
(8) Umeyama, T.; Tezuka, N.; Kawashima, F.; Seki, S.; Matano, Y.; Nakao, Y.; Shishido, T.; Nishi, M.; Hirao, K.; Lehtivuori, H.; Tkachenko, N. V.; Lemmetyinen, H.; Imahori, H. Angew. Chem. Int. Ed. 2011, 50, 4615.
(9) Zhang, Y.; Yu, Y.; Jiang, Z.; Xu, H.; Wang, Z.; Zhang, X.; Oda, M.; Ishizuka, T.; Jiang, D.; Chi, L.; Fuchs, H. Langmuir 2009, 25, 6627.
(10) Wu, Z.-Q.; Shao, X.-B.; Li, C.; Hou, J.-L.; Wang, K.; Jiang, X.-K.; Li, Z.-T. J. Am. Chem. Soc. 2005, 127, 17460.
(11) Dudic, M.; Lhotak, P.; Stibor, I.; Petrickova, H.; Lang, K. New J. Chem. 2004, 28, 85.
(12) Shoji, Y.; Tashiro, K.; Aida, T. J. Am. Chem. Soc. 2004, 126, 6570.
(13) Jakob, M.; Berg, A.; Levanon, H.; Schuster, D. I.; Megiatto, J. D. J. Phys. Chem. C 2011, 115, 24555.
(14) Wilson, S. R.; MacMahon, S.; Tat, F. T.; Jarowski, P. D.; Schuster, D. I. Chem. Commun. 2003, 226.
(15) Sessler, J. L.; Jayawickramarajah, J.; Gouloumis, A.; Torres, T.; Guldi, D. M.; Maldonado, S.; Stevenson, K. J. Chem. Commun. 2005, 1892.
(16) D'Souza, F.; Chitta, R.; Gadde, S.; Zandler, M. E.; Sandanayaka, A. S. D.; Araki, Y.; Ito, O. Chem. Commun. 2005, 1279.
(17) Echegoyen, L.; Echegoyen, L. E. Acc. Chem. Res. 1998, 31, 593.
(18) D'Souza, F.; Ito, O. Chem. Commun. 2009, 4913.
(19) Drain, C. M.; Nifiatis, F.; Vasenko, A.; Batteas, J. D. Angew. Chem. Int. Ed. 1998, 37, 2344.
(20) Varotto, A.; Todaro, L.; Vinodu, M.; Koehne, J.; Liu, G.-y.; Drain, C. M. Chem. Commun. 2008, 4921.
(21) Drain, C. M.; Varotto, A.; Radivojevic, I. Chem. Rev. 2009, 109, 1630.
(22) Mulholland, A. R.; Woodward, C. P.; Langford, S. J. Chem. Commun. 2011, 47, 1494.
(23) Babu, S. S.; Mohwald, H.; Nakanishi, T. Chem. Soc. Rev. 2010, 39, 4021.
(24) Coates, G. W.; Dunn, A. R.; Henling, L. M.; Ziller, J. W.; Lobkovsky, E. B.; Grubbs, R. H. J. Am. Chem. Soc. 1998, 120, 3641.
(25) Vilmercati, P.; Cudia, C. C.; Larciprete, R.; Cepek, C.; Zampieri, G.; Sangaletti, L.; Pagliara, S.; Verdini, A.; Cossaro, A.; Floreano, L.; Morgante, A.; Petaccia, L.; Lizzit, S.; Battocchio, C.; Polzonetti, G.; Goldoni, A. Surf. Sci. 2006, 600, 4018.
(26) Boyd, P. D. W.; Hodgson, M. C.; Rickard, C. E. F.; Oliver, A. G.; Chaker, L.; Brothers, P. J.; Bolskar, R. D.; Tham, F. S.; Reed, C. A. J. Am. Chem. Soc. 1999, 121, 10487.
(27) Li, H.; Zhou, B.; Lin, Y.; Gu, L.; Wang, W.; Fernando, K. A. S.; Kumar, S.; Allard, L. F.; Sun, Y.-P. J. Am. Chem. Soc. 2004, 126, 1014.

(28) Sgobba, V.; Rahman, G. M. A.; Guldi, D. M.; Jux, N.; Campidelli, S.; Prato, M. Adv. Mat. 2006, 18, 2264.
(29) Tasis, D.; Tagmatarchis, N.; Bianco, A.; Prato, M. Chem. Rev. 2006, 106, 1105.
(30) Ariga, K.; Hill, J. P.; Ji, Q. Phys. Chem. Chem. Phys. 2007, 9, 2319.
(31) Ariga, K.; Sakakibara, K.; Richards, G. J.; Hill, J. P. Supramolecular Chem. 2011, 23, 183.
(32) Sakakibara, K.; Hill, J. P.; Ariga, K. Small 2011, 7, 1288.
(33) Kim, D. Multiporphyrin Arrays: Fundamentals and Applications; CRC Press: Boca Raton, 2012.
(34) Radivojevic, I.; Varotto, A.; Farley, C.; Drain, C. M. Energy & Environmental Science 2010, 3, 1897.
(35) Jurow, M.; Schuckman, A. E.; Batteas, J. D.; Drain, C. M. Coordination Chemistry Reviews 2010, 254, 2297.
(36) Drain, C. M.; Smeureanu, G.; Patel, S.; Gong, X. C.; Garno, J.; Arijeloye, J. New Journal of Chemistry 2006, 30, 1834.
(37) Drain, C. M.; Bazzan, G.; Milic, T.; Vinodu, M.; Goeltz, J. C. Israel Journal of Chemistry 2005, 45, 255.
(38) Drain, C. M.; Batteas, J. D.; Flynn, G. W.; Milic, T.; Chi, N.; Yablon, D. G.; Sommers, H. Proceedings of the National Academy of Sciences of the United States of America 2002, 99, 6498.
(39) Deak, D. S.; Porfyrakis, K.; Castell, M. R. Chem. Commun. 2007, 2941.
(40) Dietz, P.; Fostiropoulos, K.; Krätschmer, W.; Hansma, P. K. Citation: Appl. Phys. Lett. 1992, 60, 62.

5. Zr(IV) Porphyrinoids on Graphene Oxide by Axial Ligation

(1) Loh, K. P.; Bao, Q.; Eda, G.; Chhowalla, M. Nat Chem 2010, 2, 1015.
(2) Dreyer, D. R.; Park, S.; Bielawski, C. W.; Ruoff, R. S. Chemical Society Reviews 2010, 39, 228.
(3) Lerf, A.; He, H.; Forster, M.; Klinowski, J. The Journal of Physical Chemistry B 1998, 102, 4477.
(4) Kim, J.; Cote, L. J.; Kim, F.; Yuan, W.; Shull, K. R.; Huang, J. Journal of the American Chemical Society 2010, 132, 8180.
(5) Shih, C.-J.; Lin, S.; Sharma, R.; Strano, M. S.; Blankschtein, D. Langmuir 2011, 28, 235.
(6) Liu, Z.; Robinson, J. T.; Sun, X.; Dai, H. Journal of the American Chemical Society 2008, 130, 10876.
(7) Sun, X.; Liu, Z.; Welsher, K.; Robinson, J.; Goodwin, A.; Zaric, S.; Dai, H. Nano Research 2008, 1, 203.
(8) Luo, Z.; Vora, P. M.; Mele, E. J.; Johnson, A. T. C.; Kikkawa, J. M. Applied Physics Letters 2009, 94, 111909.
(9) Yao, C.; Yan, L.-K.; Guan, W.; Liu, C.-G.; Song, P.; Su, Z.-M. Dalton Trans. 2010, 39, 7645.
(10) Arnold, M. S.; Zimmerman, J. D.; Renshaw, C. K.; Xu, X.; Lunt, R. R.; Austin, C. M.; Forrest, S. R. Nano Letters 2009, 9, 3354.
(11) Tung, V. C.; Huang, J.-H.; Tevis, I.; Kim, F.; Kim, J.; Chu, C.-W.; Stupp, S. I.; Huang, J. Journal of the American Chemical Society 2011, 133, 4940.

(12) Tung, V. C.; Kim, J.; Cote, L. J.; Huang, J. Journal of the American Chemical Society 2011, 133, 9262.
(13) Xu, Y.; Liu, Z.; Zhang, X.; Wang, Y.; Tian, J.; Huang, Y.; Ma, Y.; Zhang, X.; Chen, Y. Advanced Materials 2009, 21, 1275.
(14) Karousis, N.; Sandanayaka, A. S. D.; Hasobe, T.; Economopoulos, S. P.; Sarantopoulou, E.; Tagmatarchis, N. Journal of Materials Chemistry 2011, 21, 109.
(15) Bala Murali Krishna, M.; Venkatramaiah, N.; Venkatesan, R.; Narayana Rao, D. Journal of Materials Chemistry 2012, 22, 3059.
(16) Chunder, A.; Pal, T.; Khondaker, S. I.; Zhai, L. The Journal of Physical Chemistry C 2010, 114, 15129.
(17) Malig, J.; Jux, N.; Kiessling, D.; Cid, J.-J.; Vázquez, P.; Torres, T.; Guldi, D. M. Angewandte Chemie International Edition 2011, 50, 3561.
(18) Wang, X.; Zhi, L.; Mullen, K. Nano Letters 2007, 8, 323.
(19) Brand, H.; Arnold, J. Coordination Chemistry Reviews 1995, 140, 137.
(20) Falber, A.; Burton-Pye, B. P.; Radivojevic, I.; Todaro, L.; Saleh, R.; Francesconi, L. C.; Drain, C. M. European Journal of Inorganic Chemistry 2009, 2009, 2459.
(21) Radivojevic, I.; Bazzan, G.; Burton-Pye, B. P.; Ithisuphalap, K.; Saleh, R.; Durstock, M. F.; Francesconi, L. C.; Drain, C. M. J. Phys. Chem. C 2012, ASAP, dx.doi.org/10.1021/jp301853d.
(22) Liao, M.-S.; Scheiner, S. J. Chem. Phys. 2002, 117.
(23) Varotto, A.; Nam, C.-Y.; Radivojevic, I.; P. C. Tomé, J.; Cavaleiro, J. A. S.; Black, C. T.; Drain, C. M. Journal of the American Chemical Society 2010, 132, 2552.
(24) Paredes, J. I.; Villar-Rodil, S.; Martínez-Alonso, A.; Tascón, J. M. D. Langmuir 2008, 24, 10560.
(25) Beletskaya, I.; Tyurin, V. S.; Tsivadze, A. Y.; Guilard, R.; Stern, C. Chemical Reviews 2009, 109, 1659.
(26) Zhang, L.; Xia, J.; Zhao, Q.; Liu, L.; Zhang, Z. Small 2010, 6, 537.
(27) Treossi, E.; Melucci, M.; Liscio, A.; Gazzano, M.; Samorì, P.; Palermo, V. J. Am. Chem. Soc. 2009, 131, 15576.
(28) Bazzan, G.; Smith, W.; Francesconi, L. C.; Drain, C. M. Langmuir 2008, 24, 3244.
(29) Becerril, H. A.; Mao, J.; Liu, Z.; Stoltenberg, R. M.; Bao, Z.; Chen, Y. ACS Nano 2008, 2, 463.
(30) Li, D.; Muller, M. B.; Gilje, S.; Kaner, R. B.; Wallace, G. G. Nat Nano 2008, 3, 101.
(31) Jin, M.; Jeong, H.-K.; Yu, W. J.; Bae, D. J.; Kang, B. R.; Lee, Y. H. Journal of Physics D: Applied Physics 2009, 42, 135109.
(32) Chang, C.-H.; Fan, X.; Li, L.-J.; Kuo, J.-L. The Journal of Physical Chemistry C 2012.
(33) Zhao, X.; Zhang, Q.; Hao, Y.; Li, Y.; Fang, Y.; Chen, D. Macromolecules 2010, 43, 9411.
(34) Luo, D.; Zhang, G.; Liu, J.; Sun, X. The Journal of Physical Chemistry C 2011, 115, 11327.